

# Adaptive Control of Plants with Input Saturation: An Approach for Performance Improvement

Dissertation  
zur  
Erlangung des akademischen Grades  
Doktor-Ingenieur (Dr.-Ing)  
der Fakultät für Informatik und Elektrotechnik  
der Universität Rostock

vorgelegt von  
Frederik Manus Thiel  
aus Hamburg

Gutachter:

Prof. Dr.-Ing. Torsten Jeinsch  
Institut für Automatisierungstechnik, Universität Rostock

Prof. Dr.-Ing. Herbert Werner  
Institute of Control Systems, Technische Universität Hamburg

Prof. Dr.-Ing. Dirk Söffker  
Lehrstuhl Steuerung, Regelung und Systemdynamik, Universität Duisburg-Essen

Jahr der Einreichung: 2017  
Jahr der Verteidigung: 2019



---

## Abstract

The general concept of adaptive control originates from an intuitive and promising idea for the control of plants with uncertain or even changing parameters. Instead of designing a robust controller that accounts for parameter uncertainties of the plant, the parameters of the plant or the controller are identified online. Hence, the controller can be adjusted during operation in order to permanently achieve a predefined closed-loop performance.

After the first introduction of adaptive control, it became very popular in the 1960s in flight control research. However, unexpected difficulties such as the lack of robustness of the applied algorithms prevented acceptance of adaptive methods in industry. Today extensions and modifications exist which make classical adaptive algorithms applicable to systems that suffer from typical practical issues. Yet, some of these extensions only provide unsatisfactory solutions for industrial control challenges in terms of performance. Input saturation of the plant is a common challenge which always plays a very important role when controlling technical systems with high-performance requirements.

In this work, a new method for adaptive control of plants with input saturation is presented. The new anti-windup scheme can be shown to result in bounded closed-loop states under certain conditions on the plant and the initial closed-loop states. As an improvement in comparison to existing methods in adaptive control, a new degree of freedom is introduced in the control scheme. It allows to improve the closed-loop response when actually encountering input saturation without changing the closed-loop performance for unconstrained inputs. Besides the step-by-step introduction of the new adaptive anti-windup scheme for state-feedback as well as for output-feedback, a mathematical analysis of its properties is given and simulation examples are shown in order to present the capabilities of the method to improve the closed-loop performance. Furthermore, numerous remarks and guidelines are stated and verified by simulations in order to reduce the initial effort for the application of the introduced method.

Finally, the new method is applied to a helicopter benchmark experiment and the position control of an electronic throttle plate. The results of these experiments confirm the simulation results and demonstrate the capabilities of the introduced method as well as its applicability to real-world plants. In addition, the experimental results point out the general benefits of adaptive control algorithms for the control of uncertain plants and for the automatic tuning of controller parameters.

ADAPTIVE CONTROL, SELF TUNING, AUTOMATIC TUNING, INPUT SATURATION, INPUT CONSTRAINTS

## Zusammenfassung

Das grundlegende Konzept der adaptiven Regelung entstammt einer intuitiven und vielversprechenden Idee für die Regelung von Strecken mit unsicheren oder veränderlichen Parametern. Anstatt einen Regler robust gegen Parameterunsicherheiten auszulegen, werden die Regler- oder Streckenparameter während des Betriebs identifiziert. Der Regler passt sich somit stetig an sich ändernde Bedingungen an, um permanent eine vorher definierte Regelgüte des geschlossenen Regelkreises zu erreichen.

Nach der ersten Vorstellung adaptiver Regleralgorithmen wurden diese in den 1960er Jahren vielfach in der Forschung zur Flugregelung untersucht. Unerwartete Schwierigkeiten und fehlende Robustheit der angewendeten Algorithmen führten jedoch dazu, dass sich adaptive Verfahren nicht in industriellen Anwendungen etablierten. Noch immer ist die adaptive Regelung in der Industrie nur selten zu finden, was nicht zuletzt auf den hohen Aufwand bei dessen Anwendung zurückzuführen ist. Dieser resultiert unter anderem aus den Erweiterungen der Standardalgorithmen, die bei der Anwendung in realen Systemen notwendig werden und eine gute Systemkenntnis der Regelstrecke voraussetzen. Zudem stellen einige dieser Erweiterungen nur unzureichende Lösungen für übliche industrielle Herausforderungen im Hinblick auf die Regelgüte dar. Eine Stellgrößenbegrenzung der Regelstrecke ist eine häufig auftretende Herausforderung, die Erweiterungen der Algorithmen benötigt und bei allen technischen Systemen mit hohen Anforderungen an die Regelung eine wichtige Rolle spielt.

Diese Arbeit präsentiert eine neue Methode für die adaptive Regelung von Strecken mit Stellgrößenbegrenzung. Für das neue anti-windup Verfahren wird gezeigt, dass die Zustände des geschlossenen Regelkreises begrenzt bleiben, wenn dessen initiale Werte und die Regelstrecke bestimmte Bedingungen erfüllen. Eine Verbesserung im Vergleich zu existierenden Methoden wird durch die Einführung eines zusätzlichen Freiheitsgrades erzielt. Dieser erlaubt die Verbesserung der Regelgüte des geschlossenen Regelkreises wenn das Eingangssignal sich in der Limitierung befindet, ohne die Regelgüte bei einem unbeschränkten Eingangssignal zu verändern. Neben einer Schritt für Schritt Einführung des neuen adaptiven anti-windup Verfahrens für Zustandsrückführung als auch für Ausgangsrückführung und einer mathematischen Analyse von dessen Eigenschaften, wird die verbesserte erreichbare Regelgüte anhand von Simulationsbeispielen gezeigt. Um den Aufwand für die initiale Anwendung der neuen Methode zu senken, sind zudem zahlreiche Hinweise und Richtlinien für dessen Verwendung genannt, die an Simulationsbeispielen verifiziert werden.

Zum Abschluss wird die neue Methode auf ein Helikopter Benchmark Experiment und auf die Positionsregelung einer elektronischen Drosselklappe angewendet. Die Ergebnisse der Experimente bestätigen die Simulationsergebnisse und zeigen die Vorteile und den Nutzen der neuen Methode sowie ihre Anwendbarkeit auf reale Strecken. Weiterhin heben die Ergebnisse die grundsätzlichen Vorteile und den Nutzen adaptiver Regelalgorithmen für Systeme mit unsicheren Parametern sowie für die automatische Reglereinstellung hervor.



# Contents

|   |           |
|---|-----------|
| <b>Nomenclature</b>   | <b>v</b>  |
| <b>1 Introduction</b>   | <b>1</b>  |
| <b>2 Presentation of Selected Adaptive Control Methods</b>                        | <b>7</b>  |
| 2.1 Basic Concepts of Adaptive Control . . . . .                                  | 7         |
| 2.2 Selected Adaptive Control Methods . . . . .                                   | 10        |
| 2.2.1 Model Reference Adaptive Control for State-Feedback . . . . .               | 11        |
| 2.2.2 Model Reference Adaptive Control for Output-Feedback . . . . .              | 18        |
| 2.2.3 Indirect Adaptive Pole Placement Control for Output-Feedback . . . . .      | 25        |
| 2.2.4 Closed-Loop Reference Model (CRM) . . . . .                                 | 34        |
| 2.2.5 Robustness of Adaptive Control . . . . .                                    | 37        |
| <b>3 Adaptive Systems with Input Saturation</b>                                   | <b>41</b> |
| 3.1 Effects of Input Saturation on Adaptive Systems . . . . .                     | 42        |
| 3.2 Model Recovery Anti-Windup (MRAW) . . . . .                                   | 46        |
| 3.3 Existing Adaptive Control Methods for Systems with Input Saturation . . . . . | 49        |
| 3.4 Anti-Windup by Kárason and Annaswamy (KAAW) . . . . .                         | 51        |
| 3.5 Conclusion . . . . .  | 54        |
| <b>4 Adaptive Model Recovery Anti-Windup: Derivation</b>                          | <b>55</b> |
| 4.1 Direct Adaptive Model Recovery Anti-Windup for State-Feedback . . . . .       | 56        |
| 4.2 Direct Adaptive Model Recovery Anti-Windup for Output-Feedback . . . . .      | 64        |
| 4.3 Indirect Adaptive Model Recovery Anti-Windup for Output-Feedback . . . . .    | 72        |
| <b>5 Adaptive Model Recovery Anti-Windup: Remarks and Simulations</b>             | <b>77</b> |
| 5.1 Direct Adaptive Model Recovery Anti-Windup for State-Feedback . . . . .       | 77        |

|          |   |            |
|----------|---|------------|
| 5.1.1    | Remarks . . . . .   | 78         |
| 5.1.2    | Simulations . . . . .   | 81         |
| 5.2      | Direct Adaptive Model Recovery Anti-Windup for Output-Feedback . . . .                  | 92         |
| 5.2.1    | Remarks . . . . .   | 92         |
| 5.2.2    | Simulations . . . . .   | 93         |
| 5.3      | Indirect Adaptive Model Recovery Anti-Windup for Output-Feedback . . .                  | 95         |
| 5.3.1    | Simulations . . . . .   | 96         |
| <b>6</b> | <b>Experimental Results</b>   | <b>103</b> |
| 6.1      | Helicopter Benchmark Experiment . . . . .   | 103        |
| 6.1.1    | Experimental Setup and Plant Description . . . . .                                      | 103        |
| 6.1.2    | Closed-Loop Stability for Frequent Saturation of the Input . . . . .                    | 106        |
| 6.1.3    | Performance Adjustments and Parameter Adaptation . . . . .                              | 108        |
| 6.1.4    | Adaptation to Changing Plant Parameters . . . . .                                       | 109        |
| 6.2      | Electronic Throttle Plate . . . . .   | 112        |
| 6.2.1    | Experimental Setup and Plant Description . . . . .                                      | 113        |
| 6.2.2    | Application and Results . . . . .   | 116        |
| <b>7</b> | <b>Summary and Future Work</b>  | <b>121</b> |
| <b>A</b> | <b>Definitions, Theorems and Lemma regarding Stability Analysis of Adaptive Systems</b> | <b>123</b> |
| A.1      | Lyapunov Stability . . . . .  | 123        |
| A.2      | Barbalat's Lemma . . . . .  | 125        |
| A.3      | Meyer-Kalman-Yakubovich (MKY) Lemma . . . . .   | 125        |
| A.4      | Properties of Least-Squares Estimation with Covariance Resetting . . . . .              | 126        |
| <b>B</b> | <b>Proofs</b>   | <b>127</b> |
| B.1      | Second Part of Proof of Theorem 4.1 . . . . .   | 127        |
| B.2      | Proof of Theorem 4.2 . . . . .  | 132        |
| B.3      | Second Part of Proof of Theorem 4.3 . . . . .   | 137        |
| <b>C</b> | <b>Examples: Additional Results</b>   | <b>143</b> |

# Nomenclature

In the following list, several symbols and abbreviations are described that are frequently used throughout this work. Symbols that are used only locally or that have special contextual meanings are not listed here. However, all symbols in this work are properly explained when introduced.

Since this work deals with adaptive control algorithms, estimated parameters are used frequently. Their denotation differs for parameters of the plant and parameters of the control algorithms. The vector of real parameters of the plant model is usually denoted by  $\theta_p$  and its estimation by  $\hat{\theta}_p$ . In difference, the estimated controller parameters  $\theta_c$  are not highlighted by additional symbols. Instead, the ideal values of the controller parameter vector  $\theta_c^*$ , which lead to the desired closed-loop behavior for a given plant, are marked with the star as subscript. In cases where confusion between the estimations and the real or ideal parameters could easily occur, the time dependence of the estimated parameters is explicitly stated. The estimation errors  $\hat{\theta}_p(t) - \theta_p$  and  $\theta_c(t) - \theta_c^*$  are denoted by a tilde, i.e.  $\tilde{\theta}_p = \hat{\theta}_p(t) - \theta_p$  and  $\tilde{\theta}_c = \theta_c(t) - \theta_c^*$ , respectively.

Single entries of a vector, e.g.  $\theta$ , are denoted by  $\theta_1, \theta_2, \dots$  and so on. If a vector is denoted with an additional subscript, e.g.  $\theta_p$ , the numbering of its entries is separated by a comma:  $\theta_{p,1}, \theta_{p,2}, \dots$  and so on. Hence,  $\theta_{p1}$  does not denote an entry of the vector  $\theta_p$ . Similar to the vector, the coefficients of polynomials, e.g.  $Z(s)$ , are denoted as  $Z(s) = s^n + z_{n-1} s^{n-1} + \dots + z_1 s + z_0$ . Note that small letters are used for the coefficients of polynomials.

## Abbreviations

|       |                                      |
|-------|--------------------------------------|
| AMRAW | Adaptive model recovery anti-windup  |
| APPC  | Adaptive pole placement control      |
| CRM   | Closed-loop reference model          |
| KAAW  | Anti-windup by Káráson and Annaswamy |
| MIMO  | Multiple inputs multiple outputs     |
| MRAC  | Model reference adaptive control     |
| MRAW  | Model recovery anti-windup           |

PE Persistent excitation / persistently exciting

SISO Single input single output

### List of frequently used symbols

$\Delta u$  Effect of saturation represented as an input disturbance

$\lambda$  Input gain of a plant

$\mathcal{S}$  Set of feasible plant parameters

$\phi_p$  Vector of signals of the estimated plant model

$\theta$  Vector of parameters of the control law in output-feedback MRAC

$\theta_{aw}$  Vector of parameters of the anti-windup controller for output-feedback AMRAW

$\theta_{nl}$  Vector of parameters of the matched uncertainty  $\theta_{nl}^T f_{nl}(\cdot)$

$\theta_p$  Vector of parameters of a plant

$A_{awr}$  Desired anti-windup dynamics

$A_d$  Desired closed-loop denominator for indirect APPC

$A_p$  System matrix of a plant

$A_{ref}$  System matrix of the reference model

$B_p$  Input matrix of a plant

$B_{ref}$  Input matrix of the reference model

$c$  Reference gain for output-feedback MRAC

$C_p$  Output matrix of a plant

$C_{ref}$  Output matrix of the reference model

$D \triangleq \frac{d}{dt}$  Differential operator

$e$  Tracking error of the state

$e_2$  Auxiliary error for output-feedback MRAC

$e_y$  Tracking error of the output

$f_{nl}(\cdot)$  Vector of arbitrary known nonlinear functions depending on the plant state or the plant output

$I_{n \times n}$  Identity matrix of order  $n$

---

|                    |   |
|--------------------|---|
| $k_{\Delta}$       | Estimated parameter such that $B_{\text{ref}} k_{\Delta}^* = B_p \lambda$ |
| $K_{\text{aw}}$    | Gain on state of the anti-windup controller for state-feedback AM-RAW     |
| $k_a$              | Auxiliary state as estimation for $\frac{1}{c}$ for output-feedback MRAC  |
| $k_p$              | High frequency gain of a plant  |
| $k_r$              | Reference gain for state-feedback MRAC                                    |
| $K_x$              | State gain for state-feedback MRAC  |
| $L_{\text{ref}}$   | Gain of the closed-loop reference model                                   |
| $M(D), P(D), L(D)$ | Controller polynomials of indirect APPC                                   |
| $n$                | Degree of nominator polynomial of a plant                                 |
| $n$                | Order of a plant  |
| $n^*$              | Relative degree of a plant  |
| $P$                | Solution of Lyapunov equation   |
| $P_{\text{ls}}$    | Covariance matrix of least-squares algorithm                              |
| $Q(D)$             | Internal model of the reference signal                                    |
| $r$                | Reference signal for the closed-loop system                               |
| $R_p$              | Denominator polynomial of a plant   |
| $u$                | Input of a plant and output of a controller                               |
| $u_{\text{aw}}$    | Output of the anti-windup controller                                      |
| $u_{\text{lim}}$   | Saturated plant input   |
| $V$                | Lyapunov function (candidate)   |
| $w_1, w_2$         | States of the the control law for output-feedback MRAC                    |
| $x$                | State of a system specified by an additional subscript                    |
| $x_{\text{aw}}$    | State of the anti-windup scheme   |
| $y$                | Output of a system, specified by an additional subscript                  |
| $y_{\text{aw}}$    | Output of the anti-windup plant model                                     |
| $Z_p$              | Numerator polynomial of a plant   |

**Subscripts**

|     |                    |
|-----|--------------------|
| aw  | Anti-Windup Scheme |
| p   | Plant              |
| ref | Reference Model    |

# Chapter 1

## Introduction

The degree of automation in industrial systems as well as in technical consumer goods is increasing quickly [79, 80]. Since automation always involves automatic control, this trend comes along with an increasing demand for solutions to control engineering tasks. Not only the quantity of these tasks is growing but also their diversity. For example in automotive industries the automatic position control of the electronic throttle plate is a long known control task [35, 127], which still affects all modern gasoline engines and has been approached with many different control algorithms (see e.g. [16, 27, 128, 137]). Recent challenges for automotive control engineers are given e.g. by the control of electric valve timing systems, parking control algorithms, and the control of autonomous driving vehicles, which require different and partially novel control approaches [65, 97, 135].

In order to handle the increasing demand for solutions to control tasks, the applied control algorithms have to work reliably with a desired performance and need to be applicable with a reasonable effort. In the context of industrial control, e.g. in automotive industry, the notions of performance, reliability, and effort should be understood as follows:

**Performance** Performance requirements in industry are usually stated in time-domain and make demands on the rise-time, the settling-time and maximal overshoots for desired setpoint changes of the plant output. Furthermore, the offset during constant setpoints needs to be as small as possible. A good performance can therefore be achieved if set point changes can be accomplished as quickly as possible, with reasonable small overshoots, and zero steady-state offsets [81, 142, 146].

**Reliability** A controlled system works reliable<sup>1</sup> if it works for its whole lifetime with the desired performance. Therefore, the applied controller has to be able to handle a changing behavior of the system, which might arise due to aging, changing environments, and small defects. Moreover, the control algorithm has to work for several instances of the same system, which potentially differ due to e.g. poor production quality or production tolerances.

---

<sup>1</sup>Note that this property is often called robustness in control theory. However, the notion of robustness will be used in a different context in this work.

**Effort** A control algorithm for practical problems should be applicable with a reasonable effort. This requires that it is straight forward to understand and that it can deal with common practical control challenges. The effort further decreases if the tuning of the controller can be done in an intuitive way and without the expert knowledge of a control engineer. In addition, a reasonable application effort involves the feasibility of the implementation of the control algorithm on an electronic control unit, that is common for the particular system.

When addressing the requirements of performance and reliability, methods from the field of adaptive control are highly appealing. The basic idea of adaptive control algorithms is to include a self-adjusting mechanism into the controller. This mechanism is intended to adapt the controller to uncertain or even changing conditions in order to achieve a constant closed-loop performance. Loosely speaking, adaptive controllers adjust themselves such that a desired performance can be achieved for an uncertain or even changing behavior of the controlled system. This is done by using the plant feedback not only to compute the controlled input like in constant controllers such as PID-controllers or controllers from the field of robust control but also utilize to the information in the feedback as a basis for a parameter adaptation of the control algorithms. This makes such algorithms especially useful for

**Control of Systems with Uncertain Parameters** Adaptive control methods permanently adjust the controller parameters for the purpose of achieving a desired closed-loop performance even if the plant parameters are uncertain. Hence, their reliability is imposed by the adjustment of the controller as a reaction to an uncertain or changing plant behavior. Traditionally, the application to flight control, as e.g. in [94, 134, 162], is the main application example for adaptive control. Additional applications can be found e.g. for robotics and automotive plants [23, 103, 131].

**Automatic Tuning** Automatic tuning applications use adaptive methods to tune controller parameters in limited time periods. That means the controller parameters are held constant as long as the closed-loop performance meets its requirements. Once the system behavior becomes unacceptable, the adaptive algorithm is started to update the controller parameters automatically. Examples of automatic tuning methods, which are highly relevant for industrial use, can be found e.g. in [14, 129, 169].

Despite their very attracting idea, numerous application possibilities, and the fact that first adaptive controllers have already been introduced more than 60 years ago, such methods are rarely used in industries [17]. Considering the potential benefits of adaptive control, this lack of application is unexpected. However, applying adaptive control algorithms to real-world systems involves high effort due to their complexity and due to necessary extensions regarding practical issues [31]. For example, neglected system dynamics in the plant model, external disturbances, and measurement noise require special extensions of basic adaptive control methods in order to guarantee closed-loop stability [60, 112, 136]. Evaluation of the right situation and the right way to use such extensions



requires extensive system knowledge in the first place [31]. Moreover, it also involves the knowledge about the properties of the basic adaptive methods, about the properties of its possible extensions, and about the way in which these extensions affect the controlled system.

An issue that always needs to be considered when controlling real technical plants is an input saturation, i.e. a limited amplitude of the plant input. Since the input of any technical system is limited, this issue is highly relevant for control applications in industrial systems. An input saturation becomes even more problematic in adaptively controlled systems compared to closed-loop systems with a constant controller due to the additional parameter adjustments. Especially with high-performance requirements regarding the settling time, the controlled input will encounter its limits frequently so that the input saturation needs to be treated with care in the control design. As a first effect of input saturation, the reduced available input amplitude might degrade the closed-loop performance. Hence, performance requirements that are feasible for unsaturated systems might not be realizable anymore if saturation is encountered. Secondly, the reduced input amplitude might lead to situations, where an open-loop unstable system can not be stabilized anymore. The presence of input saturation, therefore, requires the examination of closed-loop stability as well as its performance and reliability. These aspects are treated in this work for adaptive systems by introducing a new adaptive anti-windup scheme.

## Main Contribution

The introduction of adaptive control in the 1950s came with some interesting, promising and appealing ideas. However, since that time a lot of theoretical and practical research on the topic of adaptive systems has been necessary. This research mainly regarded the stability and the robustness of adaptive systems in the presence of issues that might arise in real-world applications. The results of this research allow a safe application of modern adaptive control algorithms in real-world systems. Some of these results are presented in Chapter 2 and Chapter 3 of this work.

Input saturation is one of the challenges a control engineer has to deal with when considering real technical systems. For adaptive systems, the issue of input saturation becomes even more challenging due to the parameter adjustments of the controller. Some of the aforementioned theoretical and practical research has already been dealing with several different approaches for input saturated adaptive systems, which are shortly summarized in Chapter 3. However, these approaches mostly only aim to preserve or establish stability of the closed-loop system. The closed-loop performance, which is very important for industrial applications, has so far not been examined for existing adaptive methods regarding input saturation. This is where the main contribution of this work begins.

This work deals with the development of a new adaptive anti-windup method that allows for performance considerations in adaptively controlled systems. The construction of the new method is based on standard adaptive control algorithms. Therefore, many of the properties and practical considerations of the standard methods do also apply for the new method presented in this work. The derivation of the new anti-windup scheme in Chapter

4 is explicitly done by a combination of two existing anti-windup concepts. Since one of these concepts originally stems from control theory for plants with known parameters, it is brought into a form suitable for the adaptive framework. This form has first been presented by the author of this work. The derivation of the new method is completed by the choice of a suitable control law and, equally important, by the development of suitable parameter estimation schemes. For the resulting closed-loop systems stability results are established by rigorous analysis of the closed-loop equations, wherever such results have been possible to establish for the author. These are verified and augmented by results from simulation examples.

The new method is based on an extension of the basic adaptive control algorithms, and hence leads to a higher effort when it comes to the application of the resulting control scheme. Since the application effort has been mentioned as an important point for the applicability of control methods in industrial systems, the second part of the contribution of this work deals with the reduction of the application effort. For this purpose, remarks about the newly introduced adaptive anti-windup scheme are given in Chapter 5. Some of the remarks comment on the stability of the closed-loop and give hints for the implementation of the method. However, the majority of the remarks are meant to give the control engineer an interpretation of how the new methods work and how their tuning parameters can be chosen to achieve an improved closed-loop behavior when actually encountering input saturation.

As the last part of the contribution of this work, simulations and real-world experiments have been carried out with the new adaptive anti-windup methods. The results of the simulations and the experiments do not only verify the effectiveness of the newly developed methods, but they also illustrate the benefits of adaptive control even in the presence of input saturation. Moreover, the presentation of the simulations and experiments is meant to further facilitate the transfer of the presented methods from theory to practical usage.

## Chapter Outline

**Chapter 2** serves as an introduction to adaptive control. Firstly, the basic concepts of adaptive control are introduced and some references to the most familiar realizations of these concepts are presented without mathematical derivations. Moreover, some references to topics of active research on adaptive control are given. Subsequently, the methods of model reference adaptive control (MRAC) for state-feedback and for output-feedback as well as the method of adaptive pole placement control (APPC) are presented as explicit realizations of the adaptive control concept. In order to reduce the application effort of these methods for the reader, all the necessary equations are summed up and issues that might arise during implementation are discussed in several remarks. Furthermore, some properties of the aforementioned adaptive control schemes are illustrated by simulation examples. Finally, some extensions are introduced which address practical issues of adaptive control aside from input saturation. All presented methods in this chapter are adopted from the literature and form the basis for the derivations in the following chapters.

**Chapter 3** focuses on the issues that arise if the input amplitude in adaptive systems saturates. Based on several simulations, different effects of a limited input amplitude on the closed-loop system are illustrated and explained. As a first basis for the derivation of a new adaptive anti-windup scheme, the idea of the model-based method of model recovery anti-windup (MRAW) is presented for systems with known parameters. The transition to plants with uncertain parameters is given afterwards by an overview of existing adaptive control methods for input saturated plants from the literature. Finally, the method from [75] is presented in detail, since besides the basic adaptive control methods from Chapter 2 and MRAW it forms the third basis for the derivations in the subsequent chapter.

In **Chapter 4** the main contribution of this work is presented. Based on the methods introduced in Chapter 2 and in Chapter 3, a new adaptive anti-windup scheme is derived. The derivations are done in several consecutive steps, which introduce the different concepts of the new scheme separately. For the anti-windup schemes based on MRAC a rigorous stability analysis is carried out, which verifies boundedness of the closed-loop signals under certain conditions on its initial states. Additionally, for scalar plants a performance result is derived, which allows for a systematic tuning of the anti-windup scheme, such that the influence of the saturation in the closed-loop is reduced. Parts of the results of Chapter 4 have already been published by the author in [152–154].

In **Chapter 5** the results from the previous chapter are examined from an engineering point of view. Questions and issues that might arise when considering the application of the newly introduced methods are discussed in several remarks. These remarks are partially based on the examination of the mathematical results of Chapter 4. Other parts of the remarks are based on simulation examples, whose results are shown subsequently to the remarks. The simulation results do not only verify stability of the proposed adaptive control schemes, but also show their capability of influencing the closed-loop performance during saturation of the input.

In **Chapter 6** the new adaptive anti-windup scheme is applied to real-world experimental applications. State-feedback model reference adaptive control together with the new anti-windup scheme is applied to a helicopter benchmark experiment. Several results are shown, which further verify the results of Chapter 4 and 5. Moreover, the experiments illustrate the benefits of adaptive control for plants with uncertain or changing parameters even in the presence of a saturation on the input amplitude. In the second part of chapter 6 the method of adaptive pole placement control with the new anti-windup scheme is applied to an electronic throttle plate, which is a typical plant in automotive industries. The presented results show that the new method allows for a fast automatic tuning without the need of a special excitation of the system and without the need to avoid saturation of the input amplitude.

In **Chapter 7** a concluding summary and an outline of future work is given.



# Chapter 2

## Presentation of Selected Adaptive Control Methods

It has often been tried in the literature to uniformly define the field of adaptive control (see e.g. [11, 13, 116]). The fact that none of the proposed definitions has established itself shows that it is very difficult to express all aspects of adaptive control in a single definition. Instead of making another attempt to define adaptive control in this work, a short overview of some of its basic concepts is given in Section 2.1. Selected methods of adaptive control, that serve as a basis for subsequent examinations in this work, are described in more detail afterwards in Section 2.2.

### 2.1 Basic Concepts of Adaptive Control

In order to present some basic concepts of adaptive control, the general plant representation

$$\begin{aligned}\dot{x}_p(t) &= f_p(x_p(t), u_c(t), \theta_p), \\ y_p(t) &= g_p(x_p(t), u_c(t), \theta_p),\end{aligned}\tag{2.1}$$

is considered, where the dynamic of the plant state  $\dot{x}_p$  is a function of a controlled input  $u_c$ , the plant state  $x_p$ , and the uncertain plant parameters  $\theta_p$ . Also the measurable plant output  $y_p$  is a function of the aforementioned variables. Note that no time dependence is stated for the plant parameters, since they are usually supposed to be constant or quasi-stationary for adaptive control. A general assumption for adaptive control can be stated similar to [87] as follows: There exists a controller with a known structure

$$\begin{aligned}\dot{x}_{ctr}(t) &= f_c(x_{ctr}(t), y_p(t), r(t), \theta_c(t)), \\ u_c(t) &= g_c(x_{ctr}(t), y_p(t), r(t), \theta_c(t)),\end{aligned}\tag{2.2}$$

where  $x_{ctr}(t)$  and  $\theta_c(t)$  are the controller state and the controller parameters, respectively, that can achieve the desired closed-loop behavior for any value of the plant parameters  $\theta_p$ . After defining a controller structure, which is equivalent to an explicit definition of  $f_c$  and  $g_c$  in (2.2), it remains to find a suitable way to adapt the controller parameters  $\theta_c(t)$

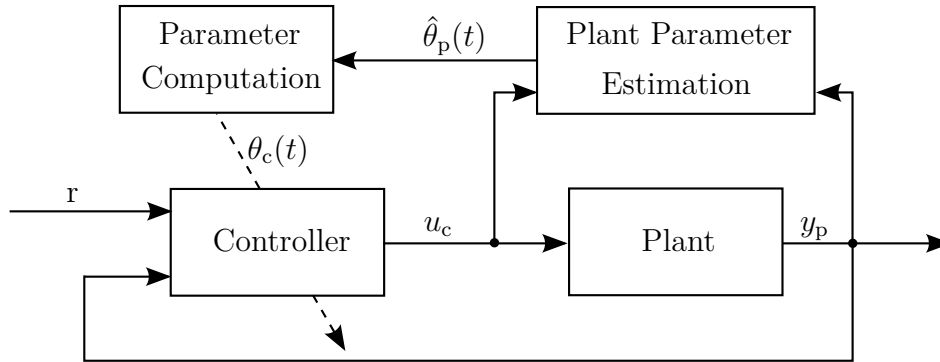


Figure 2.1: Indirect adaptive control scheme.

such that the desired closed-loop behavior will be achieved. Hence, the way the controller is updated differentiates the several adaptive control methods. Common approaches are shortly presented below.

The indirect methods represent the probably most intuitive approach for adaptive control. According to [13, 116, 140] it has been firstly presented by Kalman in 1958. Indirect adaptive controllers combine a control law with a recursive parameter estimation scheme for the plant. The controller parameters can, therefore, be computed during operation based on the estimated plant parameters [13, 60, 87]. Hence, the desired closed-loop behavior is implicitly incorporated in the computation methods for  $\theta_c$ . This approach is often referred to as certainty equivalence principle because the estimated plant parameters are used as if they were known to be the true plant parameters. The indirect approach basically allows combining arbitrary controller structures with arbitrary recursive parameter estimation schemes, as long as a computation of the controller parameters is feasible during operation. However, closed-loop stability has so far only been guaranteed for certain combinations of controller structures and estimation schemes, which are presented e.g. in [24, 34, 56, 83]. A schematic illustration of indirect adaptive control is shown in Figure 2.1, where  $\hat{\theta}_p(t)$  denotes the estimation of the plant parameters  $\theta_p$ . In Section 2.2.3 an indirect adaptive controller is presented in more detail.

Another concept of adaptive control is given by the direct adaptive control methods, which are based on direct estimations of the controller parameters and often require the desired closed-loop performance to be specified in form of a reference model. The idea of a reference model has first been introduced in [161] and became popular in flight control in the 1960s [60, 116, 147]. However, the flight accident in 1967 [33] showed that stability and robustness of adaptive control have not been well understood at that time. Modern model reference adaptive control (MRAC) is based on rigorous stability analysis, which yields stable parameter estimation laws and a stable closed-loop system. In addition, the issue of robustness in adaptive control can be addressed with several extensions of the basic methods. Some important results on stability and robustness of MRAC can be found in [106, 108, 113, 114, 116] and [58, 60, 112], respectively. Moreover, recent results regarding performance and stability show that MRAC is still a topic of active research [7, 43, 44, 53, 54, 90, 148]. For discrete-time systems the implicit self-tuning regulator [12] gained a lot of interest and is closely related to MRAC [13, 88]. Nonlinear

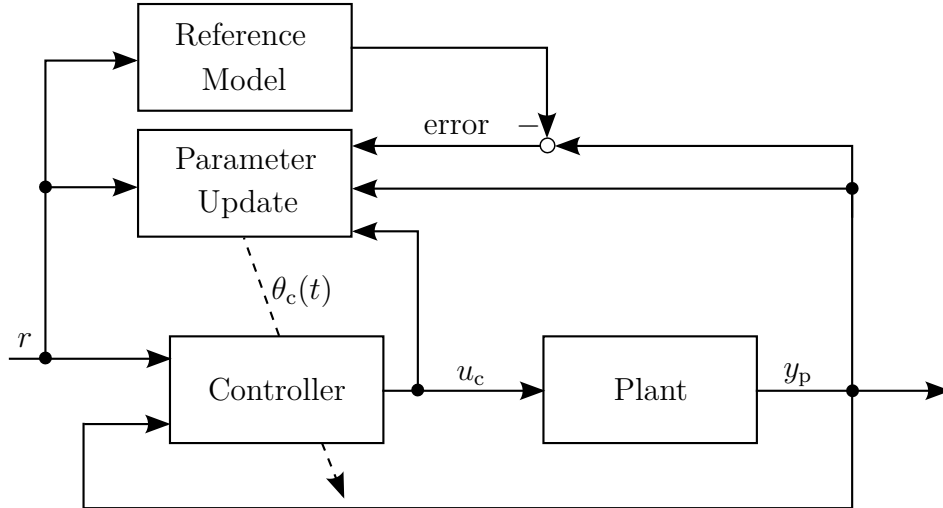


Figure 2.2: Direct adaptive control scheme: MRAC.

direct adaptive control methods are often based on adaptive backstepping or on adaptive feedback linearization as e.g. in [82, 85, 139]. A schematic illustration of model reference adaptive control is shown in Figure 2.2. MRAC schemes for state-feedback and output-feedback will be presented in more detail in Section 2.2.1 and 2.2.2, respectively.

Since the first introduction of the aforementioned ideas, different approaches have been developed in the framework of adaptive control. Some of them are based on the indirect and direct adaptive control methods and some of them have introduced new concepts. The method of composite model reference adaptive control combines indirect and direct adaptive control [30, 91, 144]. It has been demonstrated without a formal proof, that this method leads to improved transient performance. Note that in the framework of adaptive control, transient performance means the closed-loop behavior during parameter adaptation. Instead of updating the parameters of a controller, the controlled input is directly adjusted by the methods of iterative learning control, repetitive control, and run to run control based on a desired closed-loop trajectory [10, 138, 141]. However, these methods usually require the desired trajectories of a process to be repeated periodically. Other approaches have combined switching and adaptive control [102, 109–111]. Their idea is based on multiple models

$$\begin{aligned}\dot{\hat{x}}_{\text{pi}}(t) &= f_{\text{p}}(\hat{x}_{\text{pi}}(t), u_{\text{c}}(t), \hat{\theta}_{\text{pi}}), \\ \hat{y}_{\text{pi}}(t) &= g_{\text{p}}(\hat{x}_{\text{pi}}(t), u_{\text{c}}(t), \hat{\theta}_{\text{pi}}),\end{aligned}$$

of the plant, where each model is based on a different estimation  $\hat{\theta}_{\text{pi}}$  of the plant parameters  $\theta_{\text{p}}$ . Therefore, this model is referred to as multiple model adaptive control. The model parameters  $\theta_{\text{pi}}$  are distributed in the admissible set of the plant parameters  $\hat{\theta}_{\text{p}}$  and for each of the models a robust controller

$$\begin{aligned}\dot{x}_{\text{ctri}}(t) &= f_{\text{c}}(x_{\text{ctri}}(t), y_{\text{p}}(t), r(t), \theta_{\text{ci}}), \\ u_{\text{ci}}(t) &= g_{\text{c}}(x_{\text{ctri}}(t), y_{\text{p}}(t), r(t), \theta_{\text{ci}}),\end{aligned}$$

with constant plant parameters  $\theta_{ci}$  is designed that fulfills the performance specifications, if it is applied to the respective model. During operation, all of the model states are updated so that for each model an error  $e_i = y_{pi} - y_p$  can be computed permanently. Based on this error a so-called supervisor decides which model is the best representation of the real process. The respective controller is then used to close the loop. Research about extensions of this method led to mixing of different control signals [86], a combination of multiple model adaptive control with direct or indirect adaptive control, and the use of multiple models to improve parameter estimation [117, 118]. An overview of multiple model adaptive control can be found in [50].

The effort of applying multiple model adaptive control is quite high, in the sense that it requires high implementation costs as well as high computational costs. The methods of iterative learning control, repetitive control, and run to run control require a process with repeated desired trajectories, which strongly restricts its applications to special plants. For the above-mentioned reasons, the recent advances in MRAC, and its wide applicability, the method of model reference adaptive control is further examined in this work. In addition, an indirect method is part of the following examinations because it represents an easily applicable and understandable adaptive control method. Moreover, indirect methods are well suited for automatic tuning applications. Note that for the sake of simplicity, time dependencies of signals and variables are only stated in this work, where omitting them could lead to confusion.

## 2.2 Selected Adaptive Control Methods

In the following Sections 2.2.1-2.2.3, the basic methods of MRAC for state-feedback, MRAC for output-feedback and adaptive pole placement control (APPC) are presented. Direct versions of MRAC are introduced, while the presented APPC scheme is an indirect adaptive control scheme. In order to unify the presentation, the aforementioned control schemes are introduced in five steps. After a short summary of the control scheme, an explicit structure for the plant (2.1) is defined in the first step and it is shown how the desired performance of the closed-loop system can be specified. In the second step, it is assumed that all plant parameters are known. Based on this assumption the parameters of an explicit constant control law are specified, such that the desired closed-loop properties are achieved. The constant control law serves as the basis to present an adaptive control scheme in the third step, where the parameter update laws for an adaptive version of the control law are presented. In a fourth step a summary of the respective adaptive control method is given, that allows a quick comparison of the different schemes. In addition, some questions and issues, that might arise during implementation, are discussed in several remarks. Finally, simulation examples are shown in the fifth step, in order to point out some characteristics of the control schemes.

After the introduction of the basic adaptive control methods, extensions of them are presented in Sections 2.2.4 and 2.2.5, which address the transient performance and robustness of adaptive systems. If adaptive control methods are applied to real technical processes,



considering the extensions for robustness is absolutely necessary in order to guarantee stability of the closed-loop system.

### 2.2.1 Model Reference Adaptive Control for State-Feedback

In this section, the direct method of model reference adaptive control for state-feedback plants is presented. In order to force the closed-loop system to follow a desired reference model, a basic control structure with a gain on each state of the plant, a gain on the reference signal, and a direct compensation of matched uncertainties are introduced. Since a direct version of MRAC is presented here, the parameters of the controller are estimated during operation. The corresponding update laws follow from a stability analysis of the adaptive closed-loop system. Direct MRAC for state-feedback can be found in slightly different versions in the literature [11, 56, 60, 116]. The following presentation is done in accordance with [94].

#### Plant Structure and Performance Specifications

The plant

$$G_{\text{nl}} : \quad \dot{x}_{\text{p}} = A_{\text{p}} x_{\text{p}} + B_{\text{p}} \lambda \left( u + \theta_{\text{nl}}^{\text{T}} f_{\text{nl}}(x_{\text{p}}) \right) \quad (2.3)$$

is considered, where  $A_{\text{p}} \in \mathbb{R}^{n \times n}$ ,  $\lambda > 0 \in \mathbb{R}$ , and  $\theta_{\text{nl}} \in \mathbb{R}^l$  are unknown but constant. The input vector  $B_{\text{p}} \in \mathbb{R}^n$  is known and the vector  $f_{\text{nl}}(x_{\text{p}}) \in \mathbb{R}^l$  contains known nonlinear functions, that depend on the system state and that are bounded for bounded  $x_{\text{p}}$ :

$$f_{\text{nl}}(x_{\text{p}}) = \left[ f_{\text{nl},1}(x_{\text{p}}) \quad f_{\text{nl},2}(x_{\text{p}}) \quad \dots \quad f_{\text{nl},l}(x_{\text{p}}) \right]^{\text{T}}.$$

Thus, the linear combination  $\theta_{\text{nl}}^{\text{T}} f_{\text{nl}}(x_{\text{p}})$  represents a matched uncertainty of the system. The aim of using MRAC, is to force the closed-loop system to follow a given reference model

$$G_{\text{ref}} : \quad \dot{x}_{\text{ref}} = A_{\text{ref}} x_{\text{ref}} + B_{\text{ref}} r, \quad (2.4)$$

where the stable matrix  $A_{\text{ref}} \in \mathbb{R}^{n \times n}$  and the input vector  $B_{\text{ref}} \in \mathbb{R}^n$  are design parameters. That means, the desired performance of the closed-loop system can be chosen in form of a linear time-invariant (LTI) system.

#### Control Law for known Plant Parameters

Perfect model following, i.e.  $x_{\text{ref}} \equiv x_{\text{p}}$ , can be achieved with the ideal control law

$$u^* = K_x^* x_{\text{p}} + k_r^* r - \theta_{\text{nl}}^{\text{T}} f_{\text{nl}}(x_{\text{p}}), \quad (2.5)$$

if the ideal controller parameters  $K_x^* \in \mathbb{R}^n$  and  $k_r^* \in \mathbb{R}$  satisfy the matching conditions

$$\begin{aligned} A_{\text{p}} + B_{\text{p}} \lambda K_x^* &= A_{\text{ref}}, \\ B_{\text{p}} \lambda k_r^* &= B_{\text{ref}}. \end{aligned} \quad (2.6)$$

Inserting (2.5) into (2.3) and using the matching conditions (2.6) directly yields the reference system  $G_{\text{ref}}$ . Thus, the desired closed-loop behavior can be achieved by a direct compensation of the matched uncertainty, proper gains on the states, and a proper gain on the reference signal.

### Adaptive Control Law for Unknown Plant Parameters

Since the calculation of the ideal control law (2.5) is only possible for known plant parameters, an adaptive version of it

$$u = K_x^T(t) x_p + k_r(t) r - \hat{\theta}_{\text{nl}}^T(t) f_{\text{nl}}(x_p), \quad (2.7)$$

with the estimated parameters  $K_x(t)$  and  $k_r(t)$ , and the estimation  $\hat{\theta}_{\text{nl}}(t)$  of  $\theta_{\text{nl}}$  is introduced. Note that the time dependency for the estimated parameters is explicitly stated here in order to clearly distinguish them from the ideal parameters. In order to guarantee stability of the closed-loop system and to satisfy the performance requirements, suitable estimation schemes for the controller parameters have to be derived. This can be done by a stability analysis of the tracking error  $e = x_p - x_{\text{ref}}$ .

In order to get rid of the unknown system matrix  $A_p$  in the equations of the closed-loop system, the term  $B_p \lambda (K_x^{*T} x_p + k_r^* r)$  is added and subtracted to the plant equation (2.3), which together with the matching conditions in (2.6) yields

$$\dot{x}_p = A_{\text{ref}} x_p + B_{\text{ref}} r + B_p \lambda \left( u - K_x^{*T} x_p - k_r^* r + \theta_{\text{nl}}^T f_{\text{nl}}(x_p) \right). \quad (2.8)$$

The dynamics of the tracking error can then be obtained by subtracting (2.4) from (2.8) and inserting the control law (2.7), which results in

$$\dot{e} = A_{\text{ref}} e + B_p \lambda \left( (K_x - K_x^*)^T x_p + (k_r - k_r^*) r - (\hat{\theta}_{\text{nl}} - \theta_{\text{nl}})^T f_{\text{nl}}(x_p) \right). \quad (2.9)$$

Introduction of the parameter estimation errors  $\tilde{K}_x = K_x(t) - K_x^*$ ,  $\tilde{k}_r = k_r(t) - k_r^*$ ,  $\tilde{\theta}_{\text{nl}}(t) = \hat{\theta}_{\text{nl}} - \theta_{\text{nl}}$ , and the Lyapunov-function candidate

$$V = e^T P e + \lambda \left( \tilde{K}_x^T \Gamma_x^{-1} \tilde{K}_x + \frac{1}{\gamma_r} \tilde{k}_r^2 + \tilde{\theta}_{\text{nl}}^T \Gamma_{\text{nl}}^{-1} \tilde{\theta}_{\text{nl}} \right), \quad (2.10)$$

allows a suitable choice of the update laws

$$\begin{aligned} \dot{\tilde{K}}_x &= \dot{K}_x = -\Gamma_x x_p e^T P B_p, \\ \dot{\tilde{k}}_r &= \dot{k}_r = -\gamma_r r e^T P B_p, \\ \dot{\tilde{\theta}}_{\text{nl}} &= \dot{\hat{\theta}}_{\text{nl}} = \Gamma_{\text{nl}} f_{\text{nl}}(x_p) e^T P B_p, \end{aligned} \quad (2.11)$$

which result in  $\dot{V} \leq 0$ . Based on this results the following theorem can be stated.

**Theorem 2.1.** *The control law (2.7) with a bounded reference signal  $r(t)$  together with the parameter update laws (2.11) applied to the system  $G_{nl}$  in (2.3) results in a closed-loop system, that guarantees global asymptotic stability of the tracking error:*

$$\lim_{t \rightarrow \infty} \|x_p(t) - x_{ref}(t)\| = 0.$$

Moreover, all signals of the closed-loop system are guaranteed to stay bounded.

*Proof.* A proof of the theorem can be found e.g. in [94] or for slightly different versions of MRAC in e.g. [60, 116].  $\square$

## Summary and Remarks

The complete control scheme is given by the control law in (2.7), the parameter update laws in (2.11), and the reference model  $G_{ref}$ . Designing a state-feedback MRAC requires the choice of several design parameters. At first, a stable system  $G_{ref}$  has to be defined, which satisfies the performance requirements of the closed-loop system. In addition, the state matrices  $A_{ref}$  and  $B_{ref}$  need to be chosen, such that the matching conditions (2.6) can be satisfied for known plant parameters. A comment on that is given in Remark 2.2. For the parameter update laws, the gains  $\Gamma_x$ ,  $\gamma_r$ , and  $\Gamma_{nl}$ , as well as the matrix  $Q$ , which determines  $P$ , needs to be defined. All of these parameters act as gains on the parameter updates. Consequently, the designer can choose  $Q$  arbitrarily but positive definite and tune the gains  $\Gamma_x$ ,  $\gamma_r$ , and  $\Gamma_{nl}$  as stated in Remark 2.4. An overview of the control scheme is given in Table 2.1. Some of the properties of MRAC are illustrated in Simulation Example 2.1.

**Remark 2.1.** The input vector  $B_p$  of  $G_{nl}$  has been assumed to be known and just an uncertainty of the input gain  $\lambda$  has been introduced. This is equivalent to the assumption of a known control direction, as it is also assumed for the MRAC scheme presented in [60]. A MRAC scheme that does not require this assumption is given in [116], but just guarantees local stability. Since the assumption of the known control direction is not restrictive for many technical systems, the MRAC scheme with the stronger stability result is considered in this work. Other approaches that deal with uncertain control directions can be found in [99, 120, 165]

**Remark 2.2.** The matching conditions (2.6) require the structure of  $A_p$  to be known. That means that the position of the uncertain parameters in the  $A_p$ -matrix is known, so that  $A_{ref}$  can be chosen such that an ideal gain  $K_x^*$  exists. This is equivalent to the basic assumption of an existing control structure, that can achieve the performance requirements. For many technical systems that is usually true. However, the matching conditions restrict the choice of the reference model. A MRAC method for output tracking with state-feedback that does not require a known structure of the system matrix is given e.g. in [147].

**Remark 2.3.** The controller parameters of the introduced MRAC scheme are not guaranteed to converge to the ideal values  $K_x^*$ ,  $k_r^*$  and  $\theta_{nl}$ . However, since the asymptotic

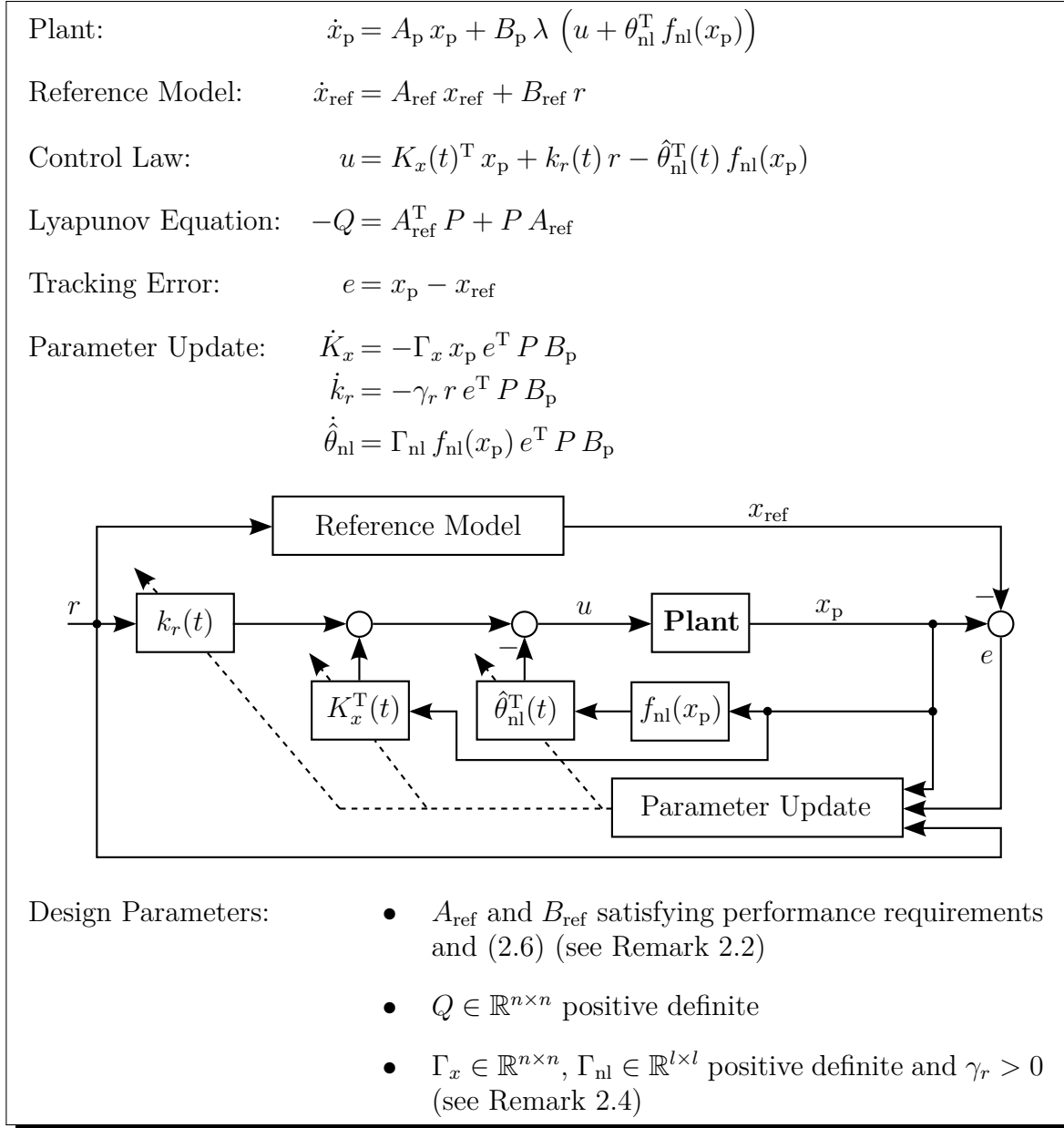


Table 2.1: Summary of state-feedback MRAC.

convergence of the tracking error  $e$  to zero is guaranteed, asymptotic convergence of the parameter errors  $\tilde{K}_x$ ,  $\tilde{k}_r$ , and  $\tilde{\theta}_{nl}$  is not required for the control task. If the estimation of the ideal controller parameters is part of the task, a sufficient excitation of the system is needed. For parameter estimation and adaptive systems, this involves the notion of persistent excitation (PE), which is discussed e.g. in [11, 115, 116]. In this context also the notion of dual control should be mentioned, which addresses the control problem and the parameter identification in parallel and with the same priority. Dual controllers start to excite the plant automatically with the controlled input if the uncertainty of the plant parameters becomes too large [11, 156, 164].

**Remark 2.4.** The positive definite gains  $\Gamma_x$ ,  $\Gamma_{nl}$  and  $\gamma_r$  in the Lyapunov function (2.10) introduce additional degrees of freedom for the parameter update laws (2.11). These gains can be used as tuning parameters to adjust the convergence speed of the estimations. However, there does not exist a systematic way to choose these gains. Typical choices are diagonal matrices with entries that are as high as possible to establish fast parameter estimation but still small enough to avoid high-frequency oscillations of the closed-loop system. Such oscillations occur in adaptive systems due to the influence of the parameter estimations on the controller input. In Section 2.2.4 an extension of the classical MRAC scheme is presented, which addresses the issue of oscillatory closed-loop behavior.

**Simulation Example 2.1.** A second order mechanical plant of the form

$$G_{\text{ex1}} : \quad \dot{x}_p = \begin{pmatrix} 0 & 1 \\ -\frac{k_1}{m} & -\frac{d_1}{m} \end{pmatrix} x_p + \begin{pmatrix} 0 \\ \frac{b}{m} \end{pmatrix} (F_{\text{in}} - F_k - F_r) \quad (2.12)$$

with measurable state  $x_p = [x_{p,1} \ x_{p,2}]^T$ , where  $x_{p,1}$  and  $x_{p,2}$  are the position and the velocity, respectively, is considered as an example. A schematic picture of the plant is shown in Figure 2.3. The parameters of  $G_{\text{ex1}}$  are given as follows. The mass, the linear

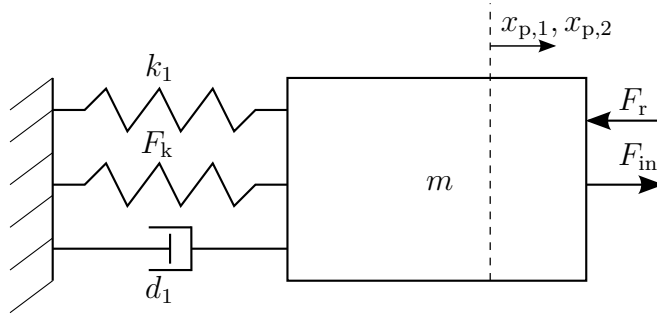


Figure 2.3: Schematic representation of  $G_{\text{ex1}}$ .

stiffness and the damping are given as  $m = 1$ ,  $k_1 = 15$  and  $d_1 = 1$ , respectively. The input gain for the external controlled force  $F_{\text{in}}$  takes the value  $b = 3.7$ . In addition, a nonlinear spring with the characteristic  $F_k = 3 \arctan\left(\frac{x_{p,1}}{10}\right)$  and a quadratic resistance  $F_r = 0.4 \left(\frac{x_{p,2}}{15}\right)^2 \text{sign}(x_{p,2})$ , similar to an air resistance, are part of the plant. Hence the plant description becomes

$$\begin{aligned} \dot{x}_p &= \begin{pmatrix} 0 & 1 \\ -15 & -1 \end{pmatrix} x_p + \begin{pmatrix} 0 \\ 3.7 \end{pmatrix} \left( F_{\text{in}} - 3 \arctan\left(\frac{x_{p,1}}{10}\right) - 0.4 \left(\frac{x_{p,2}}{15}\right)^2 \text{sign}(x_{p,2}) \right) \\ &= \begin{pmatrix} 0 & 1 \\ -15 & -1 \end{pmatrix} x_p + \begin{pmatrix} 0 \\ 3.7 \end{pmatrix} \left( F_{\text{in}} + \begin{bmatrix} 3 & 0.4 \end{bmatrix} \begin{pmatrix} -\arctan\left(\frac{x_{p,1}}{10}\right) \\ -\left(\frac{x_{p,2}}{15}\right)^2 \text{sign}(x_{p,2}) \end{pmatrix} \right), \end{aligned} \quad (2.13)$$

which can be shown to be open-loop stable. Note that since this is a simulation example no units are stated for the parameters or the states.

The objective is to control the position  $x_{p,1}$  of the plant with a desired closed-loop performance chosen as the LTI model

$$\dot{x}_{\text{ref}} = \begin{pmatrix} 0 & 1 \\ -100 & -20 \end{pmatrix} x_{\text{ref}} + \begin{pmatrix} 0 \\ 100 \end{pmatrix} r, \quad (2.14)$$

which has two poles at -10 and a unit steady state gain for  $x_{\text{ref},1}$ .

In order to present the capability of MRAC to control an uncertain plant with the desired performance, the initial controller parameters have been computed with the matching equation (2.6), based on rough estimations of the plant parameters, which are assumed to be  $\hat{k}_1 = 30$ ,  $\hat{d}_1 = 3$ ,  $\hat{b} = 6.6$ ,  $\hat{F}_k = 6 \arctan\left(\frac{x_{p,1}}{10}\right)$ , and  $\hat{F}_r = 0.2 \left(\frac{x_{p,2}}{15}\right)^2 \text{sign}(x_{p,2})$ . This leads to the following initially estimated controller parameters and the respective ideal parameters:

| initial parameters   | ideal parameters  |
|--|---|
| $K_x(0) = \begin{pmatrix} -10.5105 \\ -2.7027 \end{pmatrix}$             | $K_x^* = \begin{pmatrix} -22.9730 \\ -5.1351 \end{pmatrix}$     |
| $k_r(0) = 15.0150$   | $k_r^* = 27.0270$   |
| $\hat{\theta}_{\text{nl}}(0) = \begin{pmatrix} 6.0 \\ 0.2 \end{pmatrix}$ | $\theta_{\text{nl}} = \begin{pmatrix} 3.0 \\ 0.4 \end{pmatrix}$ |

The simulation results shown in Figure 2.4 have been achieved by applying a MRAC controller as given in Table 2.1 to the plant  $G_{\text{ex}1}$  with  $Q = I_{2 \times 2}$ ,  $\Gamma_x = \Gamma_{\text{nl}} = 0.1 I_{2 \times 2}$  and  $\gamma_r = 0.1$ . As reference signal  $r$  a repeated step sequence with an amplitude of 20 has been provided. For the first 10 seconds of simulation, the parameter adaptation has been turned off. The closed-loop response with the initial controller parameters can be seen in the first graph of Figure 2.4.

After starting the adaptation, the closed-loop response quickly changes but does not follow the reference signal perfectly. The corresponding controlled input signal  $u$  is shown in the second graph. After the start of adaptation, it undergoes some strong high-frequency oscillations when the reference signal changes. These oscillations occur frequently in adaptive systems and have been mentioned in Remark 2.4. The third graph in Figure 2.4 shows the system response at the end of adaptation and for one step back and forth after the adaptation have been turned off at  $t = 510\text{s}$ . It can be seen, that the closed-loop system follows the reference signal better, while adaptation is turned on. This is emphasized by the scaled output tracking error  $\bar{e}_y = 30(x_{p,1} - x_{\text{ref},1})$ , which is clearly higher after adaptation has been switched off. This observation confirms Remark 2.3, because it shows that the tracking error of the adaptive system can be small without the need of ideal parameters for the direct MRAC controller. It further shows that the tracking error during adaptation is not necessarily a good indicator for the tracking error after adaptation, which is important if the presented adaptive controller is used for automatic tuning purposes. Finally, the fourth graph shows the estimated controller parameters, which slowly converge to their ideal values. However, the estimated parameters at the end of simulation

$$K_x(t = 510\text{s}) = \begin{pmatrix} -23.932 \\ -5.0467 \end{pmatrix}, \quad k_r(t = 510\text{s}) = 27.916, \quad \hat{\theta}_{\text{nl}}(t = 510\text{s}) = \begin{pmatrix} 5.3679 \\ -1.6084 \end{pmatrix},$$

did not reach their ideal value (see Remark 2.3). As mentioned in Remark 2.4, faster adaptation can be achieved with higher adaptation gains, but will also lead to stronger

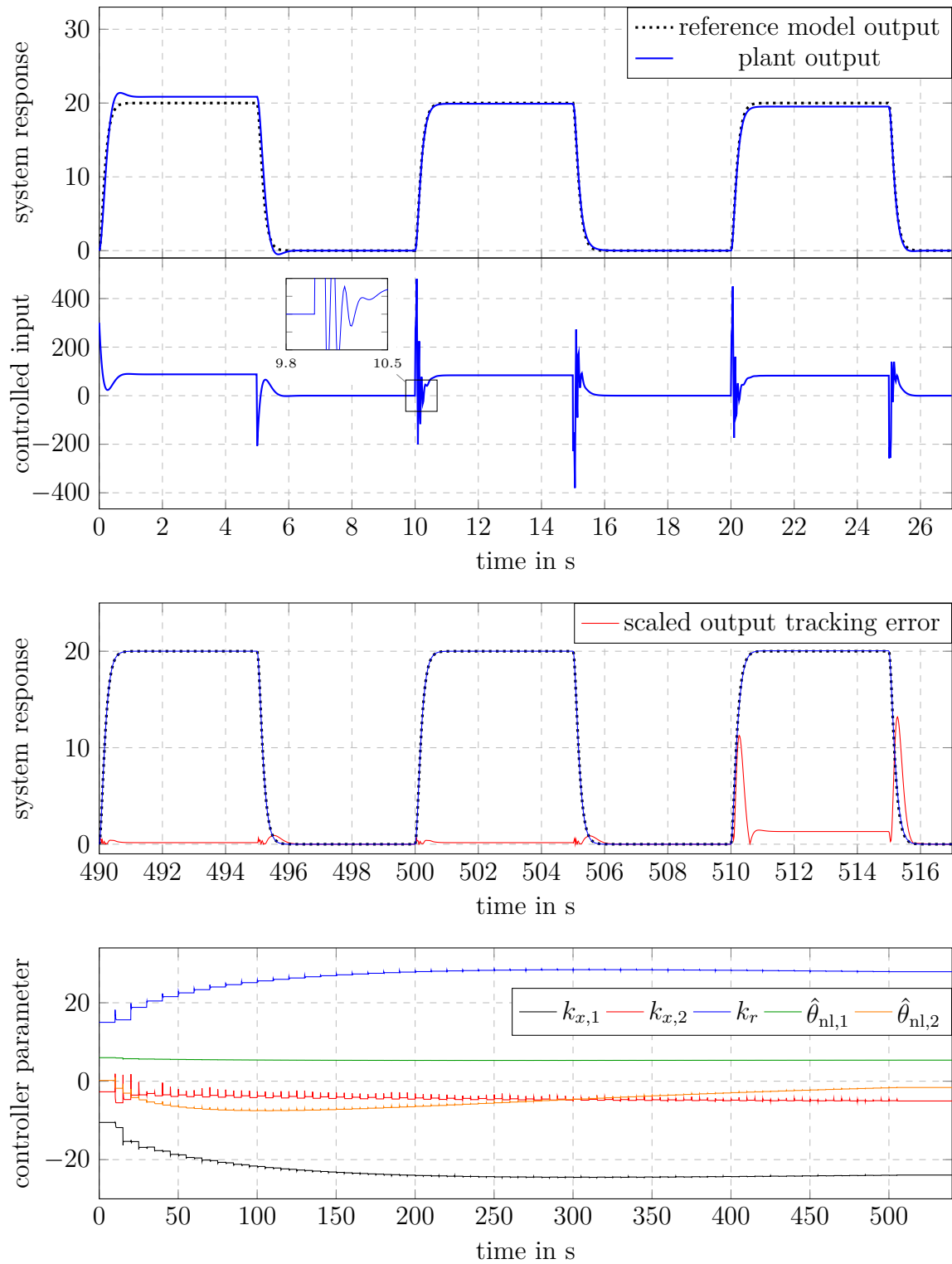


Figure 2.4: Results of Simulation Example 2.1 for MRAC with state-feedback. First and second graph: System response and controlled input at beginning of adaptation. Third graph: Closed-loop response and output tracking error after 480s of adaptation. Fourth graph: Estimations of controller parameters.

oscillations of the closed-loop as it is shown in Simulation Example 2.4. Applying an appropriate reference signal which causes a stronger excitation of the closed-loop system is another way to speed up the parameter estimation. Simulation result with such a reference signal are shown in Appendix C.

### 2.2.2 Model Reference Adaptive Control for Output-Feedback

Model reference adaptive control for output-feedback plants basically uses the same principle as in the state-feedback case. However, since only the output is available for measurement, a dynamical controller is necessary. Furthermore, different relative degrees of the plant require different parameter update laws. For relative degrees higher than one, the stability analysis of the closed-loop system needs to be done separately from the stability analysis of the parameter estimations, which increases the effort of the design procedure in comparison to the state-feedback case. The following presentation of MRAC for output-feedback plants is based on [60] and [116], but can also be found in [140, 147].

#### Plant Structure and Performance Specifications

The transfer function of a linear plant

$$G_{\text{lin}} : \quad y_{\text{p}} = k_{\text{p}} \frac{s^m + z_{m-1} s^{m-1} + \cdots + z_1 s + z_0}{s^n + r_{n-1} s^{n-1} + \cdots + r_1 s + r_0} u = k_{\text{p}} \frac{Z_{\text{p}}(s)}{R_{\text{p}}(s)} u \quad (2.15)$$

is considered under the following assumptions:

- A1) The degrees  $m$  of  $Z_{\text{p}}(s)$  and  $n$  of  $R_{\text{p}}(s)$  are known. Thus, the relative degree  $n^* = n - m \geq 1$  is known.
- A2) The numerator polynomial  $Z_{\text{p}}(s)$  is Hurwitz.
- A3) The sign of  $k_{\text{p}}$  is known.

The state-space representation of the plant  $G_{\text{lin}}$  is given by

$$\begin{aligned} \dot{x}_{\text{p}} &= A_{\text{p}} x_{\text{p}} + B_{\text{p}} u, \\ y_{\text{p}} &= C_{\text{p}} x_{\text{p}}, \end{aligned} \quad (2.16)$$

where  $A_{\text{p}} \in \mathbb{R}^{n \times n}$ ,  $B_{\text{p}} \in \mathbb{R}^n$ ,  $C_{\text{p}} \in \mathbb{R}^{1 \times n}$  depend on the unknown constant parameters  $z_i, r_j$  for  $i = 0, \dots, m - 1$  and  $j = 0, \dots, n - 1$ . As in the state-feedback case, a desired closed-loop behavior can be specified by a linear time-invariant (LTI) reference model

$$G_{\text{ref}} : \quad y_{\text{ref}} = k_{\text{ref}} \frac{Z_{\text{ref}}(s)}{R_{\text{ref}}(s)} r, \quad (2.17)$$

where the monic polynomials  $Z_{\text{ref}}(s)$  and  $R_{\text{ref}}(s)$  are of order  $m_{\text{ref}} = m$  and  $n_{\text{ref}} = n$ , respectively. A state-space model of  $G_{\text{ref}}$  is given by

$$\begin{aligned} \dot{x}_{\text{ref}} &= A_{\text{ref}} x_{\text{ref}} + B_{\text{ref}} r, \\ y_{\text{ref}} &= C_{\text{ref}} x_{\text{ref}}. \end{aligned} \quad (2.18)$$



### Control Law for Known Plant Parameters

If the plant parameters  $z_i, r_j$  for  $i = 0, \dots, m-1$  and  $j = 0, \dots, n-1$  are known, ideal parameters  $\theta_1^* \in \mathbb{R}^{n-1}$ ,  $\theta_2^* \in \mathbb{R}^{n-1}$ ,  $\theta_3^* \in \mathbb{R}$ , and  $c^* \in \mathbb{R}$  of the control law

$$u^* = \theta_1^{*\text{T}} \frac{\alpha_{n-2}(s)}{\Lambda(s)} u^* + \theta_2^{*\text{T}} \frac{\alpha_{n-2}(s)}{\Lambda(s)} y_p + \theta_3^* y_p + c^* r \quad (2.19)$$

with  $\Lambda = Z_{\text{ref}} \Lambda_0$  and

$$\alpha_i(s) = [s^i \quad s^{i-1} \quad \dots \quad s \quad 1]^{\text{T}} \quad (2.20)$$

can be found such that the closed-loop system is equal to the reference system. The polynomial  $\Lambda_0$  of degree  $n-m-1$  can be chosen to be an arbitrary Hurwitz polynomial. Building the closed-loop system of (2.15) and (2.19) yields

$$y_p = \frac{c^* k_p Z_p \Lambda^2}{\Lambda [(\Lambda - \theta_1^{*\text{T}} \alpha_{n-2}) R_p - k_p Z_p (\theta_2^{*\text{T}} \alpha_{n-2} + \theta_3^* \Lambda)]} r. \quad (2.21)$$

For perfect model following, i.e.  $y_p \equiv y_{\text{ref}}$ , it follows that

$$\frac{c^* k_p Z_p \Lambda^2}{\Lambda [(\Lambda - \theta_1^{*\text{T}} \alpha_{n-2}) R_p - k_p Z_p (\theta_2^{*\text{T}} \alpha_{n-2} + \theta_3^* \Lambda)]} = k_{\text{ref}} \frac{Z_{\text{ref}}}{R_{\text{ref}}}$$

has to be satisfied, which requires  $2n-2$  pole-zero cancellations and the controller parameters have to satisfy the matching conditions

$$c^* = \frac{k_{\text{ref}}}{k_p} \quad (2.22)$$

and

$$\theta_1^{*\text{T}} \alpha_{n-2} R_p + k_p Z_p (\theta_2^{*\text{T}} \alpha_{n-2} + \theta_3^* \Lambda) = \Lambda R_p - Z_p \Lambda_0 R_{\text{ref}}. \quad (2.23)$$

In [60] it is shown that (2.23) always has a solution, if assumptions A1)-A3) and the requirements about the reference model  $G_{\text{ref}}$  are satisfied.

A similar procedure can be done for the state-space representation (2.16) and the state-space representation of the control law (2.19)

$$\begin{aligned} \dot{w}_1 &= F w_1 + g u, \\ \dot{w}_2 &= F w_2 + g y, \\ u^* &= \begin{pmatrix} \theta_1^{*\text{T}} & \theta_2^{*\text{T}} & \theta_3^* & c^* \end{pmatrix} \begin{pmatrix} w_1 \\ w_2 \\ y_p \\ r \end{pmatrix} = \theta^{*\text{T}} w, \end{aligned} \quad (2.24)$$

where  $F, g$  satisfy

$$\left( s I_{(n-1) \times (n-1)} - F \right)^{-1} g = \frac{\alpha_{n-2}(s)}{\Lambda(s)}.$$

The closed-loop system of (2.16) and (2.24) becomes

$$\begin{aligned} \dot{x}_c &= \underbrace{\begin{pmatrix} A_p + B_p \theta_3^* C_p & B_p \theta_1^{*\top} & B_p \theta_2^{*\top} \\ g \theta_3^* C_p & F + g \theta_1^{*\top} & g \theta_2^{*\top} \\ g C_p & 0 & F \end{pmatrix}}_{A_{\text{refc}}} x_c + \underbrace{\begin{pmatrix} B_p \\ g \\ 0 \end{pmatrix}}_{B_c} c^* r, \\ y_p &= \underbrace{\begin{pmatrix} C_p & 0 & 0 \end{pmatrix}}_{C_c} x_c, \end{aligned} \quad (2.25)$$

which is a nonminimal state-space representation ( $2n - 2$  pole-zero cancellations, which follow from the transfer function argumentation) of the reference model  $G_{\text{ref}}$ , if the controller parameters satisfy (2.22) and (2.23). Therefore (2.25) can be written as a nonminimal state-space representation of the reference model with the state  $x_{\text{refc}}$ :

$$\begin{aligned} \dot{x}_{\text{refc}} &= A_{\text{refc}} x_{\text{refc}} + B_{\text{refc}} r, \\ y_{\text{ref}} &= C_c x_{\text{refc}}. \end{aligned} \quad (2.26)$$

### Adaptive Control Law for Unknown Plant Parameters

If the plant parameters  $z_i, r_j$  for  $i = 0, \dots, m - 1$  and  $j = 0, \dots, n - 1$  are unknown, an adaptive version

$$u = \theta_1^\top(t) \frac{\alpha_{n-2}(s)}{\Lambda(s)} u + \theta_2^\top(t) \frac{\alpha_{n-2}(s)}{\Lambda(s)} y_p + \theta_3(t) y_p + c(t) r = \theta^\top(t) w \quad (2.27)$$

of (2.19) is used with the time-dependent estimated controller parameters  $\theta_1(t)$ ,  $\theta_2(t)$ ,  $\theta_3(t)$  and  $c(t)$ . In order to find suitable update laws for the controller parameters, the tracking error  $e_y = y_p - y_{\text{ref}}$  needs to be expressed in terms of the parameter errors  $\tilde{\theta}_1(t) = \theta_1(t) - \theta_1^*$ ,  $\tilde{\theta}_2(t) = \theta_2(t) - \theta_2^*$ ,  $\tilde{\theta}_3(t) = \theta_3(t) - \theta_3^*$  and  $\tilde{c}(t) = c(t) - c^*$ . Similar to the state-feedback case, this can be achieved by adding and subtracting the term  $B_p \theta^{*\top} w$  and substituting  $u = \theta^\top w$  in (2.16), which yields

$$\begin{aligned} \dot{x}_c &= A_{\text{refc}} x_c + B_c \left( \tilde{\theta}^\top w + c^* r \right) = A_{\text{refc}} x_c + B_{\text{refc}} \left( \frac{1}{c^*} \tilde{\theta}^\top w + r \right), \\ y_p &= C_c x_c, \end{aligned} \quad (2.28)$$

where  $B_{\text{refc}} = B_c c^*$  follows from (2.21), (2.25), and (2.26). Since  $A_{\text{refc}}$ ,  $B_{\text{refc}}$  and  $C_c$  are matrices for a nonminimal state-space representation of  $G_{\text{ref}}$ , the state-space equations for the tracking error  $e_y = y_p - y_{\text{ref}}$  become

$$\begin{aligned} \dot{e} &= A_{\text{refc}} e + B_{\text{refc}} \frac{1}{c^*} \tilde{\theta}^\top w, \\ e_y &= C_c e, \end{aligned} \quad (2.29)$$

with the transfer function

$$e_y = G_{\text{ref}}(s) \frac{1}{c^*} \tilde{\theta}^\top w. \quad (2.30)$$

A distinction for the cases of relative degree  $n^* = 1$  and relative degree  $n^* \geq 2$  is necessary to derive parameter update laws. The procedure for  $n^* = 1$  is straight forward and allows to establish stability for the parameter estimations and the closed-loop system with a single stability analysis. For the case of  $n^* \geq 2$  a stable adaptive closed-loop system requires some extensions in comparison to the case  $n^* = 1$ . In this work the method from [116] is presented. It requires a separate stability analysis of the parameter estimations and the remaining closed-loop signals, which makes it not as straight forward to apply as the method for  $n^* = 1$ .

**$n^* = 1$ :**

For relative degree unity, the reference model  $G_{\text{ref}}$  has to be strictly positive real (SPR). If in addition the parameter update law is chosen to be

$$\dot{\theta} = -\Gamma e_y w \text{sign}(c^*) \quad (2.31)$$

the function

$$V = \frac{1}{2} \left( e^T P_c e + \frac{1}{|c^*|} \tilde{\theta}^T \Gamma^{-1} \tilde{\theta} \right) \quad (2.32)$$

with the gain matrix  $\Gamma = \Gamma^T > 0 \in \mathbb{R}^{2n \times 2n}$  can be shown to be a Lyapunov function.

**$n^* \geq 2$ :**

For a relative degree greater than one, a separate stability analysis for the parameter estimations and the remaining closed-loop signals is necessary. Various approaches exist, that result in different parameter estimation schemes. However, in the following the method 1 from [116] is presented.

The tracking error  $e_y$  is extended by the auxiliary error

$$e_2 = \left( \theta^T G_{\text{REF}} - G_{\text{ref}} \theta^T \right) w. \quad (2.33)$$

such that  $e_{y2} = e_y + k_a(t) e_2$ , where  $k_a(t)$  is an estimation of  $\frac{1}{c^*}$  and  $G_{\text{REF}}$  is a diagonal  $2n \times 2n$  MIMO transfer function, where each nonzero entry is  $G_{\text{ref}}$ . With the definition of the parameter error  $\tilde{k}_a = k_a(t) - \frac{1}{c^*}$ , the extended error can be written as

$$\begin{aligned} e_{y2} &= G_{\text{ref}} \frac{1}{c^*} \tilde{\theta}^T w + \tilde{k}_a e_2 + \frac{1}{c^*} e_2 \\ &= \frac{1}{c^*} \theta^T G_{\text{REF}} w + \tilde{k}_a e_2 + \frac{1}{c^*} G_{\text{ref}} \tilde{\theta}^T w - \frac{1}{c^*} G_{\text{ref}} \theta^T w \\ &= \frac{1}{c^*} \theta^T G_{\text{REF}} w + \tilde{k}_a e_2 - \frac{1}{c^*} G_{\text{ref}} \theta^{*\text{T}} w. \end{aligned} \quad (2.34)$$

Addition and subtraction of  $\frac{1}{c^*} \theta^{*\text{T}} G_{\text{REF}} w$  yields

$$e_{y2} = \frac{1}{c^*} \tilde{\theta}^T G_{\text{REF}} w + \tilde{k}_a e_2 + \underbrace{\frac{1}{c^*} \theta^{*\text{T}} G_{\text{REF}} w - \frac{1}{c^*} G_{\text{ref}} \theta^{*\text{T}} w}_{\delta}, \quad (2.35)$$

where  $\delta$  decays exponentially due to the stable linear system  $G_{\text{ref}}$  and the constant vector  $\theta^*$  of the ideal controller parameters. Hence,  $\delta$  can be neglected in the following, as shown in detail in [116].

The extended error  $e_{y2}$  allows the derivation of the parameter update laws

$$\dot{\theta} = -\text{sign}(c^*) \Gamma \frac{e_{y2} \phi_w}{1 + \phi_w^T \phi_w}, \quad (2.36)$$

$$\dot{k}_a = -\gamma_a \frac{e_{y2} e_2}{1 + \phi_w^T \phi_w}, \quad (2.37)$$

with  $\phi_w = G_{\text{REF}} w$ , which lead to bounded parameter estimations. This can be shown with the Lyapunov function

$$V = \frac{1}{2} \left( \frac{1}{|c^*|} \tilde{\theta}^T \Gamma^{-1} \tilde{\theta} + \frac{1}{\gamma_a} \tilde{k}_a^2 \right), \quad (2.38)$$

where the matrix  $\Gamma = \Gamma^T > 0 \in \mathbb{R}^{2n \times 2n}$  and the scalar  $\gamma_a > 0$  are gains for the parameter estimations.

For the presented MRAC scheme for output-feedback, the following theorem can be formulated.

**Theorem 2.2.** *The control law (2.27) with a bounded reference signal  $r(t)$  together with the parameter update law (2.31) for  $n^* = 1$  or update laws (2.36)-(2.37) for  $n^* \geq 2$  and the reference model (2.17) applied to the plant  $G_{\text{lin}}$  in (2.15) results in global asymptotic stability of the tracking error:*

$$\lim_{t \rightarrow \infty} \|y_p(t) - y_{\text{ref}}(t)\| = 0.$$

Moreover, all signals of the closed-loop system are guaranteed to stay bounded.

*Proof.* The proof of the theorem can be found e.g. in [60] and [116].  $\square$

## Summary and Remarks

The complete control scheme is given by the controller structure in (2.27), the reference model  $G_{\text{ref}}$  in (2.17), and the parameter update law (2.31) for  $n^* = 1$  and the update laws (2.36)-(2.37) for  $n^* \geq 2$ . The design of output-feedback MRAC requires the choice of several design parameters. Similar to the state-feedback case, a reference model  $G_{\text{ref}}$  and the gains  $\Gamma$  and  $\gamma_a$  for the parameter updates need to be defined. Comments on that and other similarities of state-feedback and output-feedback MRAC are stated in Remark 2.5. In Remark 2.10 an idea of the choice of the filter polynomial  $\Lambda_0$  for the control law is explained. An overview of the control scheme is given in Table 2.2. Some of the properties of MRAC for output-feedback plants are shown in Simulation Example 2.2.

**Remark 2.5.** Some similarities do appear for MRAC of output-feedback systems and state-feedback systems:



- For output-feedback systems, the gains for the parameter updates,  $\Gamma$  and  $\gamma_a$ , have been introduced. These gains have a similar meaning and effect as the gains for state-feedback systems, which are mentioned in Remark 2.4.
- The assumption of a known sign of  $c^*$  is similar to the assumption of a known control direction of the plant. For state-feedback MRAC a comment on that is given in Remark 2.1.
- The parameter estimations are not guaranteed to converge to their ideal values for output-feedback MRAC and for state-feedback MRAC. Remark 2.3 for the state-feedback case does also apply to the parameters of output-feedback MRAC.

**Remark 2.6.** The method of MRAC for output-feedback plants can also be applied to plants, where only an upper bound  $\bar{n}$  for the exact plant order  $n$  is known (see [60, 116]). However, in order to simplify the discussion, the plant order is assumed to be known in this work.

**Remark 2.7.** For the case of  $n^* \geq 2$  the parameter update laws of output-feedback MRAC become more complicated and are not as straight forward to apply compared to the case with  $n^* = 1$ . In order to guarantee closed-loop stability, it is even necessary to introduce the additional state  $k_a$ . For the special case  $n^* = 2$  a similar method to the method for  $n^* = 1$  can be used (see [60, 116]) in order to reduce the complexity. In [60] the procedure of stability analysis for  $n^* = 1$  is even extended for the case of higher relative degrees. However, this extension leads to control laws with high complexity and does not have a general advantage over the method presented in this work.

**Remark 2.8.** In difference to state-feedback MRAC, the adaptive control law for output-feedback has been presented for a purely linear plant. An output-feedback MRAC scheme for a class of nonlinear systems is presented in [74].

**Remark 2.9.** The assumption of a minimum-phase plant ( $Z_p$  Hurwitz) is necessary, since pole zero cancellation will take place in order to make the closed-loop system equal to the reference model. If  $Z_p$  has roots in the right half plane, unstable pole zero cancellations are necessary, which lead to unbounded closed-loop states. More detailed comments on that can be found in [60]. An approach to deal with plants that have unstable zeros has been introduced in [76] and has been extended in [4].

**Remark 2.10.** In addition to the gains of the parameter updates, output-feedback MRAC introduces the coefficients of  $\Lambda_0 = \frac{\Lambda}{Z_{\text{ref}}}$  as design parameters. Testing different choices is a common way to get well-suited coefficients of  $\Lambda_0$ . In [104] the influence of  $\Lambda_0$  on the closed-loop performance has been examined in a systematic way under the assumption that the parameters  $\theta^*$  lie in a known convex set.

**Simulation Example 2.2.** A similar plant to  $G_{\text{ex1}}$  from Simulation Example 2.1 is considered, but without the matched uncertainty, which can not be addressed by the presented MRAC scheme for output-feedback. Hence, the plant model

$$G_{\text{ex2}} : \begin{aligned} \dot{x}_p &= \begin{pmatrix} 0 & 1 \\ -\frac{k_1}{m} & -\frac{d_1}{m} \end{pmatrix} x_p + \begin{pmatrix} 0 \\ \frac{b}{m} \end{pmatrix} F_{\text{in}}, \\ y_p &= [1 \quad 0] x_p, \end{aligned} \quad (2.39)$$

where the parameters  $m = 1$ ,  $k_1 = 15$  and  $d_1 = 1$  are the same as for  $G_{\text{ex1}}$ . The reference model is chosen as

$$\begin{aligned} \dot{x}_{\text{ref}} &= \begin{pmatrix} 0 & 1 \\ -100 & -20 \end{pmatrix} x_{\text{ref}} + \begin{pmatrix} 0 \\ 100 \end{pmatrix} r, \\ y_{\text{ref}} &= \begin{bmatrix} 1 & 0 \end{bmatrix} x_{\text{ref}}, \end{aligned} \quad (2.40)$$

which is the same as in Example 2.1, but only its output is used for the parameter updates. An initial rough estimate of the plant parameters, which are assumed to be  $\hat{k}_1 = 30$ ,  $\hat{d}_1 = 3$ ,  $\hat{b} = 6.6$ , have been used to compute the initial controller parameters, which are given in the following table together with the ideal plant parameters.

| initial parameters   | ideal parameters  |
|--|---|
| $\theta(0) = \begin{pmatrix} -18.0 \\ 78.3784 \\ -7.8078 \\ 15.0150 \end{pmatrix}$ | $\theta^* = \begin{pmatrix} -19.0 \\ 77.027 \\ -22.9730 \\ 27.0270 \end{pmatrix}$ |
| $k_a(0) = 0.0666$  | $k_a^* = 0.0370$  |

From this starting point, the same experiments as in Example 2.1 have been done with the MRAC algorithm in Table 2.2 for relative degrees  $n^* \geq 2$ . The adaptive gains have been set to  $\Gamma = 10^4 I_{4 \times 4}$ ,  $\gamma_a = 10$  and the filter polynomial has been chosen as  $\Lambda_0 = s + 1$ . The results for a repeated step sequence of the reference signal are shown in Figure 2.5.

In the first and second graph, it can be seen that at the beginning of adaptation, the tracking error is clearly higher than in the state-feedback case, presented in Simulation Example 2.1, but the input signal is less oscillatory. Since the parameter adaptation is faster than in the state-feedback case in this example, as can be seen in the fourth graph of Figure 2.5, the simulation has already been stopped at  $t = 240$ s. The simulation results at the end of adaptation are shown in the third graph. As in the state-feedback case, the scaled tracking error  $\bar{e}_y = 30 (x_{p,1} - x_{1\text{ref},1})$  is smaller during adaptation and becomes bigger after adaptation has been deactivated. From  $t = 201$ s seconds to  $t = 205$ s the steady-state tracking error vanishes slowly for a constant value of the reference model output. In contrast to that, the tracking error stays constant in the time from  $t = 211$ s to  $t = 215$ s, where again a constant value of the reference signal is demanded. From this result it can be concluded that the adaptation for the present problem has a similar effect to an integrator in a non-adaptive control law. As for Simulation Example 2.1, simulation results for a reference signal that is more appropriate for parameter estimation are shown in Appendix C.

### 2.2.3 Indirect Adaptive Pole Placement Control for Output-Feedback

In this section the polynomial approach for adaptive pole placement control adopted from [60], is presented. The same method can also be found in [147]. An extension of the

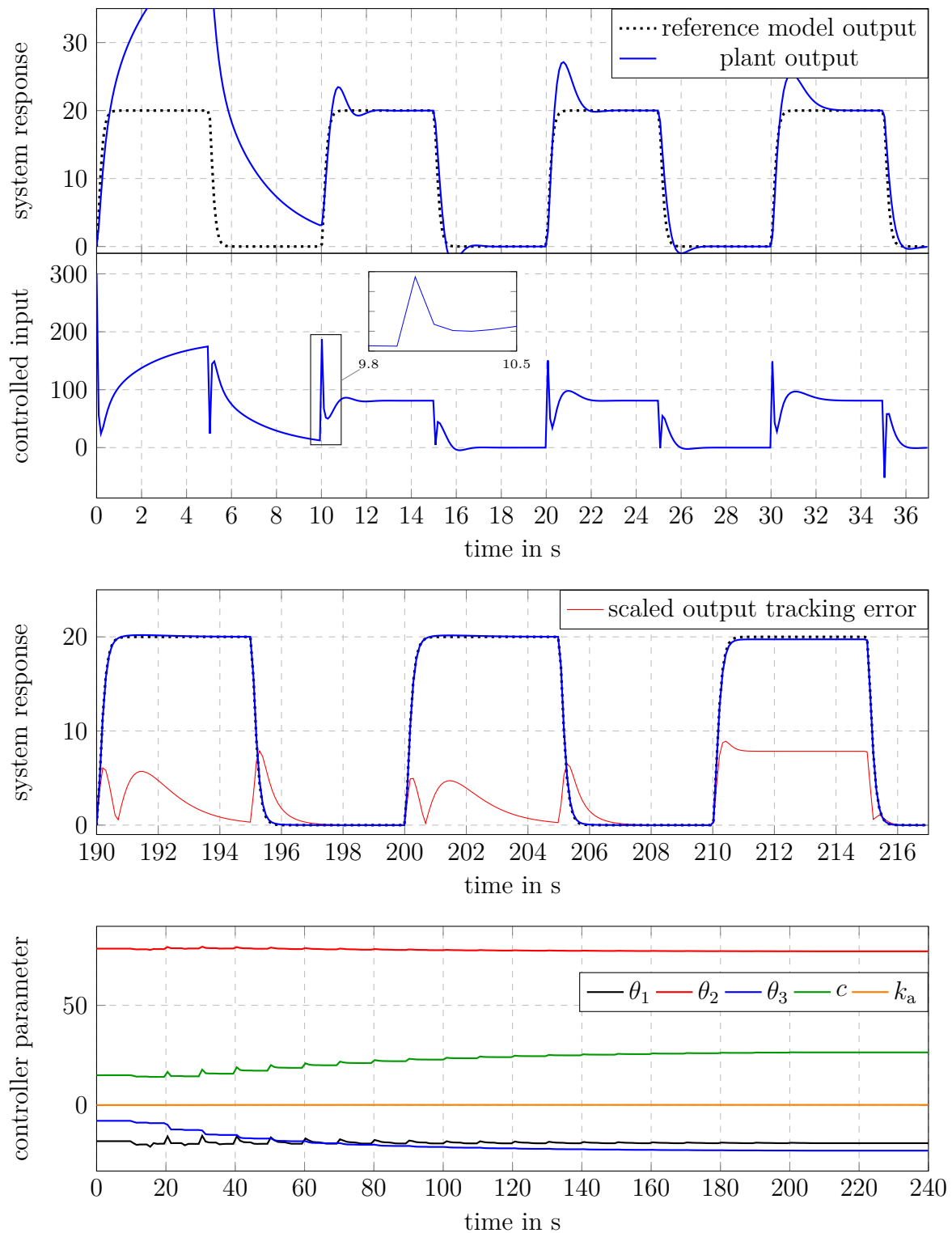


Figure 2.5: Results of Simulation Example 2.2 for MRAC with output-feedback. First and second graph: System response and controlled input at beginning of adaptation. Third graph: Closed-loop response and output tracking error after 180s of adaptation. Fourth graph: Estimations of controller parameters.



method from the literature is done here in order to account for matched uncertainties. In contrast to the foregoing presentations, the APPC scheme is presented as an indirect adaptive control method based on the certainty equivalence principle.

### Plant Structure and Performance Specifications

A strictly proper input-output plant model of the form

$$G_{\text{nl}2} : R_p(D) y_p = Z_p(D) \left( u + \theta_{\text{nl}}^T f_{\text{nl}}(y_p) \right) \quad (2.41)$$

is considered, where  $D \triangleq \frac{d}{dt}$ , the degree  $n$  of the polynomial  $R_p = D^n + r_{n-1} D^{n-1} + \dots + r_0$  is known, the polynomials  $Z_p = z_m D^m + z_{m-1} D^{m-1} + \dots + z_0$  and  $R_p$  are known to be coprime, but the constant parameters  $z_i, r_j$  for  $i = 0, \dots, m$  and  $j = 0, \dots, n-1$  are unknown. The term  $\theta_{\text{nl}}^T f_{\text{nl}}(y_p)$  represents a matched uncertainty, where the nonlinear functions

$$f_{\text{nl}}(y_p) = \left[ f_{\text{nl},1}(y_p) \quad \dots \quad f_{\text{nl},l}(y_p) \right]^T$$

are known and bounded for bounded  $y_p$ . The constant parameters in  $\theta_{\text{nl}} \in \mathbb{R}^l$  are unknown. Note that the differential operator  $D \triangleq \frac{d}{dt}$  instead of the Laplace variable  $s$  is used here, as it has been done e.g. in [38, 74, 77], in order to avoid confusion about frequency and time domain.

The objective of APPC is to place the poles of the closed-loop system at the poles of a desired denominator polynomial  $A_d(D)$ . In addition, the closed-loop system is supposed to follow the bounded reference signal  $r$ . For this reason, an internal model  $Q(D)$  with degree  $q$  of the reference signal has to be defined that satisfies  $Q(D)r = 0$  and has no common roots with  $Z_p(D)$ . The control-law, which will be introduced below, applied to the plant  $G_{\text{lin}}$  results in a closed-loop system of order  $2n + q - 1$ . Accordingly, the degree of  $A_d(D)$  has to be  $2n + q - 1$ :

$$A_d(D) = D^{2n+q-1} + a_{d,2n+q-2} D^{2n+q-2} + \dots + a_{d,0}.$$

### Control Law for known Plant Parameters

For known plant parameters the control law

$$u = -\frac{P^*(D)}{Q(D)L^*(D)} y_p + \frac{M^*(D)}{Q(D)L^*(D)} r - \theta_{\text{nl}}^T f_{\text{nl}}(y_p) \quad (2.42)$$

with the constant and ideal polynomials  $L^*(D)$ ,  $P^*(D)$  and  $M^*(D)$  is considered. The degree of these controller polynomials is  $n-1$  and  $n+q-1$ , for  $L^*(D)$  and  $P^*(D)$ , respectively. If tracking of a constant reference signal is desired and  $z_0 \neq 0$ ,  $M^*$  can be chosen to be a scalar. In all other cases,  $M^*(D)$  has to be chosen as a polynomial of order  $n+q-1$ . Application of (2.42) to the plant  $G_{\text{nl}2}$  leads to the closed-loop system

$$y_p = \frac{Z_p(D) M^*(D)}{L^*(D) Q(D) R_p(D) + P^*(D) Z_p(D)} r. \quad (2.43)$$

If the controller parameters satisfy

$$L^* Q R_p + P^* Z_p = A_d, \quad (2.44)$$

the poles of the closed-loop system lie at the desired positions. If  $z_0 \neq 0$  the computation

$$M^* = \frac{a_{d,0}}{z_0} \quad (2.45)$$

leads to a closed-loop steady-state gain of one, which is especially useful for piecewise constant reference signals. For other reference signals or  $z_0 = 0$ , the equation

$$e_{yr} = y_p - r = \frac{Z_p}{A_d} (M^* - P^*) r - \frac{L^* R_p}{A_d} Q r \quad (2.46)$$

of the tracking error suggests the choice of

$$M^* = P^* \quad (2.47)$$

to achieve  $e_{yr}(t) \rightarrow 0$  exponentially. In [60] it is shown that (2.44) always has a solution if all the aforementioned assumptions about  $Z_p$ ,  $R_p$  and  $Q$  are satisfied. Hence, if (2.44) has a solution, at least (2.47) has a solution and leads to an admissible choice of  $M^*(D)$ .

### Adaptive Control Law for Unknown Plant Parameters

If the plant parameters  $z_i, r_j$  for  $i = 0, \dots, m$  and  $j = 0, \dots, n-1$ , and  $\theta_{nl}$  are unknown, an adaptive version of (2.42) has to be used:

$$u = -\frac{P(D)}{Q(D)L(D)} y_p + \frac{M(D)}{Q(D)L(D)} r - \hat{\theta}_{nl}^T f_{nl}(y_p). \quad (2.48)$$

In (2.48) the constant controller parameters have been replaced by their estimations  $L$ ,  $P$ ,  $M$ , and  $\hat{\theta}_{nl}$ . Since an indirect APPC is considered here, an estimation scheme for the plant parameters rather than for the controller parameters has to be applied. Based on the certainty equivalence principle, the controller parameters are then calculated during operation with (2.44) and (2.45) or (2.47) based on the estimations  $\hat{Z}_p$ ,  $\hat{R}_p$  and  $\hat{\theta}_{nl}$  of the plant parameters.

Many recursive parameter estimation schemes exist, that are suitable for indirect adaptive control. Some of them can be found in [56, 60, 61, 98, 147] and usually require the system description to be in a linear parametric form. For  $G_{nl2}$  this can be achieved by multiplying both sides of (2.41) with  $R_p(D)$  and then filtering them with a stable polynomial  $\Lambda_e(D)$  of degree  $n$ , which results in

$$\frac{D^n y_p}{\Lambda_e(D)} = -\theta_y^T \frac{\alpha_{n-1}(D)}{\Lambda_e(D)} y_p + \theta_u^T \frac{\alpha_m(D)}{\Lambda_e(D)} u + \theta_{znlm}^T \frac{D^m}{\Lambda_e(D)} f_{nl}(y_p) + \dots + \theta_{znl0}^T \frac{1}{\Lambda_e(D)} f_{nl}(y_p), \quad (2.49)$$

where

$$\alpha_i(D) = \begin{bmatrix} D^i & D^{i-1} & \dots & D & 1 \end{bmatrix}^T, \quad (2.50)$$

$\theta_y = [r_{n-1} \ \dots \ r_0]^\top$ ,  $\theta_u = [z_m \ \dots \ z_0]^\top$ , and  $\theta_{z_{nli}} = z_i \theta_{nl}$  for  $i = 0, \dots, m$ . Equation (2.49) can be written in a compact form as

$$y_f = \theta_p^\top \phi_p \quad (2.51)$$

with

$$\begin{aligned} y_f &= \frac{D^n y_p}{\Lambda_e(D)}, \\ \theta_p &= [\theta_y^\top \ \theta_u^\top \ \theta_{z_{n1,m}}^\top \ \dots \ \theta_{z_{n1,0}}^\top]^\top, \text{ and} \\ \phi_p &= \left[ -\frac{\alpha_{n-1}^\top}{\Lambda_e(D)} y_p \quad \frac{\alpha_m^\top}{\Lambda_e(D)} u \quad \frac{D^m}{\Lambda_e(D)} f_{nl}(y_p)^\top \quad \dots \quad \frac{1}{\Lambda_e(D)} f_{nl}(y_p)^\top \right]^\top. \end{aligned}$$

The well known recursive least-squares estimation with covariance resetting can then be applied to (2.51). Hence, the update law for the estimated plant parameters  $\hat{\theta}_p$  becomes

$$\begin{aligned} \epsilon &= \frac{y_f - \hat{\theta}_p^\top \phi_p}{1 + \phi_p^\top \phi_p}, \\ \dot{\hat{\theta}}_p &= P_{ls} \epsilon \phi_p, \\ \dot{P}_{ls} &= -\frac{P_{ls} \phi_p \phi_p^\top P_{ls}}{1 + \phi_p^\top \phi_p}, \quad P_{ls}(0) = P_{ls0}, \quad P_{ls}(t_r) = \rho_r I_{p \times p}, \end{aligned} \quad (2.52)$$

with the covariance matrix  $P_{ls} = P_{ls}^\top > 0 \in \mathbb{R}^{p \times p}$  and  $p = n + m + l + ml + 1$ . The covariance matrix is set to  $\rho_r I_{p \times p}$  at time  $t_r$ , where the minimal eigenvalue of the covariance matrix becomes  $\lambda_{\min}(P_{ls}) < \rho_s$ . The parameters  $P_{ls0}$  and  $\rho_r > \rho_s > 0$  can be chosen as design parameters. The presented least-squares algorithm (2.52) guarantees the parameter estimations and their derivatives with respect to time to be bounded. Additional properties of the given recursive least-squares algorithm with covariance resetting are stated in Appendix B.

Calculation of the controller parameter estimations can be done with equations (2.44) and (2.45) or (2.47), where the plant parameters have to be replaced by their estimations. An estimation of the nonlinear parameters can be achieved by

$$\hat{\theta}_{nl} = \frac{\hat{\theta}_{z_{nli}}}{\hat{z}_i}, \quad (2.53)$$

for any  $i = 0, \dots, m$ .

## Summary and Remarks

The complete control scheme is given by the controller structure (2.48), the plant parameter estimation scheme in (2.52), and the rules for controller parameter calculation in (2.44), (2.45) or (2.47). A comment on the choice of the tuning parameters  $A_d$ ,  $\Lambda_e$ ,  $P_{ls}(0)$ ,  $\rho_0$ , and  $\rho_1$  is given in Remark 2.12. No stability result has been stated for the APCC scheme in this section. Remark 2.13 gives an idea of a possible proof of stability

for the closed-loop system. The lack of a solution for equation (2.44) is a potential issue of the APPC scheme and shortly discussed in Remark 2.14. An overview of the complete control scheme is given in Table 2.3. Some properties of the APPC method are illustrated in Simulation Example 2.3.

**Remark 2.11.** In the presentation of APPC, a least-squares algorithm with covariance reset has been chosen as plant parameter estimation method. This has been done, because this estimation scheme has shown superior performance in comparison to other methods, like gradient methods or the least-mean square estimation (these schemes can be found e.g. in [56, 60, 61]). In addition, many extensions of the least-squares algorithm exist that e.g. allow for identification of time-varying parameters ([11, 119]).

**Remark 2.12.** The performance of the closed-loop system is mainly determined by the choice of the stable desired denominator polynomial  $A_d(D)$ . That means, the performance in terms of speed of the closed-loop response can be estimated by a linear system with poles at the roots of  $A_d(D)$ . However, the designer has to keep in mind additional influences, like the nonlinear nature of the closed-loop system due to parameter updates, and the zeros of the closed-loop system, that are determined by the zeros of the plant and the choice of  $M(D)$  (see (2.43)). The parameter estimation will be influenced by the choice of the stable filter polynomial  $\Lambda_e$ . It can be chosen, such that undesired high-frequency contents of the output signal, e.g. measurement noise, are filtered out. However, since there is no systematic way to choose  $\Lambda_e$ , experiments on the plant are often necessary.  $P_{1s}(0)$  determines the initial gain for the parameter estimation. A high gain is necessary if the plant parameters are completely unknown. If a good estimation of the plant parameters is available, only a low gain is necessary. The values of  $\rho_0$ , and  $\rho_1$  can then be chosen according to  $P_{1s}(0)$ .

**Remark 2.13.** For the presented APPC scheme in this section a standard proof of stability does not exist in the literature, since it has been extended by a direct compensation of nonlinearities which act as matched uncertainties. For a purely linear plant a stability proof is given in [60, 147]. Due to the properties of the least squares algorithm, stated in Appendix A, boundedness of the estimated parameters can be guaranteed for the presented control scheme. If in addition an upper bound  $f_{nlmax} \geq \|f_{nl}\|$  for the nonlinearities exists, stability of all closed-loop signals can be established in the framework of robust adaptive control in the presence of bounded disturbances [60, 147]. However, since no stability analysis has been carried out for the presented APPC scheme, it should only be used for limited time periods of adaptation under well known and save environmental conditions. Hence, automatic tuning applications are still well suited for the presented scheme.

**Remark 2.14.** A solution for the controller parameters calculated by (2.44) is guaranteed, as long as  $Z_p$  and  $R_p$  are coprime. However, for an adaptive control scheme, the plant polynomials are substituted by their estimations so that it can no longer be guaranteed that a solution for (2.44) always exists. In order to simplify the discussion, it is assumed for the rest of this work that such a solution always exists. A more detailed discussion about that issue is given in [60], where also some ways are proposed to enforce the existence of a solution. One of them restricts the estimated plant parameters to lie in a convex set. This

|                                   |   |
|-----------------------------------|---|
| Plant:                            | $y_p = \frac{Z_p(D)}{R_p(D)} \left( u + \theta_{nl}^T f_{nl}(y_p) \right)$  |
| Control Law:                      | $u = -\frac{P(D)}{Q(D)L(D)} y_p + \frac{M(D)}{Q(D)L(D)} r - \hat{\theta}_{nl}^T f_{nl}(y_p)$<br>$Q(D) r = 0$  |
| Plant Parameter Estimation:       | $\dot{\hat{\theta}}_p = P_{ls} \epsilon \phi_p$<br>$\dot{P}_{ls} = -\frac{P_{ls} \phi_p \phi_p^T P_{ls}}{1 + \phi_p^T \phi_p}, \quad P_{ls}(0) = P_{ls0}, \quad P_{ls}(t_r) = \rho_r I_{p \times p}$<br>$\epsilon = \frac{y_f - \hat{\theta}_p^T \phi_p}{1 + \phi_p^T \phi_p}$<br>$y_f = \frac{D^n y_p}{\Lambda_e(D)}, \quad \hat{\theta}_p = \left[ \hat{\theta}_y^T \quad \hat{\theta}_u^T \quad \hat{\theta}_{znl,m}^T \quad \dots \quad \hat{\theta}_{znl,0}^T \right]^T$<br>$\phi_p^T = \left[ -\frac{\alpha_{n-1}^T}{\Lambda_e(D)} y_p \quad \frac{\alpha_m^T}{\Lambda_e(D)} u \quad \frac{D^m}{\Lambda_e(D)} f_{nl}^T(y_p) \quad \dots \quad \frac{1}{\Lambda_e(D)} f_{nl}^T(y_p) \right]$ |
| Controller Parameter Calculation: | $A_d(D) = L(D) Q(D) \hat{R}_p(D) + P(D) \hat{Z}_p(D)$<br>$M = \begin{cases} \frac{a_{d0}}{\hat{z}_0}, & \text{for piecewise constant } r \text{ and } z_0 \neq 0 \\ P, & \text{otherwise} \end{cases}$<br>$\hat{\theta}_{nl} = \frac{\hat{\theta}_{znl,i}}{\hat{z}_i}, \text{ for any } i = 0, \dots, m, \quad \hat{\theta}_u = \left[ \hat{z}_m \quad \dots \quad \hat{z}_0 \right]^T$<br>$\hat{Z}_p(D) = \hat{\theta}_u^T \alpha_m$<br>$\hat{R}_p(D) = D^n + \hat{\theta}_y^T \alpha_{n-1}(D)$<br>$\alpha_i(D) = \left[ D^i \quad D^{i-1} \quad \dots \quad D \quad 1 \right]^T$  |
|                                   |   |
| Design Parameters:                | <ul style="list-style-type: none"> <li>• polynomial <math>A_d</math> with roots at desired closed-loop poles</li> <li>• <math>\Lambda_e</math> of degree <math>n</math> (see Remark 2.12)</li> <li>• <math>P_{ls}(0)</math>, <math>\rho_0</math>, and <math>\rho_r</math> (see Remark 2.12)</li> </ul>  |

Table 2.3: Summary of the polynomial approach of output-feedback APPC with compensation of matched uncertainty.

is done by a projection algorithm, which is an extension for basic parameter estimation schemes and is shortly introduced in Section 2.2.5.

**Simulation Example 2.3.** A similar plant to  $G_{\text{ex1}}$  from Simulation Example 2.1 is considered:

$$G_{\text{ex3}} : \begin{aligned} \dot{x}_{\text{p}} &= \begin{pmatrix} 0 & 1 \\ -\frac{k_1}{m} & -\frac{d_1}{m} \end{pmatrix} x_{\text{p}} + \begin{pmatrix} 0 \\ \frac{b}{m} \end{pmatrix} (F_{\text{in}} - F_k), \\ y_{\text{p}} &= [1 \quad 0] x_{\text{p}}. \end{aligned} \quad (2.54)$$

This plant equation can also be written as

$$\left( D^2 + \frac{d_1}{m} D + \frac{k_1}{m} \right) y_{\text{p}} = \frac{b}{m} (F_{\text{in}} - F_k). \quad (2.55)$$

The parameters  $m = 1$ ,  $k_1 = 15$  and  $d_1 = 1$  in (2.54) are the same as for  $G_{\text{ex1}}$ . In difference to the MRAC methods, no reference model needs to be defined. However, with the requirement of tracking of a piecewise constant reference signal, which leads to  $Q(D) = D$ , a choice of  $2n + q - 1$  desired closed-loop poles is necessary. All of them have been chosen to lie at  $-25$ , which results in a desired closed-loop dynamic that is similar to the dynamics of the reference models in the preceding simulation examples. For the calculation of the controller parameter  $M$ , equation (2.45) has been used.

As in the previous examples, the controller has been initiated with a rough estimate of the plant parameters, which are given as  $\hat{k}_1 = 30$ ,  $\hat{d}_1 = 3$ ,  $\hat{b} = 6.6$ ,  $\hat{F}_k = 6 \arctan\left(\frac{x_1}{10}\right)$ . Consequently, the initial controller parameters and the ideal controller parameters for the control scheme in Table 2.3 become:

| initial parameters                                   | ideal parameters                                    |
|--|---|
| $P = 529.13 D^2 + 8.9 \cdot 10^3 D + 5.9 \cdot 10^4$ | $P^* = 982.7 D^2 + 1.6 \cdot 10^4 D + 1 \cdot 10^5$ |
| $L = D + 98$   | $L^* = D + 99$                                      |
| $M = 5.9 \cdot 10^4$                                 | $M^* = 1 \cdot 10^5$                                |
| $\hat{\theta}_{\text{nl}} = 6$                       | $\theta_{\text{nl}} = 3$                            |

The linear parametric model for the plant parameter estimation is given by

$$\begin{aligned} \frac{D^2 y_{\text{p}}}{\Lambda_e} &= \theta_{\text{p}}^{\text{T}} \phi_{\text{p}} \quad \text{with} \\ \theta_{\text{p}}^{\text{T}} &= \left[ \frac{d_1}{m} \quad \frac{k_1}{m} \quad \frac{b}{m} \quad -\frac{b\theta_{\text{nl}}}{m} \right] \quad \text{and} \\ \phi_{\text{p}}^{\text{T}} &= \left[ -\frac{D y_{\text{p}}}{\Lambda_e} \quad -\frac{y_{\text{p}}}{\Lambda_e} \quad \frac{u}{\Lambda_e} \quad -\frac{\arctan\left(\frac{y_{\text{p}}}{10}\right)}{\Lambda_e} \right]. \end{aligned}$$

where the filter polynomial  $\Lambda_e(s)$  has been chosen to have two poles at  $-150$  and the remaining tuning parameters for the estimation method have been set to  $P_{\text{ls0}} = 10^5 I_{4 \times 4}$ ,  $\rho_r = 5 \cdot 10^4$  and  $\rho_s = 1$ .

The results for a similar simulation procedure as in Simulation Examples 2.1 and 2.2 are shown in Figure 2.6. In difference to the foregoing examples, the parameter adaptation

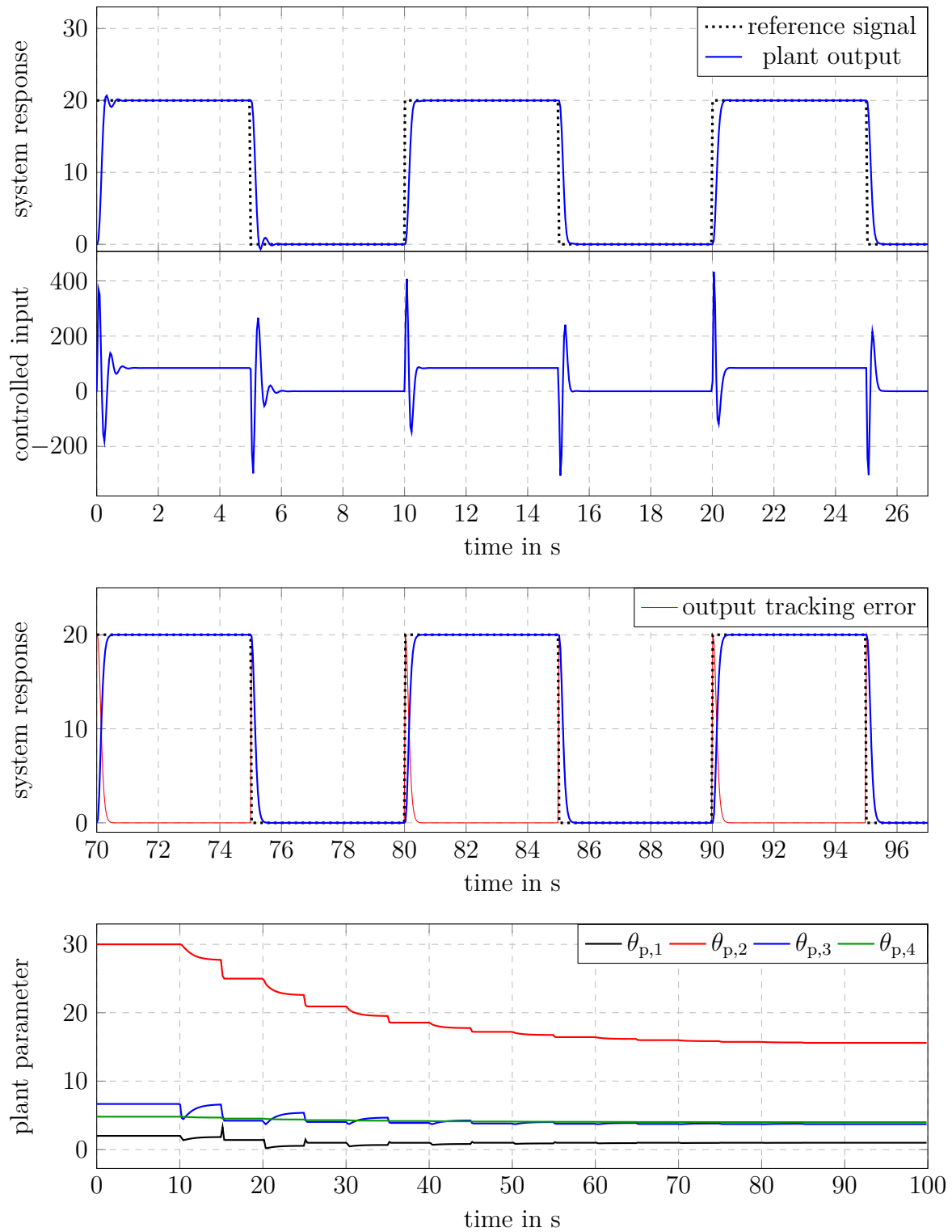


Figure 2.6: Results of Simulation Example 2.3 for APPC. First and second graph: System response and controlled input at beginning of adaptation. Third graph: Closed-loop response and output tracking error after 80s of adaptation. Fourth graph: Estimations of controller parameters.

has already been stopped after 90 seconds. The parameter adaptation is rather quick in this example so that a longer simulation is not necessary. Although the parameter estimation is very fast, undesired oscillations can not be observed in the system output or in the controlled input. In addition, the third graph in Figure 2.6 shows that the tracking error does not become larger after the adaptation has been switched off, which is a consequence of the integrator in the controller that has implicitly been introduced by the internal model  $Q(s)$ . This result shows that the APPC scheme is suitable for automatic-tuning purposes. As in the preceding examples, the parameter estimation is shown for a different reference signal that causes stronger excitation of the closed-loop in Appendix C.

### 2.2.4 Closed-Loop Reference Model (CRM)

In Remark 2.4 it has been mentioned that the choice of the gains for the parameter update laws in model reference adaptive control is not trivial. High adaptation rates will lead to high-frequency oscillations of the system and the estimated parameters as shown in [44, 94, 145]. On the other hand, slow adaptation rates will lead to high tracking errors at the beginning of adaptation. In order to improve this transient behavior in a systematic way, the closed-loop reference (CRM) model has been introduced and examined in [44].

For the control scheme given in Table 2.1 the CRM is defined as

$$\dot{x}_{\text{ref}} = A_{\text{ref}} x_{\text{ref}} + B_{\text{ref}} r - L_{\text{ref}} (x_{\text{p}} - x_{\text{ref}}), \quad (2.56)$$

where  $L_{\text{ref}} \in \mathbb{R}^{n \times n}$  is a gain matrix for the tracking error  $e = x_{\text{p}} - x_{\text{ref}}$ . As can be seen in (2.56), the tracking error  $e = x_{\text{p}} - x_{\text{ref}}$  is fed back to the reference model, so that a closed-loop system with feedback-gain  $L_{\text{ref}}$  results. Using the same procedure as in Section 2.2.1 with a CRM leads to the closed-loop equation

$$\dot{e} = (A_{\text{ref}} + L_{\text{ref}}) e + B_{\text{p}} \lambda \left( \tilde{K}_x^T x_{\text{p}} + \tilde{k}_r r - \tilde{\theta}_{\text{nl}}^T f_{\text{nl}}(x_{\text{p}}) \right) \quad (2.57)$$

of the tracking error dynamics. Stability of MRAC with CRM can be proven the same way as for MRAC with an open-loop reference model, if the Lyapunov equation

$$(A_{\text{ref}} + L_{\text{ref}})^T P + P (A_{\text{ref}} + L_{\text{ref}}) = -Q \quad \text{for } Q = Q^T > 0 \quad (2.58)$$

is satisfied. Furthermore, the properties stated in Theorem 2.1 also apply to state-feedback MRAC with CRM.

As the main benefit of a CRM it is shown in [44] for linear plants that the choices

$$\begin{aligned} \Gamma_x &= \gamma_c I_{n \times n}, \quad \gamma_r = \gamma_c, \\ L_{\text{ref}} &= -A_{\text{ref}} - g I_{n \times n}, \\ Q &= g I_{n \times n} \Rightarrow P = \frac{1}{2} I_{n \times n}, \end{aligned} \quad (2.59)$$

for the estimation gains and the CRM-gain with  $\gamma_c > 0$  and  $g = \gamma_c > 0$  lead to significant improvement of the transient closed-loop behavior in the sense of a reduced square integral



of the tracking error and the parameter derivatives with respect to time. It is also shown that the closed-loop response, as well as the parameter estimation, are less oscillatory. In [94] an alternative procedure is shown to tune  $L_{\text{ref}}$  which is similar to observer tuning.

Two different interpretations on how the CRM improves closed-loop performance can be given. The first one follows from equation (2.57) and the computation of  $L_{\text{ref}}$  in (2.59). It can be seen that the feedback of  $e$  to the reference model shifts the reference state  $x_{\text{ref}}$  in the direction of the plant state  $x_{\text{p}}$ . Hence, not only the closed-loop state approaches the reference state, but also the other way round. This, as it is stated in [44], reduces the burden of tracking on the adaptive system. The second interpretation is adopted from arguments of observer-based control. From equation (2.57) it follows that  $L_{\text{ref}}$  can be chosen such that the stable dynamics of the tracking error is faster than that of the open-loop reference model. Hence, the tracking error is reduced faster than the closed-loop system is desired to respond to the reference signal  $r$ . This reduces the influence of the transients of  $e$  on the closed-loop system. A similar argument stems from observer based control where the dynamics of the observer is demanded to be faster than that of the closed-loop system in order to reduce the influence of the observer error transients on the closed-loop system (see e.g. [60, 100]).

Application of state-feedback MRAC with CRM is very similar to MRAC with open-loop reference model in Table 2.1. It is only necessary to replace the reference model equation and the Lyapunov equation by (2.57) and (2.58), respectively. Calculation of  $L_{\text{ref}}$  can then be done by (2.59). Similar results for output-feedback MRAC with CRM can be found in [43].

**Simulation Example 2.4.** In order to compare MRAC for state-feedback with and without closed-loop reference model, the plant  $G_{\text{ex1}}$  from Example 2.1 is considered. The initial estimates of the parameters, as well as the requirements on the closed-loop are also adopted from Example 2.1. The remaining tuning parameters have been chosen to be  $Q = I_{2 \times 2}$ ,  $\Gamma_x = \Gamma_{\text{nl}} = 200 I_{2 \times 2}$  and  $\gamma_r = 200$ . Note that the estimation gains are 2000 times larger than in Example 2.1. The closed-loop reference model becomes

$$\dot{x}_{\text{ref}} = \begin{pmatrix} 0 & 1 \\ -100 & -20 \end{pmatrix} x_{\text{ref}} + \begin{pmatrix} 0 \\ 100 \end{pmatrix} r - L_{\text{ref}} (x_{\text{p}} - x_{\text{ref}}), \quad (2.60)$$

where

$$L_{\text{ref}}^{\text{T}} = \begin{pmatrix} -2 & -1 \\ 100 & 18 \end{pmatrix}$$

has been computed according to (2.59) with  $g = 200$ . The simulation results are shown in Figure 2.7, where the results for MRAC with standard reference model are depicted in the left column.

A first difference of the CRM can be seen in the system response at the beginning of adaptation in the first graph of Figure 2.7. The responses of the CRM and the closed-loop system do not differ, even before adaptation is started at  $t = 10\text{s}$ . The reason for that is the feedback of  $x_{\text{p}}$  to the reference model in (2.4) which pulls the reference trajectories closer to the plant trajectories. Another difference can be observed for the controlled input of the plant, which is shown in the second graph. For the standard

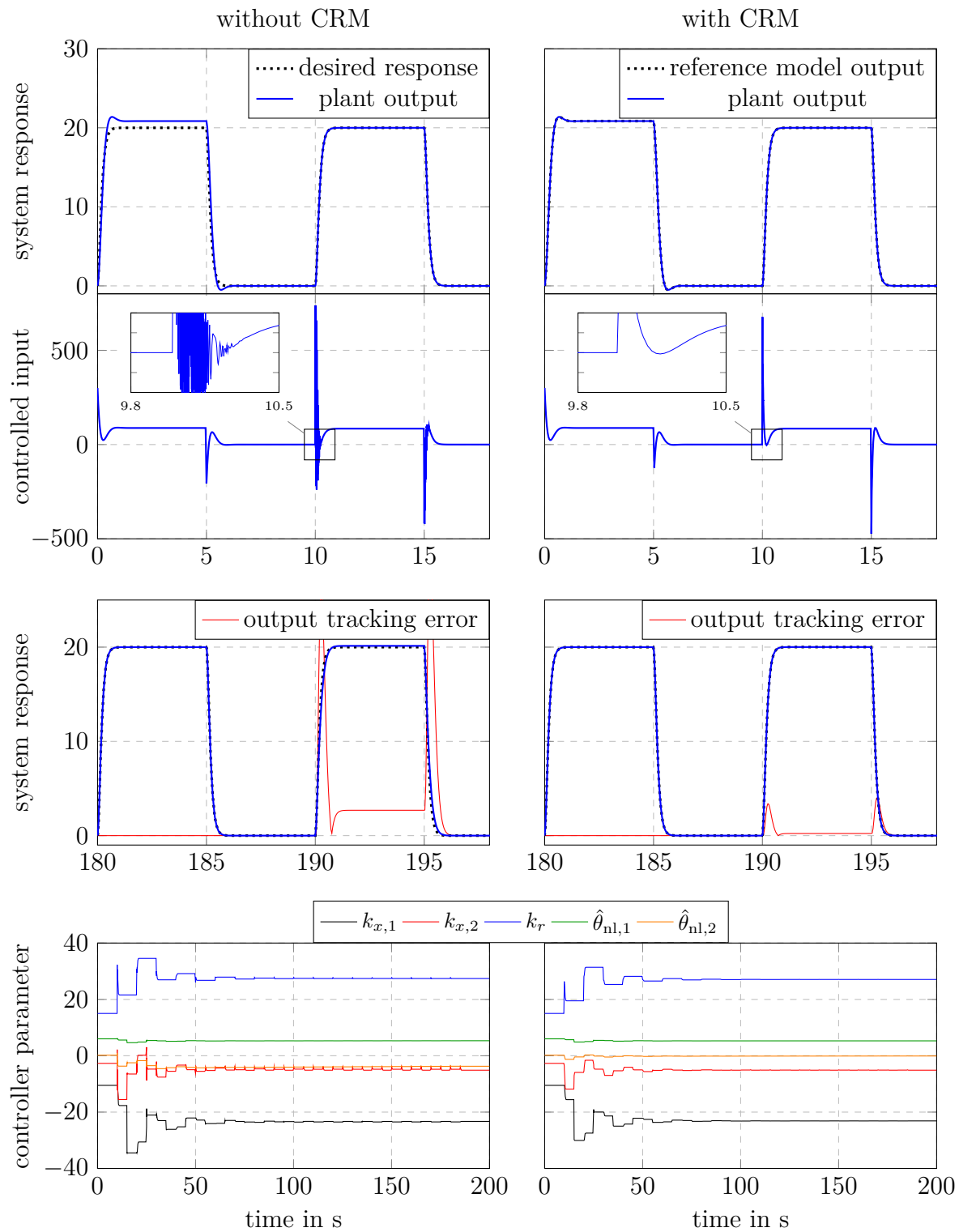


Figure 2.7: Comparison of MRAC with and without CRM. First and second graph: System response and controlled input at beginning of adaptation. Third graph: Closed-loop response and output tracking error after 180s of adaptation. Fourth graph: Estimations of controller parameters.

MRAC strong oscillations occur, which are even stronger than in Example 2.1 due to the higher estimation gain. In contrast to that, the controlled input of MRAC with CRM shows no oscillations at all. This is a great improvement, since for technical systems strong oscillation can be critical for actuators or other wear parts of the system. Finally, the last graph of Figure 2.7 shows that parameter estimation with CRM is quicker in this example and results in less oscillatory peaks of the estimated parameters. After adaptation is switched off at  $t = 190s$  the scaled tracking error  $\bar{e}_y = 20(x_{p,1} - x_{ref,1})$  is smaller for the closed-loop system with CRM as can be seen in the third graph of Figure 2.7. Note that the scaled tracking error for MRAC with CRM as well as for standard MRAC has been computed with  $x_{ref,1}$  of the constant reference model (2.14) in order to guarantee comparability.

## 2.2.5 Robustness of Adaptive Control

The plant descriptions  $G_{nl}$  in (2.3),  $G_{nl2}$  in (2.41), and  $G_{lin}$  in (2.15) are models of real processes. Modeling such processes always involves neglecting some characteristics of it such as nonlinearities or dynamics at high frequencies, which are often referred to as unmodeled dynamics. In addition, the process inputs and outputs are usually corrupted by noise and disturbances of rarely known frequency and amplitude. Since neither unmodeled dynamics nor noise or unknown disturbances can be represented by the introduced plant models, none of these effects is considered in the controller synthesis presented in Sections 2.2.1-2.2.4.

Unfortunately, unmodeled dynamics, noise, and disturbances have unselectable influence on the robustness of adaptive systems. For adaptive controllers, it has been shown in [136], that unmodeled dynamics can lead to unstable closed-loop responses due to diverging parameter estimations. Instability can also be caused by disturbances on the adaptive system [11, 60], even if the disturbances act as noise on the inputs or outputs of the process. For indirect adaptive control systems, these effects can be explained in an intuitive way as follows. For the recursive plant model identification, the available plant parameters are defined in advance by defining the linear parametric model (2.51). The definition of a plant model always involves negligence of plant dynamics, for example at high frequencies, in order to keep the model as simple as possible. However, if the plant is excited such that the unmodeled dynamics contribute to the plant output, the plant behavior can not be represented by the model. For the least squares algorithm in (2.52), this would lead to an estimation error  $\epsilon \neq 0$  and hence to a parameter update. Since this update would not stop as long as the unmodeled dynamics contribute to the plant output, parameter divergence results. Similar interpretations can be given for disturbances and measurement noise.

Some known extension of adaptive algorithms can be used to make the adaptive system robust against unmodeled dynamics, noise, and disturbances. These can be found e.g in [11, 60, 116, 147]. The idea of these extensions is shortly given below, where the general notion of modeling errors is used for unmodeled dynamics, noise, and disturbances.

## Leakage

Leakage modifications introduce an additional term in parameter update laws, like (2.11) or (2.52), that prevents the estimated parameters to become unbounded. Loosely speaking, an additional leakage term is introduced, that pushes the estimated parameters back in a certain parameter space, when the estimations become too large. In terms of Lyapunov stability, the leakage term in the update law guarantees the derivative of the Lyapunov function with respect to time to become negative when the parameter estimations exceed certain bounds.

Three different leakage modifications are well known in the literature. The  $\sigma$ -modification [59] is the simplest method that guarantees boundedness of the parameters, but does not preserve the properties of the original estimation schemes. Most important, the  $\sigma$ -modification generates nonzero estimation errors, even in the absence of modeling errors [116]. The method of  $e_1$ -modification [115] was shown to recover the possibility of nonzero estimation errors, but only if the plant is persistently excited. The third method, called switching  $\sigma$ -modification [55], preserves all ideal properties of the original estimation schemes at the cost of the knowledge of an admissible convex set for the estimated parameters.

## Dead Zone

If the estimation error  $\epsilon$  of the parameter update law is small, modeling errors will have a dominant influence on  $\epsilon$ . In order to prevent a parameter update based on modeling errors, the estimation of the plant parameters can be stopped, if the estimation error is small. This results in a dead zone for the parameter updates, which has to be defined with a known upper bound for the modeling errors. A parameter update modified by a suitable dead zone guarantees the estimated parameters to be bounded, but a convergence of the estimation error to zero can not be established [60, 116].

## Parameter Projection

In most practical applications, the plant parameters and therefore also the ideal controller parameters are known to lie in a convex set  $\mathcal{S}$ . A simple idea to keep the parameters in this set is given by the parameter projection. As long as the parameters are inside  $\mathcal{S}$ , the original parameter update law stays unchanged. If the estimated parameters get outside of  $\mathcal{S}$ , they are projected on the boundary  $\delta\mathcal{S}$  of the set. For the least-squares algorithm

in (2.52) the parameter projection is given in [60] by

$$\begin{aligned} \dot{\hat{\theta}}_p &= \begin{cases} P_{ls} \in \phi_p, & \hat{\theta}_p \in \mathcal{S} \\ & \text{or } \hat{\theta}_p \in \delta\mathcal{S} \text{ and } (P \in \phi_p)^T \nabla g \leq 0, \\ P_{ls} \in \phi_p - P_{ls} \frac{\nabla g \nabla g^T}{\nabla g^T P_{ls} \nabla g} P_{ls} \in \phi_p, & \text{otherwise,} \end{cases} \\ \dot{P}_{ls} &= \begin{cases} -\frac{P_{ls} \phi_p \phi_p^T P_{ls}}{1 + \phi_p^T \phi_p}, & \hat{\theta}_p \in \mathcal{S} \\ & \text{or } \hat{\theta}_p \in \delta\mathcal{S} \text{ and } (P \in \phi_p)^T \nabla g \leq 0, \\ 0, & \text{otherwise,} \end{cases} \end{aligned} \quad (2.61)$$

$$P_{ls}(0) = P_{ls0}, \quad P_{ls}(t_r) = \rho_r,$$

where  $g(\hat{\theta}_p)$ , defines the known set as  $\mathcal{S} = \{\hat{\theta}_p \in \mathbb{R}^p \mid g(\hat{\theta}_p) \leq 0\}$  and  $\nabla g$  is the gradient of  $g$ . The parameter projection in (2.61) preserves all the properties of the least-squares algorithm given in Appendix A ([60]). Parameter projection for MRAC can be found in [84, 94].



# Chapter 3

## Adaptive Systems with Input Saturation

In the previous chapter, basic adaptive control methods have been introduced with necessary extensions that address transient performance as well as issues with unmodeled dynamics, noise, and disturbances. However, the presented methods are not well suited for constraints on the plant input. Since the input of real technical systems is always limited due to physical constraints on the actuators, application of adaptive control requires a suitable consideration of these constraints.

In the subsequent chapters of this work, limitations of the input amplitudes in adaptive systems are considered. It is well known that input limitations can lead to undesired closed-loop behavior like oscillations and slow convergence to steady state values even for controllers without adaptation [52, 150]. These effects have firstly been attributed to windup of the integral part of the controller, which has been examined and treated e.g. in [21, 45, 157, 158]. However, not only the integral part can cause undesired closed-loop behavior, but also eigenvalues of the controller close to the imaginary axis [52]. Moreover, the properties of the controlled plant itself can give rise to windup effects if the maximal input amplitude is too small to control all states of the plant with a desired dynamic. A good example of such effects can be given in terms of the mechanical plant introduced in Simulation Example 2.1 in the following way. A fast position control of the mechanical plant  $G_{\text{ex1}}$  requires a high velocity of the plant. Close to the desired position the velocity needs to be reduced very quickly in order to stop the plant in time. However, if the maximal available force is too small to reduce the velocity quick enough, the plant will overshoot and might oscillate around the desired position. This effect is called plant windup in [52]. Most importantly, if an unstable plant is subjected to input saturation, the feasible plant states are restricted to lie in a certain region, since the range of the input amplitude is not sufficient to stabilize the plant at arbitrarily large set points [52, 150].

A lot of different anti-windup strategies exist that deal with the effects of windup in different ways. The publication in [18] shows a bibliography of theoretical and practical results for control of systems with input constraints up to the year 1995. Modern anti-

windup strategies, as can be found e.g. in [42, 149–151], introduce additional degrees of freedom in order to allow for closed-loop performance improvements as shown in [122, 123].

Additional effects of input saturation can be observed in adaptive systems, where the parameter estimations represent additional closed-loop states that can cause windup. Consequently, even if a constant controller results in an acceptable closed-loop behavior, an adaptive version of it can cause undesired effects, which require special consideration. This chapter builds the basis for the derivation of a new anti-windup method for adaptive systems that addresses the windup phenomena under consideration of the closed-loop performance. The chapter is structured as follows. Several effects of input saturation which can occur if the limited input is not explicitly considered in adaptive and non-adaptive closed-loop systems, are explained and presented in Section 3.1 based on simulation examples. The method of model recovery anti-windup (MRAW) addresses these issues for the case of known plant parameters and is presented in Section 3.2. The basic concept of MRAW will be used in Chapter 4 to derive a new anti-windup scheme for adaptive systems. The transition to adaptive systems comes in Section 3.3, where an overview of already existing adaptive control methods for input saturated systems is given. An especially well-suited method for MRAC is then presented in detail in Section 3.4. Its basic concept is combined with MRAW for the derivation of the new adaptive anti-windup scheme in Chapter 4. Finally a conclusion in Section 3.5 sums up the findings of this chapter.

### 3.1 Effects of Input Saturation on Adaptive Systems

Before the effects of input limitations will be illustrated with an exemplary plant, a definition of the input saturation is necessary. A limitation of the input amplitude is considered as

$$u_{\text{lim}}(t) = \text{sat}_{u_{\text{max}}}(u(t)) \triangleq \begin{cases} u(t) & \text{if } |u(t)| \leq u_{\text{max}}, \\ u_{\text{max}} \text{sign}(u(t)) & \text{otherwise,} \end{cases} \quad (3.1)$$

with the maximal input amplitude  $u_{\text{max}} > 0$ . If this saturation limits the input of the plant  $G_{\text{nl}}$  in (2.3), the plant description becomes

$$G_{\text{nls}} : \quad \dot{x}_{\text{ps}} = A_{\text{p}} x_{\text{ps}} + B_{\text{p}} \lambda \left( u_{\text{lim}} + \theta_{\text{nl}}^{\text{T}} f_{\text{nl}}(x_{\text{ps}}) \right). \quad (3.2)$$

Note that the “s” in the subscript of  $G_{\text{nls}}$  stands for “saturation” and will be used frequently in the sequel in order to specify an already defined plant, where an input saturation has been introduced.

In order to illustrate some effects of saturation on the closed-loop behavior, a linear version of  $G_{\text{nls}}$ , i.e.  $\theta_{\text{nl}} = f_{\text{nl}} = 0$ , is considered. The explicit description of the plant for the simulation examples in this section is given by

$$G_{\text{ex4}} : \quad \dot{x}_{\text{ps}} = \begin{pmatrix} 0 & 1 \\ 2 & 2 \end{pmatrix} x_{\text{ps}} + \begin{pmatrix} 0 \\ 3.7 \end{pmatrix} u_{\text{lim}}, \quad (3.3)$$



which has a stable pole at  $-0.73$  and an unstable pole at  $2.73$ . The maximal input amplitude of  $u_{\text{lim}}$  in  $G_{\text{ex4}}$  is given by  $u_{\text{max}} = 100$ . A mechanical interpretation of the plant (3.3) like in Figure 2.3 would require the introduction of a negative stiffness and a negative damping, which does not exist for real technical systems. However, the introduced plant in (3.3) is a good example to illustrate multiple effects of saturation with a single system. As the desired closed-loop behavior a reference model

$$\dot{x}_{\text{ref}} = \begin{pmatrix} 0 & 1 \\ -484 & -44 \end{pmatrix} x_{\text{ref}} + \begin{pmatrix} 0 \\ 484 \end{pmatrix} r \quad (3.4)$$

is defined, which has two real poles at  $-22$  and a steady-state gain of one for  $x_{\text{ref},1}$ . The reference signal has been chosen as a step sequence like in Example 2.1.

A first effect of the limited input amplitude is shown in Figure 3.1, where the adaptation for a state-feedback MRAC from Table 2.1 has been switched off, and the controller parameters are set to their ideal values  $K_x^{*\text{T}} = [-131.35 \quad -12.43]$  and  $k_r^* = 130.81$ , which can be computed with the matching equations (2.6). It can be seen that the input

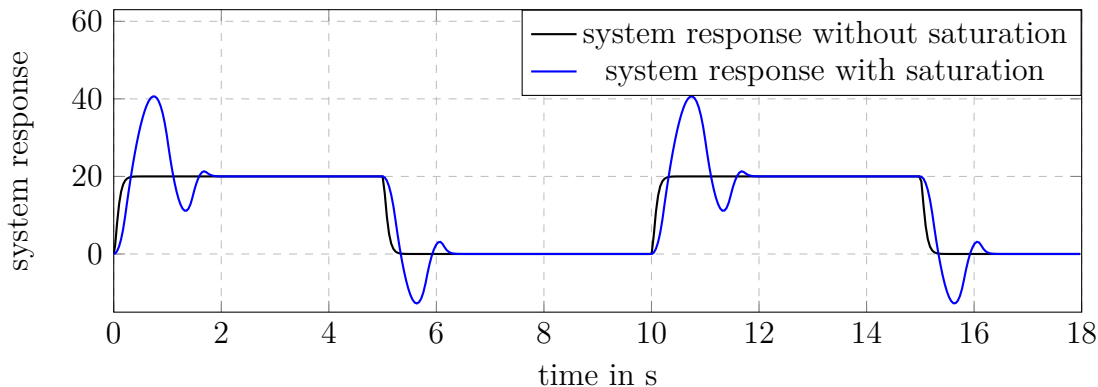


Figure 3.1: MRAC with ideal and constant controller parameters applied to the unstable input saturated plant  $G_{\text{ex4}}$ .

limitation leads to an oscillatory closed-loop response, which leads to an increased settling time. In addition, the rise time of the closed-loop with saturation is higher than specified by the reference model, which is an expected effect, since the available input energy is less than in the unsaturated case. Both effects, the slower convergence to the desired set points as well as the oscillatory behavior reduces the closed-loop performance and can also appear if the parameter adaptation is activated as it is shown in Section 3.4. An even more critical effect of saturation is shown in the simulation results for initial conditions  $x_{\text{ps}}^{\text{T}}(0) = [0 \quad 50]$  of the plant states in Figure 3.2. The range of the input amplitude is too small to stabilize the unstable open-loop plant with these initial conditions, so that the closed-loop trajectories become unstable.

Since the estimated parameters of MRAC introduce new states in the closed-loop system, their initial values are as important for the closed-loop stability as the initial values of the other closed-loop states. In order to illustrate that statement, the initial plant parameters have been set to  $x_{\text{ps}}^{\text{T}}(0) = [0 \quad 25]$  and adaptation has been activated at the beginning of

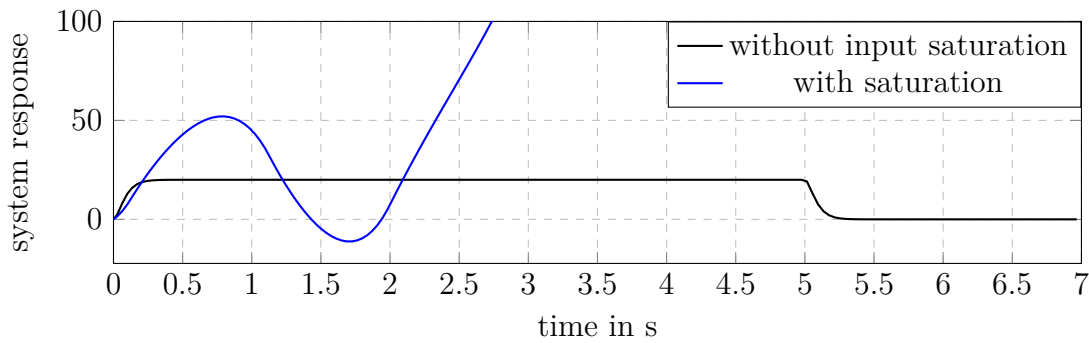


Figure 3.2: MRAC with ideal and constant controller parameters applied to the unstable input saturated plant  $G_{\text{ex4}}$ , with inappropriate initial conditions for the plant state.

simulation. This has been done in two experiments, where the initial parameter estimates have firstly been chosen to be the ideal controller parameters. In the second experiment the initial parameter estimations have been set to  $k_r(0) = 250$  and  $K_x(0) = K_x^*$ . In both experiments the parameter update gains have been set to  $\Gamma_x = 0.1 I_{2 \times 2}$ ,  $\gamma_r = 0.1$  and  $\gamma_\Delta = 0.1$ . The system responses of both simulation examples and an additional simulation without saturation are shown in Figure 3.3. It can be seen that the closed-loop system

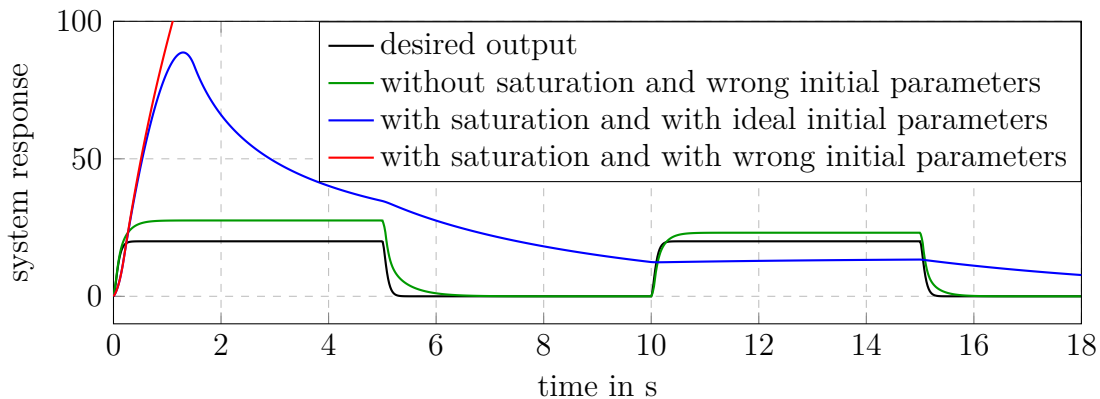


Figure 3.3: Comparison of simulation results for MRAC without anti-windup and with different initial conditions for the controller parameters.

stays stable, if the initial parameter estimates are given as the ideal parameters. In difference to that, the wrong initial condition for the parameter  $k_r$  renders the closed-loop system unstable. The reason for the instability can be explained as follows. For unstable plants the uncertainty of the plant parameters might lead to initial controller parameters that do not stabilize the closed-loop system or leads to a system response, that is very different from the response of the reference system. Hence, the states of the plant might grow until they are in a region, where the range of the input amplitude is not sufficient anymore to stabilize the closed-loop system with the available range of the input amplitude. That means, even if the controller parameters has become equal to their ideal values in the meantime, there is no chance to stabilize the closed-loop system. The

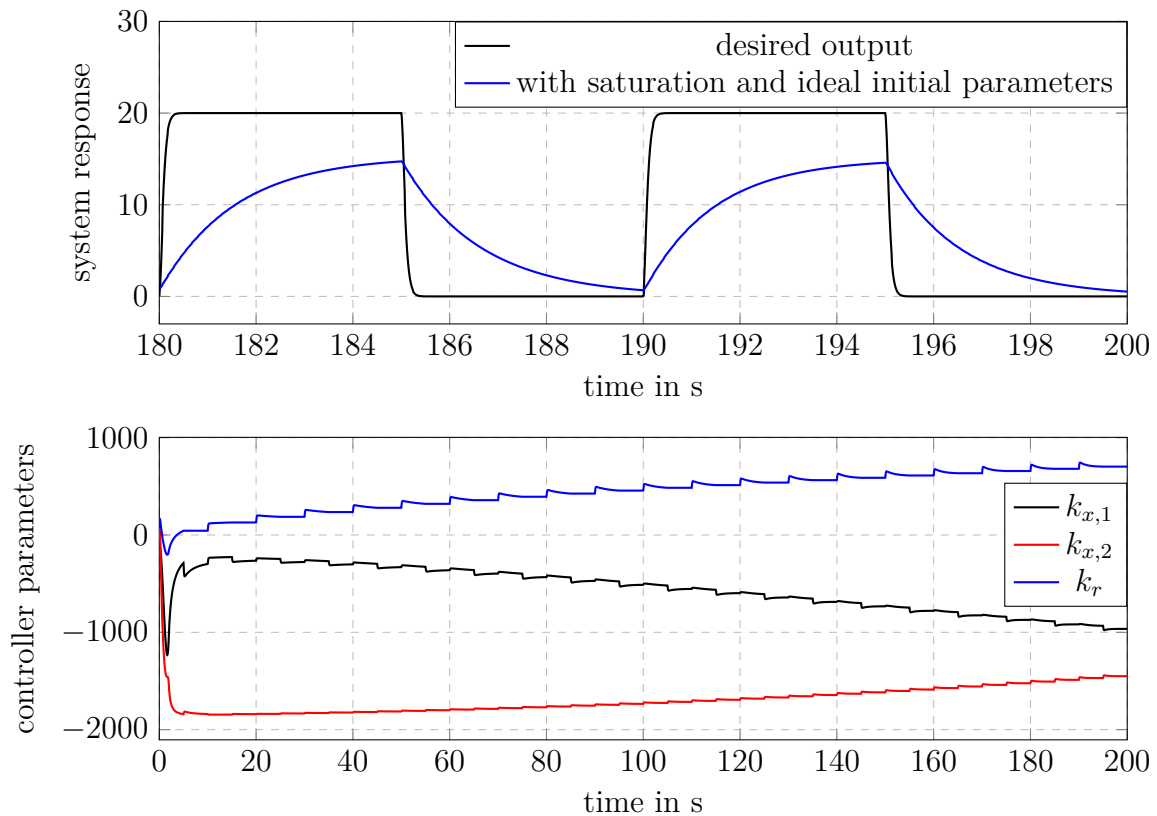


Figure 3.4: Simulation results of the parameter estimations for MRAC without anti-windup applied to  $G_{\text{ex4}}$ .

initial conditions of the controller parameters are therefore also crucial for the closed-loop stability.

With ideal initial parameters, the closed-loop system stays stable, but the performance becomes very bad as can be seen at the beginning of adaptation in Figure 3.3. Further simulation of this example leads to the results depicted in Figure 3.4, where the system response of  $G_{\text{ex4}}$  controlled by MRAC is shown for the last 20 seconds of simulation. In addition, the estimated parameters are shown for the whole time of simulation. It can be seen that the system output after 180s of adaptation is still bounded, but is very different from the output shown in Figure 3.1 with constant ideal controller parameters. The reason for that are the quickly diverging parameter estimations. Based on the plant description of  $G_{\text{nls}}$  in (3.2) this additional effect of input saturation on adaptive systems without an anti-windup method can be explained in a general way as follows. It is assumed that the adaptive controller from Table 2.1, parametrized with the ideal parameters  $K_x^*$ ,  $k_r^*$ , and  $\theta_{\text{nl}}$  that satisfy (2.6), is applied to  $G_{\text{nls}}$ . It is further assumed that the given reference signal  $r$  leads to saturation of the controlled input, i.e.  $|u| > u_{\text{max}}$ , during changes of set points. Therefore, the input is saturated for limited periods of time  $t_{\text{sat}} = \{t \in \mathbb{R} \mid |u(t)| > u_{\text{max}}\}$ . From (2.5) and (2.6) it follows that the closed-loop system can only follow the reference model  $G_{\text{ref}}$  perfectly if the controlled input is equal to the ideal control input  $u^*$ . However, this can not always be achieved due to the saturation, which leads to a tracking error

$e = x_{\text{ps}} - x_{\text{ref}} \neq 0$ , that will not vanish if  $t \in t_{\text{sat}}$ . This in turn will lead to updates of the estimated parameters, as can be seen in the parameter update laws (2.11). Hence, the controller parameters will be updated, even if they are equal to their ideal values. Since the tracking error can not become zero with any values of the parameters as long as the input is saturated, the parameters will diverge as they do in the simulation results shown in Figure 3.4. This will be referred to as parameter windup in the following.

All the effects of input saturation described above are clearly undesired. Therefore, a proper consideration of input saturation is always necessary in order to avoid the presented effects. Different existing methods that address input constraints are presented in the subsequent sections of this chapter. A way to consider input constraints in non-adaptive systems is presented in the directly following section and will be extended to adaptive systems in Chapter 4.

## 3.2 Model Recovery Anti-Windup (MRAW)

This section briefly explains the basic concept of model recovery anti-windup for the case of known plant parameters. Note that the presentation of MRAW is done in an intuitive way in this section. Formal proofs and derivations for MRAW can be found in [42, 122, 149, 151, 155] and the references therein. It is worth mentioning that MRAW in this section is introduced for plants with known parameters so that no adaptation is necessary. The concept of the presented method is used in Chapter 4 to derive a novel adaptive anti-windup scheme.

The linear plant

$$G_{\text{lins}} : \begin{aligned} \dot{x}_{\text{ps}} &= A_{\text{p}} x_{\text{ps}} + B_{\text{p}} u_{\text{lim}}, \\ y_{\text{ps}} &= C_{\text{p}} x_{\text{ps}}, \end{aligned} \quad (3.5)$$

with a limited input amplitude is considered, where all parameters of  $A_{\text{p}}$ ,  $B_{\text{p}}$ , and  $C_{\text{p}}$  as well as the maximal input amplitude  $u_{\text{max}}$  as defined in (3.1) are assumed to be known. Note that the following discussion applies for output-feedback as well as state-feedback, i.e.  $C_{\text{p}} = I$ .

It is assumed that a suitable controller  $C_{\text{k}}$  for the unsaturated plant  $G_{\text{lin}}$  is available, so that the closed-loop system without input saturation satisfies the performance requirements. Hence, the controller design of  $C_{\text{k}}$  does not involve consideration of the input saturation. The method of MRAW allows to avoid or at least reduce windup phenomena by an extension of the closed-loop system without the need of a modification of  $C_{\text{k}}$ . This extension of the closed-loop system is depicted in Figure 3.5 and is described below.

For the explanation of the anti-windup scheme the effect of saturation on the input of the plant is considered as an input disturbance

$$\Delta u = u_{\text{lim}} - u, \quad (3.6)$$

which can be calculated with the knowledge of  $u_{\text{max}}$  of the saturation (3.1). Note that  $\Delta u$  describes that part of the amplitude of  $u$  that can not be applied to the plant due to

saturation. As the first part of the anti-windup scheme, the negative of the disturbance signal  $-\Delta u$  is fed into the model

$$M_G : \begin{aligned} \dot{x}_{aw} &= A_p x_{aw} + B_p (u_{aw} - \Delta u), \\ y_{aw} &= C_p x_{aw}, \end{aligned} \quad (3.7)$$

inside the anti-windup scheme, which represents the plant dynamics of  $G_{lin}$  without saturation. The output  $y_{aw}$  of  $M_G$  is added to the measured plant output  $y_{ps}$  and the resulting signal is fed back to the controller  $C_k$ . As the second part of MRAW, an anti-windup controller  $C_{kaw}$  is considered in the anti-windup scheme. Since the computation of  $x_{aw}$  is done with the model (3.7), the anti-windup controller has access to the complete anti-windup state  $x_{aw}$ . The explicit structure of  $C_{kaw}$  is not important for the basic idea of MRAW and is therefore not defined in this section. Feedback of the anti-windup control signal  $u_{aw}$  to  $M_G$  builds a closed-loop system inside of the anti-windup structure. Moreover, the controller output  $u_{aw}$  is subtracted from the output  $u_c$  of the original controller, so that the unsaturated input becomes  $u = u_c - u_{aw}$ .

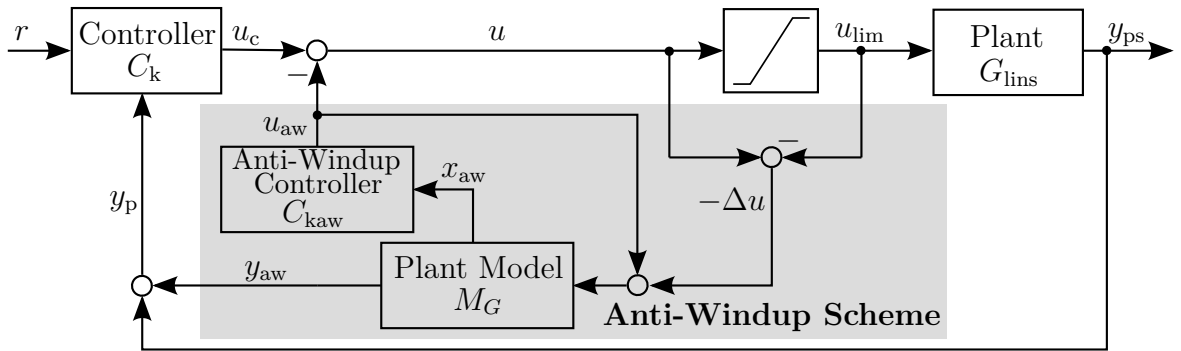


Figure 3.5: Basic structure of model recovery anti-windup.

It follows from Figure 3.5 and its description above, that MRAW manipulates two signals of the original closed-loop system. The benefit of adding  $y_{aw}$  to  $y_{ps}$  becomes clear, when actually doing the summation of the respective equations (3.5) and (3.7)

$$\begin{aligned} \dot{x}_{ps} + \dot{x}_{aw} &= A_p (x_{ps} + x_{aw}) + B_p u_c, \\ y_{ps} + y_{aw} &= C_p (x_{ps} + x_{aw}), \end{aligned} \quad (3.8)$$

where  $u_{lim} = u_c - u_{aw} + \Delta u$  has been substituted in (3.5). Since the only input  $u_c$  of the resulting system in (3.8) is the same as for  $G_{lin}$ , the output  $y_p$  of the system without input limitation is recovered by the summation under the assumption of known initial conditions<sup>1</sup> of  $x_{aw}$ . More precisely, it is achieved that  $x_{ps} + x_{aw} = x_p$  and  $y_{ps} + y_{aw} = y_p$ , which results in the same feedback to the original controller  $C_k$ , as if it was applied to  $G_{lin}$ .

<sup>1</sup>The assumption of known initial conditions for  $x_{aw}$  is not restrictive for practical use of the anti-windup scheme. When a technical system is put into operation, no influence of past input limitations are present, so that  $x_{aw}(0) = 0$ .

Since the effect of saturation on the input is represented by the input disturbance  $\Delta u$  and the output of the anti-windup scheme is a result of its external input  $-\Delta u$ , the signal  $y_{aw}$  can be interpreted as the effect of the saturation on the plant output  $y_{ps}$ , but with inverted sign. Therefore, the summation  $y_{aw} + y_{ps}$  can be taken as a subtraction of the saturation influence from the plant output. It has been illustrated in Section 3.1 that the influence of saturation often leads to a degradation of the closed-loop performance. For this reason the effect of saturation on the plant output, which is represented by  $y_{aw}$ , is subsequently referred to as the unwanted behavior.

The method of MRAW addresses the closed-loop performance by introducing the anti-windup controller  $C_{kaw}$ . This controller is supposed to efficiently regulate the unwanted behavior  $y_{aw}$  to zero and therefore to recover the behavior of the closed-loop system without saturation as good as possible. It has to be designed such that the behavior due to the disturbance  $-\Delta u$  inside the anti-windup scheme is regulated by the control signal  $u_{aw}$ . Since the unwanted behavior of the plant is a result of the input disturbance  $\Delta u$ , the anti-windup control signal with inverted sign  $-u_{aw}$  is supposed to reduce the influence of saturation on the closed-loop system. Hence, the control signal  $u$  consists of the original signal  $u_c$ , which is supposed to realize the desired performance when the input is not saturated, and the anti-windup signal  $-u_{aw}$ , which is supposed to reduce the unwanted behavior when saturation is actually encountered.

From the description of MRAW above and Figure 3.5 it follows that the complete anti-windup scheme can be described by the equations

$$\begin{aligned} \dot{x}_{aw} &= A_p x_{aw} - B_p (\Delta u - u_{aw}), \\ y_{aw} &= C_p x_{aw}, \\ u_{aw} &= C_{kaw}(x_{aw}). \end{aligned} \tag{3.9}$$

A summary of MRAW can be given as follows. A plant model in the anti-windup scheme is used to calculate the effect of saturation. Removing this effect from the plant output makes it invisible for the controller  $C_k$ . This allows the controller to work as if no input saturation was present. In addition, an anti-windup controller  $C_{kaw}$  is designed to eliminate the effect of input saturation independently of the original plant controller  $C_k$ . Therefore, the anti-windup controller is highly relevant for the closed-loop performance if input saturation occurs. However, choosing an explicit structure and the corresponding parameters of  $C_{kaw}$  is not trivial. Systematic ways to tune the anti-windup controller for known plant parameters in order to achieve a good closed-loop performance are given e.g. in [122–124, 155] and require the solution of convex optimization problems and the knowledge of the plant parameters.

No simulation example for MRAW is presented in this section since a lot of simulations and experimental results are shown in Chapters 5 and 6, which will illustrate the properties of the anti-windup method.

### 3.3 Existing Adaptive Control Methods for Systems with Input Saturation

This section represents the transition to anti-windup methods for adaptive systems. After the excursus to a non-adaptive method in the foregoing section, adaptive anti-windup methods from the literature are presented here and references to the respective publications are stated. Since this section is intended to give an overview of the basic ideas, it is not restricted to continuous time methods but begins with a short introduction of discrete time methods. After that, methods suitable for the adaptive control schemes presented in Chapter 2.2 are summarized. It is distinguished between practical approaches which are only valid for very particular problems, approaches for indirect adaptive control schemes, and approaches for direct adaptive control schemes.

For discrete time adaptive control the computation of the control signal and the parameter updates is based on current and past values of the plant output and input [46, 47]. In order to deal with input limitations, these computations have to be done with the limited values of the past inputs, as stated in [1, 2, 9, 37, 132, 163]. It is therefore guaranteed that the computations are done with the input values which have actually been applied to the plant. The methods in [1, 2] extend this concept by an adjustment of the reference trajectories to make them feasible for the closed-loop system. The reference signal does therefore represent a trajectory which can actually be achieved by the closed-loop system even with the limited input amplitude. This approach has been proven to lead to bounded closed-loop signals if it is applied to stable open-loop plants. A similar procedure and stability result is given in [132]. A slightly stronger stability result for the same approach for discrete-time adaptive control of plants with limited input amplitude can be found in [168] and [167]. It is shown there that the control scheme results in a stable closed-loop system, if it is applied to plants with at most one pole on the unit circle, whereas all other poles lie strictly inside the unit circle. This result is extended in [37] to plants with multiple poles on the unit circle. The discrete-time adaptive control scheme presented in [9] is based on the same concept as the schemes mentioned before. However, it guarantees boundedness of the closed-loop signals, if it is applied to stable input saturated plants. If the plant is unstable, the closed-loop can be shown to have bounded trajectories if the initial conditions of the closed-loop signals do not exceed certain values. Therefore this scheme can also be applied to plants with poles outside the unit circle if the closed-loop initial conditions are admissible.

A slightly different anti-windup approach for discrete-time adaptive control is proposed in [125]. The presented method adjusts the reference model of a discrete-time model reference adaptive controller during operation. This is done in a way such that it stays asymptotically stable and minimizes the settling time, under the condition that the closed-loop plant can follow this reference model without violating maximal input values and maximal increments of the input value. However, no explicit algorithm is given to calculate such a reference model for a general plant, which makes the algorithm to a rather heuristic approach. Even the authors of [125] state that such an algorithm is not straight forward

to realize. Therefore, the given global stability result is only valid, if an algorithm can be found for a given plant.

Rather practical approaches have also been developed for continuous time adaptive control of plants with a limited input amplitude. These include deactivation of the parameter estimation during phases of a saturated input as in [73], which is equivalent to switching to a constant controller during saturation. Combined with the methods in Section 2.2 it can, therefore, be shown that this approach results in bounded closed-loop signals if it is applied to an open-loop stable plant. The same method is proposed in [126], where the authors additionally propose to add a leakage term to the parameter estimation in order to minimize parameter windup effects. In [20] multiple practical anti-windup methods are compared for an aircraft model. The first method scales the controlled input until it satisfies the constraints while preserving the input direction. It is also proposed there to modify the reference signal and the reference model in order to relax the control requirements. Finally, the authors of [20] propose an anti-windup scheme that is based on the re-calculation of an input that fulfills the constraints and results in an acceleration of the aircraft, which is as similar as possible to an acceleration produced by the unconstrained input. A comparison of simulations for the different approaches results in similar performance for all methods proposed in [20].

An early analysis of classical indirect adaptive control of continuous time input limited systems can be found in [38]. The authors use the filtered limited input for calculation of the control signal and the parameter estimations. This is similar to the approach for discrete-time methods since the limited input which is actually applied to the plant is used for further computations. Boundedness of the closed-loop signals can be shown for stable plants with at most one pole at the origin. A first approach to introduce the method of MRAW in indirect adaptive control has been presented in [69] for plants with measurable states. In this work the authors extend an adaptive linear quadratic controller by MRAW and show boundedness of all closed-loop signals if the open-loop plant is asymptotically stable. However, the method requires the solution of linear matrix inequalities during operation, which is connected to high computational effort. The method is extended to input rate saturation in [70] and applied to soaring control of a glider in [71, 72].

For continuous time direct adaptive control of plants with limited input amplitudes three main anti-windup concepts from the literature can be distinguished. The first concept is based on modifications of the parameter update laws, such that the adaptive control scheme is applicable to input saturated plants [3, 159]. This concept mainly prevents the estimated parameters from diverging. The second concept deals with input saturation by modifying the reference signal, such that the closed-loop system can follow the reference without violating the maximal input amplitude. For the respective method in [32] no stability result is given. In difference, the method presented in [95, 96], which can be applied to input affine nonlinear system, guarantees boundedness of the closed-loop signals. Finally, the third concept is based on modifications of the reference model, such that it is feasible for the closed-loop system. This is done by incorporating the effect of saturation in the reference model. The concept can be shown to be equivalent to an augmentation of the tracking error between the closed-loop system and the reference system as it has been introduced in [105]. The idea has been further analyzed in [8, 75], where it is shown that



the resulting adaptive control method leads to bounded closed-loop signals if it is applied to a stable open-loop plant. For unstable open-loop plants, the method guarantees the closed-loop system to have bounded trajectories, if the initial conditions of the closed-loop signals lie in certain limits. The same concept has been applied to a gyroscope in [64] and is analyzed in the framework of adaptive backstepping in [171]. Another application of the basic concept is shown in [25, 26], but with a constant extension of the reference model by a model of the actuator. A detailed explanation of the basic concept from [8, 75], which is called Kárason Annaswamy anti-windup (KAAW) in the sequel, is given in the next section. Note that the method of pseudo control hedging (PCH) proposed in [67] and further examined in [68, 166] uses the same concept as KAAW, if it is applied to address input saturation. An extension to KAAW is introduced in [89, 92, 93] and is called positive  $\mu$ -modification. It additionally modifies the control signal such that saturation can be avoided. Similar stability results as for KAAW are derived.

### 3.4 Anti-Windup by Kárason and Annaswamy (KAAW)

The method introduced by Kárason and Annaswamy in [75] represents a well suited anti-windup scheme for MRAC since it can be interpreted as an extension of the reference model. This idea has already been used to derive extensions of KAAW and has been shown to work effectively in real applications. Therefore the concept of an extended reference model is also used as a fundamental part of the novel adaptive anti-windup scheme, which is derived in Chapter 4.

For the presentation of KAAW the plant  $G_{\text{nls}}$  from equation (3.2) with input saturation and with measurable states<sup>2</sup> is considered. Similar to the presentation of MRAW, the input saturation (3.1) is represented by a measurable input disturbance  $\Delta u$ , which has been introduced in (3.6). Therefore, the plant description becomes

$$\dot{x}_{\text{ps}} = A_{\text{p}} x_{\text{ps}} + B_{\text{p}} \lambda \left( u + \Delta u + \theta_{\text{nl}}^{\text{T}} f_{\text{nl}}(x_{\text{ps}}) \right). \quad (3.10)$$

Building the tracking error dynamics with the reference model  $G_{\text{ref}}$  in (2.4), as it has been done in Section 2.2.1, yields

$$\dot{e} = A_{\text{ref}} e + B_{\text{p}} \lambda \left( \tilde{K}_x^{\text{T}} x_{\text{ps}} + \tilde{k}_r r - \tilde{\theta}_{\text{nl}}^{\text{T}} f_{\text{nl}}(x_{\text{ps}}) \right) + B_{\text{p}} \lambda \Delta u. \quad (3.11)$$

Following the idea of KAAW in [75], the tracking error has to be extended by  $e_{\Delta}$  with the dynamic

$$\dot{e}_{\Delta} = A_{\text{ref}} e_{\Delta} + B_{\text{ref}} k_{\Delta}(t) \Delta u. \quad (3.12)$$

The term  $B_{\text{ref}} k_{\Delta}(t) \Delta u$  is an estimation of  $B_{\text{p}} \lambda \Delta u$ , such that the ideal value  $k_{\Delta}^*$  satisfies

$$B_{\text{ref}} k_{\Delta}^* = B_{\text{p}} \lambda. \quad (3.13)$$

---

<sup>2</sup>In this section the idea of KAAW is presented, which is simpler to do in the framework of state-feedback MRAC. However, the same idea can be used for output-feedback MRAC as shown in [8, 75].

Hence, the extension  $e_{\text{sat}} = e - e_{\Delta}$  results in

$$\dot{e}_{\text{sat}} = A_{\text{ref}} e_{\text{sat}} + B_{\text{p}} \lambda \left( \tilde{K}_x^{\text{T}} x_{\text{ps}} + \tilde{k}_r r - \tilde{\theta}_{\text{nl}}^{\text{T}} f_{\text{nl}}(x_{\text{ps}}) \right) - B_{\text{ref}} \tilde{k}_{\Delta} \Delta u, \quad (3.14)$$

with the estimation errors known from MRAC in Section 2.2.1 and the additional estimation error  $\tilde{k}_{\Delta} = k_{\Delta}(t) - k_{\Delta}^*$ .

However, a more intuitive way to achieve the tracking error dynamics in (3.14) is given by an extension of the reference model  $G_{\text{ref}}$ . From the MRAC presentation in Section 2.2.1 it follows that the application of the ideal control law (2.5) to the plant  $G_{\text{nl}}$  leads to the desired dynamics of reference model (2.4). Applying the same control law  $u^*$  from (2.5) to  $G_{\text{nls}}$  yields

$$\dot{x}_{\text{ps}} = A_{\text{ref}} x_{\text{ps}} + B_{\text{ref}} r + B_{\text{p}} \lambda \Delta u, \quad (3.15)$$

where the matching conditions (2.6) have been used. The system in (3.15) is very similar to the original reference model (2.4), but has an additional term  $B_{\text{p}} \lambda \Delta u$  that introduces the effect of saturation in the reference dynamics. This additional term makes the dynamics of (3.15) feasible for the closed-loop system. However, an implementation of (3.15) is not possible, due to the uncertain parameter  $\lambda$ . Therefore, the input gain of the disturbance  $\Delta u$  has to be estimated by  $B_{\text{ref}} k_{\Delta}(t)$ , so that an adaptive reference model

$$G_{\text{refs}} : \quad \dot{x}_{\text{refs}} = A_{\text{ref}} x_{\text{refs}} + B_{\text{ref}} r + B_{\text{ref}} k_{\Delta}(t) \Delta u, \quad (3.16)$$

is achieved, where the ideal value  $k_{\Delta}^*$  of  $k_{\Delta}(t)$  satisfies (3.13). Derivation of the tracking error as in Section 2.2.1 yields  $e_{\text{sat}}$  from (3.14). Note that similar to the naming of the plants, the subscript "s" for the reference model denotes that the effect of saturation is present in the reference system.

The choice of the Lyapunov function candidate

$$V = e_{\text{sat}}^{\text{T}} P e_{\text{sat}} + \lambda \left( \tilde{K}_x^{\text{T}} \Gamma_x^{-1} \tilde{K}_x + \frac{1}{\gamma_r} \tilde{k}_r^2 + \tilde{\theta}_{\text{nl}}^{\text{T}} \Gamma_{\text{nl}}^{-1} \tilde{\theta}_{\text{nl}} \right) + \frac{1}{\gamma_{\Delta}} \tilde{k}_{\Delta}^2, \quad (3.17)$$

and the parameter update laws

$$\begin{aligned} \dot{K}_x &= -\Gamma_x x_{\text{ps}} e_{\text{sat}}^{\text{T}} P B_{\text{p}} \\ \dot{k}_r &= -\gamma_r r e_{\text{sat}}^{\text{T}} P B_{\text{p}} \\ \dot{\theta}_{\text{nl}} &= \Gamma_{\text{nl}} f_{\text{nl}}(x_{\text{ps}}) e_{\text{sat}}^{\text{T}} P B_{\text{p}} \\ \dot{k}_{\Delta} &= \gamma_{\Delta} e_{\text{sat}} \Delta u P B_{\text{ref}} \end{aligned} \quad (3.18)$$

allows the formulation of the following theorem.

**Theorem 3.1.** *The control law (2.7) with a bounded reference signal  $r(t)$  together with the parameter update laws (3.18) applied to the system  $G_{\text{nls}}$  in (3.2) results in bounded parameter estimations and a bounded tracking error  $e_{\text{sat}}$ .*

*Proof.* The proof of the theorem can be found in [8, 75]. □

Note that different from classical MRAC the result of Theorem 3.1 does not directly lead to boundedness of the remaining closed-loop signals since due to  $\Delta u$  the reference state  $x_{\text{refs}}$  is not guaranteed to be bounded. However, results for the boundedness of the remaining closed-loop signals for a purely linear plant with limited input amplitude can be found in [8, 75]. The derivation of this result is not shown here, because the proofs for the new adaptive anti-windup method in Chapter 4 are done in a similar way. In order to apply MRAC with KAAW, the reference model and the parameter update laws in Table 2.1 has to be replaced by (3.16) and (3.18), respectively. The following simulation example presents the difference between MRAC with and without the extension of KAAW.

**Simulation Example 3.1.** In order to illustrate the capability of KAAW to deal with input limited plants, the simulation example from Section 3.1 is continued. Consequently, the plant in (3.3) and the reference model in (3.4) are considered for the application of MRAC with KAAW and the controller parameters have again been set to their ideal values and the initial condition of the plant state have been  $x_{\text{ps0}}^T = [0 \ 25]$ . The additional KAAW parameter is given by  $k_{\Delta}(0) = k_{\Delta}^* = 0.0076$ . The closed-loop response for the last 20 seconds of adaptation and the estimated parameters are shown in Figure 3.6. It can be seen that in difference to the standard MRAC algorithm, whose parameters diverged as shown in Figure 3.4, the parameters stay constant at their ideal values. Consequently, the system response with KAAW is the same as for the constant control law, shown in Figure 3.1. The simulation example clearly shows, that in difference to basic MRAC, the method

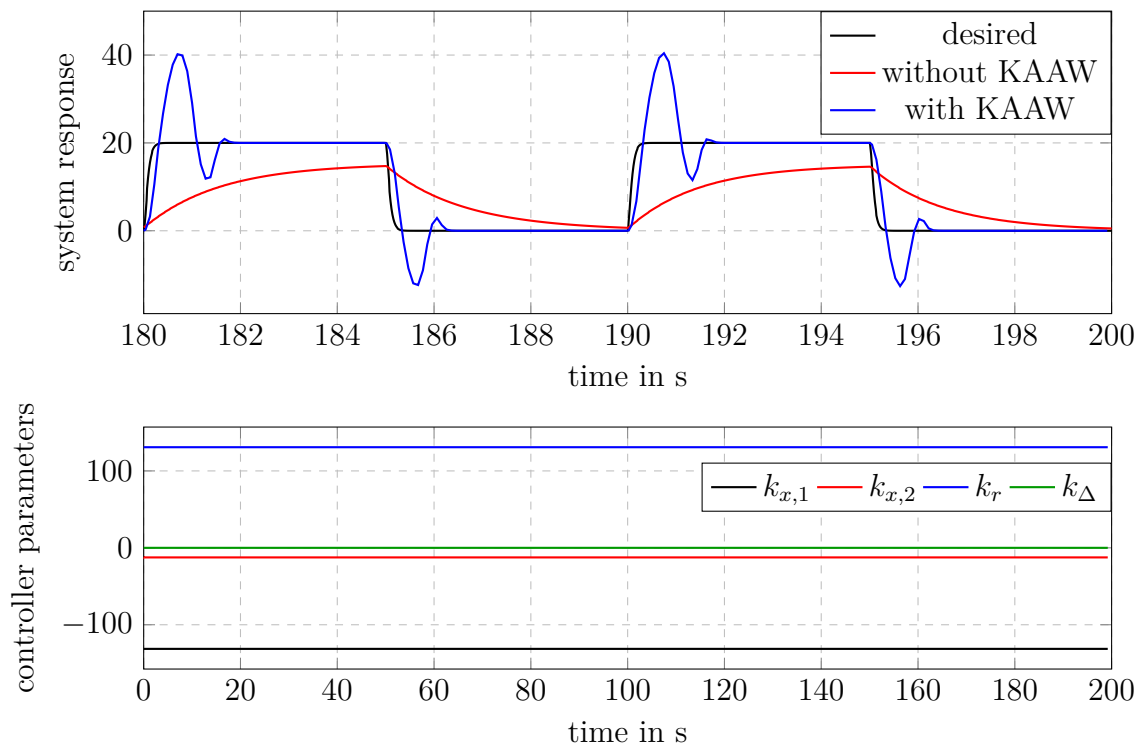


Figure 3.6: Simulation results for MRAC with and without KAAW applied to  $G_{\text{ex4}}$ . The second graph shows the estimated parameters with KAAW, where their initial values have been set to the ideal parameters.

of KAAW avoids parameter windup and leads to bounded closed-loop signals. However, the tracking performance in this example is not desirable due to the strong oscillations of the plant output around the desired set points.

## 3.5 Conclusion

The simulation results in Section 3.1 have shown that a proper consideration of saturation effects is absolutely necessary for adaptive as well as non-adaptive systems. Many of the adaptive anti-windup schemes for continuous-time systems mentioned in Section 3.3 can be applied to the adaptive control methods presented in Chapter 2 in order to make them applicable to plants with input constraints. For some of these methods the boundedness of the closed-loop has been proven, for others it has been verified with numerical simulations. However, these methods do not provide additional degrees of freedom to improve the closed-loop performance during saturation and hence for none of them a performance analysis has been carried out in either way. Positive  $\mu$ -modification in [92] even aims at avoiding saturation of the input in order to reduce the control deficiency. The same purpose is presented for the method in [95, 96]. Therefore, both of these anti-windup concepts sacrifices achievable speed and range of the system in order to reduce the control deficiency.

It has been shown in Section 3.4 that the method of KAAW avoids parameter windup and, therefore, allows for an application of adaptive control to plants with a limited input amplitude. However, with KAAW the performance during saturation of the input can only be influenced by changing the reference model, which also changes the performance when no saturation occurs. Since the method of MRAW, which has been presented in Section 3.2, can address performance issues during saturation with the additional anti-windup controller, a combination of it with KAAW is done in this work in order to simultaneously address parameter-windup and closed-loop performance of adaptive systems.

It is worth mentioning that MRAW has already been combined with an indirect adaptive control scheme in [69]. However, the method shown there has only been presented for state-feedback and is based on solutions of a linear matrix inequality, which is computed during operation. Therefore, it comes with high computational costs and increases the effort of its application. In Section 4.3 an indirect adaptive method is presented that can be applied to output-feedback plants without solving a linear matrix inequality. Hence, it can be used with lower computational costs and is therefore more suitable for common industrial control challenges.

# Chapter 4

## Adaptive Model Recovery Anti-Windup: Derivation

In the preceding chapter, it has been shown that the basic adaptive control methods presented in Chapter 2 suffer from input saturation. Multiple undesired effects of a limited input have been illustrated, which can partially be addressed with existing methods from the literature (see Section 3.3). Most of these methods have been developed to avoid parameter windup and to guarantee boundedness of the closed-loop signals. Some of them also allow for a reduction of control deficiency in the presence of saturation. However, for none of the methods mentioned in Section 3.3 a performance analysis has been carried out.

In this chapter a new adaptive anti-windup scheme will be introduced, which extends the adaptive controllers presented in Chapter 2. This new method establishes an additional degree of freedom that allows for performance considerations in input saturated adaptive systems. The presentations in this chapter are based on the methods of KAAW and MRAW, which have been presented in sections 3.2 and 3.4, respectively. Hence, in order to follow the derivations of the new method in the subsequent sections, it is advisable to first get familiar with the basic concepts presented there.

In order to unify the following presentations, the derivation of the anti-windup scheme for the different control structures are done in a similar way. For the direct adaptive control schemes, an adaptive anti-windup system based on MRAW is introduced in a first step. Similar to KAAW the reference model is then extended in order to account for the saturation effects as well as for the influence of the anti-windup system on the closed-loop system. In the third step, a stability analysis of the closed-loop system is carried out in order to derive the parameter update laws and to introduce conditions for guaranteed boundedness of the plant states and the remaining closed-loop signals. At the end of the respective sections, a summary of the new adaptive anti-windup scheme is given. In difference to the direct schemes, no extension of a reference model needs to be considered for the indirect method and also no stability analysis needs to be done to derive the parameter update laws. Hence, for the introduction of the indirect adaptive

anti-windup scheme, these steps are substituted by the presentation of a modified linear parametric model, which can be used to estimate the plant parameters.

Note that this chapter only presents the derivation of the new anti-windup method. Remarks about its properties, possible tuning procedures and implementation issues will be given in Chapter 5 based on illustrative simulation examples.

## 4.1 Direct Adaptive Model Recovery Anti-Windup for State-Feedback

The method of adaptive model recovery anti-windup (AMRAW), presented in this section, extends the MRAC scheme from Section 2.2.1 in order to take saturation of the input amplitude into account. This is done by introducing an adaptive anti-windup structure similar to MRAW and by an extended reference model similar to KAAW. For the following presentation the plant

$$G_{\text{nls}} : \quad \dot{x}_{\text{ps}} = A_{\text{p}} x_{\text{ps}} + B_{\text{p}} \lambda \left( u_{\text{lim}} + \theta_{\text{nl}}^{\text{T}} f_{\text{nl}}(x_{\text{ps}}) \right),$$

which has already been defined in (3.2) with unknown parameters  $A_{\text{p}}$ ,  $\lambda$  and  $\theta_{\text{nl}}$  is considered. As an additional assumption on the plant, a linear function is supposed to be known as an upper bound for the nonlinear function of the matched uncertainty:

$$\|f_{\text{nl}}(x_{\text{ps}})\| \leq o_{\text{nl}} + c_{\text{nl}} \|x_{\text{ps}}\| \quad \text{with} \quad o_{\text{nl}} > 0, \quad c_{\text{nl}} > 0. \quad (4.1)$$

Note that this additional assumption is not restrictive for technical systems.

### Anti-Windup Scheme

Following the idea of MRAW, the basic MRAC controller structure given in (2.7) is not changed. Instead, an additional anti-windup scheme is introduced into the closed-loop in order to recover the output of the plant  $G_{\text{nl}}$  introduced in equation (2.3) and to reduce the influence of the saturation on the plant. The plant equation with the modified input and the representation of the input limitation as a disturbance becomes

$$\dot{x}_{\text{ps}} = A_{\text{p}} x_{\text{ps}} + B_{\text{p}} \lambda \left( u_{\text{c}} - u_{\text{aw}} + \Delta u + \theta_{\text{nl}}^{\text{T}} f_{\text{nl}}(x_{\text{ps}}) \right), \quad (4.2)$$

where explicit terms for  $u_{\text{c}}$  and  $u_{\text{aw}}$  will be defined below and  $\Delta u = u_{\text{lim}} - u$  as defined in (3.6). For known plant parameters a suitable choice for the anti-windup system model is given by

$$\dot{x}_{\text{aw}} = A_{\text{p}} x_{\text{aw}} + B_{\text{p}} \lambda \left( -\Delta u + u_{\text{aw}} + \theta_{\text{nl}}^{\text{T}} (f_{\text{nl}}(x_{\text{ps}} + x_{\text{aw}}) - f_{\text{nl}}(x_{\text{ps}})) \right). \quad (4.3)$$

Summation of (4.2) and (4.3) leads to

$$\dot{x}_{\text{ps}} + \dot{x}_{\text{aw}} = A_{\text{p}} (x_{\text{ps}} + x_{\text{aw}}) + B_{\text{p}} \lambda \left( u_{\text{c}} + \theta_{\text{nl}}^{\text{T}} f_{\text{nl}}(x_{\text{ps}} + x_{\text{aw}}) \right). \quad (4.4)$$

Since (4.4) does not suffer from any effect of input saturation, the summation  $x_{\text{ps}} + x_{\text{aw}}$  recovers the output of the plant  $G_{\text{nl}}$ , and hence can be used for feedback to the standard MRAC control law

$$u_c = K_x(t)^T (x_{\text{ps}} + x_{\text{aw}}) + k_r(t) r - \hat{\theta}_{\text{nl}}^T(t) f_{\text{nl}}(x_{\text{ps}} + x_{\text{aw}}). \quad (4.5)$$

However, the anti-windup scheme requires the knowledge of the plant parameters. Hence, the anti-windup system (4.3) and therefore also the control law (4.5) are not implementable. A modification of the anti-windup scheme that renders it implementable will be derived on the basis of (4.3) after the introduction of the anti-windup controller.

In order to regulate the unwanted behavior  $x_{\text{aw}}$ , resulting from the effect of input saturation  $\Delta u$ , to zero, an anti-windup controller needs to be introduced. The explicit structure of this controller is given by

$$u_{\text{aw}} = K_{\text{aw}}(t)^T x_{\text{aw}} - \hat{\theta}_{\text{nl}}^T(t) (f_{\text{nl}}(x_{\text{ps}} + x_{\text{aw}}) - f_{\text{nl}}(x_{\text{ps}})), \quad (4.6)$$

which is similar to the MRAC control law in (4.5). Since no steady-state value different from  $x_{\text{aw}} = 0$  is desired for the unwanted behavior, a reference signal for any anti-windup state and a corresponding gain are not necessary. The ideal value  $K_{\text{aw}}^*$  of  $K_{\text{aw}}(t)$  is defined to satisfy the matching equation

$$A_p + B_p \lambda K_{\text{aw}}^{*\text{T}} = A_{\text{awr}}, \quad (4.7)$$

so that the desired anti-windup dynamic  $A_{\text{awr}}$  introduces an additional degree of freedom, which can be chosen by the designer in a similar way as  $A_{\text{ref}}$  for the reference model in MRAC. Note that Remark 2.2 for the MRAC matching conditions also applies for matching condition (4.7). The complete control scheme therefore becomes

$$u = u_c - u_{\text{aw}} = K_x(t)^T (x_{\text{ps}} + x_{\text{aw}}) + k_r(t) r - K_{\text{aw}}(t)^T x_{\text{aw}} - \hat{\theta}_{\text{nl}}^T(t) f_{\text{nl}}(x_{\text{ps}}). \quad (4.8)$$

The structure of the anti-windup controller can now be used to find an implementable version of the anti-windup scheme. One possibility of doing that is illustrated in Figure 4.1, where the block-diagram **I** shows the initial scheme, which follows from equation (4.3). Since the signal  $u_{\text{aw}}$  builds an internal closed-loop in the anti-windup scheme, the anti-windup system can be directly represented by the resulting closed-loop equation. Furthermore, since the desired dynamics of the anti-windup scheme are known and chosen by the designer, the ideal control law rather than the adaptive version can be considered for the internal feedback as shown in block diagram **II** of Figure 4.1. Together with matching condition (4.7) this results in

$$\dot{x}_{\text{aw}} = A_{\text{awr}} x_{\text{aw}} - B_p \lambda \Delta u,$$

which is illustrated in block diagram **III**. In order to get rid of the unknown term  $B_p \lambda \Delta u$ , the estimation  $B_{\text{ref}} k_{\Delta}(t)$  for  $B_p \lambda$  is introduced as it has been done for the method of KAAW in Section 3.4. The final anti-windup system is therefore given by

$$M_{\text{aw}} : \quad \dot{x}_{\text{aw}} = A_{\text{awr}} x_{\text{aw}} - B_{\text{ref}} k_{\Delta}(t) \Delta u, \quad (4.9)$$

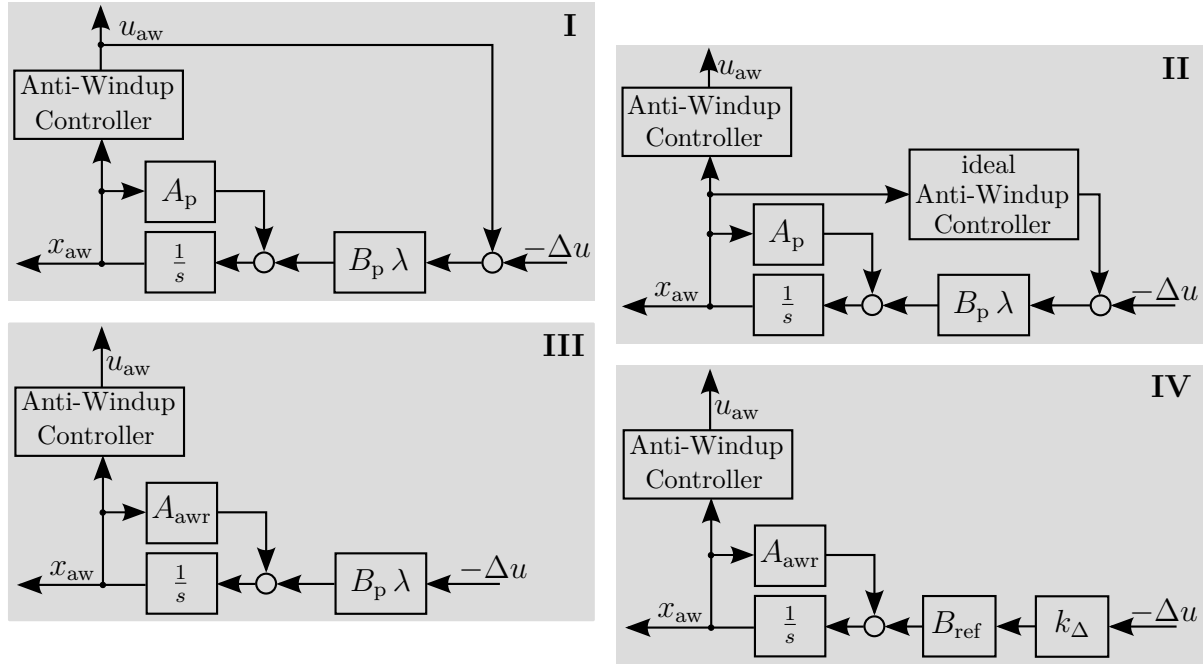


Figure 4.1: Schematic illustration of the derivation of the adaptive anti-windup scheme. Note that the ideal anti-windup controller denotes the controller with ideal parameters.

which is shown in block diagram **IV** of Figure 4.1. Hence, the computation of the anti-windup state is done with the desired dynamics and an adaptive input gain  $k_\Delta$ . Therefore,  $M_{aw}$  can be interpreted as a reference model for the unwanted behavior of the plant and it remains to find the ideal parameters for the anti-windup controller, which lead to the corresponding behavior of the real plant. As for basic MRAC, this can be done by suitable parameter update laws, which will be derived after the introduction of the reference model.

## Reference Model

In order to derive the reference model the same procedure as for KAAW in Section 3.4 is done. The reference model is determined by considering it as the actual plant, fed by the ideal version of the control signal (4.8). For AMRAW the ideal control signal  $u^*$  is given by

$$u^* = u_c^* - u_{aw}^* = K_x^{*\top} (x_{ps} + x_{aw}) + k_r^* r - K_{aw}^{*\top} x_{aw} - \theta_{nl}^\top(t) f_{nl}(x_{ps}).$$

Substitution of  $u^*$  for  $u$  in  $G_{nls}$  yields

$$\dot{x}_{ps} = \left( A_p + B_p \lambda K_x^{*\top} \right) x_{ps} + B_p \lambda k_r^* r + B_p \lambda \left( K_x^{*\top} - K_{aw}^{*\top} \right) x_{aw} + B_p \lambda \Delta u.$$

The matching conditions (2.6) and (4.7) as well as a substitution of the estimation  $B_p k_\Delta \Delta u$  for  $B_{ref} \lambda \Delta u$  finally results in the reference model

$$G_{refaw} : \quad \dot{x}_{refs} = A_{ref} (x_{refs} + x_{aw}) + B_{ref} r + B_{ref} k_\Delta(t) \Delta u - A_{awr} x_{aw}, \quad (4.10)$$



where  $x_{\text{ps}}$  has been replaced by  $x_{\text{refs}}$  to clarify that it is the state of the reference model. It has been shown in Section 3.4 that the method of KAAW can be interpreted as an extension of the reference model in order to incorporate the effect of saturation into it. This effect is also represented in  $G_{\text{refaw}}$  by the term  $B_{\text{ref}} k_{\Delta}(t) \Delta u$ . Since AMRAW introduces an additional anti-windup structure that affects the closed-loop, its influence also has to be incorporated into the reference model in order to make it feasible for the closed-loop system. In  $G_{\text{refaw}}$  the effect of the anti-windup scheme is represented by the terms  $A_{\text{ref}} x_{\text{aw}}$  and  $-A_{\text{awr}} x_{\text{aw}}$ .

### Parameter Updates and Closed-Loop Stability

Derivation of the parameter update laws requires the development of the closed-loop system. Similar to the procedure for MRAC the term

$$B_p \lambda \left( K_x^{*\text{T}} (x_{\text{ps}} + x_{\text{aw}}) + k_r^* r - K_{\text{aw}}^{*\text{T}} x_{\text{aw}} \right)$$

is added and subtracted from the plant equation of  $G_{\text{nls}}$  in (3.2). Together with matching conditions (2.6) it results in

$$\begin{aligned} \dot{x}_{\text{ps}} = & A_{\text{ref}} x_{\text{ps}} + B_{\text{ref}} r + B_p \lambda \left( u + \Delta u + \theta_{\text{nl}}^{\text{T}} f_{\text{nl}}(x_{\text{ps}}) - K_x^{*\text{T}} (x_{\text{ps}} + x_{\text{aw}}) + K_x^{*\text{T}} x_{\text{aw}} \right. \\ & \left. - k_r^* r \pm K_{\text{aw}}^{*\text{T}} x_{\text{aw}} \right). \end{aligned}$$

Inserting the control law (4.8) and using the matching condition (4.7) yields

$$\begin{aligned} \dot{x}_{\text{ps}} = & A_{\text{ref}} x_{\text{ps}} + B_{\text{ref}} r + B_p \lambda \left( \Delta u + \tilde{K}_x^{\text{T}} (x_{\text{ps}} + x_{\text{aw}}) + \tilde{k}_r r - \tilde{\theta}_{\text{nl}}^{\text{T}} f_{\text{nl}}(x_{\text{ps}}) - \tilde{K}_{\text{aw}}^{\text{T}} x_{\text{aw}} \right) \\ & + (A_p - A_{\text{awr}}) x_{\text{aw}} + B_p \lambda K_x^{*\text{T}} x_{\text{aw}}. \end{aligned}$$

Usage of matching condition (2.6) finally results in the closed-loop equation

$$\begin{aligned} \dot{x}_{\text{ps}} = & A_{\text{ref}} (x_{\text{ps}} + x_{\text{aw}}) + B_{\text{ref}} r - A_{\text{awr}} x_{\text{aw}} \\ & + B_p \lambda \left( \Delta u + \tilde{K}_x^{\text{T}} (x_{\text{ps}} + x_{\text{aw}}) + \tilde{k}_r r - \tilde{\theta}_{\text{nl}}^{\text{T}} f_{\text{nl}}(x_{\text{ps}}) - \tilde{K}_{\text{aw}}^{\text{T}} x_{\text{aw}} \right), \end{aligned} \quad (4.11)$$

where  $\tilde{K}_x = K_x(t) - K_x^*$ ,  $\tilde{k}_r = k_r(t) - k_r^*$ ,  $\tilde{K}_{\text{aw}} = K_{\text{aw}}(t) - K_{\text{aw}}^*$  and  $\tilde{\theta}_{\text{nl}} = \hat{\theta}_{\text{nl}}(t) - \theta_{\text{nl}}$  are the parameter estimation errors. The dynamics of the tracking error  $e_{\text{sat}} = x_{\text{ps}} - x_{\text{refs}}$  of the closed-loop system with saturation becomes

$$\dot{e}_{\text{sat}} = A_{\text{ref}} e_{\text{sat}} + B_p \lambda \left( \tilde{K}_x^{\text{T}} (x_{\text{ps}} + x_{\text{aw}}) + \tilde{k}_r r - \tilde{\theta}_{\text{nl}}^{\text{T}} f_{\text{nl}}(x_{\text{ps}}) - \tilde{K}_{\text{aw}}^{\text{T}} x_{\text{aw}} \right) - B_{\text{ref}} \tilde{k}_{\Delta} \Delta u,$$

where  $\tilde{k}_{\Delta} = k_{\Delta}(t) - k_{\Delta}^*$ .

Considering the Lyapunov function candidate

$$V = e_{\text{sat}}^{\text{T}} P e_{\text{sat}} + \lambda \left( \tilde{K}_x^{\text{T}} \Gamma_x^{-1} \tilde{K}_x + \frac{1}{\gamma_r} \tilde{k}_r^2 + \tilde{K}_{\text{aw}}^{\text{T}} \Gamma_{\text{aw}}^{-1} \tilde{K}_{\text{aw}} + \tilde{\theta}_{\text{nl}}^{\text{T}} \Gamma_{\text{nl}}^{-1} \tilde{\theta}_{\text{nl}} \right) + \frac{1}{\gamma_{\Delta}} \tilde{k}_{\Delta}^2 \quad (4.12)$$

and its derivative with respect to time

$$\begin{aligned}
\dot{V} = & e_{\text{sat}}^{\text{T}} \left( P A_{\text{ref}} + A_{\text{ref}}^{\text{T}} P \right) e_{\text{sat}} \\
& + 2 \lambda \left( \tilde{K}_x^{\text{T}} (x_{\text{ps}} + x_{\text{aw}}) e_{\text{sat}}^{\text{T}} P B_{\text{p}} + \tilde{K}_x^{\text{T}} \Gamma_x^{-1} \dot{\tilde{K}}_x \right. \\
& \quad + \tilde{k}_r^{\text{T}} r e_{\text{sat}}^{\text{T}} P B_{\text{p}} + \frac{1}{\gamma_r} \tilde{k}_r \dot{\tilde{k}}_r \\
& \quad - \tilde{K}_{\text{aw}}^{\text{T}} x_{\text{aw}} e_{\text{sat}}^{\text{T}} P B_{\text{p}} + \tilde{K}_{\text{aw}}^{\text{T}} \Gamma_{\text{aw}}^{-1} \dot{\tilde{K}}_{\text{aw}} \\
& \quad \left. - \tilde{\theta}_{\text{nl}}^{\text{T}} f(x_{\text{ps}}) e_{\text{sat}}^{\text{T}} P B_{\text{p}} + \tilde{\theta}_{\text{nl}}^{\text{T}} \Gamma_{\text{nl}}^{-1} \dot{\tilde{\theta}}_{\text{nl}} \right) \\
& - 2 \tilde{k}_{\Delta} \Delta u e_{\text{sat}}^{\text{T}} P B_{\text{ref}} + \frac{2}{\gamma_{\Delta}} \tilde{k}_{\Delta} \dot{\tilde{k}}_{\Delta}
\end{aligned}$$

suggests the choice of

$$\begin{aligned}
\dot{K}_x &= -\Gamma_x (x_{\text{ps}} + x_{\text{aw}}) e_{\text{sat}}^{\text{T}} P B_{\text{p}}, \\
\dot{K}_{\text{aw}} &= \Gamma_{\text{aw}} x_{\text{aw}} e_{\text{sat}}^{\text{T}} P B_{\text{p}}, \\
\dot{k}_r &= -\gamma_r r e_{\text{sat}}^{\text{T}} P B_{\text{p}}, \\
\dot{\theta}_{\text{nl}} &= \Gamma_{\text{nl}} f_{\text{nl}}(x_{\text{ps}}) e_{\text{sat}}^{\text{T}} P B_{\text{p}}, \\
\dot{k}_{\Delta} &= \gamma_{\Delta} \Delta u e_{\text{sat}}^{\text{T}} P B_{\text{ref}},
\end{aligned} \tag{4.13}$$

for the parameter update laws. In (4.12) and (4.13),  $P$  is the solution of the Lyapunov equation  $A_{\text{ref}}^{\text{T}} P + P A_{\text{ref}} < -Q$  for  $Q = Q^{\text{T}} > 0$  and the gains  $\Gamma_x = \Gamma_x^{\text{T}} > 0$ ,  $\Gamma_{\text{aw}} = \Gamma_{\text{aw}}^{\text{T}} > 0$ ,  $\Gamma_{\text{nl}} = \Gamma_{\text{nl}}^{\text{T}} > 0$ ,  $\gamma_r > 0$ , and  $\gamma_{\Delta} > 0$  are introduced as tuning parameters for the parameter updates. Note that Remark 2.4 for the corresponding gains of MRAC also applies for AMRAW. The preceding derivations allow the formulation of the following theorem.

**Theorem 4.1.** *The control law (4.8) with a bounded reference signal  $|r(t)| \leq r_{\text{max}}(t)$  together with the parameter update laws (4.13) and the reference model (4.10) applied to the plant  $G_{\text{nls}}$  in (3.2) results in bounded closed-loop signals if the plant is open-loop stable. Boundedness of the closed-loop signals for an unstable open-loop plant  $G_{\text{nls}}$  can be established under the following conditions:*

i) *The initial state of the closed-loop system satisfies*

$$x_{\text{ps}}(t_0)^{\text{T}} P_W x_{\text{ps}}(t_0) \leq \lambda_{\min}(P_W) \left( \frac{2 p_b \lambda (u_{\text{max}} - \|\theta_{\text{nl}}\| o_{\text{nl}})}{|-q_0 + 2 p_b \lambda \|\tilde{K}_x^*\| + \|\theta_{\text{nl}}\| c_{\text{nl}}|} \right)^2. \tag{4.14}$$

ii) *The reference signal does not exceed*

$$r_{\text{max}} \leq \frac{q_0 (u_{\text{max}} - \|\theta_{\text{nl}}\| o_{\text{nl}}) - \rho \eta D_{\text{aw}} \|x_{\text{aw}}\|}{\rho \eta |k_r^*|}. \tag{4.15}$$

iii) *The initial value of (4.12) does not exceed*

$$\begin{aligned}
V(t_0) &\leq \\
&\frac{\lambda}{\lambda_{\max}(\Gamma_x)} \left( \frac{q_0 (2 p_b \lambda (u_{\text{max}} - \|\theta_{\text{nl}}\| o_{\text{nl}})) - 2 p_b \lambda \rho \eta (|k_r^*| r_{\text{max}} + D_{\text{aw}} \|x_{\text{aw}}(t_0)\|)}{N_{\text{max}}} \right)^2
\end{aligned} \tag{4.16}$$

with

$$\begin{aligned}
N_{\max} = & \\
& 2 p_b \lambda \left[ \rho \eta \left( \|x_{\text{aw}}(t_0)\| \left[ 1 + \sqrt{\frac{\lambda_{\min}(\Gamma_{\text{aw}})}{\lambda_{\min}(\Gamma_x)}} \right] + r_{\max} \sqrt{\frac{\gamma_r}{\lambda_{\min}(\Gamma_x)}} + o_{\text{nl}} \sqrt{\frac{\lambda_{\min}(\Gamma_{\text{nl}})}{\lambda_{\min}(\Gamma_x)}} \right) \right. \\
& \left. + \left( 1 + c_{\text{nl}} \sqrt{\frac{\lambda_{\min}(\Gamma_{\text{nl}})}{\lambda_{\min}(\Gamma_x)}} \right) (2 p_b \lambda [u_{\max} - \|\theta_{\text{nl}}\| o_{\text{nl}}]) \right]
\end{aligned}$$

The matrix  $P_{\text{W}} = P_{\text{W}}^{\text{T}} > 0$  is the solution of the linear equation  $A_{\text{ref}}^{\text{T}} P_{\text{W}} + P_{\text{W}} A_{\text{ref}} = -Q_{\text{W}}$  with  $Q_{\text{W}} = Q_{\text{W}}^{\text{T}} > 0$  and  $q_0$  is the minimal eigenvalue of  $Q_{\text{W}}$ . In conditions (i) – (iii) the definitions of  $p_b \triangleq \|P_{\text{W}} B_{\text{p}}\|$ ,  $\eta \triangleq |-q_0 + 2 p_b \lambda \|K_{\text{x}}^*\| + \|\theta_{\text{nl}}\| c_{\text{nl}}|$ ,  $D_{\text{aw}} \geq \|K_{\text{x}}^* - K_{\text{aw}}^*\|$  and  $\rho \triangleq \sqrt{\frac{\lambda_{\max}(P_{\text{W}})}{\lambda_{\min}(P_{\text{W}})}}$  have been used, where  $\lambda_{\min}(\cdot)$  and  $\lambda_{\max}(\cdot)$  are the minimal and maximal eigenvalue, respectively.

*Proof.* The boundedness of the parameter estimations directly follows from the fact that  $V$  in (4.12) is a Lyapunov function if the parameter update laws are chosen as those given in (4.13).

If the plant  $G_{\text{nl}s}$  is open-loop stable, a bounded input  $u_{\text{lim}}$  directly leads to a bounded state  $x_{\text{ps}}$ . Since the boundedness of  $e_{\text{sat}}$  can be deduced from the Lyapunov function  $V$ , also the reference state  $x_{\text{refs}}$  is bounded. Summation of the dynamical system of the reference model (4.10) and the anti-windup scheme (4.9) yields

$$\dot{x}_{\text{aw}} + \dot{x}_{\text{refs}} = A_{\text{ref}} (x_{\text{aw}} + x_{\text{refs}}) + B_{\text{ref}} r,$$

which is a stable system with bounded input  $r$ . Hence,  $x_{\text{aw}} + x_{\text{refs}}$  is bounded and therefore  $x_{\text{aw}}$  is bounded. From the control law (4.8) it then follows that  $u$  is bounded. The proof of boundedness for the closed-loop signals if AMRAW is applied to an unstable open-loop plant  $G_{\text{nl}s}$  is shown in Appendix B.  $\square$

An additional result to that of Theorem 4.1 can be found for first order plants

$$\dot{x}_{\text{ps}} = a_{\text{p}} x_{\text{ps}} + b_{\text{p}} \lambda \left( u_{\text{lim}} + \theta_{\text{nl}}^{\text{T}} f_{\text{nl}}(x_{\text{ps}}) \right), \quad (4.17)$$

where the same assumptions apply as for  $G_{\text{nl}s}$  but with scalar plant parameters  $a_{\text{p}} \in \mathbb{R}$  and  $b_{\text{p}} \in \mathbb{R}$ . Under the assumption that the parameter update laws have adapted the controller parameters to their ideal values, the equation (4.9) for the anti-windup system can be written as

$$\begin{aligned}
\dot{x}_{\text{aw}} &= a_{\text{awr}} x_{\text{aw}} - b_{\text{p}} \lambda \Delta u, \\
&= a_{\text{p}} x_{\text{aw}} + b_{\text{p}} \lambda k_{\text{aw}}^* x_{\text{aw}} - b_{\text{p}} \lambda \Delta u, \\
&= a_{\text{p}} x_{\text{aw}} + b_{\text{p}} \lambda k_{\text{aw}}^* x_{\text{aw}} - b_{\text{p}} \lambda (\text{sat}(u_{\text{c}} - k_{\text{aw}}^* x_{\text{aw}}) - u_{\text{c}} + k_{\text{aw}}^* x_{\text{aw}}), \\
&= a_{\text{p}} x_{\text{aw}} + b_{\text{p}} \lambda (u_{\text{c}} - \text{sat}(u_{\text{c}} - k_{\text{aw}}^* x_{\text{aw}})).
\end{aligned} \quad (4.18)$$

With the interpretation of the state  $x_{\text{aw}}$  as the unwanted behavior of the plant, as it has been introduced in Section 3.2, a small value of  $\|x_{\text{aw}}\|$  is desirable. Therefore,  $x_{\text{aw}}$

is a reasonable measure for the closed-loop performance during saturation of the input. Consequently, increasing the closed-loop performance is equivalent to a reduced influence of the saturation on the system. The same argumentation is also used e.g. in [122, 155] to derive anti-windup controllers that optimize the closed-loop performance. The following theorem implicitly gives an indication of how to choose the desired anti-windup pole  $a_{awr} < 0 \in \mathbb{R}$  in order to increase closed-loop performance.

**Theorem 4.2.** *For the first order plant (4.17) with limited input amplitude, the choice of two different AMRAW parameters  $k_{aw1}^* \in \mathbb{R}$  and  $k_{aw2}^* \in \mathbb{R}$  such that*

$$a_p + b_p k_{aw1}^* = a_{awr1} < a_p + b_p k_{aw2}^* = a_{awr2} < a_p$$

*with  $a_{awri} < 0$  for  $i = 1, 2$ , will lead to  $|x_{aw1}| \leq |x_{aw2}| \quad \forall t > t_0$  for the corresponding unwanted behaviors  $x_{awi}$ ,  $i = 1, 2$ , if*

- i) the input  $u_c$  is the same for both systems,*
- ii) the initial conditions fulfill  $|x_{aw1}(t_0)| \leq |x_{aw2}(t_0)|$ ,  
where  $\text{sign}(x_{aw1}(t_0)) = \text{sign}(x_{aw2}(t_0))$ ,*
- iii) the unwanted behaviors  $x_{aw1}$  and  $x_{aw2}$  do not change sign.*

*Proof.* The proof is based on an examination of all possible combinations of  $u_c$  and  $\text{sat}(u_c - k_{aw}^* x_{aw})$  in (4.18) and on the effect of these combinations on the anti-windup state  $x_{aw}$ . The different combinations are compared for two closed-loop systems with gains  $k_{aw1}^*$  and  $k_{aw2}^*$  respectively, which makes a conclusion about the growth or decay of  $x_{aw1}$  and  $x_{aw2}$  possible. The detailed proof of Theorem 4.2 is given in Appendix B.  $\square$

## Summary

The complete control scheme of AMRAW with state-feedback is given by the control law (4.8), the adaptive anti-windup scheme  $M_{aw}$  in (4.9), the adaptive reference model  $G_{refaw}$  in (4.10), and the parameter update laws in (4.13). All necessary equations and tuning parameters for the implementation of AMRAW for state-feedback plants are summarized in Table 4.1. Since AMRAW extends the method of MRAC, all Remarks 2.1-2.4 from Section 2.2.1 does also apply to the method of AMRAW. However, since AMRAW introduces additional states, parameter estimations, and tuning parameters in the closed-loop system, additional considerations are necessary, which are presented in several remarks in Chapter 5 based on the results of simulation examples.

Plant:  $\dot{x}_{ps} = A_p x_{ps} + B_p \lambda \left( u_{lim} + \theta_{nl}^T f_{nl}(x_{ps}) \right)$

Reference Model:  $\dot{x}_{refs} = A_{ref} (x_{refs} + x_{aw}) + B_{ref} r + B_{ref} k_{\Delta}(t) \Delta u - A_{awr} x_{aw}$   
 $\Delta u = u_{lim} - u$

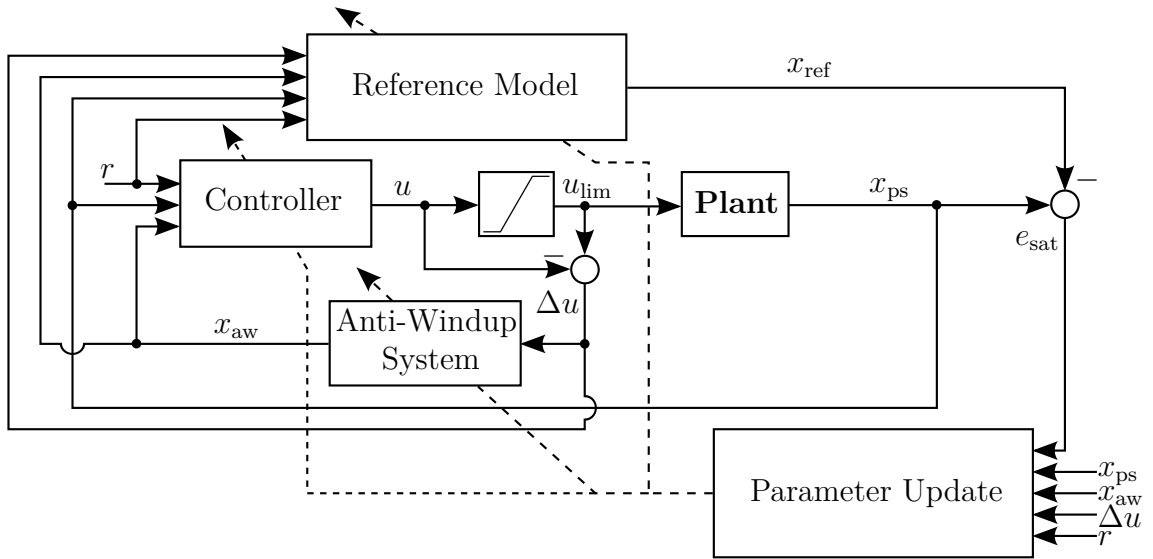
Control Law:  $u = K_x(t)^T (x_{ps} + x_{aw}) + k_r(t) r - K_{aw}(t)^T x_{aw}$   
 $-\hat{\theta}_{nl}(t)^T f_{nl}(x_{ps})$

Anti-Windup:  $\dot{x}_{aw} = A_{awr} x_{aw} - B_{ref} k_{\Delta}(t) \Delta u$

Lyapunov Equation:  $-Q = A_{ref}^T P + P A_{ref}$

Tracking Error:  $e_{sat} = x_{ps} - x_{refs}$

Parameter Update:  $\dot{K}_x = -\Gamma_x (x_{ps} + x_{aw}) e_{sat}^T P B_p$   
 $\dot{k}_r = -\gamma_r r e_{sat}^T P B_p$   
 $\dot{\theta}_{nl} = \Gamma_{nl} f_{nl}(x_{ps}) e_{sat}^T P B_p$   
 $\dot{K}_{aw} = \Gamma_{aw} x_{aw} e_{sat}^T P B_p$   
 $\dot{k}_{\Delta} = \gamma_{\Delta} \Delta u e_{sat}^T P B_{ref}$



- Design Parameters:
- $A_{ref}$  and  $B_{ref}$  satisfying performance requirements and (2.6)
  - $A_{awr}$  satisfying (4.7) (see Remark 5.2)
  - $Q \in \mathbb{R}^{n \times n}$  positive definite
  - $\Gamma_x, \Gamma_{aw} \in \mathbb{R}^{n \times n}$ ,  $\Gamma_{nl} \in \mathbb{R}^{l \times l}$  positive definite and  $\gamma_r, \gamma_{\Delta} > 0$  (see Remark 2.4)

Table 4.1: Summary of AMRAW with state-feedback.

## 4.2 Direct Adaptive Model Recovery Anti-Windup for Output-Feedback

The method of adaptive model recovery anti-windup for output-feedback, presented in this section extends the MRAC scheme from Section 2.2.2 in order to take saturation of the input amplitude into account. The derivation of the new control scheme follows the same idea as in the state-feedback case in the preceding section, in the sense that an adaptive anti-windup scheme is introduced and that the reference model is extended like in KAAW. However, in difference to the state-feedback case a dynamical controller is used and hence its state has to be taken into account. This leads to the necessity of taking the anti-windup controller states into account in the basic control law.

For the following presentation the plant

$$G_{\text{lins}} : y_p = k_p \frac{s^m + z_{m-1} s^{m-1} + \dots + z_1 s + z_0}{s^n + r_{n-1} s^{n-1} + \dots + r_1 s + r_0} u_{\text{lim}} = k_p \frac{Z_p(s)}{R_p(s)} u_{\text{lim}} \quad (4.19)$$

with the same assumptions as for the plant  $G_{\text{lin}}$  in (2.15) is considered. The state-space model of  $G_{\text{lins}}$  has already been defined in (3.5) as

$$\begin{aligned} \dot{x}_{\text{ps}} &= A_p x_{\text{ps}} + B_p u_{\text{lim}}, \\ y_{\text{ps}} &= C_p x_{\text{ps}}, \end{aligned} \quad (4.20)$$

which is assumed to be in observability canonical form for the following derivations. Therefore, the additional assumption of an observable plant  $G_{\text{lins}}$  is necessary. The limited input  $u_{\text{lim}}$  in (4.19) has been defined in (3.1).

### Anti-Windup Scheme

Derivation of the anti-windup scheme requires the combined open-loop state-space model of the plant  $G_{\text{lins}}$  in (4.19) and the controller dynamics

$$\begin{aligned} \underbrace{\begin{pmatrix} \dot{x}_{\text{ps}} \\ \dot{w}_{1s} \\ \dot{w}_{2s} \end{pmatrix}}_{\dot{x}_{\text{cs}}} &= \underbrace{\begin{pmatrix} A_p & 0 & 0 \\ 0 & F & 0 \\ g C_p & 0 & F \end{pmatrix}}_{A_c} \underbrace{\begin{pmatrix} x_{\text{ps}} \\ w_{1s} \\ w_{2s} \end{pmatrix}}_{x_{\text{cs}}} + \underbrace{\begin{pmatrix} B_p \\ g \\ 0 \end{pmatrix}}_{B_c} (u_c - u_{\text{aw}} + \Delta u), \\ y_{\text{ps}} &= \underbrace{\begin{pmatrix} C_p & 0 & 0 \end{pmatrix}}_{C_c} x_{\text{cs}}, \end{aligned} \quad (4.21)$$

where  $u_c$  is the signal of the basic controller,  $u_{\text{aw}}$  is the signal of the anti-windup controller, and  $F$  and  $g$  are defined as in Section 2.2.2. The effect of saturation is represented as the input disturbance  $\Delta u = u_{\text{lim}} - u$ . The combined open-loop equation (4.21) differs from that of the standard MRAC scheme, since the limited input  $u_{\text{lim}}$  instead of  $u$  is fed back to the controller. This is similar to KAAW for output-feedback plants in [75]. Explicit definitions of the basic control law, as well as the anti-windup control law, will be derived below.

For known plant parameters, the anti-windup system model can be chosen as

$$\underbrace{\begin{pmatrix} \dot{x}_{aw} \\ \dot{w}_{1aw} \\ \dot{w}_{2aw} \end{pmatrix}}_{\dot{x}_{awc}} = \underbrace{\begin{pmatrix} A_p & 0 & 0 \\ 0 & F & 0 \\ gC_p & 0 & F \end{pmatrix}}_{A_c} \underbrace{\begin{pmatrix} x_{aw} \\ w_{1aw} \\ w_{2aw} \end{pmatrix}}_{x_{awc}} + \underbrace{\begin{pmatrix} B_p \\ g \\ 0 \end{pmatrix}}_{B_c} (u_{aw} - \Delta u), \quad (4.22)$$

$$y_{aw} = (C_p \ 0 \ 0) x_{awc}.$$

Summation of the states  $x_{cs}$  and  $x_{awc}$  yields

$$\dot{x}_{cs} + \dot{x}_{awc} = A_c (x_{cs} + x_{awc}) + B_c u_c. \quad (4.23)$$

In the equation above no influence of the saturation on the input is present, while the parameters are the same as for (4.21). Hence, the state of the combined state-space representation of (2.16) and (2.24) for the unsaturated case is recovered and can be fed back to the basic control law

$$u_c = \begin{pmatrix} \theta_1^T & \theta_2^T & \theta_3 & c \end{pmatrix} \begin{pmatrix} w_{1s} + w_{1aw} \\ w_{2s} + w_{2aw} \\ y_{ps} + y_{aw} \\ r \end{pmatrix} = \theta^T w_{us}. \quad (4.24)$$

However, since the anti-windup scheme in (4.22) requires the knowledge of the exact plant parameters, it can not be implemented. An implementable scheme will be derived on the basis of (4.22) after the introduction of the anti-windup controller.

The anti-windup controller structure

$$u_{aw} = \theta_{1aw}^T(t) \frac{\alpha_{n-2}(s)}{\Lambda(s)} (u_{aw} - \Delta u) + \theta_{2aw}^T(t) \frac{\alpha_{n-2}(s)}{\Lambda(s)} y_{aw} + \theta_{3aw}(t) y_{aw} = \theta_{aw}^T(t) w_{aw} \quad (4.25)$$

follows from the anti-windup state-space model (4.22). As for the standard output-feedback MRAC, the parameters of  $\Lambda_0(s)$  in  $\Lambda(s) = \Lambda_0(s) Z_{ref}(s)$  can be chosen by the designer, but have to be the same as for the basic controller. The ideal controller parameters  $\theta_{1aw}^*$ ,  $\theta_{2aw}^*$  and  $\theta_{3aw}^*$  of (4.25) are defined to satisfy

$$A_c x_{awc} + B_c \theta_{aw}^{*T} w_{aw} = A_{awrc} x_{awc}, \quad (4.26)$$

where the desired dynamic  $A_{awrc}$  is the non-minimal representation of  $A_{awr}$ , which can be chosen by the designer. The complete control scheme therefore becomes

$$u = u_c - u_{aw} = \theta^T w_{us} - \theta_{aw}^T w_{aw}. \quad (4.27)$$

The derivation of the final anti-windup scheme is done with the same procedure as for the state-feedback case, which is illustrated in Figure 4.1. Instead of the control signal  $u_{aw}$  based on the estimated parameters, the ideal control law

$$u_{aw}^* = \theta_{1aw}^{*T} \frac{\alpha_{n-2}(s)}{\Lambda(s)} (u_{aw}^* - \Delta u) + \theta_{2aw}^{*T} \frac{\alpha_{n-2}(s)}{\Lambda(s)} y_{aw} + \theta_{3aw}^* y_{aw} = \theta_{aw}^{*T} w_{aw}$$

is used for feedback inside the anti-windup scheme, so that the internal closed-loop system can be derived by substitution of  $u_{aw}^*$  in (4.22). Together with (4.26) this yields

$$\begin{aligned} \dot{x}_{awc} &= \underbrace{\begin{pmatrix} A_p + B_p \theta_{3aw}^* C_p & B_p \theta_{1aw}^{*T} & B_p \theta_{2aw}^{*T} \\ g \theta_{3aw}^* C_p & F + g \theta_{1aw}^{*T} & g \theta_{2aw}^{*T} \\ g C_p & 0 & F \end{pmatrix}}_{A_{awrc}} x_{awc} - \underbrace{\begin{pmatrix} B_p \\ g \\ 0 \end{pmatrix}}_{B_c} \Delta u, \\ y_{aw} &= \underbrace{\begin{pmatrix} C_p & 0 & 0 \end{pmatrix}}_{C_c} x_{awc}. \end{aligned} \quad (4.28)$$

With the same arguments as for standard output-feedback MRAC in Section 2.2.2, it can be shown that (4.28) is a non-minimal representation of

$$\begin{aligned} \dot{x}_{aw} &= A_{awr} x_{aw} - \frac{1}{c^*} B_{ref} \Delta u, \\ y_{aw} &= C_p x_{aw}. \end{aligned}$$

Similar to the state-feedback case the anti-windup system can be made implementable by using an estimation  $k_\Delta(t)$  for the unknown input gain  $\frac{1}{c^*}$ , which yields the anti-windup scheme

$$M_{aw} : \begin{aligned} \dot{x}_{aw} &= A_{awr} x_{aw} - k_\Delta B_{ref} \Delta u, \\ y_{aw} &= C_p x_{aw}. \end{aligned} \quad (4.29)$$

Note that  $C_p = [1 \ 0 \ \dots \ 0]$  due to the assumption of the observability canonical form of (4.20). Hence, the anti-windup scheme for output-feedback is similar to the scheme in (4.9) for state-feedback. However, a difference is clearly given by the fact that the structure of the anti-windup controller and the necessary consideration of the anti-windup controller states for the basic controller in (4.24).

## Reference Model

The reference model describes the desired behavior of the closed-loop system and consequently can be achieved if the ideal version of (4.27)

$$u^* = \theta^{*T} w_{us} - \theta_{aw}^{*T} w_{aw} \quad (4.30)$$

is used as the input signal to  $G_{lins}$ . Inserting the ideal control law in (4.21) and taking (2.25) and (4.28) into account, yields

$$\dot{x}_{cs} = A_{refc} (x_{cs} + x_{awc}) + B_{refc} \left( r + \frac{1}{c^*} \Delta u \right) - A_{awrc} x_{awc}.$$

As for the anti-windup scheme, the estimation  $k_\Delta(t)$  for the gain  $\frac{1}{c^*}$  is introduced, so that a minimal, implementable, and feasible representation of the reference model is given by

$$G_{refaw} : \dot{x}_{refs} = A_{ref} (x_{refs} + x_{aw}) + B_{ref} (r + k_\Delta \Delta u) - A_{awr} x_{aw}, \quad (4.31)$$

where the closed-loop state has been renamed as  $x_{refs}$ . In  $G_{refaw}$  the effect of saturation on the input is present as the input disturbance  $\Delta u$  and also the effect of the anti-windup scheme is represented by the terms  $A_{ref} x_{aw}$  and  $-A_{awr} x_{aw}$ .



## Parameter Updates and Closed-Loop Stability

A description of the closed-loop system with AMRAW can be derived by adding and subtracting  $B_c (\theta^{*\text{T}} w_{\text{us}} + \theta_{\text{aw}}^{*\text{T}} w_{\text{aw}})$  to the combined open-loop equations in (4.21), which results in

$$\begin{aligned} \dot{x}_{\text{cs}} = & A_{\text{refc}} (x_{\text{cs}} + x_{\text{aw}}) + B_{\text{refc}} r + B_{\text{refc}} \frac{1}{c^*} (\Delta u + u_c - u_{\text{aw}} - \theta^{*\text{T}} w_{\text{us}} + \theta_{\text{aw}}^{*\text{T}} w_{\text{aw}}) \\ & - A_{\text{awrc}} x_{\text{awc}}. \end{aligned} \quad (4.32)$$

Substitution of the control law (4.27) for  $u_c - u_{\text{aw}}$  and subtraction of the reference model (4.31) from the minimal representation of (4.32) leads to the closed-loop tracking error dynamics

$$\dot{e}_{\text{sat}} = A_{\text{ref}} e_{\text{sat}} + B_{\text{ref}} \frac{1}{c^*} (\tilde{\theta}^{\text{T}} w_{\text{us}} - \tilde{\theta}_{\text{aw}}^{\text{T}} w_{\text{aw}} - \tilde{k}_{\Delta} \Delta u), \quad (4.33)$$

with the parameter estimation errors  $\tilde{\theta} = \theta - \theta^*$ ,  $\tilde{\theta}_{\text{aw}} = \theta_{\text{aw}} - \theta_{\text{aw}}^*$ ,  $\tilde{k}_{\Delta} = c^* k_{\Delta} - 1$  and the transfer function

$$e_{\text{ys}} = \frac{1}{c^*} G_{\text{ref}} (\tilde{\theta}^{\text{T}} w_{\text{us}} - \tilde{\theta}_{\text{aw}}^{\text{T}} w_{\text{aw}} - \tilde{k}_{\Delta} \Delta u), \quad (4.34)$$

that can be used to derive the necessary parameter update laws for the complete control-law in (4.27). As for the standard MRAC, this requires a differentiation between the two cases of relative degree  $n^* = 1$  and  $n^* \geq 2$  of the plant  $G_{\text{lins}}$ .

$n^* = 1$

For the case  $n^* = 1$ , the reference model  $G_{\text{ref}}$  has to be SPR. If the parameter update laws are chosen to be

$$\dot{\theta} = -\Gamma w_{\text{us}} e_{\text{ys}} \text{sign}(c^*), \quad (4.35)$$

$$\dot{\theta}_{\text{aw}} = \Gamma_{\text{aw}} w_{\text{aw}} e_{\text{ys}} \text{sign}(c^*), \quad (4.36)$$

$$\dot{k}_{\Delta} = \gamma_{\Delta} \Delta u e_{\text{ys}}, \quad (4.37)$$

the function

$$V_1 = e_{\text{sat}}^{\text{T}} P e_{\text{sat}} + \frac{1}{|c^*|} (\tilde{\theta}^{\text{T}} \Gamma^{-1} \tilde{\theta} + \tilde{\theta}_{\text{aw}}^{\text{T}} \Gamma_{\text{aw}}^{-1} \tilde{\theta}_{\text{aw}}) + \frac{1}{\gamma_{\Delta} c^{*2}} \tilde{k}_{\Delta}^2, \quad (4.38)$$

with  $P$  as the solution for  $A_{\text{ref}}^{\text{T}} P + P A_{\text{ref}} = Q$  with  $Q = Q^{\text{T}} < 0$ , can be shown to be a Lyapunov function of (4.33) and (4.35)-(4.37). This result is derived in more detail in the proof of Theorem 4.3.

$n^* \geq 2$

For higher relative degrees an augmentation of the error dynamics (4.34), as it was done in Section 2.2.2 for basic MRAC, is necessary. The auxiliary error

$$e_{2\text{s}} = (\theta_{\text{cl}}^{\text{T}} G_{\text{REF}} - G_{\text{ref}} \theta_{\text{cl}}^{\text{T}}) w_{\text{cl}}$$

is used for the augmentation  $e_{\text{y}2\text{s}} = e_{\text{ys}} + k_{\text{a}} e_{2\text{s}}$ , which results in

$$e_{\text{y}2\text{s}} = \frac{1}{c^*} \tilde{\theta}_{\text{cl}}^{\text{T}} G_{\text{REF}} w_{\text{cl}} - \tilde{k}_{\Delta} G_{\text{ref}} \Delta u + \tilde{k}_{\text{a}} e_{2\text{s}} + \underbrace{\frac{1}{c^*} \theta_{\text{cl}}^{*\text{T}} G_{\text{REF}} w_{\text{cl}} - \frac{1}{c^*} G_{\text{ref}} \theta_{\text{cl}}^{*\text{T}} w_{\text{cl}}}_{\rightarrow 0 \text{ exponentially}}, \quad (4.39)$$

with  $\tilde{\theta}_{\text{cl}} = [\tilde{\theta}^{\text{T}} \quad \tilde{\theta}_{\text{aw}}^{\text{T}}]^{\text{T}}$ ,  $w_{\text{cl}} = [w_{\text{us}}^{\text{T}} \quad -w_{\text{aw}}^{\text{T}}]^{\text{T}}$ ,  $\tilde{k}_{\text{a}} = k_{\text{a}} - \frac{1}{c^*}$  and  $\tilde{k}_{\Delta} = \frac{1}{c^*} \tilde{k}_{\Delta}$ . The transfer function  $G_{\text{REF}}$  has already been defined in Section 2.2.2 as a diagonal MIMO system, where all nonzero entries are  $G_{\text{ref}}$ . The parameter update laws

$$\dot{\theta}_{\text{cl}} = -\text{sign}(c^*) \Gamma_{\text{cl}} \frac{e_{y2s} \phi_{\text{cl}}}{1 + \phi_{\text{cl}}^{\text{T}} \phi_{\text{cl}}} \quad (4.40)$$

$$\dot{k}_{\text{a}} = -\gamma_{\text{a}} \frac{e_{y2s} e_{2s}}{1 + \phi_{\text{cl}}^{\text{T}} \phi_{\text{cl}}} \quad (4.41)$$

$$\dot{k}_{\Delta} = \gamma_{\Delta} \frac{e_{y2s} \phi_u}{1 + \phi_{\text{cl}}^{\text{T}} \phi_{\text{cl}}} \quad (4.42)$$

with  $\phi_{\text{cl}} = G_{\text{REF}} w_{\text{cl}}$  and  $\phi_u = G_{\text{ref}} \Delta u$  result in boundedness for the estimated parameters, which can be shown with the Lyapunov function candidate

$$V_2 = \frac{1}{2} \left( \frac{1}{|c^*|} \tilde{\theta}_{\text{cl}}^{\text{T}} \Gamma_{\text{cl}}^{-1} \tilde{\theta}_{\text{cl}} + \frac{1}{\gamma_{\Delta}} \tilde{k}_{\Delta}^2 + \frac{1}{\gamma_{\text{a}}} \tilde{k}_{\text{a}}^2 \right). \quad (4.43)$$

This result is derived in more detail in the proof of Theorem 4.3.

Since all necessary equations to implement AMRAW for an output-feedback system  $G_{\text{lims}}$  have been derived above, the following theorem can be stated:

**Theorem 4.3.** *The control law (4.27) with a bounded reference signal  $|r(t)| \leq r_{\text{max}}(t)$  together with the parameter update laws (4.35)-(4.37) for  $n^* = 1$  or (4.40)-(4.42) for  $n^* \geq 2$  and the reference model (4.31) applied to the plant  $G_{\text{lims}}$  in (4.19) results in a bounded state of (4.21), if the plant is open-loop stable. Boundedness of the state for an unstable open-loop plant  $G_{\text{lims}}$  can be established under the following conditions:*

i) *The initial condition of the closed-loop state fulfills*

$$x_{\text{cs}}(0)^{\text{T}} P_{\text{W}} x_{\text{cs}}(0) \leq \lambda_{\min}(P_{\text{W}}) \left( \frac{2 p_{\text{b}} u_{\text{max}}}{|-q_0 + 2 p_{\text{b}} \|\tilde{\theta}^*\| \|C_{\text{t}}\|} \right)^2. \quad (4.44)$$

ii) *The reference signal does not exceed*

$$r_{\text{max}}(t) \leq \frac{u_{\text{max}} q_0 - \rho \eta D_{\text{aw}} \|C_{\text{t}}\| \|x_{\text{awc}}\|}{\rho \eta |c^*|}. \quad (4.45)$$

iii) *The initial values of the Lyapunov functions  $V$  in (4.38) and (4.43) fulfill*

$$\begin{aligned} & \sqrt{V(t_0)} \leq \\ & \sqrt{\frac{1}{|c^*| \lambda_{\max}(\Gamma)} \left( \frac{2 p_{\text{b}} u_{\text{max}} q_0 - 2 \rho \eta p_{\text{b}} \|c^*\| r_{\text{max}} - 2 \rho \eta p_{\text{b}} D_{\text{aw}} \|C_{\text{t}}\| \|x_{\text{awc}}(t_0)\|}{N_{\text{max}}} \right)} \end{aligned} \quad (4.46)$$

with

$$N_{\text{max}} = 2 \rho \eta p_{\text{b}} \|C_{\text{t}}\| \|x_{\text{awc}}(t_0)\| \left( 1 + \frac{\lambda_{\min}(\Gamma_{\text{aw}})}{\lambda_{\min}(\Gamma)} \right) + 2 \rho \eta p_{\text{b}} r_{\text{max}} + 4 p_{\text{b}}^2 u_{\text{max}} \|C_{\text{t}}\|.$$

The matrix  $P_W = P_W^T > 0$  is the solution of the linear equation  $A_{\text{ref}}^T P_W + P_W A_{\text{ref}} = -Q_W$  with  $Q_W = Q_W^T > 0$  and  $q_0$  is the minimal eigenvalue of  $Q_W$ . In conditions (i) – (iii) the definitions of  $\bar{\theta} = [\theta_1^T \ \theta_2^T \ \theta_3^T]^T$ ,  $p_b \triangleq \|P_W B_c\|$ ,  $\eta \triangleq |2 p_b \|\bar{\theta}^*\| \|C_t\| - q_0|$ ,  $D_{\text{aw}} \geq \|(\bar{\theta}^{*\text{T}} - \theta_{\text{aw}}^{*\text{T}})\|$  and  $\rho \triangleq \sqrt{\frac{\lambda_{\max}(P_W)}{\lambda_{\min}(P_W)}}$  have been used, where  $\lambda_{\min}(\cdot)$  and  $\lambda_{\max}(\cdot)$  are the minimal and maximal eigenvalue, respectively. The matrix

$$C_t \triangleq \begin{pmatrix} 0 & I_{n-1 \times n-1} & 0 \\ 0 & 0 & I_{n-1 \times n-1} \\ C_p & 0 & 0 \end{pmatrix}$$

defines the mappings  $\bar{w} = C_t x_{\text{cs}}$  and  $w_{\text{aw}} = C_t x_{\text{awc}}$ .

*Proof.* The derivative with respect to time of  $V_1$  in (4.38) is given by

$$\begin{aligned} \dot{V}_1 = e_{\text{sat}}^T & \left( P A_{\text{ref}} + A_{\text{ref}}^T P \right) e_{\text{sat}} + 2 e_{\text{sat}}^T P B_{\text{ref}} \frac{1}{c^*} \left( \tilde{\theta}^T w_{\text{us}} - \tilde{\theta}_{\text{aw}}^T w_{\text{aw}} - \tilde{k}_\Delta \Delta u \right) \\ & + \frac{2}{|c^*|} \tilde{\theta}^T \Gamma^{-1} \dot{\tilde{\theta}} + \frac{2}{|c^*|} \tilde{\theta}_{\text{aw}}^T \Gamma_{\text{aw}}^{-1} \dot{\tilde{\theta}}_{\text{aw}} + \frac{2}{\gamma_\Delta c^{*2}} \tilde{k}_\Delta \dot{\tilde{k}}_\Delta \end{aligned} \quad (4.47)$$

Since  $G_{\text{ref}}$  is SPR, it follows from the MKY-Lemma that  $P B_{\text{ref}} = C_{\text{ref}}^T$  which leads to  $e_{\text{sat}}^T P B_{\text{ref}} = e_{\text{ys}}$ . Therefore, the update laws (4.35)-(4.37) lead to  $\dot{V}_1 \leq 0$  and hence to bounded parameter estimations of the adaptive system with a plant of relative degree  $n^* = 1$ . Since  $V_1$  is a Lyapunov function, the state  $e_{\text{sat}}$  is bounded. If the open-loop plant  $G_{\text{lims}}$  is stable, a bounded input  $u_{\text{lim}}$  will lead to a bounded plant state and therefore to a bounded state  $x_{\text{refs}}$  of the reference model. Summation of the anti-windup scheme (4.29) and the reference model (4.31) leads to the stable system

$$\dot{x}_{\text{aw}} + \dot{x}_{\text{refs}} = A_{\text{ref}} (x_{\text{aw}} + x_{\text{refs}}) + B_{\text{ref}} r,$$

with the bounded input  $r$ . Hence,  $x_{\text{aw}} + x_{\text{refs}}$  is bounded and therefore  $x_{\text{aw}}$  is bounded.

The derivative with respect to time of  $V_2$  in (4.43) is given by

$$\dot{V}_2 = \frac{1}{|c^*|} \tilde{\theta}_{\text{cl}}^T \Gamma_{\text{cl}}^{-1} \dot{\tilde{\theta}}_{\text{cl}} + \frac{1}{\gamma_\Delta} \tilde{k}_\Delta \dot{\tilde{k}}_\Delta + \frac{1}{\gamma_a} \tilde{k}_a \dot{\tilde{k}}_a, \quad (4.48)$$

where  $\dot{\tilde{k}}_\Delta = \frac{1}{c^*} \dot{\tilde{k}}_\Delta = \dot{k}_\Delta$ . Substitution of the parameter update laws (4.40)-(4.42) yields

$$\dot{V}_2 = \frac{e_{y2s}}{1 + \phi_{\text{cl}}^T \phi_{\text{cl}}} \left( -\frac{1}{c^*} \tilde{\theta}_{\text{cl}}^T \phi_{\text{cl}} + \tilde{k}_\Delta \phi_u - \tilde{k}_1 e_{2s} \right). \quad (4.49)$$

From (4.39) it follows that  $\tilde{k}_a e_{2s} = e_{y2s} - \frac{1}{c^*} \tilde{\theta}_{\text{cl}}^T \phi_{\text{cl}} + \tilde{k}_\Delta \phi_u$  which results in

$$\dot{V}_2 = -\frac{e_{y2s}^2}{1 + \phi_{\text{cl}}^T \phi_{\text{cl}}} \leq 0 \quad (4.50)$$

and bounded parameter estimations for the adaptive closed-loop system for a plant of relative degree  $n^* \geq 2$ . If the open-loop plant  $G_{\text{lims}}$  is stable, the bounded input  $u_{\text{lim}}$  directly leads to boundedness of the states of (4.21). Boundedness of the states of (4.21) for the case of an unstable open-loop plant is given in Appendix B.  $\square$

## Summary

The complete control scheme of direct AMRAW for output-feedback plants is given by the control law (4.27), the anti-windup scheme (4.29), the reference model (4.31), and the parameter update laws (4.35)-(4.37) for  $n^* = 1$  and (4.40)-(4.42) for  $n^* \geq 2$ . All equations and tuning parameters, which are necessary to implement direct AMRAW for output-feedback plants, are summarized in Table 4.2. A schematic illustration of AMRAW for output-feedback plants is shown in Figure 4.2. Since the presented method is an extension of direct MRAC with output-feedback, Remarks 2.5-2.10 do also apply to AMRAW. Additional remarks and examinations are given in Chapter 5.

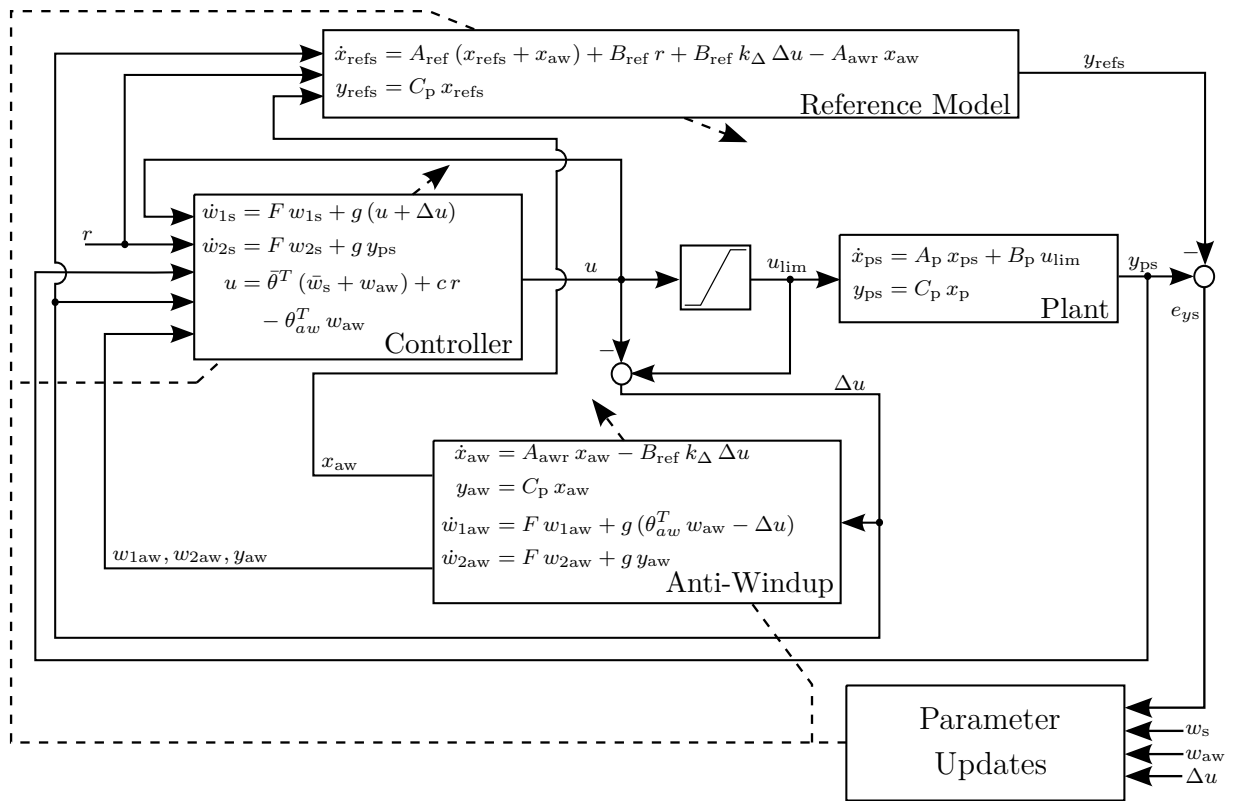


Figure 4.2: Schematic illustration of AMRAW for output-feedback plants. Note that for  $n^* \geq 2$  the calculation of  $e_{y2s}$ ,  $e_{2s}$ ,  $\phi_{\text{cl}}$ , and  $\phi_u$  is part of the parameter update block.

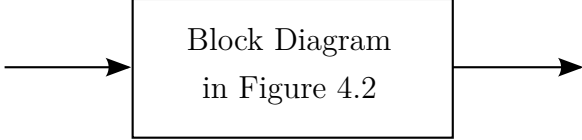
|   |  |
|---|--|
| Plant:  | $y_{ps} = k_p \frac{Z_p(s)}{R_p(s)} u_{lim}$   |
| Reference Model:  | $\begin{aligned} \dot{x}_{refs} &= A_{ref} (x_{refs} + x_{aw}) + B_{ref} (r + k_\Delta \Delta u) \\ &\quad - A_{awr} x_{aw} \\ y_{refs} &= C_p x_{refs} \end{aligned}$   |
| Control Law:  | $\begin{aligned} u &= \bar{\theta}^T (\bar{w}_s + w_{aw}) + c r - \theta_{aw}^T w_{aw} \\ w_s &= [\bar{w}_s^T \quad r]^T, \quad \theta = [\bar{\theta}^T \quad c]^T \\ w_{aw}, \theta_{aw} &\text{ from (4.25)} \end{aligned}$   |
| Anti-Windup:  | $\begin{aligned} \dot{x}_{aw} &= A_{awr} x_{aw} - k_\Delta B_{ref} \Delta u \\ y_{aw} &= [1 \quad 0 \quad \dots \quad 0] x_{aw} \end{aligned}$   |
| Tracking Error:   | $e_{ys} = y_{ps} - y_{refs}$   |
| Parameter Updates:  | $n^* = 1 : \quad \begin{aligned} \dot{\theta} &= -\Gamma w_{us} e_{ys} \text{sign}(c^*); \quad w_{us} \text{ from (4.24)} \\ \dot{\theta}_{aw} &= \Gamma_{aw} w_{aw} e_{ys} \text{sign}(c^*) \\ \dot{k}_\Delta &= \gamma_\Delta \Delta u e_{ys} \end{aligned}$<br>$n^* \geq 2 : \quad \begin{aligned} e_{2s} &= (\theta_{cl}^T G_{REF} - G_{ref} \theta_{cl}^T) w_{cl}, \quad G_{REF} = G_{ref} I_{2n \times 2n} \\ w_{cl} &= [w_{us}^T \quad -w_{aw}^T]^T; \quad \theta_{cl} = [\theta^T \quad \theta_{aw}^T]^T \\ \phi_{cl} &= G_{REF} w_{cl}; \quad \phi_u = G_{ref} \Delta u \\ e_{y2s} &= e_{ys} + k_a e_{2s} \\ \dot{\theta}_{cl} &= -\text{sign}(c^*) \Gamma_{cl} \frac{e_{y2s} \phi_{cl}}{1 + \phi_{cl}^T \phi_{cl}} \\ \dot{k}_a &= -\gamma_a \frac{e_{y2s} e_{2s}}{1 + \phi_{cl}^T \phi_{cl}} \\ \dot{k}_\Delta &= \gamma_\Delta \frac{e_{y2s} \phi_u}{1 + \phi_{cl}^T \phi_{cl}} \end{aligned}$ |
|  <p style="text-align: center;">Block Diagram<br/>in Figure 4.2</p> |  |
| Design Parameters:  | <ul style="list-style-type: none"> <li>• <math>A_{ref}, B_{ref}</math> satisfy performance requirements (see also Remark 2.6 and Remark 2.9).</li> <li>• <math>A_{awr}</math> determines the desired anti-windup dynamics (see Section 5.2.1)</li> <li>• <math>\Lambda_0</math> of degree <math>n - m - 1</math> (see Remark 2.10)</li> <li>• <math>\Gamma = \Gamma^T &gt; 0, \Gamma_{aw} = \Gamma_{aw}^T &gt; 0, \Gamma_{cl} = \text{diag}(\Gamma_{aw}, \Gamma_{cl}), \gamma_\Delta &gt; 0, \gamma_a &gt; 0</math> (see Remark 2.5)</li> </ul>  |

Table 4.2: Summary of AMRAW for output-feedback.

### 4.3 Indirect Adaptive Model Recovery Anti-Windup for Output-Feedback

The indirect method of adaptive model recovery anti-windup for output-feedback presented in this section, extends the APPC scheme from Section 2.2.3 in order to take saturation of the input amplitude into account. Since an indirect adaptive method is derived here, the certainty equivalence principle rather than a stability analysis is used to introduce suitable parameter update laws.

For the following presentation the plant

$$G_{nl2s} : \quad y_{ps} = \frac{Z_p(D)}{R_p(D)} \left( u_{lim} + \theta_{nl}^T f_{nl}(y_{ps}) \right) \quad (4.51)$$

is considered, with the same assumptions as for  $G_{nl2}$  in (2.41) and  $u_{lim}$  from the definition in (3.1). The state-space equation of the plant is given by

$$\begin{aligned} \dot{x}_{ps} &= A_p x_{ps} + B_p \left( u_{lim} + \theta_{nl}^T f_{nl}(y_{ps}) \right), \\ y_{ps} &= C_p x_{ps}. \end{aligned} \quad (4.52)$$

#### Anti-Windup Scheme

The state-space equation (4.52) is very similar to the plant description for the direct state-feedback AMRAW. The only difference is given by the measurement of the output  $y_{ps}$  instead of the complete state. Therefore, the same arguments as for direct AMRAW with state-feedback can be used to show that the summation of  $y_{ps}$  and the output of the anti-windup system

$$\begin{aligned} \dot{x}_{aw} &= A_p x_{aw} + B_p \left( -\Delta u + u_{aw} + \theta_{nl}^T (f_{nl}(y_{ps} + y_{aw}) - f_{nl}(y_{ps})) \right), \\ y_{aw} &= C_p x_{aw}, \end{aligned} \quad (4.53)$$

recovers the output of the plant  $G_{nl2}$  in (2.41). In difference to the direct AMRAW methods, the uncertain system parameters are estimated so that an implementable version of (4.53) is given by

$$\begin{aligned} \dot{x}_{aw} &= \hat{A}_p x_{aw} + \hat{B}_p \left( -\Delta u + u_{aw} + \hat{\theta}_{nl}^T (f_{nl}(y_{ps} + y_{aw}) - f_{nl}(y_{ps})) \right), \\ y_{aw} &= \hat{C}_p x_{aw}, \end{aligned} \quad (4.54)$$

where  $\hat{A}_p$ ,  $\hat{B}_p$ , and  $\hat{C}_p$  are in controller canonical form and can be build from the estimations of  $z_i, r_j$  for  $i = 0, \dots, m-1$  and  $j = 0, \dots, n-1$  in  $G_{nl2s}$ . The parameter vector  $\hat{\theta}_{nl}$  is an estimation of  $\theta_{nl}$ . Usage of the recovered output of the plant  $G_{nl2}$  allows the calculation of the basic control law

$$u_c = -\frac{P(D)}{Q(D)L(D)} (y_{ps} + y_{aw}) + \frac{M(D)}{Q(D)L(D)} r - \hat{\theta}_{nl}^T f_{nl}(y_{ps} + y_{aw}), \quad (4.55)$$

where the computation of the controller parameters has to be done with equations (2.44) and (2.45).

In order to regulate the unwanted behavior  $y_{aw}$  to zero a state-feedback controller with nonlinear compensation

$$u_{aw} = K_{aw}^T(t) x_{aw} - \hat{\theta}_{nl}^T (f_{nl}(y_{ps} + y_{aw}) - f_{nl}(y_{ps})) \quad (4.56)$$

is introduced into the anti-windup scheme. The time depending gain for the states is calculated by

$$\hat{A}_p + \hat{B}_p K_{aw}(t)^T = A_{awr}, \quad (4.57)$$

where the matrix  $A_{awr}$  can be chosen by the designer to have desired closed-loop poles for the anti-windup scheme. Hence, the complete control scheme is given by

$$u = u_c - u_{aw} = -\frac{P(D)}{Q(D)L(D)}(y_{ps} + y_{aw}) + \frac{M(D)}{Q(D)L(D)}r - \hat{\theta}_{nl}^T f_{nl}(y_{ps}) - K_{aw}^T x_{aw}. \quad (4.58)$$

Note that in difference to the direct methods of AMRAW, which have been presented in the preceding sections, the structure of the anti-windup controller in (4.56) is different from the structure of the basic controller in (4.55). A state-feedback gain  $K_{aw}^T$  has been chosen, because it does not introduce additional controller states in the closed-loop system and it is straight forward to compute with (4.57).

Since the calculation of  $K_{aw}$  in (4.57), the control law (4.56), and the anti-windup system in (4.54) are based on estimated parameters, it is always true that

$$\begin{aligned} \dot{x}_{aw} &= \hat{A}_p x_{aw} + \hat{B}_p \left( -\Delta u + u_{aw} + \hat{\theta}_{nl}^T (f_{nl}(y_{ps} + y_{aw}) - f_{nl}(x_{ps})) \right) \\ &= A_{awr} x_{aw} - \hat{B}_p \Delta u, \end{aligned} \quad (4.59)$$

so that the anti-windup system can be implemented as

$$M_{aw} : \begin{aligned} \dot{x}_{aw} &= A_{awr} x_{aw} - \hat{B}_p \Delta u, \\ y_{aw} &= \hat{C}_p x_{aw}. \end{aligned} \quad (4.60)$$

## Parameter Updates

Similar to the method of APPC, many different estimation schemes can be used to estimate the plant parameters. As for the APPC scheme in Section 2.2.3, a least-squares algorithm with covariance resetting is chosen for the indirect AMRAW scheme. No modifications for this algorithm are necessary for its application in the AMRAW scheme. However, in order to account for the input saturation, the linear parametric model needs to be slightly modified in comparison to (2.51). It becomes

$$y_{fs} = \theta_p^T \phi_{ps} \quad (4.61)$$

with

$$y_{\text{fs}} = \frac{D^n y_{\text{ps}}}{\Lambda_e(s)},$$

$$\theta_{\text{p}} = \left[ \theta_y^{\text{T}} \quad \theta_u^{\text{T}} \quad \theta_{\text{znl},m}^{\text{T}} \quad \dots \quad \theta_{\text{znl},0}^{\text{T}} \right]^{\text{T}}, \text{ and}$$

$$\phi_{\text{ps}} = \left[ -\frac{\alpha_{n-1}^{\text{T}}}{\Lambda_e(D)} y_{\text{ps}} \quad \frac{\alpha_m^{\text{T}}}{\Lambda_e(D)} u_{\text{lim}} \quad \frac{D^m}{\Lambda_e(D)} f_{\text{nl}}(y_{\text{ps}})^{\text{T}} \quad \dots \quad \frac{1}{\Lambda_e(D)} f_{\text{nl}}(y_{\text{ps}})^{\text{T}} \right]^{\text{T}},$$

where  $\alpha_i(D)$  has been defined in (2.50),  $\theta_y = [r_{n-1} \quad \dots \quad r_0]^{\text{T}}$ ,  $\theta_u = [z_m \quad \dots \quad z_0]^{\text{T}}$ ,  $\theta_{\text{znl},i} = z_i \theta_{\text{nl}}$  for  $i = 0, \dots, m$ , and an arbitrary but Hurwitz polynomial  $\Lambda_e(s)$  of degree  $n$ . Hence, the modification is done for the definition of  $\phi_{\text{ps}}$ , which includes the saturated input  $u_{\text{lim}}$  instead of the unsaturated input as in (2.51). For the linear parametric model (4.61) the least-squares algorithm (2.52) can be used to estimate the plant parameters. Since the estimation scheme is the same as for basic APPC the estimated plant parameters have the same properties stated in Appendix A.

## Summary

The complete control scheme of indirect AMRAW for output-feedback plants is given by the control law (4.58), the plant parameter estimation scheme (2.52) for the linear parametric model (4.61) and the rules for the controller parameter calculation in (2.44), (2.45) or (2.47), and (4.57). Since the presented method is based on indirect APPC, the Remarks 2.12-2.14 do also apply for indirect AMRAW. All equations and tuning parameters, which are necessary to implement indirect AMRAW for output-feedback plants, are summarized in Table 4.3. Additional remarks and examinations are given in Chapter 5.



|                                   |   |
|-----------------------------------|---|
| Plant:                            | $y_{ps} = \frac{Z_p}{R_p} \left( u_{lim} + \theta_{nl}^T f_{nl}(y_{ps}) \right)$  |
| Control Law:                      | $u = -\frac{P}{Q_L} (y_{ps} + y_{aw}) + \frac{M}{Q_L} r - \hat{\theta}_{nl}^T f_{nl}(y_{ps}) - K_{aw}^T x_{aw}$<br>$Q r = 0$  |
| Anti-Windup:                      | $\dot{x}_{aw} = A_{awr} x_{aw} - \hat{B}_p \Delta u$<br>$\dot{y}_{aw} = \hat{C}_p x_{aw}$   |
| Plant Parameter Estimation:       | $\dot{\hat{\theta}}_{ps} = P_{ls} \epsilon_s \phi_{ps}$<br>$\dot{P}_{ls} = -\frac{P_{ls} \phi_{ps} \phi_{ps}^T P_{ls}}{1 + \phi_{ps}^T \phi_{ps}}, \quad P_{ls}(0) = P_{ls0}, \quad P_{ls}(t_r) = \rho_r I_{p \times p}$<br>$\epsilon_s = \frac{y_{fs} - \hat{\theta}_p^T \phi_p}{1 + \phi_{ps}^T \phi_{ps}}$<br>$y_{fs} = \frac{D^n y_{ps}}{\Lambda_e}, \quad \hat{\theta}_p = \left[ \hat{\theta}_y^T \quad \hat{\theta}_u^T \quad \hat{\theta}_{znl,m}^T \quad \dots \quad \hat{\theta}_{znl,0}^T \right]^T$<br>$\phi_{ps}^T = \left[ -\frac{\alpha_{n-1}^T}{\Lambda_e} y_{ps} \quad \frac{\alpha_m^T}{\Lambda_e} u_{lim} \quad \frac{D^m f_{nl}^T(y_{ps})}{\Lambda_e} \quad \dots \quad \frac{1}{\Lambda_e} f_{nl}^T(y_{ps}) \right]$ |
| Controller Parameter Calculation: | $A_d(D) = L(D) Q(D) \hat{R}_p(D) + P(D) \hat{Z}_p(D)$<br>$M = \begin{cases} \frac{a_{d,0}}{\hat{z}_0}, & \text{for piecewise constant } r \text{ and } z_0 \neq 0 \\ P, & \text{otherwise} \end{cases}$<br>$A_{awr} = \hat{A}_p + \hat{B}_p K_{aw}^T$<br>$\hat{\theta}_{nl} = \frac{\hat{\theta}_{znl,i}}{\hat{z}_i}, \text{ for any } i = 0, \dots, m, \quad \hat{\theta}_u = \left[ \hat{z}_m \quad \dots \quad \hat{z}_0 \right]^T$<br>$\hat{R}_p(D) = D^n + \hat{\theta}_y^T \alpha_{n-1}(D), \quad \hat{Z}_p(D) = \hat{\theta}_u^T \alpha_m$<br>$\alpha_i(D) = \left[ D^i \quad D^{i-1} \quad \dots \quad D \quad 1 \right]^T$   |
|                                   |   |
| Design Parameters:                | <ul style="list-style-type: none"> <li>• <math>A_d</math> with roots at desired closed-loop poles and <math>A_{awr}</math> with desired anti-windup dynamic (see Remark 5.2)</li> <li>• <math>\Lambda_e</math> of degree <math>n</math> (see Remark 2.12)</li> <li>• <math>P_{ls}(0)</math>, <math>\rho_0</math>, and <math>\rho_r</math> (see Remark 2.12)</li> </ul>  |

Table 4.3: Summary of indirect AMRAW based on the polynomial approach of APPC.



# Chapter 5

## Adaptive Model Recovery Anti-Windup: Remarks and Simulations

The AMRAW schemes derived in the previous chapter extend the basic adaptive methods presented in Chapter 2. In order to deal with limited input amplitudes of the controlled plants these extensions introduce additional dynamics and parameters in the closed-loop system. For the control engineer, it might not directly be clear how to use these additional degree of freedom and what kind of considerations are necessary before applying AMRAW. Therefore, some interpretations and information about the newly introduced anti-windup scheme are given in this chapter in the form of several remarks. Some of the discussions and comments in the remarks are based on observations in the results of multiple simulations and experiments. Selected simulation results are shown in this chapter, whereas the experimental results and a detailed explanation of these experiments can be found in the next chapter.

### 5.1 Direct Adaptive Model Recovery Anti-Windup for State-Feedback

In comparison to basic MRAC summarized in Table 2.1, the AMRAW scheme given in Table 4.1 adds an additional degree of freedom represented by the anti-windup controller. This additional degree of freedom has been introduced to allow for performance considerations for input saturated systems. Remark 5.1 gives an idea of how to use this additional degree of freedom and how its influence on the closed-loop performance can be interpreted.

For many technical plants, a good system knowledge might be sufficient for the control engineer to tune an anti-windup scheme like MRAW. Furthermore, some tuning procedures for known plant parameters exist, that lead to a systematic parametrization of the anti-windup scheme. However, if the plant parameters are uncertain or even changing during operation, an initial choice of the desired anti-windup dynamics might not work

well for the whole lifetime of the system. Since AMRAW has been introduced in order to account for such uncertain plants, some heuristic, intuitive, and practical approaches to find the desired anti-windup dynamics are given in Remark 5.2.

Even if AMRAW provides the possibility to influence the closed-loop performance during saturation of the input, the implementation costs and the tuning effort are clearly higher than for KAAW. Therefore, from the viewpoint of the application costs, KAAW is preferable over AMRAW. In Remark 5.3 a comment about the connection between AMRAW and KAAW is given and it is shortly discussed in which cases KAAW rather than AMRAW should be used.

Not only the decisions of when to use AMRAW and how to correctly tune its anti-windup scheme needs to be considered with care. Also, the conditions in Theorem 4.1, which guarantee stability if AMRAW is applied to unstable open-loop plants require some explanation. Therefore, the theorem and especially the conditions are shortly discussed in Remark 5.4. However, all the derived stability results are not valid anymore if AMRAW is applied to plants with uncertain maximal input amplitudes. This issue and ways to avoid it are further discussed in Remark 5.5. Finally a short comment about the usage of a CRM in AMRAW is given in Remark 5.6.

The discussions, proposals and comments in the following remarks are partially based on the results of the Simulation Examples 5.1-5.3 in Section 5.1.2. These examples show the general benefits of AMRAW and its advantages in comparison with KAAW. The method of KAAW has been chosen for comparative examinations because AMRAW is partially based on the main concept of KAAW, which has already been used successfully in different practical applications (see Section 3.3).

### 5.1.1 Remarks

**Remark 5.1 (Additional Degree of Freedom).** The anti-windup controller of AMRAW introduces an additional degree of freedom in the closed-loop system, which can be used to influence the closed-loop performance during saturation of the input. The notion of performance, in this case, is equivalent to a reduction of the unwanted behavior, represented by the anti-windup state  $x_{aw}$ , on the closed-loop behavior. Since the anti-windup controller only regulates  $x_{aw}$ , it can influence the closed-loop performance if input saturation occurs without changing it if the input does not encounter its limits. This is shown in Simulation Example 5.1. In addition to the tuning parameters of basic MRAC, AMRAW allows the control designer to choose the desired dynamics  $A_{awr}$  of the anti-windup system, which determines the ideal controller parameters of the anti-windup controller. In the Simulation Examples 5.1-5.3 it can be observed that fast anti-windup dynamics forces the input to stay longer in saturation and vice versa. An interpretation of this behavior can be given under consideration of block diagram **II** in Figure 4.1 as follows. The desired anti-windup dynamics can be achieved by feedback of the ideal control signal to the plant model inside the anti-windup scheme. Therefore, the requirement of fast dynamics of the anti-windup scheme requires high gains of the anti-windup controller and therefore results in higher amplitudes of the control signal  $u_{aw}^*$ . Since  $u_{aw}$ , as the es-

timation of  $u_{\text{aw}}^*$  contributes to the input of the plant, also the amplitude of  $u$  will become higher and therefore grows further above the maximal amplitude  $u_{\text{max}}$ . Consequently, it takes a longer time for the plant input to come out of saturation again.

**Remark 5.2 (Tuning Proposals).** Similar to standard MRAC, the reference model system matrix  $A_{\text{ref}}$  and the input vector  $B_{\text{ref}}$  of  $G_{\text{refaw}}$  in (4.10) can be chosen by the control designer such that this part of the reference model represents the desired closed-loop dynamics without saturation of the plant input. An additional degree of freedom in the method of AMRAW has been introduced in order to allow for performance considerations in adaptive systems with limited input amplitude. This is possible by choosing the desired anti-windup dynamics  $A_{\text{awr}}$  in a suitable way. For first order plants, Theorem 4.2 suggests the choice of a very fast stable pole for the desired anti-windup dynamics. The absolute value of this pole is only limited by practical limitations such as measurement noise. However, already the choice of  $A_{\text{awr}}$  for second order plants is not straight forward anymore. It is shown in Simulation Examples 5.1-5.2 that the optimal choice depends on the plant, the reference model dynamics and the desired or at least acceptable closed-loop behavior during input saturation. This makes the specification of a systematic procedure to tune  $A_{\text{awr}}$  more difficult in comparison to the choice of  $A_{\text{ref}}$  and  $B_{\text{ref}}$ .

If nominal plant parameters and hence the corresponding controller parameters are known, which is usually the case for technical plants, an anti-windup tuning for the nominal case is possible. This can either be done by manual tuning or by using a systematic optimization technique presented e.g. in [122, 124]. However, for changing plant parameters no guarantees for the optimality of the anti-windup parameters can be given anymore with this tuning procedure.

For some plants a convex set of possible plant parameters is known in advance. Then the estimated controller parameters can be guaranteed to stay in the corresponding set by using parameter projection (see Section 2.2.5) and hence a bound on the parameter uncertainty is known. For such cases, optimal parameters for the anti-windup controller can be found with the methods presented in [49, 155]. However, since these methods are based on a robust approach, they might only work satisfactorily for sufficiently small parameter uncertainties. For strong uncertainties, such an approach could lead to rather conservative parametrization of the anti-windup scheme and hence to an insufficient closed-loop performance. In such cases, it is unavoidable to find a suitable  $A_{\text{awr}}$  by extensive simulations with multiple predefined or random combinations of possible plant and controller parameters. With this approach, a desired anti-windup dynamic can be found that likely leads to the best closed-loop behavior for all parameter combinations. For higher order plants, this procedure is clearly very time consuming and might therefore not be feasible. However, in some technical applications, where plant parameters change during lifetime due to aging or changing environments, the direction of the parameter changes is known in advance and only the corresponding time, where these changes occur, and the rate of change is unknown. For such plants, only a reduced number of simulations are necessary to find a suitable  $A_{\text{awr}}$ , since the knowledge about parameter changes adds additional restriction on the plant parameter set.

For some plants neither a good system knowledge is available nor extensive simulations are feasible. For these plants, the desired anti-windup dynamics  $A_{\text{awr}}$  can be made tunable. This renders a re-tuning of the desired anti-windup dynamics possible if the plant parameters change and the performance for a saturated input becomes unacceptable. This procedure is still preferable compared to an occasionally re-tuned constant controller, since the parameters of the basic controller and the anti-windup scheme in AMRAW will be adapted automatically.

**Remark 5.3 (Connection between KAAW and AMRAW).** Since the concept of an extended reference model introduced with KAAW has also been used for AMRAW, a connection between the two methods exist, which can be seen by inspection of the AMRAW control law (4.8), the reference model (4.10), and the corresponding equations (2.5) and (3.16) for KAAW. If the desired dynamics of the closed-loop and the anti-windup system are chosen such that  $A_{\text{awr}} = A_{\text{ref}}$ , it directly follows that  $K_x^* = K_{\text{aw}}^*$  for the ideal controller parameters. In such cases, the effect of the anti-windup method in the reference model as well as in the control law is canceled out, so that AMRAW and KAAW lead to the same closed-loop behavior after the controller parameters have been adapted to their ideal values. Consequently, if the best closed-loop performance is achieved for  $A_{\text{awr}} = A_{\text{ref}}$ , KAAW instead of AMRAW should be used for the following reasons. The tuning effort, the implementation costs, and the computational costs are less for KAAW, because AMRAW introduces  $2n$  additional states in the controller due to the anti-windup system and the additional parameter estimation of  $K_{\text{aw}}$ . Since AMRAW introduces  $n$  additional parameters in comparison to KAAW, a stronger excitation of the AMRAW closed-loop system is required (see Remark 2.3) if parameter estimation is part of the control task.

**Remark 5.4 (Conditions of Theorem 4.1).** In Theorem 4.1 it has been stated that the boundedness of all closed-loop signals can always be achieved if AMRAW is applied to open-loop stable plants. For unstable open-loop plants, guaranteed boundedness of the closed-loop signals requires the conditions *i) – iii)* in Theorem 4.1 to hold, which are similar to the conditions for KAAW given in [75]. However, already the conditions for KAAW are quite restrictive, such that it is very difficult to find higher order plants that actually fulfill them [19]. When applying AMRAW the additional state  $x_{\text{aw}}$  further restricts the admissible initial states of the closed-loop and the maximal reference signal. Only first order plants have been found that can fulfill condition *i) – iii)* in Theorem 4.1 with reasonable maximal admissible amplitudes of the reference signal.

Even for such low order plants already the calculation of the conditions *i) – iii)* in Theorem 4.1 is not straight forward since it requires the knowledge of a maximum  $x_{\text{awmax}} \geq \|x_{\text{aw}}(t)\|$ . If tuning of  $A_{\text{awr}}$  is done as proposed in Remark 5.2, a value for  $x_{\text{awmax}}$  can directly be deduced from extensive simulations. If such simulations are not feasible, condition *ii)* for the maximal reference signal amplitude can be calculated during operation, so that it can be reduced if boundedness can no longer be guaranteed by Theorem 4.1. However, the conditions for AMRAW and KAAW have been found out to be very conservative, so that a violation of them does not necessarily leads to unboundedness of the closed-loop signals. This is shown in Simulation Examples 5.2 and 5.3.

**Remark 5.5 (Uncertain Input Amplitude).** In the preceding derivation of AMRAW the upper and lower limit of the input amplitude has been assumed to be known and to have the same absolute value. However, for many technical applications that is not true and the maximal amplitudes might even change during operation. For these cases, the following considerations should be taken into account, in order to prevent the closed-loop system from avoidable problems. Unsymmetrical limitations of the input amplitude, i.e. different maximal values for positive and negative input amplitudes are not a problem for the application of AMRAW as long as they are taken into account correctly for the calculation of  $\Delta u$ . If boundedness for the closed-loop system needs to be guaranteed with the conditions of Theorem 4.1, the calculation of the necessary conditions needs to be done with the smallest absolute value of the input amplitude limit. For the tuning of AMRAW the different limitations also need to be taken into account. Since a tighter input limitation will lead to stronger saturation effects, the closed-loop behavior should be evaluated for the corresponding input direction.

Implementing AMRAW exactly as shown in the block diagram of Table 4.1 can avoid problems which might arise if only an estimation of the amplitude limits is available. If the shown artificial saturation in front of the plant is actually implemented such that its limitations are guaranteed to be tighter than the real input limitations of the plant, it can be avoided that the actual input amplitude of the plant is higher than that of  $u_{\text{lim}}$  used for calculation of  $\Delta u$ . However, if the maximal input amplitude of the plant is reduced during operation, e.g. due to defects of the technical system or changes of the environment, the new saturation limits might be unknown and can not directly be adjusted, so that an incorrect calculation of  $\Delta u$  results. The experiment in Section 6.1 suggests that AMRAW does not totally fail in such cases. However, conditions for guaranteed boundedness of the AMRAW closed-loop states have only been derived for known limits of the input amplitude in this work.

**Remark 5.6 (AMRAW with CRM).** It can be seen by inspection of the stability analysis for AMRAW that combining it with a CRM, which has been presented in Section 2.2.4, does not change the stability results in Theorem 4.1. In order to benefit from the properties of a CRM it is therefore advisable to also use it in combination with AMRAW.

### 5.1.2 Simulations

**Simulation Example 5.1.** The plant  $G_{\text{ex1s}}$  is considered, which differs from the plant  $G_{\text{ex1}}$  from Simulation Example 2.1 in that it has a maximal input amplitude of  $u_{\text{max}} = 100$ . This is equivalent to a maximal force that can be applied to the mechanical system and therefore makes the example more realistic. The reference model and the initially estimated plant parameters are adopted from Simulation Example 2.1. For the desired dynamics of the anti-windup scheme the system matrix

$$A_{\text{awr}} = \begin{pmatrix} 0 & 1 \\ -676 & -52 \end{pmatrix}$$

has been defined, which has two eigenvalues at  $-26$ . These specifications lead to the following initially estimated controller parameters and the respective ideal parameters of AMRAW:

| initial parameters   | ideal parameters  |
|--|---|
| $K_x(0) = \begin{pmatrix} -10.5105 \\ -2.7027 \end{pmatrix}$             | $K_x^* = \begin{pmatrix} -22.9730 \\ -5.1351 \end{pmatrix}$       |
| $k_r(0) = 15.0150$   | $k_r^* = 27.0270$   |
| $\hat{\theta}_{\text{nl}}(0) = \begin{pmatrix} 6.0 \\ 0.2 \end{pmatrix}$ | $\theta_{\text{nl}} = \begin{pmatrix} 3.0 \\ 0.4 \end{pmatrix}$   |
| $K_{\text{aw}}(0) = \begin{pmatrix} -33.93 \\ -4.50 \end{pmatrix}$       | $K_{\text{aw}}^* = \begin{pmatrix} -65.13 \\ -8.37 \end{pmatrix}$ |
| $k_{\Delta}(0) = 0.066$  | $k_{\Delta}^* = 0.037$  |

The simulation results for the same reference signals and simulation length as in Example 2.1 are shown in Figure 5.1, where the adaptation gains for the parameter update laws have been chosen as  $\Gamma_x = 0.1 I_{2 \times 2}$ ,  $\gamma_r = 0.1$ ,  $\Gamma_{\text{nl}} = 0.1 I_{2 \times 2}$ ,  $\Gamma_{\text{aw}} = 2 I_{2 \times 2}$  and  $\gamma_{\Delta} = 0.1$ . The results of the introduced method of AMRAW are compared to the results of KAAW in the first three graphs, which show the system responses before ( $t < 10$ s) and after adaptation, respectively. These results together with the estimated AMRAW parameters in the fourth graph verify that the closed-loop signals stay bounded. In addition, it can be seen in the third graph that the plant input for AMRAW stays longer in saturation than the input of KAAW. Therefore more input energy is supplied to the system, which results in a faster closed-loop response.

As a second part of this example, additional simulations have been carried out with different choices of the desired anti-windup poles, while the parameters of  $A_{\text{ref}}$  and  $B_{\text{ref}}$  have been kept constant. The resulting system responses for ideal controller parameters are shown in Figure 5.2 together with the respective saturated inputs. Note that the choice of  $-10$  for the desired anti-windup poles is equivalent to an application of KAAW (see Remark 5.7). It can be observed that for faster desired poles of the anti-windup schemes, the input stays longer in saturation, so that the closed-loop response becomes faster. However, for the desired anti-windup poles at  $-45$  the input stays too long in saturation, which results in a strong undershoot for the step response downwards. In this case it can be seen that the maximal amplitude of the force is not sufficient to stop the system with such a high velocity at the desired position. This effect has been introduced as plant-windup at the beginning of Chapter 3.

Another property of AMRAW is also shown in Figure 5.2 for a small change of the desired set point, which does not lead to saturation of the input. No difference of the closed-loop responses can be seen for this step command. These results confirm that AMRAW allows for an adjustment of the closed-loop performance during input saturation without having an influence on the behavior when the input does not exceed its maximal amplitude. Hence, the desired closed-loop performance for the unsaturated case can be defined in the same way it is done for MRAC.



In difference to AMRAW the adjustment of the performance during input saturation for KAAW requires a change of the parameters of the reference model. In order to point out the effect of changing the reference model in the given system, a third simulation has been done with

$$\dot{x}_{\text{ref}} = \begin{pmatrix} 0 & 1 \\ -676 & -52 \end{pmatrix} x_{\text{ref}} + \begin{pmatrix} 0 \\ 676 \end{pmatrix} r, \quad (5.1)$$

which has its two poles at  $-26$ , such as the system matrix  $A_{\text{awr}}$  considered so far. The results are shown in Figure 5.3. For KAAW a small overshoot of the step response upwards and a very strong undershoot of the step response downwards can be observed. This result shows that tuning of  $A_{\text{ref}}$  and  $B_{\text{ref}}$  of the reference model is not equivalent to tuning of the anti-windup dynamics  $A_{\text{awr}}$  in AMRAW. If the given reference model (5.1) is desired for small set point changes, where saturation of the input does not occur, the additional degree of freedom provided by the method of AMRAW allows to avoid the overshoots and undershoots during the large step commands of the reference signal. This is also shown in Figure 5.3, where the desired system matrix for the anti-windup scheme of AMRAW has been chosen as

$$A_{\text{awr}} = \begin{pmatrix} 0 & 1 \\ -196 & -16 \end{pmatrix}$$

with two poles at  $-13$ .

Note that additional simulations have been carried out with a better-suited reference signal regarding parameter estimation. The results are shown in Appendix C and verify that a stronger excitation of the closed-loop systems results in faster parameter estimation for AMRAW.

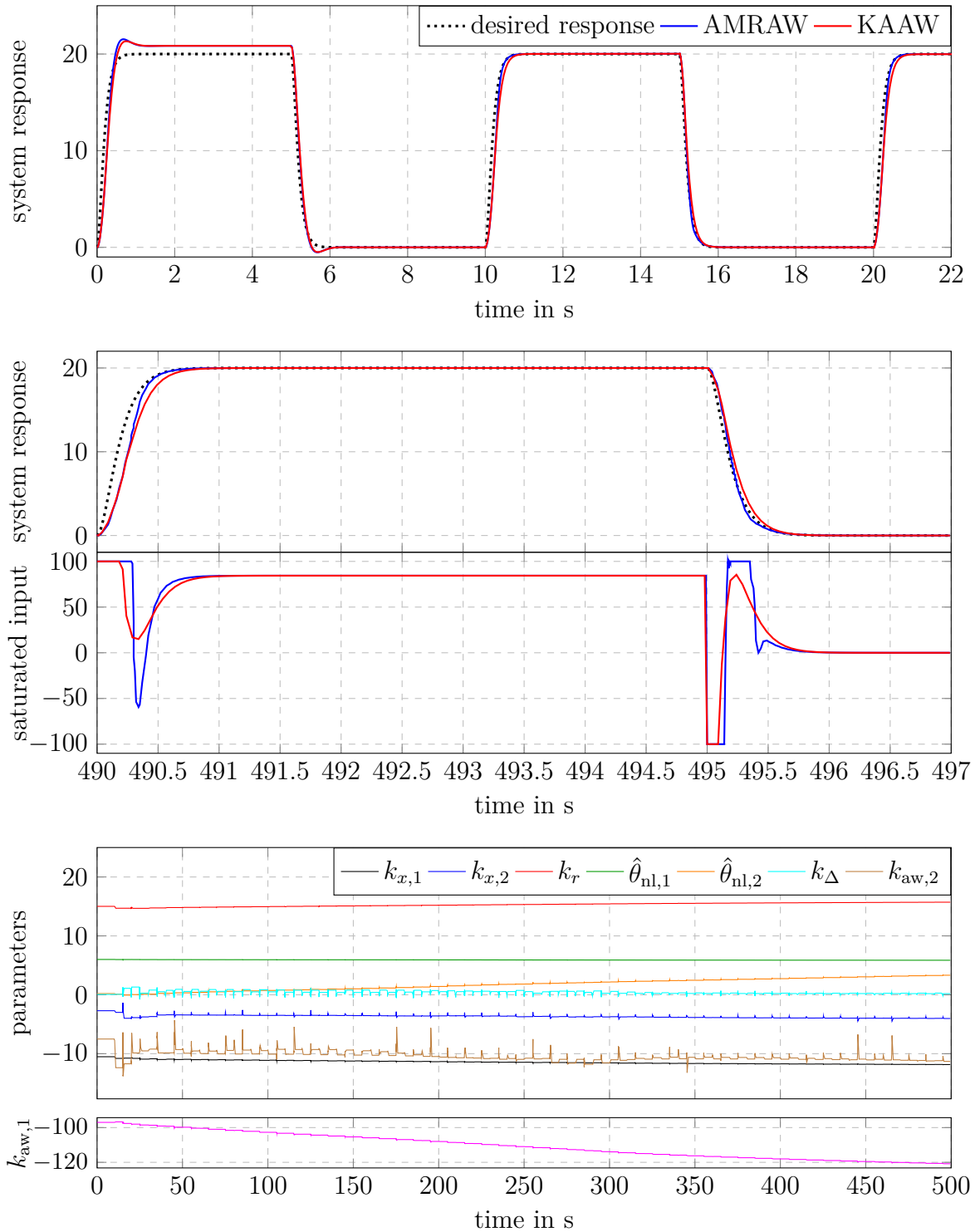


Figure 5.1: Results of Simulation Example 5.1 for KAAW and AMRAW with state-feedback before ( $t < 10$ s) and after adaptation. The last graphs show the parameter estimations of AMRAW.

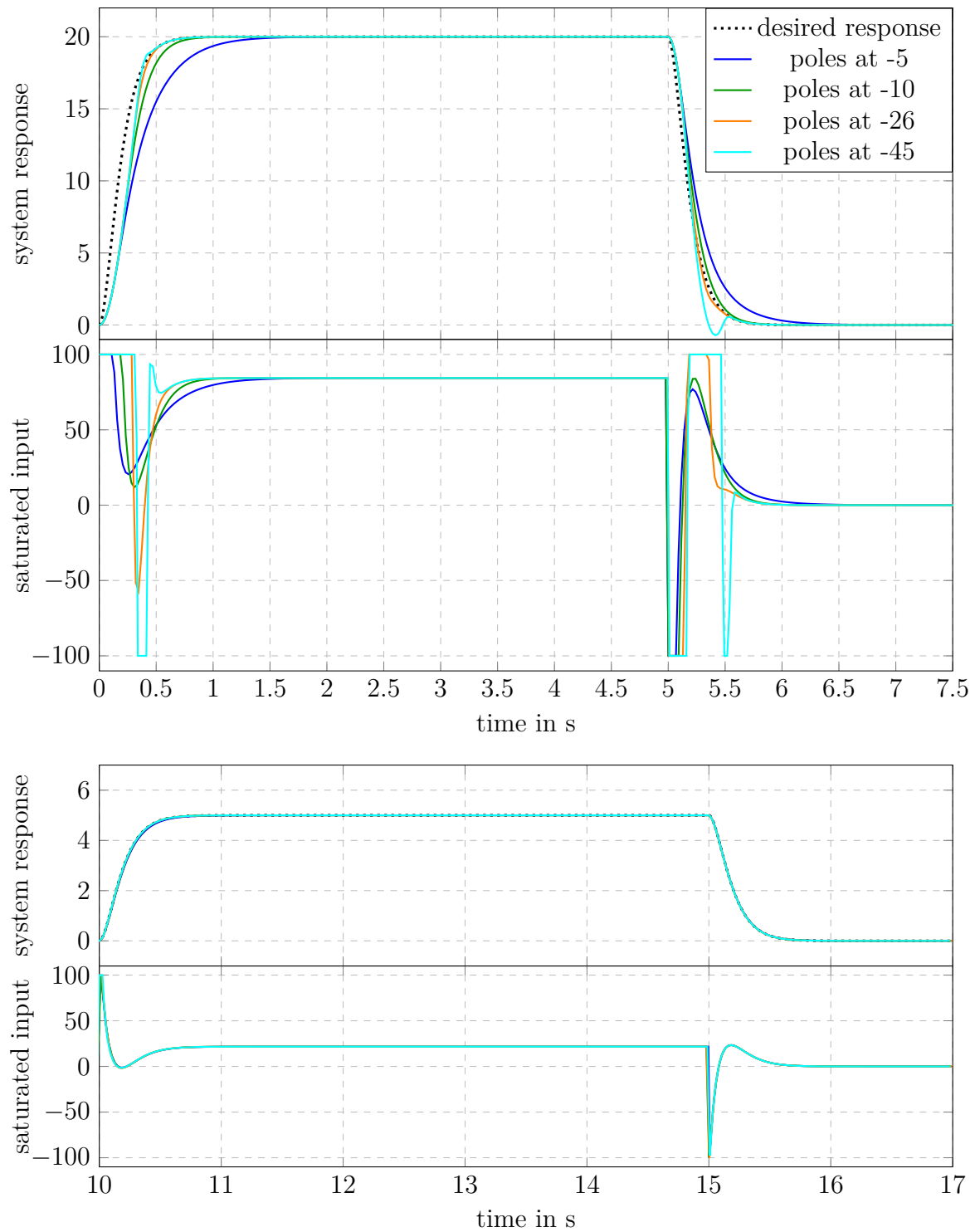


Figure 5.2: Results of Simulation Example 5.1 for AMRAW with state-feedback, ideal controller parameters and different choices of the desired anti-windup poles.

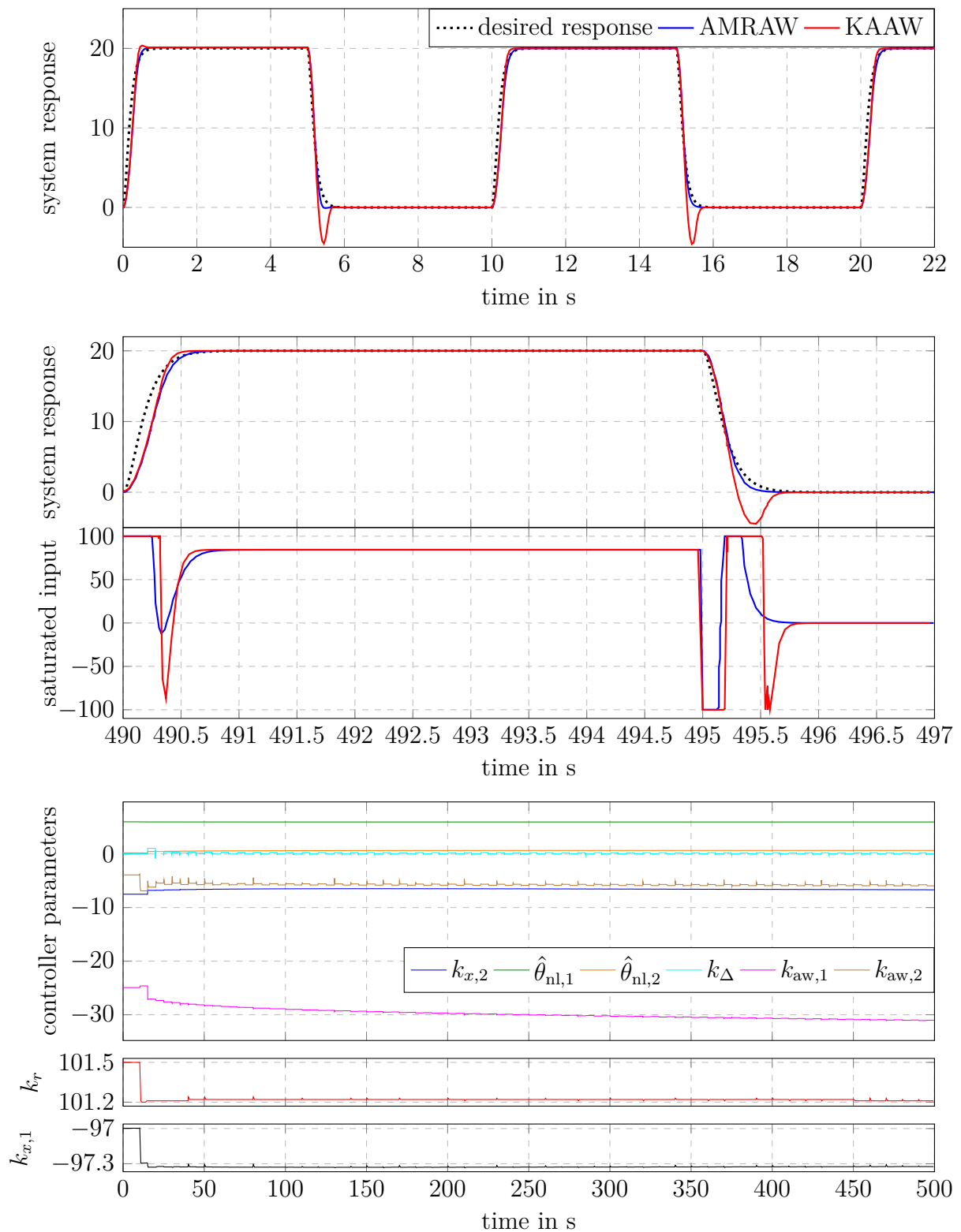


Figure 5.3: Results of the third part of Simulation Example 5.1 for KAAW and AMRAW with state-feedback before ( $t < 10$ s) and after adaptation. The last graphs show the parameter estimations of AMRAW.

**Simulation Example 5.2.** In order to show the capability of AMRAW to deal with unstable open-loop systems with an input saturation the plant  $G_{\text{ex4}}$  and the reference model (3.4) from Simulation Example 3.1 are considered. The additional desired system matrix for the anti-windup system has been chosen as

$$A_{\text{awr}} = \begin{pmatrix} 0 & 1 \\ -100 & -20 \end{pmatrix},$$

which has both poles at  $-10$ . In difference to the Example 3.1 not all the controller parameters are initialized with their ideal values:

| initial parameters   | ideal parameters  |
|--|---|
| $K_x(0) = \begin{pmatrix} -131.35 \\ -12.43 \end{pmatrix}$         | $K_x^* = \begin{pmatrix} -131.35 \\ -12.43 \end{pmatrix}$         |
| $k_r(0) = 150,$  | $k_r^* = 130.81$  |
| $K_{\text{aw}}(0) = \begin{pmatrix} -19.29 \\ -4.16 \end{pmatrix}$ | $K_{\text{aw}}^* = \begin{pmatrix} -27.56 \\ -5.94 \end{pmatrix}$ |
| $k_{\Delta}(0) = 0.0153$   | $k_{\Delta}^* = 0.0076$   |

As in Section 3.1 and Simulation Example 3.1, the initial plant state has been set to  $x_{\text{ps0}}^T = [0 \ 25]$ . The gains of the parameter update laws have been chosen to be  $\Gamma_x = 10 I_{2 \times 2}$ ,  $\gamma_r = 10$ ,  $\Gamma_{\text{aw}} = 10 I_{2 \times 2}$  and  $\gamma_{\Delta} = 10$ . These values of the initial closed-loop states, parameter estimation errors and the maximal reference amplitude lead to a violation of conditions *i*) and *ii*) in Theorem 4.1, so that boundedness of the closed-loop signals can not be guaranteed. However, the simulation results in Figure 5.4 for the same reference signal as in Simulation Example 3.1 show that the closed-loop signals stay bounded. This simulation result supports the statement that the conditions in Theorem 4.1 are conservative and a violation of them does not necessarily mean that the closed-loop signals become unbounded. It can also be observed that the given choice of  $A_{\text{awr}}$  for AMRAW results in a better closed-loop response than the application of KAAW. Similar to the previous examples, simulation results for a reference signal that is more appropriate for parameter estimation are shown in Appendix C.

**Simulation Example 5.3.** In this example the unstable first order plant

$$G_{\text{ex5}} : \quad \dot{x}_{\text{ps}} = 0.5 x_{\text{ps}} + 2 u \quad (5.2)$$

is considered, which has already been used for an example in [89]. The reference model

$$\dot{x}_{\text{ref}} = -6 x_{\text{ref}} + 6 r \quad (5.3)$$

is also adopted from the simulation example in [89]. The desired pole for the anti-windup system has been chosen as  $a_{\text{awr}} = -10$ . In order to simulate an unknown plant the controller parameters have been initialized with slightly changed plant parameters:

$$\hat{x}_{\text{ps}} = 0.45 \hat{x}_{\text{ps}} + 2.2 u. \quad (5.4)$$

Hence, the initial controller parameter and their ideal values become:

| initial parameters         | ideal parameters          |
|----------------------------|---------------------------|
| $k_x(0) = -2.93$           | $k_x^* = -3.25$           |
| $k_r(0) = 2.73$            | $k_r^* = 3$               |
| $k_{\text{aw}}(0) = -4.75$ | $k_{\text{aw}}^* = -5.25$ |
| $k_{\Delta}(0) = 0.3667$   | $k_{\Delta}^* = 0.3333$   |

For the simulation examples, the gains for the parameter adaptation have been set to  $\Gamma_x = 10^4$ ,  $\gamma_r = 10^4$ ,  $\Gamma_{\text{aw}} = 10^4$  and  $\gamma_{\Delta} = 10^4$ .

With the given initial closed-loop conditions and  $Q_W = 1$ , which leads to  $P_W = 0.0833$ , a maximal input amplitude of  $u_{\text{max}} = 1$ , a maximal reference signal of  $r_{\text{max}} = 0.8$ , and  $\lambda = 1.1$ , the conditions *i) – iii)* in Theorem 4.1 become

$$\begin{aligned} x_{\text{ps}}(t_0)^T P_W x_{\text{ps}}(t_0) &\leq 0.1594, \\ r_{\text{max}}(t) &\leq 1.5391 \quad \text{and} \\ V(0) &\leq 5.722 \cdot 10^{-4}. \end{aligned} \tag{5.5}$$

The maximal value of  $x_{\text{aw}}(t)$ , which is necessary for the computation of the results in (5.5), has been determined by simulation examples for different combinations of plant and controller parameters. For these simulations, it has been assumed that a maximal estimation error of the plant parameters are given by  $|\tilde{a}_p| = 0.1$  and  $|\tilde{b}_p| = 0.2$ . As a consequence the maximal value for the anti-windup state has been found out to be  $x_{\text{awmax}} = 0.3$ .

With the given estimation errors of the controller parameters and an initial tracking error of zero, which results from the initial plant and anti-windup state of  $x_{\text{ps}}(0) = x_{\text{aw}}(0) = 0$ , the initial value of the Lyapunov function becomes  $V(0) = 2.7384 \cdot 10^{-5}$ . Hence, all conditions in Theorem 4.1 are fulfilled for this example and boundedness of all closed-loop signals can be guaranteed.

Simulation results for AMRAW and KAAW are shown in Figure 5.5 at the beginning and at the end of adaptation. They verify the stability of the closed-loop system and show that AMRAW results in a better closed-loop performance than KAAW. In the last graph of Figure 5.5 it is demonstrated that for the given plant the excitation of the reference signal is sufficient for the parameters to converge quickly to their ideal values.

As the second part of this example, the desired pole of the anti-windup system has been varied while keeping the reference model constant. For the presented closed-loop responses in Figure 5.6, where the desired anti-windup poles are smaller than  $a_{\text{awr}} = -10$ , the conditions in Theorem 4.1 do not hold due to the increased value of  $D_{\text{aw}} \geq \|k_x^* - k_{\text{aw}}^*\|$ . However, the results show that the closed-loop signals stay bounded. Moreover, the closed-loop response can be forced to follow the reference model more closely by increasing the absolute value of the stable anti-windup pole, which verifies Theorem 4.2. This improved performance is a consequence of faster regulation of the unwanted behavior to zero, which is shown in the second graph of Figure 5.6.

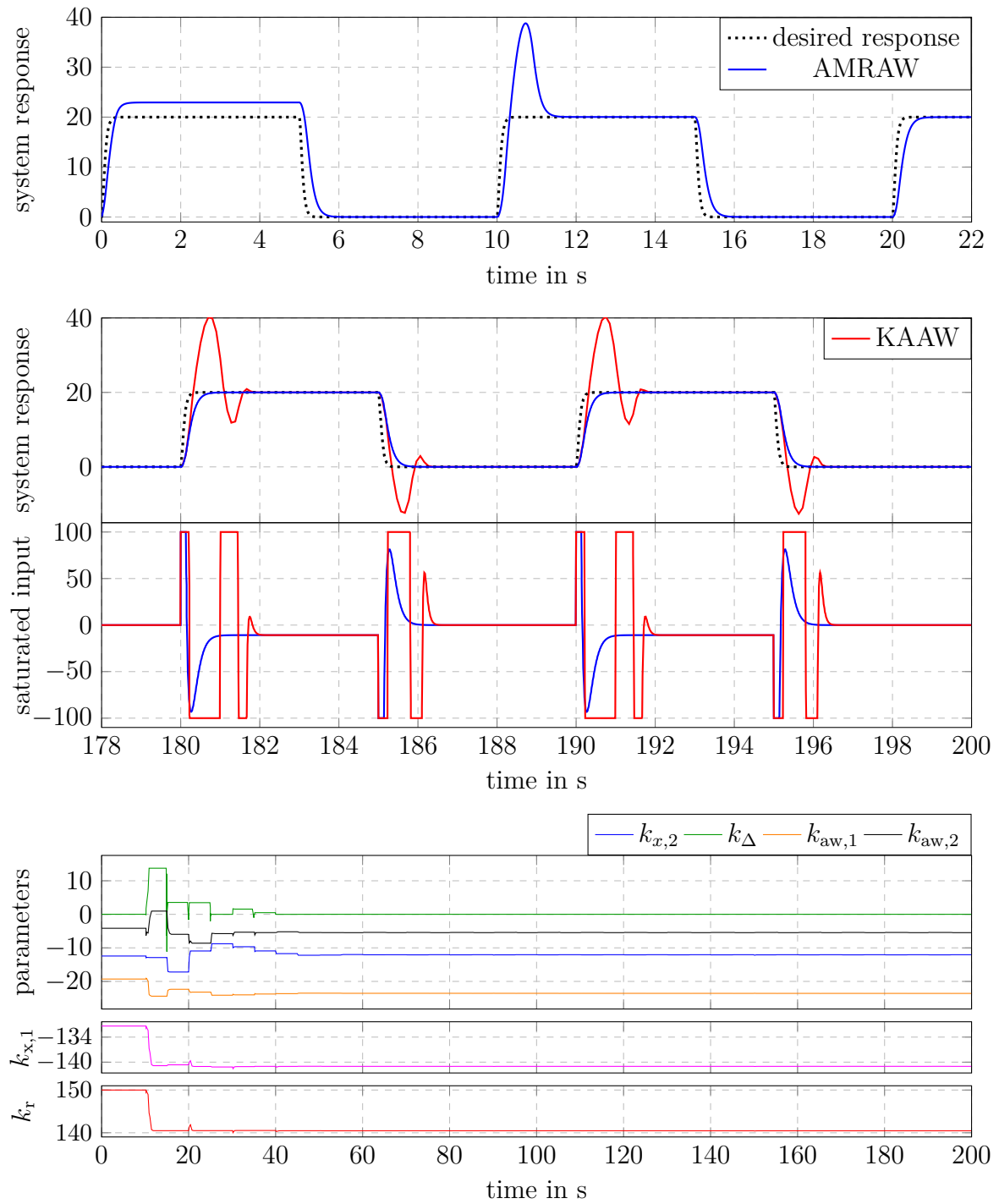


Figure 5.4: Results of Simulation Example 5.2 for AMRAW with state-feedback before ( $t < 10$ s) and after adaptation. The result at the end of adaptation is compared to KAAW with ideal controller parameters. The last graphs show the parameter estimations of AMRAW.

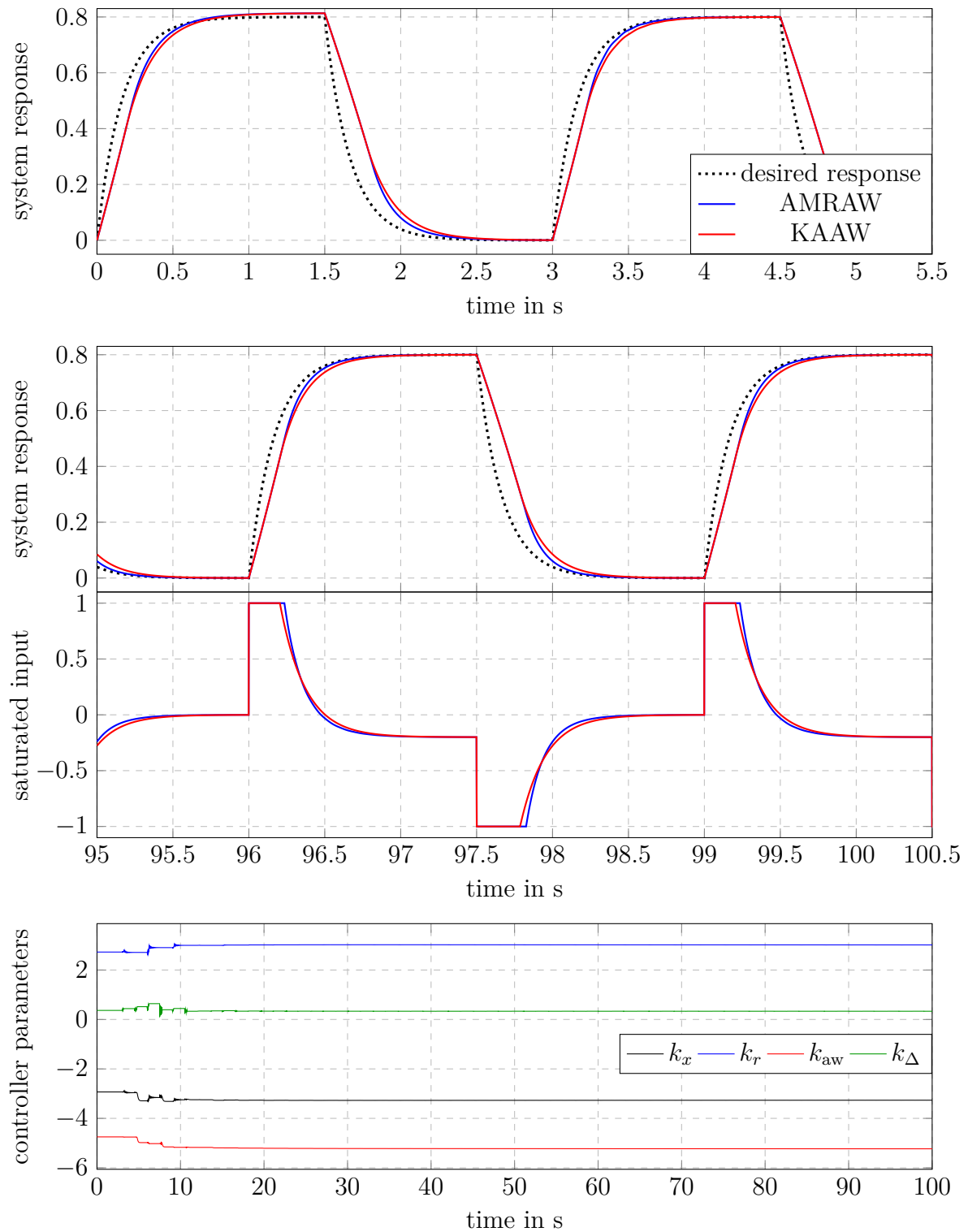


Figure 5.5: Result of Simulation Example 5.3 for KAAW and AMRAW for a first order system before ( $t < 3$ s) and after adaptation. The last graph shows the parameter estimations of AMRAW.



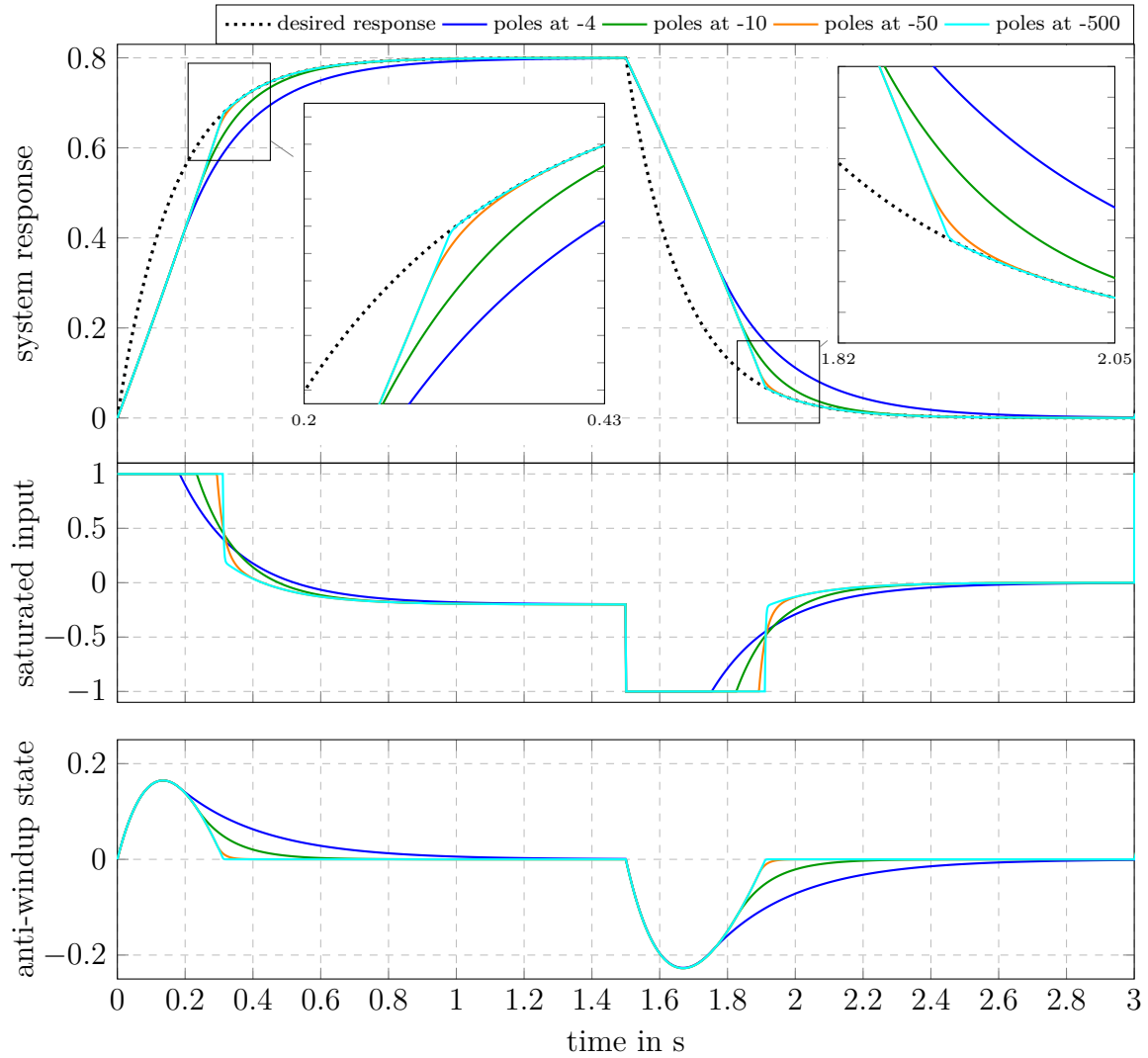


Figure 5.6: Simulation results for AMRAW for a first order system with ideal controller parameters and different choices of the desired anti-windup poles.

## 5.2 Direct Adaptive Model Recovery Anti-Windup for Output-Feedback

The basic concept of direct AMRAW for output-feedback, which is summarized in Table 4.2, is similar to that of state-feedback AMRAW. Also the effect of the additional degree of freedom, introduced by the anti-windup controller, has been found out to be similar to the state-feedback case. For this reason, Remarks 5.1 and 5.2, which comment about the influence of the anti-windup controller on the closed-loop system and possible ways to tune the desired anti-windup dynamics, respectively, do also apply for output-feedback AMRAW. Moreover, in order to avoid problems with uncertain input limitations, the considerations for the implementation of state-feedback AMRAW in Remark 5.5 should also be taken into account for AMRAW with output-feedback.

Similar to the state-feedback case, a connection between output-feedback KAAW and AMRAW can be found. This connection is described in Remark 5.7 in terms of output-feedback AMRAW. The dynamical controller in output-feedback AMRAW lead to modifications on the stability conditions in Theorem 4.3 in comparison to Theorem 4.1. These differences are pointed out in Remark 5.8.

### 5.2.1 Remarks

**Remark 5.7 (Connection between KAAW and AMRAW).** From equation (4.26) for the anti-windup controller and the presentation in Section 2.2.2 for the basic MRAC it follows that the choice of  $A_{\text{ref}} = A_{\text{awr}}$  leads to  $\theta_1^* = \theta_{1\text{aw}}^*$ ,  $\theta_2^* = \theta_{2\text{aw}}^*$ , and  $\theta_3^* = \theta_{3\text{aw}}^*$ . Therefore, if the controller parameters have been adapted to their ideal values, the influence of the anti-windup state is canceled in the control law and the reference model as can be seen in equations (4.26) and (4.31), respectively. If the best closed-loop performance is achieved for  $A_{\text{ref}} = A_{\text{awr}}$ , KAAW rather than AMRAW should be used due to the same reasons mentioned for the state-feedback case in Remark 5.3. AMRAW for output-feedback introduces  $3n - 1$  additional controller states in comparison to KAAW, where  $2n - 1$  of these states stem from the additional estimated controller parameters  $\theta_{\text{aw1}}(t)$ ,  $\theta_{\text{aw2}}(t)$ , and  $\theta_{\text{aw3}}(t)$ .

**Remark 5.8 (Conditions of Theorem 4.3).** Similar to state-feedback AMRAW, boundedness of the closed-loop states can only be guaranteed with output-feedback AMRAW if the conditions *i)–iii)* in Theorem 4.3 are satisfied. However, for output-feedback AMRAW not only the plant states and the parameter states needs to be considered for these conditions, but also the states of the basic controller and the anti-windup controller, which are included in the combined state vectors  $x_{\text{cs}}$  and  $x_{\text{awc}}$ . Therefore, the anti-windup controller states do have an influence on the maximal admissible amplitude of the reference signal in condition *ii)* of Theorem 4.3. For this reason the boundedness conditions for output-feedback AMRAW might not be satisfied in cases, where they can be satisfied by applying state-feedback AMRAW. The fact that closed-loop boundedness for the state-feedback AMRAW scheme is not equivalent to stability of output-feedback AMRAW is illustrated in Simulation Example 5.5.

## 5.2.2 Simulations

**Simulation Example 5.4.** In this example, the plant  $G_{\text{ex}2s}$  is considered, which differs from the plant  $G_{\text{ex}2}$  from Simulation Example 2.2 in that it has a maximal input amplitude of  $u_{\text{max}} = 100$ . The reference model, as well as the initially estimated plant parameters, have been adopted from Example 2.2. For the application of AMRAW, the desired anti-windup dynamics have been chosen as

$$A_{\text{awr}} = \begin{pmatrix} 0 & 1 \\ -625 & -50 \end{pmatrix},$$

which has two poles at  $-25$ .

The first simulation has been carried out in order to show boundedness of the closed-loop states. Therefore, a reference signal  $r = r_1 + r_2$  has been provided where each value of the repeated sequence  $r_1 = (20, 0, 10, 0)$  has been hold for 2 seconds and  $r_2 = 9 \sin(5t) + 6 \sin(8t)$ . The simulation results are shown in Figure 5.7, where adaptation has been started at  $t = 10\text{s}$  with the adaptation gains  $\Gamma = 10^5 I_{4 \times 4}$ ,  $\Gamma_{\text{aw}} = 10^6 I_{3 \times 3}$ ,  $\gamma_{\Delta} = \gamma_a = 100$ . It can be seen that the plant output, as well as the parameter estimations, stay bounded and that the parameters adapt to their ideal values so that the plant output follows the desired trajectory more closely.

Similar to the state-feedback case, output-feedback AMRAW has the capability to influence the closed-loop performance if the input is saturated. That is illustrated by a second simulation, whose results are shown in Figure 5.8. The simulation results have

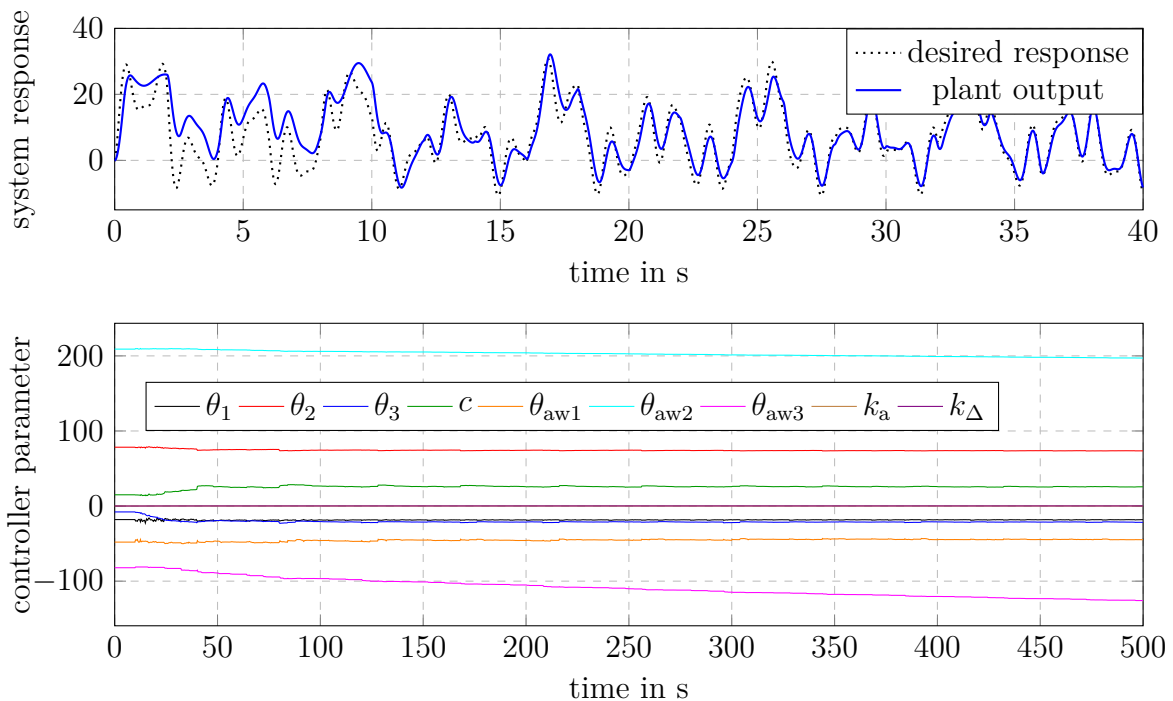


Figure 5.7: Results of Simulation Example 5.4 for AMRAW with output feedback. Adaptation has been started at  $t = 10\text{s}$ .

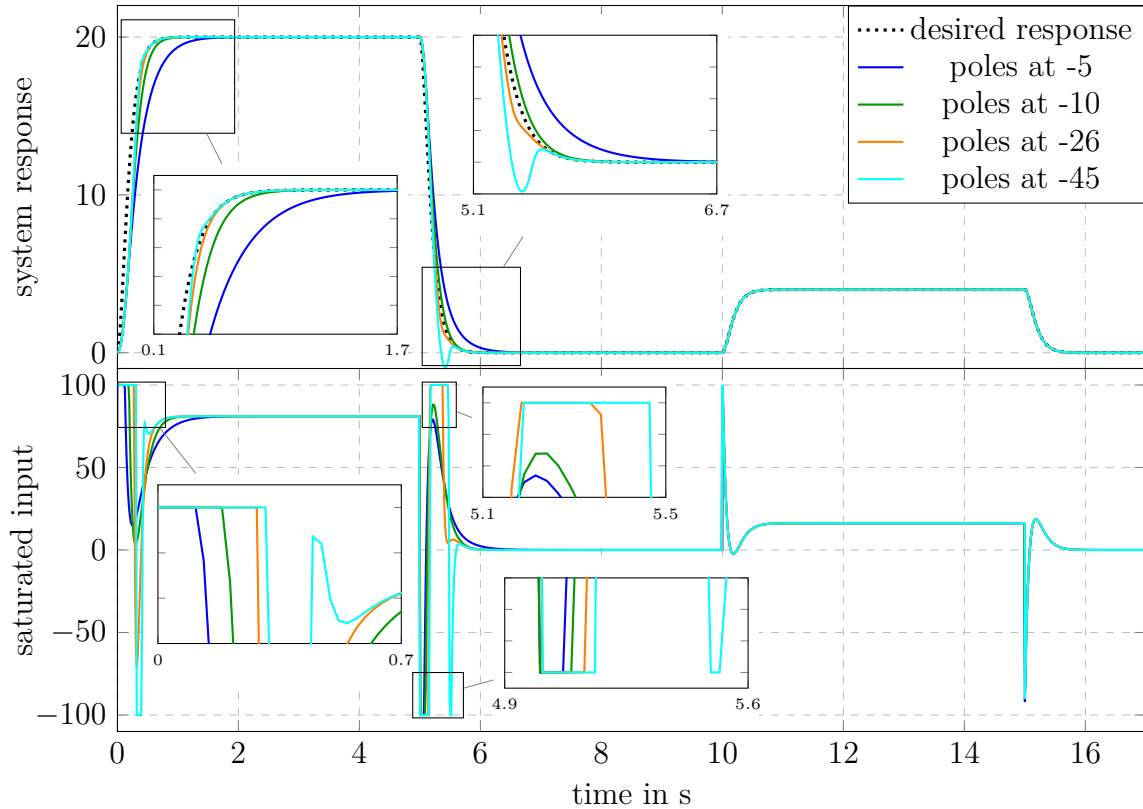


Figure 5.8: Results of Simulation Example 5.4 for AMRAW with output-feedback, ideal controller parameters and different choices of the desired anti-windup poles.

been achieved for ideal controller parameters with different choices of the desired anti-windup poles. The results look similar to the state-feedback case and can be explained in the same way (see Remark 5.1).

**Simulation Example 5.5.** As for state-feedback AMRAW, the unstable plant  $G_{\text{ex4}}$  from Section 3.1 and Simulation Example 3.1 is revisited with output-feedback AMRAW in this example. A desired anti-windup dynamics of

$$A_{\text{awr}} = \begin{pmatrix} 0 & 1 \\ -625 & -50 \end{pmatrix}$$

has been chosen, which has both poles at  $-25$ . Adaptation has been started at  $t = 10$ s with the estimation gains  $\Gamma = 10^5 I_{4 \times 4}$ ,  $\Gamma_{\text{aw}} = 10^6 I_{3 \times 3}$ ,  $\gamma_{\Delta} = \gamma_1 = 100$ . In order to simulate an uncertain plant, only the initial controller parameter  $c$  has been scaled by a small factor of 1.05, so that the initial controller has a slightly higher gain on the reference signal than in the ideal case. The simulation results are shown in Figure 5.9 for the same reference dynamics and desired anti-windup dynamics. For the given initial closed-loop states, conditions *i*) and *ii*) of Theorem 4.3 does not hold. That has also been true for the state-feedback example 5.2, whose results are shown in Figure 5.4.

It can be seen in the first ten seconds of the first graph that the slightly higher value of  $c$  results in a small offset to the desired steady-state output. After the start of the

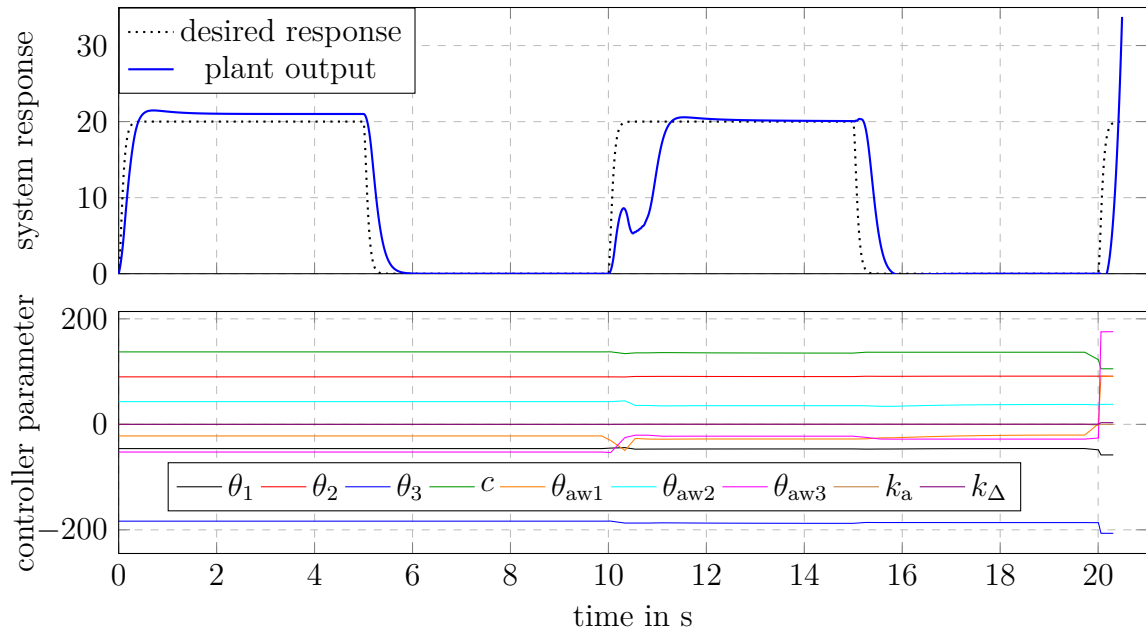


Figure 5.9: Results of Simulation Example 5.5 for AMRAW with output-feedback applied to the unstable open-loop plant  $G_{\text{ex4}}$ . Adaptation has been started at  $t = 10\text{s}$ .

parameter adaptation, the closed-loop system becomes unstable already after 10 seconds. This is different to state-feedback AMRAW, where the closed-loop trajectories with the same open-loop plant stayed bounded. This result shows that boundedness of the closed-loop system with output-feedback AMRAW is clearly not equivalent to boundedness of the closed-loop with state-feedback AMRAW.

### 5.3 Indirect Adaptive Model Recovery Anti-Windup for Output-Feedback

The basic concept of plant parameter estimation and controller parameter calculation of indirect AMRAW presented in Table 4.3 differs from the concept of the direct methods. No reference model is used for the indirect AMRAW scheme, which makes a comparison to KAAW meaningless. Consequently, no connection to KAAW can be drawn, like it is done in Remarks 5.3 and 5.7 for the direct methods. As an additional difference to the direct methods a stability analysis has not been carried out for the complete closed-loop system with indirect AMRAW. A comment on the meaning of the missing proof of stability is given in Remark 5.9.

Despite the differences to the direct methods, the effect of the anti-windup controller in indirect AMRAW has been found out to be very similar to the direct schemes. Therefore, Remark 5.1 about the general anti-windup effect, Remark 5.2 about the anti-windup tuning, and Remark 5.5 about the issue of unknown amplitude limits of the input do also apply to the indirect scheme. This is verified by the results of Simulation Example 5.6.

**Remark 5.9.** The boundedness of the closed-loop signals has not been proven for the indirect AMRAW scheme. Only boundedness of the estimated parameters is guaranteed by the properties of the least squares algorithm stated in Appendix A. Consequently, the adaptation of the indirect AMRAW scheme should only be activated for limited periods of time and under well known and save environmental conditions. The simulation examples 5.6 and 5.7 and the experimental result in Section 5.3 suggest that under optimal conditions the given control scheme results in a stable closed-loop system.

### 5.3.1 Simulations

**Simulation Example 5.6.** The plant  $G_{\text{ex3s}}$  is considered, which differs from the plant  $G_{\text{ex3}}$  from Example 2.3 in that it has a maximal input amplitude of  $u_{\text{max}} = 100$ . All closed-loop requirements and initial conditions have been adopted from Simulation Example 2.3 and the desired anti-windup dynamics for the application of indirect AMRAW has been chosen as

$$A_{\text{awr}} = \begin{pmatrix} 0 & 1 \\ -100 & -10 \end{pmatrix},$$

which has two poles at  $-10$ . Consequently, the initial controller parameters and the ideal parameters of the control scheme in Table 4.3 become:

| initial parameters                                   | ideal parameters                                    |
|--|---|
| $P = 529.13 D^2 + 8.9 \cdot 10^3 D + 5.9 \cdot 10^4$ | $P^* = 982.7 D^2 + 1.6 \cdot 10^4 D + 1 \cdot 10^5$ |
| $L = D + 98$   | $L^* = D + 99$                                      |
| $M = 5.9 \cdot 10^4$                                 | $M^* = 1 \cdot 10^5$                                |
| $\hat{\theta}_{\text{nl}} = 6$                       | $\theta_{\text{nl}} = 3$                            |
| $K_{\text{aw}}^T = [-10.51 \quad -2.70]$             | $K_{\text{aw}}^{*T} = [-22.97 \quad -5.13]$         |

In Figure 5.10 the simulation results are shown before ( $t < 10\text{s}$ ) and after parameter adaptation in the first and the second graph, respectively. In addition, the results with indirect AMRAW after adaptation are compared to a constant pole placement controller, where the parameters are set to their ideal values. The constant pole placement controller can be derived from Table 2.3 with ideal parameters. It can be observed that the closed-loop signals of the AMRAW scheme stay bounded and that a good closed-loop performance results already after a short time of parameter adaptation. In difference to that, the closed-loop performance with the constant pole placement controller without anti-windup is far from acceptable. Strong oscillations occur, which are unacceptable for any technical application. The results show that the AMRAW scheme is not only very effective in avoiding parameter windup, but also improves the overall performance significantly in comparison to the pole placement controller without anti-windup. It can also be observed that the parameter adaptation speed does not significantly differ from the estimation speed in Simulation Example 2.3.

As for the preceding examples with the direct AMRAW schemes, also for indirect AMRAW the choice of the desired anti-windup dynamics can influence the closed-loop dynamics

during input saturation, while having no influence if the input does not encounter its limits. This is shown by additional simulation results in Figure 5.11, where the controller parameters have been set to their ideal values and the poles of  $A_{\text{awr}}$  have been varied. The results look very similar to the results in Example 5.1 and 5.4 and can be explained in the same way (see Remark 5.1).

Simulations for a third part of this example have been carried out, in order to show the effect of an uncertain maximal input amplitude on indirect AMRAW. For this purpose, the input saturation limit has been reduced to  $u_{\text{max}} = 75$  without considering this reduction in the AMRAW scheme. The controller parameters have been initialized with their ideal values and adaptation has been activated at the beginning of the simulation. The results are shown in Figure 5.12. It can be seen that the range of input amplitude is not sufficient to bring the system output to the desired steady-state value. However, the closed-loop signals stay bounded. Further, it can be observed that the estimated parameters do not stay at their ideal values. The parameter estimation of  $\theta_{p3}$ , which represents the input gain of the system, is reduced very quickly. Apparently, the effect of a reduced input saturation is partially considered as a reduced input gain of the estimated plant model. However, as can be seen in Figure 5.12, also the estimations of  $\theta_{p1}$  and  $\theta_{p2}$  change and none of the parameters mentioned above reach a constant value. The values of the estimated parameters alter between different constant values for the different values of the reference signal. This observation emphasizes the fact that the effect of a reduced maximal input amplitude can not be represented by any constant combination of the plant parameters.

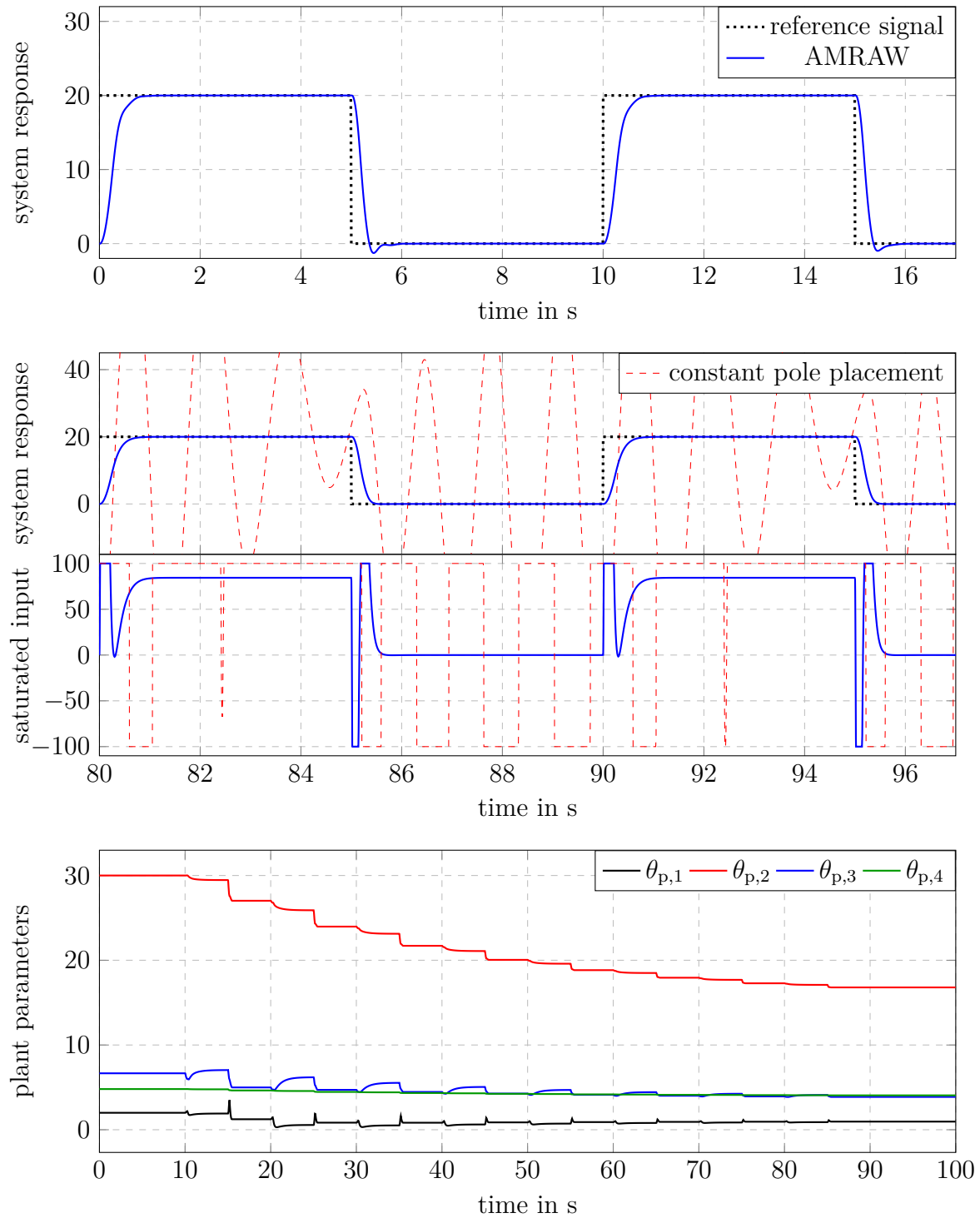


Figure 5.10: Results of Simulation Example 5.6 for indirect AMRAW with output-feedback before ( $t < 10$ s) and after adaptation. The result at the end of adaptation is compared to standard APPC with constant and ideal parameters. The last graphs shows the plant parameter estimations of the indirect AMRAW scheme.



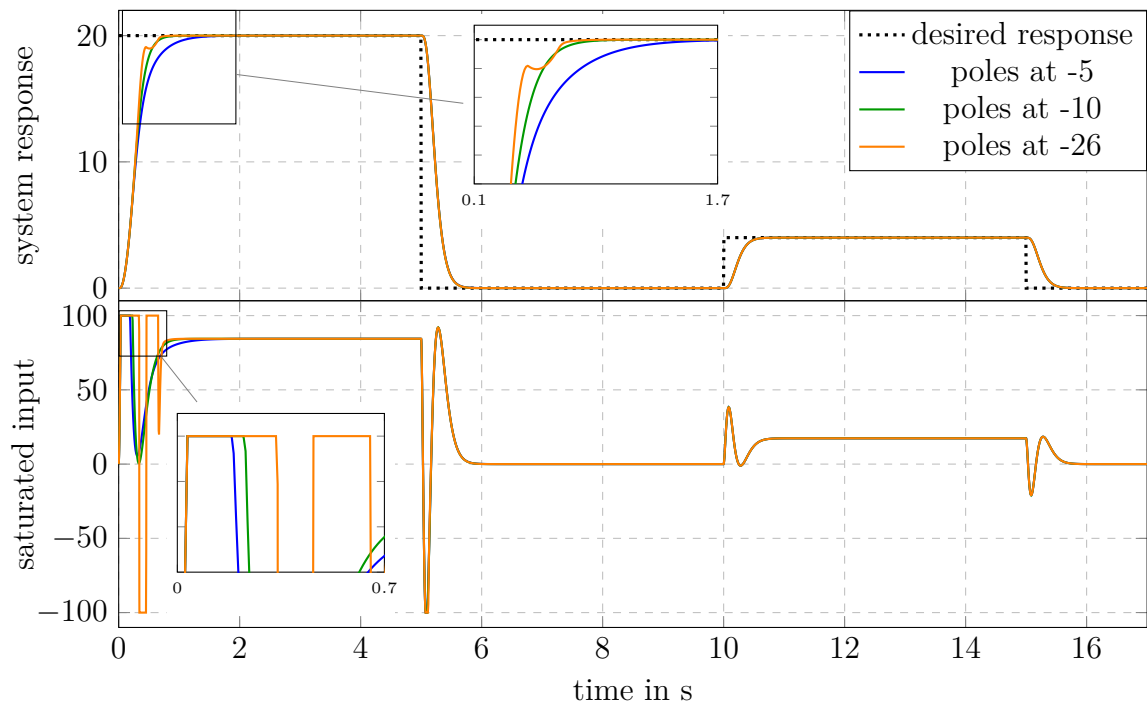


Figure 5.11: Simulation results for indirect AMRAW with output-feedback, ideal controller parameters, and different choices of the desired anti-windup poles.

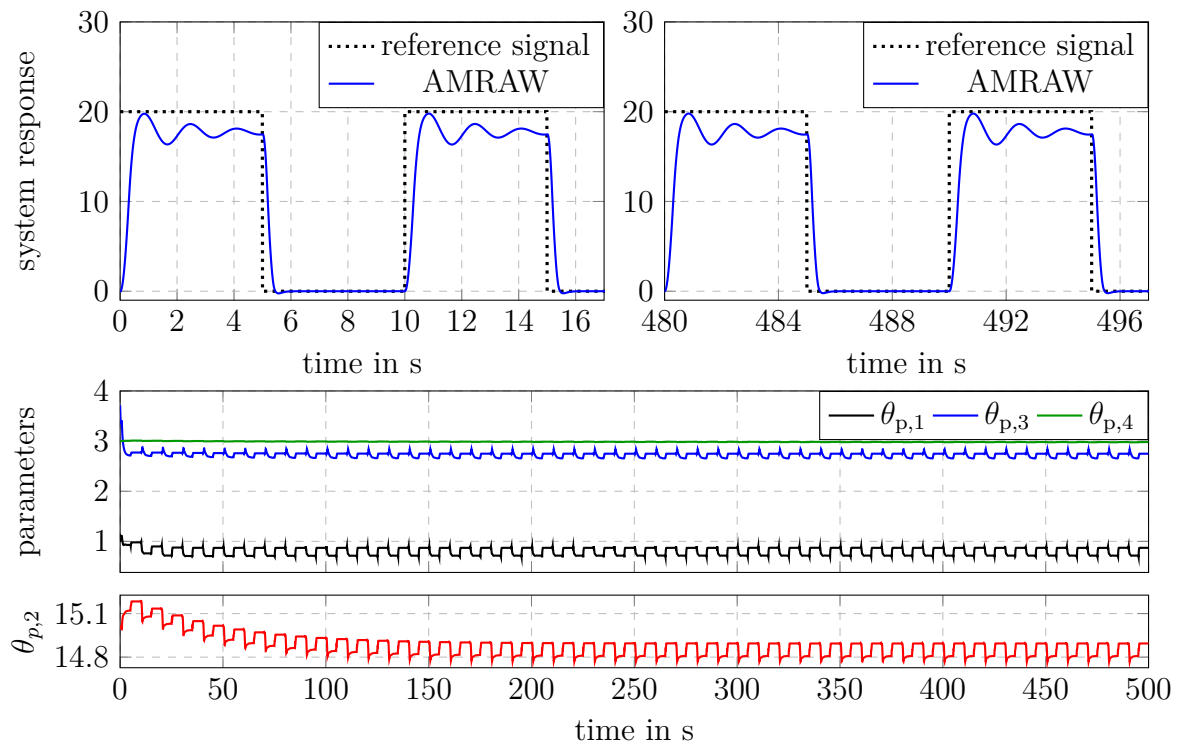


Figure 5.12: Simulation results for indirect AMRAW with output-feedback, where the input amplitude limit has been overestimated.

**Simulation Example 5.7.** In this example the unstable plant  $G_{\text{ex4}}$  with input saturation, which has been defined in (3.3), is revisited for indirect AMRAW. In order to simulate the case of uncertain plant parameters the controller parameters and the parameter estimation scheme has been initialized with the rough estimate

$$\dot{\hat{x}}_{\text{ps}} = \begin{pmatrix} 0 & 1 \\ 4 & 4 \end{pmatrix} \hat{x}_{\text{ps}} + \begin{pmatrix} 0 \\ 6.6 \end{pmatrix} u_{\text{lim}}$$

of the plant. The desired closed-loop poles of  $A_d$  have been chosen to lie at  $-25$  and the desired anti-windup system matrix has been defined as

$$A_{\text{awr}} = \begin{pmatrix} 0 & 1 \\ -100 & -10 \end{pmatrix},$$

which has two poles at  $-10$ . Therefore, the initial and ideal parameters of indirect AMRAW from Table 4.3 become

| initial parameters                                   | ideal parameters   |
|--|--|
| $P = 626.13 D^2 + 9.4 \cdot 10^3 D + 5.9 \cdot 10^4$ | $P^* = 1069.2 D^2 + 1.05 \cdot 10^4 D + 1.05 \cdot 10^5$ |
| $L = D + 104$  | $L^* = D + 102$  |
| $M = 5.9 \cdot 10^4$                                 | $M^* = 1.05 \cdot 10^5$                                  |
| $\hat{\theta}_{\text{nl}} = 6$                       | $\theta_{\text{nl}} = 3$                                 |
| $K_{\text{aw}}^{\text{T}} = [-10.51 \quad -2.70]$    | $K_{\text{aw}}^{*\text{T}} = [-27.56 \quad -5.95]$       |

The simulation results are shown in Figure 5.13, where adaptation has been started at  $t = 10\text{s}$  with the tuning parameters of the least squares algorithm set to  $P_{\text{ls0}} = 10^5 I_{3 \times 3}$ ,  $\rho_r = 5 \cdot 10^4$ ,  $\rho_s = 1$ , and  $\Lambda_e = D^2 + 30 D + 22500$ . It can be seen that the closed-loop system stays stable and that the parameter estimations converge quickly to their real values. Before the start of the parameter estimation at  $t = 10\text{s}$  undesired overshoots and undershoots at the set point changes can be observed. However, after adaptation of the parameters a good closed-loop performance results without any oscillation around the set points.

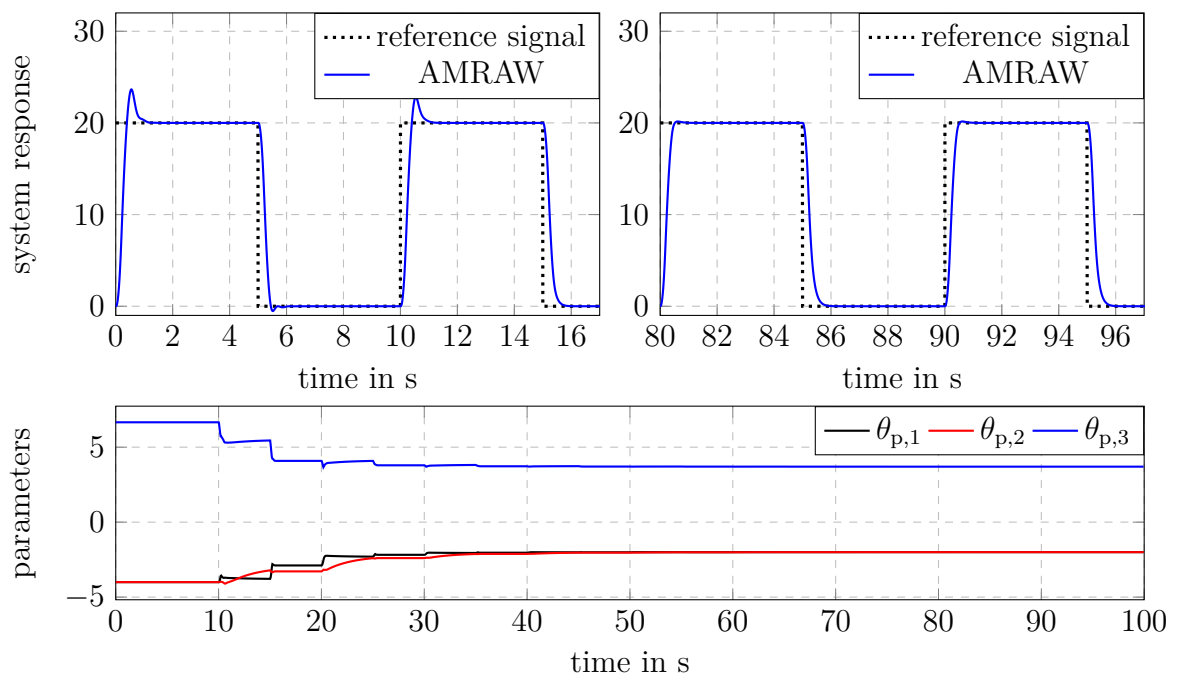


Figure 5.13: Results of Simulation Example 5.7 for indirect AMRAW applied to the unstable open-loop plant  $G_{\text{ex4}}$ .



# Chapter 6

## Experimental Results

### 6.1 Helicopter Benchmark Experiment

The helicopter benchmark experiment is a well-suited experiment for adaptive control and has already been addressed with several different adaptive control approaches [6, 22, 36, 41, 63, 121, 133]. Depending on the experimental setup and on the performance requirements, this experiment is subjected to tight limitations of the input amplitude. However, in none of the aforementioned references the influence of the limited input amplitude on the closed-loop system has been examined or explicitly considered for the controller design. In this section, it is shown that such negligence of the input saturation will lead to instability of the adaptive closed-loop system if the basic MRAC scheme with CRM is applied. In difference to that, it is shown with the results of real experiments that the application of AMRAW leads to a stable closed-loop system and allows for an improvement of the closed-loop performance during saturation of the input. Moreover, the general benefits of adaptive control are presented in this section. This is done by presenting the results of experiments which have been carried out with uncertain or even changing plant parameters.

#### 6.1.1 Experimental Setup and Plant Description

The basic setup of the helicopter benchmark experiment is shown in Figure 6.1 from two different perspectives and in a schematic illustration. The masses and lengths in the schematic picture are denoted with  $m$  and  $l$ , respectively. The experiment consists of two propellers in an orange and a green protection cover, respectively, driven by brushless DC motors and mounted in parallel with distance  $2 \cdot l_h$  on the "propeller bar". The "propeller bar" is mounted on one side of the "elevation bar" such that a pitch motion  $p$  of the "propeller bar" is possible. The suspension of the "elevation bar" allows for a motion of the whole experimental setup around the vertical axis  $v$  as well as an elevation motion  $\epsilon$ . On the other side of the "elevation bar" a counter mass  $m_c$  is mounted. In addition, a movable mass  $m_v$  with an automatically adjustable position  $x_v$  is located

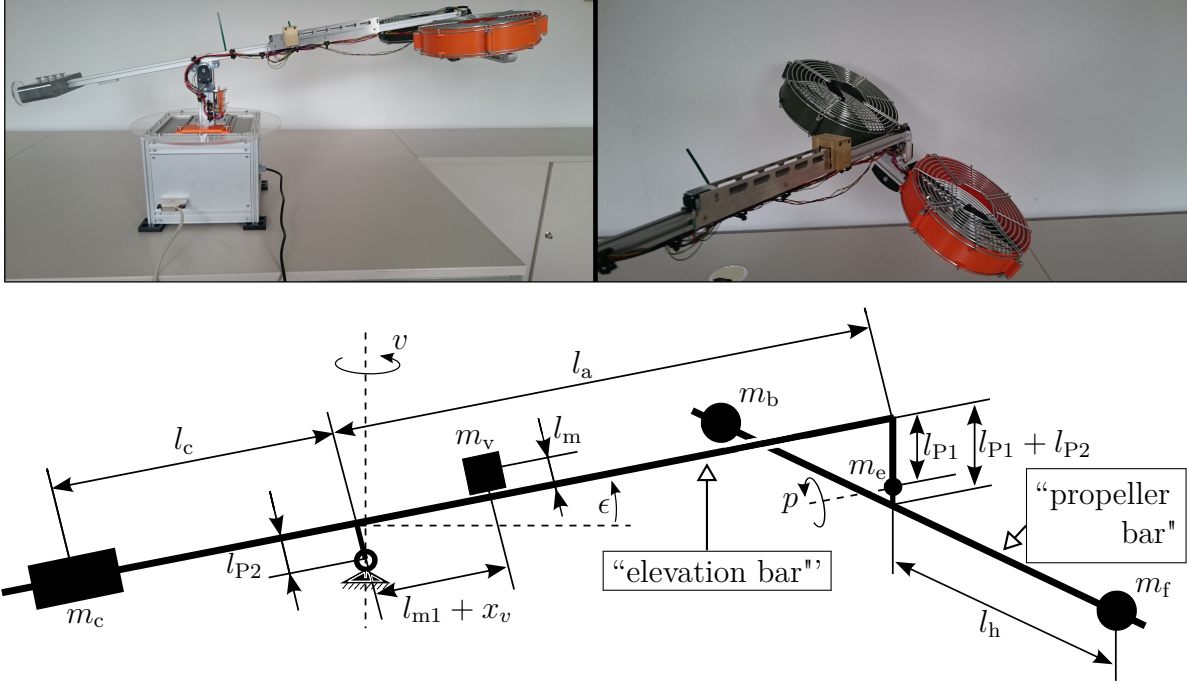


Figure 6.1: Photography and a schematic illustration of the experimental setup of the 3-DOF helicopter.

between the counter mass and the “propeller bar”. The two other length  $l_m$  and  $l_{m1}$ , which characterize the position of  $m_v$ , are fixed.

For the subsequently described experiments with the helicopter the two degrees of freedom  $v$  and  $p$  have been mechanically fixed so that only an elevation motion  $\epsilon$  has been possible. Furthermore, in order to keep the controller design as simple as possible, a simplified version of the plant has been considered to derive the equation of motion. This simplified system consists of one lumped mass  $m_f + m_e + m_b$  on the side of the “elevation bar” where the propellers are mounted, the counter mass  $m_c$  on the other side, and the movable mass  $m_v$ . Therefore, using Euler’s rotation equations of classical mechanics under the assumption of a constant inertia of the system and under consideration of the lumped masses and distances in Figure 6.1 leads to the elevation dynamic

$$\begin{aligned}
 J_\epsilon \ddot{\epsilon} = & - (m_f + m_b + m_e) g \frac{l_a}{\cos(\delta_a)} \cos(\epsilon - \delta_a) + m_c g \frac{l_c}{\cos(\delta_c)} \cos(\epsilon + \delta_c) \\
 & - m_v g \frac{l_{m1} + x_v}{\cos(\delta_v)} \cos(\epsilon - \delta_v) + l_a (F_1 + F_2) - \eta_\epsilon \dot{\epsilon}
 \end{aligned} \tag{6.1}$$

with the angles

$$\delta_a = \arctan\left(\frac{l_{P1}}{l_a}\right), \quad \delta_c = \arctan\left(\frac{l_{P2}}{l_c}\right), \quad \delta_v = \arctan\left(\frac{l_{P2} + l_m}{l_{m1} + x_v}\right),$$

the acceleration of gravity  $g$ , a linear damping  $\eta_\epsilon$ , and the forces  $F_1$  and  $F_2$  produced by the propellers. A similar model of the experimental setup has been derived in [62, 143, 170].

|                       |                      |                            |
|-----------------------|----------------------|----------------------------|
| $\eta_\epsilon = 0.1$ | $\theta_V = 2.2043$  | $\delta_a = 0.0298$        |
| $J_\epsilon = 2.2$    | $\theta_P = 27.8728$ | $\delta_c = -0.0617$       |
| $l_a = 0.705$         | $\theta_C = 26.4471$ | $\bar{\delta}_v = -0.1831$ |

Table 6.1: Plant parameters and force characteristic for helicopter benchmark experiment.

In order to transform (6.1) in a state-space model equivalent to  $G_{\text{nl}s}$  in (3.2), the parameters

$$\theta_P = (m_f + m_b + m_e) g \frac{1}{\cos(\delta_a)}, \quad \theta_C = m_c g \frac{1}{\cos(\delta_c)}, \quad \theta_V = m_v g \frac{l_{m1} + x_v}{l_a \cos(\delta_v)}$$

and the state  $x_{\text{ps}}^T = [\epsilon \quad \dot{\epsilon}]$  are introduced, which allow a formulation of the plant as

$$\begin{aligned} \dot{x}_{\text{ps}} &= \begin{pmatrix} 0 & 1 \\ 0 & -\frac{\eta_\epsilon}{J_\epsilon} \end{pmatrix} x_{\text{ps}} + \begin{pmatrix} 0 \\ \frac{l_a}{J_\epsilon} \end{pmatrix} \left( F_1 + F_2 + [\theta_P \quad \theta_C \quad \theta_V] \begin{pmatrix} -\cos(\epsilon - \delta_a) \\ +\cos(\epsilon + \delta_c) \\ -\cos(\epsilon - \bar{\delta}_v) \end{pmatrix} \right) \\ &= A_H x_{\text{ps}} + B_H \lambda \left( F_1 + F_2 + \theta_H^T f_H(\epsilon) \right), \end{aligned} \quad (6.2)$$

with  $\lambda = 1$ , and where  $\epsilon = 0$  corresponds to the horizontal position of the ‘‘elevation bar’’. Note that the angle  $\delta_v$  depends on the position  $x_v$  of the mass  $m_v$ . However, as an additional simplification, this dependence is neglected in the term  $\cos(\epsilon - \bar{\delta}_v)$  in (6.2), where  $\bar{\delta}_v$  is considered a constant angle. The dependence of the inertia  $J_\epsilon$  and the parameter  $\theta_V$  on the position of the mass  $m_v$  is considered as a parametric uncertainty, which is supposed to be addressed by the adaptive controller. All of the parameters of the plant model, which have been identified by measurements of masses and lengths with  $x_v = 0$ , are given in SI units in Table 6.1. In the same table the characteristic of the propeller forces is depicted in dependence of the PWM duty cycle, which is used to adjust the voltage supply of the brushless DC motors. These characteristics has been determined experimentally. It can be seen that the maximal force of both propellers combined is limited by  $F_{\text{max}} = 8\text{N}$ . A force in the opposite direction is not possible with the presented experimental setup. Hence, the minimal force of the propellers is given by  $F_{\text{min}} = 0$ . It is worth mentioning that for many of the following experiments the maximal amplitude of the propeller forces have been limited to  $\bar{F}_{\text{max}} = 6\text{N}$  in the software.

For all of the experiments, whose results will be shown in the following, the control algorithms have been implemented on a dSpace DS1103 system with a sampling time of 1ms. Therefore, the continuous time control schemes from tables 2.1 and 4.1 have been implemented using a Euler forward discretisation. The angular position  $\epsilon$  and the angular velocity  $\dot{\epsilon}$  have been detected by a rotary encoder with a resolution of 20000 increments per revolution. It should be mentioned that the admissible range of  $\epsilon$  is restricted to  $-0.45\text{rad} \leq \epsilon \leq 0.64\text{rad}$  due to mechanical stops, which prohibit further elevation movements.

### 6.1.2 Closed-Loop Stability for Frequent Saturation of the Input

In the first experiment, the method of MRAC without anti-windup and with AMRAW has been applied for position control of the helicopter benchmark experiment with a maximal force amplitude of  $\bar{F}_{\max} = 6\text{N}$ . The control methods given in Table 2.1 and Table 4.1, respectively, have been initialized for the plant description in (6.2) with the parameters in Table 6.1 and a specified reference model

$$\dot{x}_{\text{ref}} = \begin{pmatrix} 0 & 1 \\ -9 & -6 \end{pmatrix} x_{\text{ref}} + \begin{pmatrix} 0 \\ 9 \end{pmatrix} r, \quad (6.3)$$

which has two poles at  $-3$  and a steady state gain of one for the position. The desired anti-windup dynamic of AMRAW has been defined as

$$A_{\text{awr}} = \begin{pmatrix} 0 & 1 \\ -13.69 & -7.4 \end{pmatrix},$$

which has two poles at  $-3.7$ . Hence, the initial parameters for MRAC become

$$K_x(0) = \begin{pmatrix} -28.08 \\ -18.58 \end{pmatrix}, \quad k_r(0) = 28.08, \quad \hat{\theta}_{\text{nl}}(0) = \theta_{\text{H}} = \begin{pmatrix} 27.87 \\ 26.45 \\ 2.20 \end{pmatrix},$$

and the additional parameters for AMRAW are given by

$$K_{\text{aw}}(0) = \begin{pmatrix} -42.72 \\ -22.95 \end{pmatrix}, \quad k_{\Delta}(0) = 0.0356.$$

The estimation gains have been set to  $\Gamma_x = \Gamma_{\text{aw}} = I_{2 \times 2}$ ,  $\gamma_r = \gamma_{\Delta} = 1$ , and  $\Gamma_{\text{nl}} = I_{3 \times 3}$ . For both control schemes a CRM has been implemented, where the parameters  $\gamma_c = g = 1$  have been chosen according to (2.59) which results in

$$L_{\text{ref}} = \begin{pmatrix} -1 & -1 \\ 9 & 5 \end{pmatrix}.$$

The closed-loop responses for MRAC without anti-windup are shown in Figure 6.2 and the results for AMRAW are shown in Figure 6.3. Note that the desired system response led to a saturation of the input for the step response upwards as well as for the step response downwards, which can be observed in Figure 6.4.

It can be seen that the parameters of MRAC without anti-windup slowly diverge and the system response shows some strong overshoots and undershoots after some time of adaptation. In difference to that, the closed-loop response with AMRAW looks very similar at the beginning of adaptation and at the end of the experiment. Only a slight change of the parameters of AMRAW can be observed, which are most likely due to measurement errors of the plant parameters in Table 6.1. The results clearly show that the application of basic MRAC is not advisable for this experiment with the desired dynamics given by 6.3. However, the extension of AMRAW allows the application of the adaptive control scheme and results in a good closed-loop performance.



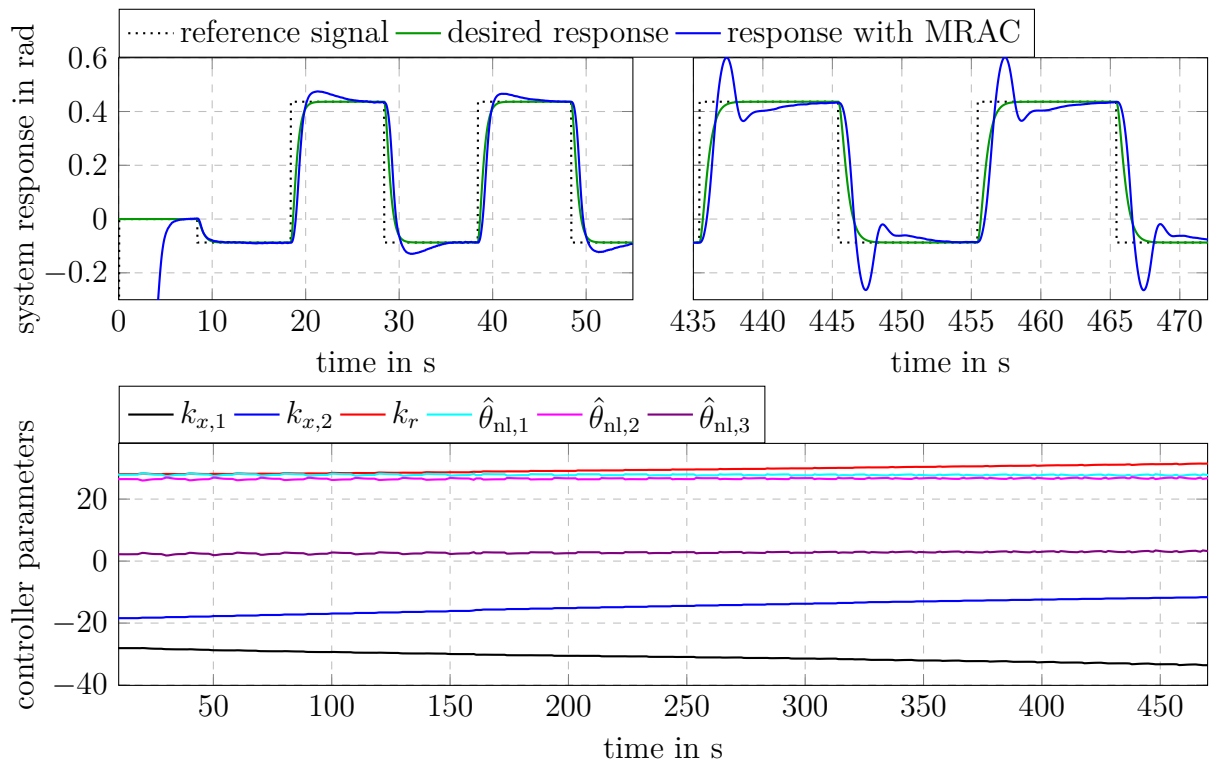


Figure 6.2: MRAC with CRM applied to helicopter experiment.

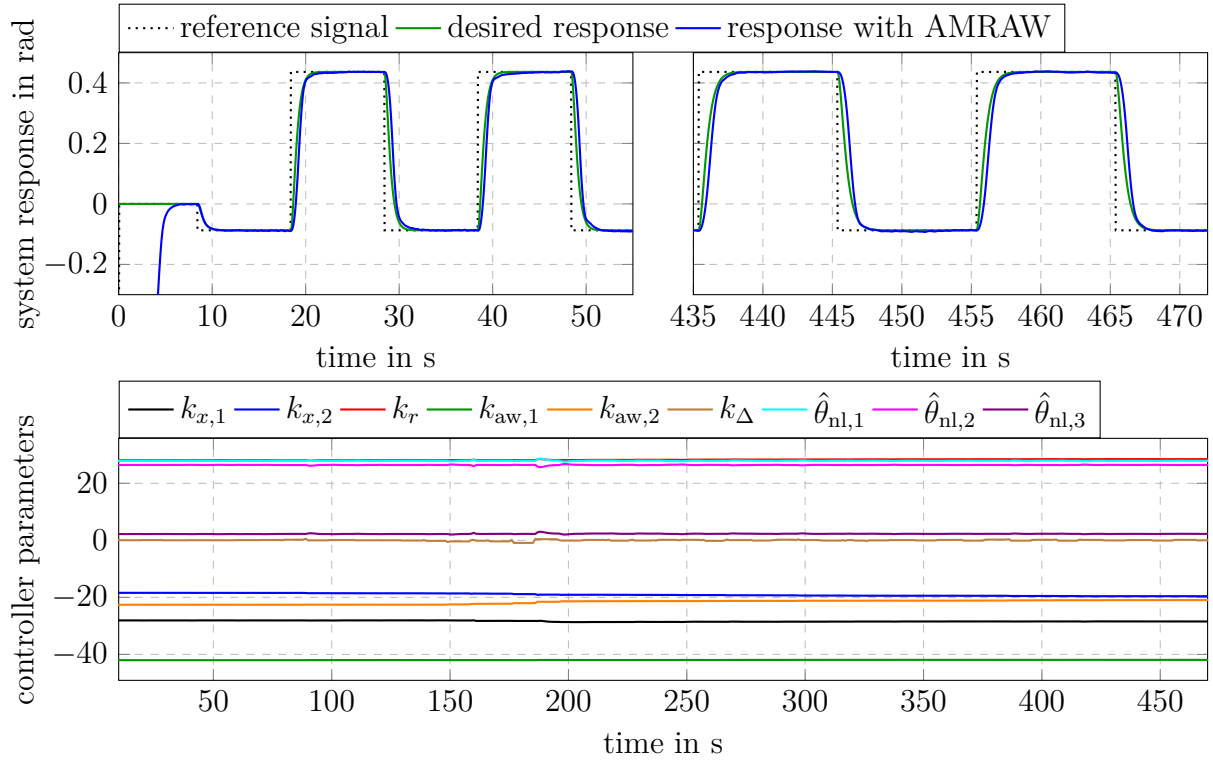


Figure 6.3: AMRAW with CRM applied to helicopter experiment.

### 6.1.3 Performance Adjustments and Parameter Adaptation

As a second experiment with the method of AMRAW different choices of  $A_{\text{awr}}$  with the desired anti-windup poles at  $-1$ ,  $-3$ ,  $-3.7$ , and  $-5$  have been carried out. Note that the poles at  $-3$  results in an equivalent closed-loop response to KAAW after adaptation to the ideal controller parameters (see Remark 5.3). After some time of adaptation, different step heights have been provided as the reference signal. Figure 6.4 shows a comparison of the experimental results for all choices of the anti-windup dynamics

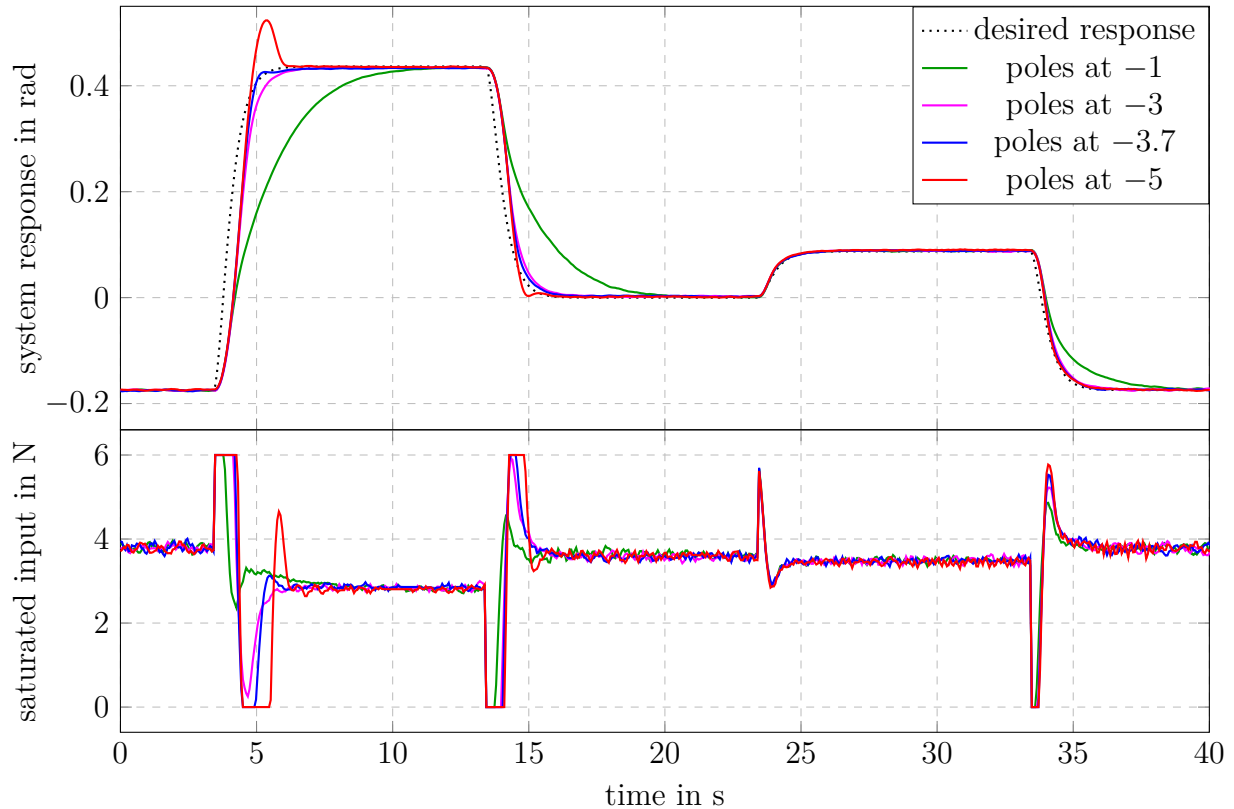


Figure 6.4: AMRAW applied to the helicopter experiment with different choices of the anti-windup poles.

It can be seen that similar to Simulation Example 5.1 the input stays longer in saturation for higher absolute values of the desired anti-windup poles. In the presented results the choice of the poles at  $-3.7$  leads to the best closed-loop performance, in the sense that the closed-loop response is most similar to the desired behavior prescribed by the reference model (6.3). It can also be observed that for smaller step sizes, where the period of saturation is shorter for all the compared cases, the different closed-loop responses look more similar to each other than for big step commands. For the step command without saturation of the input at  $t = 24\text{s}$ , no influence of the choice of the anti-windup pole can be observed. These results again verify that the desired anti-windup dynamics can be used to tune the performance when the input actually saturates without changing the performance when the input amplitude stays inside its limits.

In order to additionally show the capability of AMRAW to deal with uncertain plants, some erroneous plant parameters have been used to initialize the controller parameters. The inertia, the movable mass and the parameter  $\theta_p$  have been considered as

$$\hat{J}_\epsilon = 1.87, \quad \hat{m}_v = 0.705, \quad \hat{\theta}_p = 30.66,$$

so that the calculation of the initial controller parameters with the same specification as in Section 6.1.2 yields

$$K_x(0) = \begin{pmatrix} -23.87 \\ -15.77 \end{pmatrix}, \quad k_r(0) = 23.87, \quad \hat{\theta}_{nl}(0) = \begin{pmatrix} 30.66 \\ 26.45 \\ 2.20 \end{pmatrix},$$

$$K_{aw}(0) = \begin{pmatrix} -36.31 \\ -19.49 \end{pmatrix}, \quad k_\Delta(0) = 0.0419.$$

The experimental results are shown in Figure 6.5, where adaptation has been started at  $t = 53$ s. It can be seen that the performance with the erroneous plant parameters is very bad due to the very large offsets at steady state. After activation of the adaptation the parameter of  $\hat{\theta}_{nl}$  quickly change, so that a good tracking behavior results almost instantly after adaptation has been started. Therefore, the method of AMRAW also works very reliably for this plant when initialized with wrong parameters, due to the adaptive nature of the method.

## 6.1.4 Adaptation to Changing Plant Parameters

### Changing mass position

After showing the capability of AMRAW to deal with uncertain initial plant parameters, the following experiments are intended to show how the newly introduced method can adapt to changing plant parameters. As a simulation of a changing mass of a helicopter due to e.g. additional payload, the mass position  $x_v$  of the experiment has been changed during operation. This was done such that the distance of  $m_v$  to the propellers has been reduced and an increased propeller force is required to hold the helicopter in a constant position. The AMRAW controller parameters have been initialized like in section 6.1.2. Figure 6.6 shows the results of two experiments with activated and deactivated parameter adaptation, respectively.

It can be seen that without adaptation the closed-loop response becomes unacceptable after the mass has started to move. Due to the higher required force the closed-loop response  $\epsilon$  does not reach its desired steady state-values. For the experiment with parameter adaptation the effect of a changing mass position is barely observable in the closed-loop response. This is due to the quickly changing controller parameters  $\hat{\theta}_{nl,1}$ ,  $\hat{\theta}_{nl,2}$  and  $\hat{\theta}_{nl,3}$ , which compensate for the effect of the changing mass position. It can also be seen in Figure 6.6 that the changed position of the mass leads to an increased required force in the steady-state positions which in turn results in a longer input saturation for the steps upwards. However, no critical overshoots and undershoots can be observed for

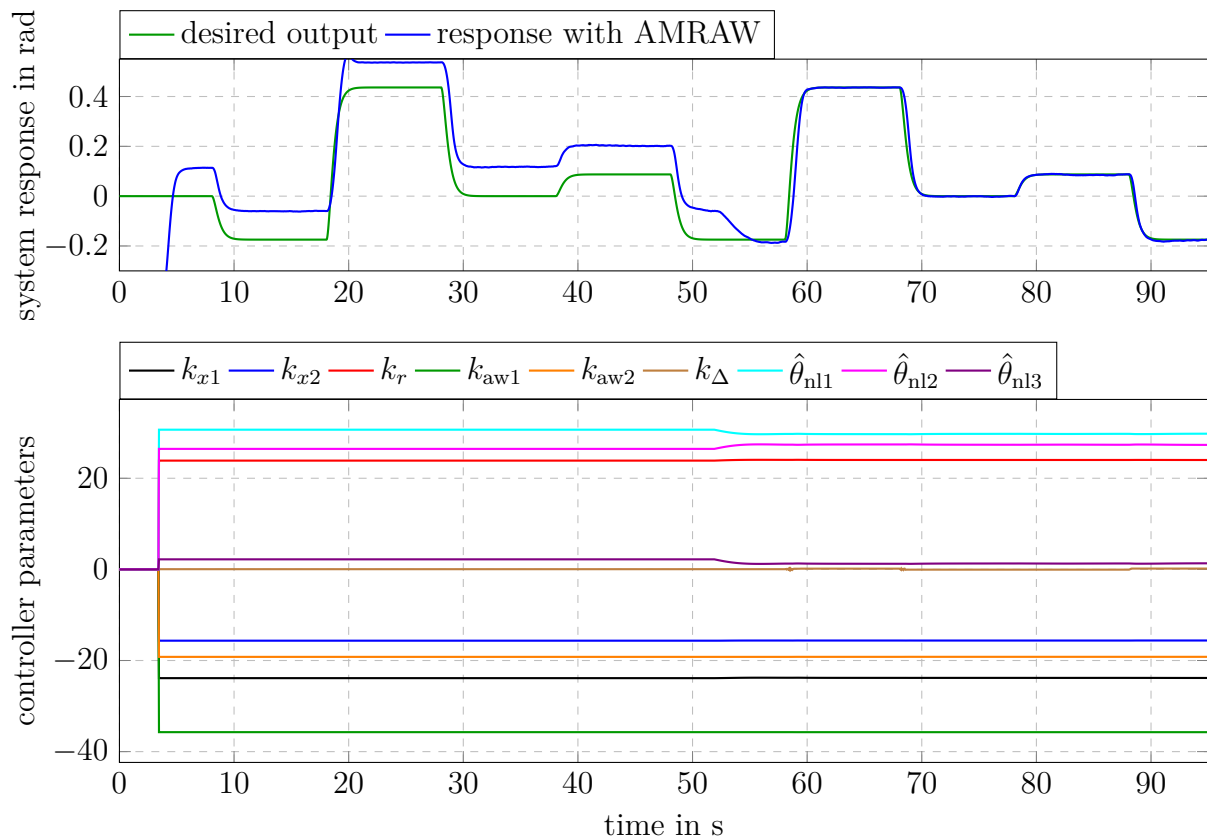


Figure 6.5: AMRAW applied to helicopter experiment with wrong initial parameters. Adaptation has been started at  $t = 52$ s.

the chosen desired anti-windup dynamics. This result shows that the initial choice of the desired anti-windup dynamic is still a good choice for the altered plant parameters.

### Reduced control effectiveness

As a last experiment with the helicopter, a defect of a propeller has been simulated. This has been done by reducing the value of  $\lambda$  in (6.2) to a value of 0.75 and by simultaneously reducing the maximal force amplitude from  $F_{\max} = 8\text{N}$  to  $\bar{F}_{\max} = 6\text{N}$  during operation. For a real helicopter, this would be equivalent to a reduced thrust and a respective reduced maximal force that can be achieved with the propellers. It is worth mentioning that these changes have been done in the software and not by actually damaging the propellers. The controller parameters of AMRAW have been initialized like in Section 6.1.2 and the initial maximal amplitude of  $F_{\max} = 8\text{N}$  has been considered in the AMRAW algorithm during the whole experiment. Hence, after reducing the maximal propeller force, the AMRAW algorithm uses a wrong assumption of the maximal amplitude of the force.

It can be seen in Figure 6.7 that the closed-loop system adapts to the reduced control effectiveness so that the tracking performance with adaptation is far better than without adaptation. It can also be observed that the parameters stay stable and do not diverge

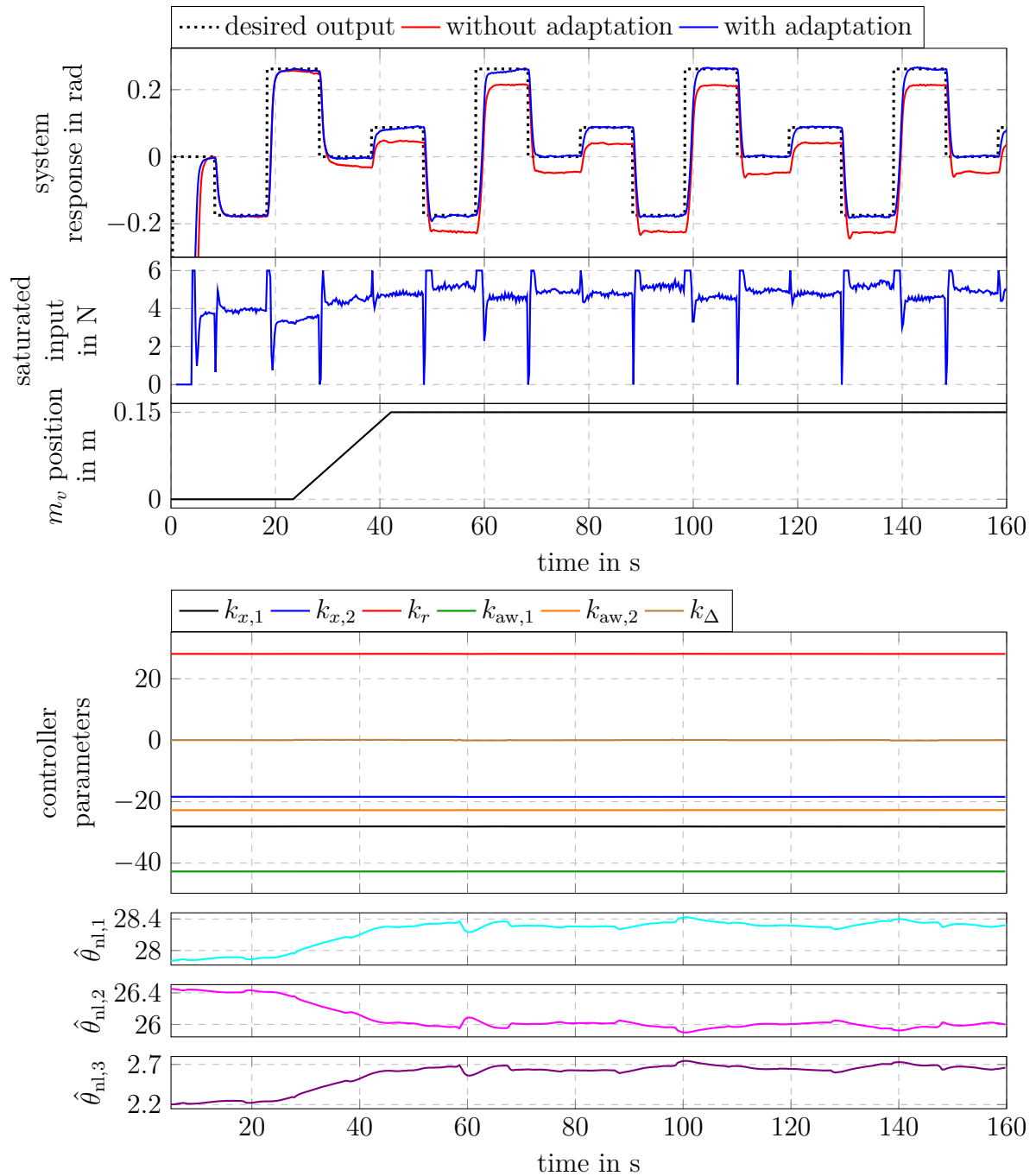


Figure 6.6: AMRAW applied to helicopter experiment with changing position of mass  $m_v$ .

during the whole time of the experiment. This experimental result suggests that the AMRAW algorithm is robust against wrong considerations of the saturation and therefore against erroneous calculations of  $\Delta u$ . However, it is necessary to mention again that this observation is only based on simulation results and experimental results. Robustness and

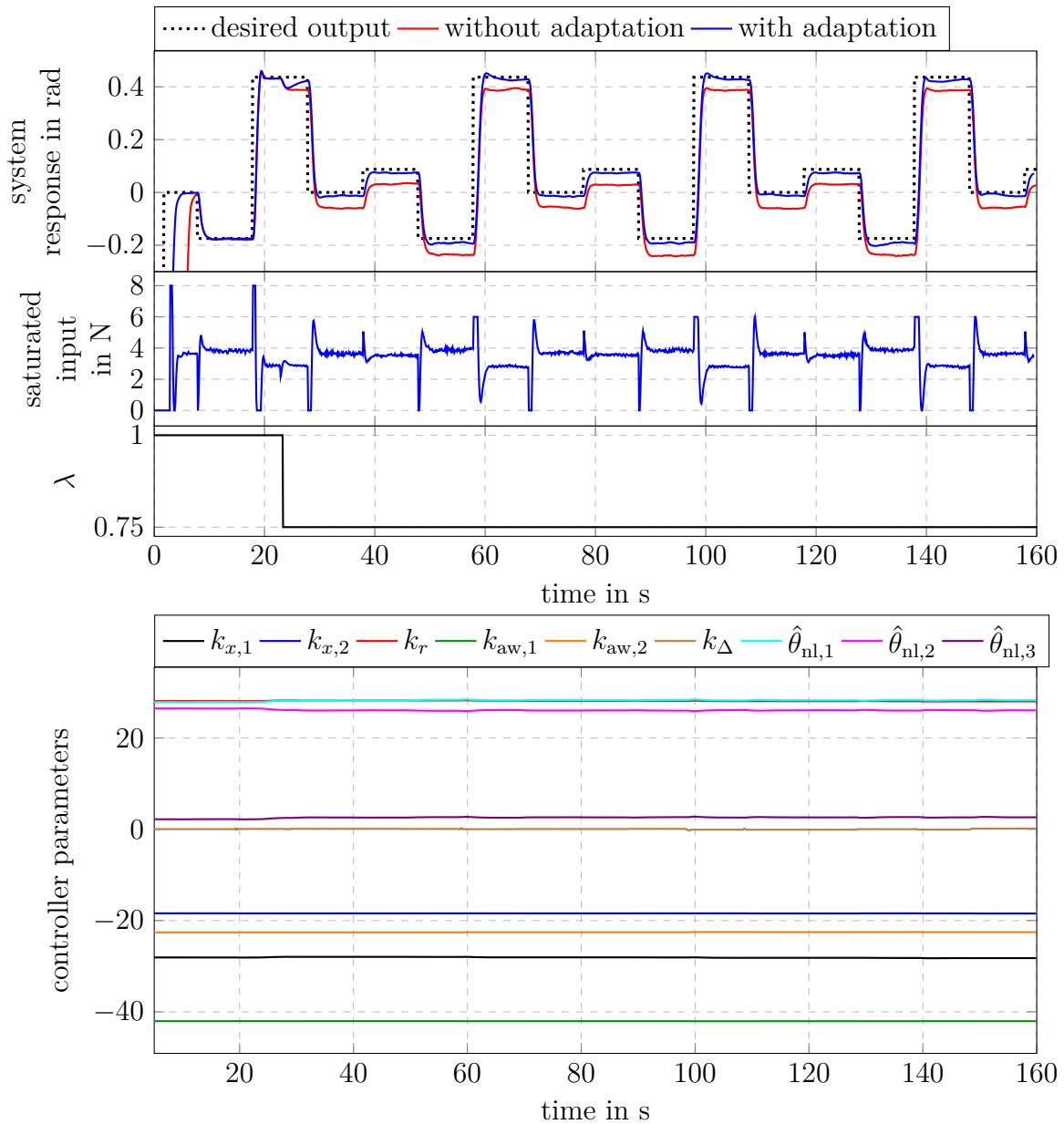


Figure 6.7: AMRAW applied to helicopter experiment with changing  $\lambda$  and a reduction of the maximal force amplitude during operation.

stability in the case of overestimated input amplitude limits can not be guaranteed based on the derivations in this work.

## 6.2 Electronic Throttle Plate

In this section, the method of indirect AMRAW from Table 4.3 is applied to the position control of an electronic throttle plate, which is a typical automotive application. The

position of the throttle plate mainly determines the airflow into the combustion chambers of an internal combustion engine. The resulting air charge, in turn, determines the engine torque of gasoline engines. More detailed information about the physical relations in the combustion engines can be found e.g. in [51]. As a consequence of the physical relations, the performance of the throttle plates position control has a strong influence on how quick the desired engine torque can be generated. Since the reference value for the position of the throttle plate is generated based on the position of the drivers gas pedal, a quick position control for the throttle plate corresponds to a dynamic driving experience.

Due to aging, altering environments and small defects, the control performance of an electronic throttle plate can decrease during lifetime. Furthermore, production tolerances can lead to altering performances for different instances of the same type of throttle plates. In order to avoid a permanent deterioration of the control performance, an automatic tuning algorithm can be applied. Such algorithms can be used to automatically re-tune the controller parameters if the performance becomes unacceptable. They also allow for an automatic initial tuning of the controller parameters, which results in a similar performance of all devices that have been tuned in this way. Some approaches for such algorithms applied to electronic throttle plates can be found in the literature [5, 27–29, 66, 107, 130, 131]. However, most of the proposed methods need special excitation signals in order to identify all parameters which are necessary for the controller design of the respective methods in the above-stated references. Furthermore, none of the above mentioned algorithms take input saturation into account explicitly. Since fast position dynamics require the input of an electronic throttle plate to frequently encounter its limits, a parameter adaptation with none of these algorithms is possible without the risk of parameter-windup for usual excitation of the plant during operation. In contrast to that, the method of indirect AMRAW will be shown in the following to allow for quick adaptation without the need of a special excitation of the throttle plate and without the need of avoiding input saturation. In addition, the algorithm will be shown to work very efficiently without special consideration of friction.

### 6.2.1 Experimental Setup and Plant Description

The setup of the electronic throttle plate experiment is shown in Figure 6.8. Two throttle plates are mounted on the top of a shelf. Each throttle plate can be controlled separately by connecting them to the additional hardware, which is mounted on the middle level of the shelf. The additional hardware consists of a power supply unit which provides 24V, a DC-DC converter to reduce the voltage down to 12V, and a motor controller that converts a PWM into DC voltage for the DC motor of the throttle plate. A dSpace Autobox 1405 is used to process the sensor data, implement the control scheme, and to generate the resulting PWM based on the computations of the control scheme. The sampling time has been chosen to be 1ms, which is similar to the sampling time of the series production throttle plate controller. Discretisations have been done with the Euler forward method.

Figure 6.9 shows the schematic structure of the throttle plate, which can be used to derive the plant description. For this purpose, the throttle plate has been divided into an electrical and a mechanical part. The electrical part represents a DC motor with resistance

$R$  and inductance  $L$ . A voltage  $u_M$  is applied to the motor that results in a current  $i_M$  and a torque  $\frac{T_M}{n_g}$ . The motor is connected to the mechanical part of the throttle plate via a gear with transmission ratio  $n_g$ . The mechanical parameters are the inertia  $J_{\text{mech}}$ , the damping  $d_{\text{mech}}$ , which is not schematically depicted in Figure 6.9, and four additional parameters that determine the torque of the spring  $T_S$ . These four parameters result from the special arrangement of two springs, which is common in usual throttle plates and shown in the undermost picture of Figure 6.9. The two springs differ such that each of them has a different initial tension  $T_{0i}$  at the equilibrium point  $\varphi = \varphi_{\text{lh}}$  and a different stiffness  $k_{ti}$ . Each spring is active in another region of the opening angle  $\varphi$  in order to force the throttle plate in the so-called “limp home position”  $\varphi_{\text{lh}}$  if no voltage is applied. In this position, the motor can be still supplied with enough air to slowly drive the car. The described spring arrangement results in the expression

$$T_S = (T_{01} - k_{t1} (\varphi - \varphi_{\text{lh}})) H(\varphi_{\text{lh}} - \varphi) + (-T_{02} - k_{t2} (\varphi - \varphi_{\text{lh}})) H(\varphi - \varphi_{\text{lh}}) \quad (6.4)$$

for the spring torque, where  $H(\cdot)$  denotes the Heaviside function

$$H(x) = \begin{cases} 0, & \text{for } x \leq 0, \\ 1, & \text{otherwise.} \end{cases} \quad (6.5)$$

It is worth mentioning that the opening angle  $\varphi$  of throttle plates is always limited by mechanical stops and that for all experiments in this section the “limp home position” has been defined to correspond to the opening angle  $\varphi = 0$ .

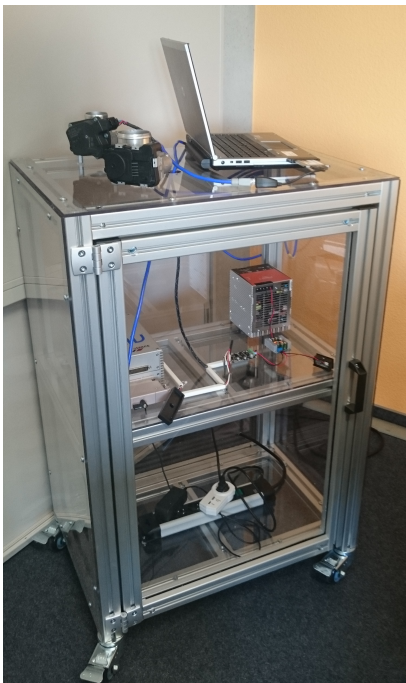


Figure 6.8: Experimental setup of the throttle plate position control.

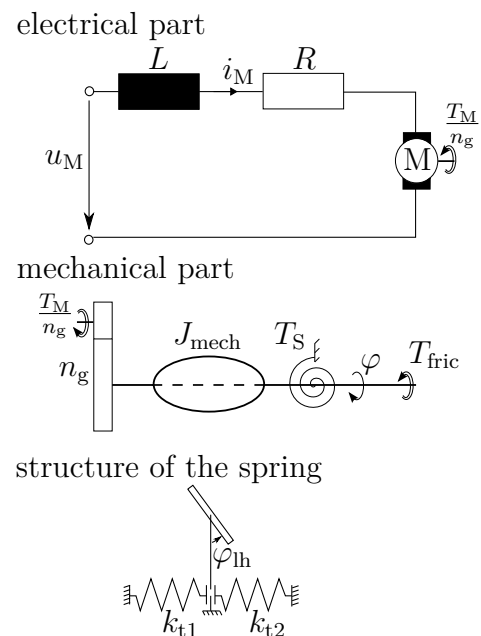


Figure 6.9: Schematic structure of the throttle plate.



In the following, the plant model is shortly presented based on the schematic illustration in Figure 6.9 and the description above. For a more detailed derivation of the system equations it is referred to [5, 48]. The equations of the plant are given by

$$u_M = K_M \dot{\varphi} + R i_M + L \frac{d i_M}{dt} \quad (6.6)$$

$$T_M = K_M i_M n_g, \quad (6.7)$$

for the electrical part and

$$J_{\text{mech}} \ddot{\varphi} = T_S + T_M - d_{\text{mech}} \dot{\varphi} + T_{\text{fric}} \quad (6.8)$$

for the mechanical part, where  $K_M$  denotes the torque constant of the DC motor. The torque  $T_{\text{fric}}$  in (6.8) describes all effects of friction. Note that these effects are usually very strong in common electronic throttle plates. However, friction is not explicitly considered for the derivation of the indirect AMRAW scheme for the throttle plate in this work. Therefore, the term  $T_{\text{fric}}$  is neglected in the following.

Additional negligence of the inductance ( $L = 0$ ), which is a common assumption for DC motors of throttle plates [5, 48], leads to

$$J_{\text{mech}} \ddot{\varphi} = T_S - \left( d_{\text{mech}} + \frac{K_M^2 n_g}{R} \right) \dot{\varphi} + \frac{K_M n_g}{R} u_M \quad (6.9)$$

after substitution of (6.6) and (6.7) in (6.8). As already mentioned in the description of the experimental setup different voltages  $u_M$  have been realized with a motor controller. This motor controller scales a constant voltage  $U$  based on a pulse-width modulation (PWM) with duty-cycle  $\tau$  such that  $u_M = \tau U$  with  $-\tau_{\text{max}} = -1 \leq \tau \leq 1 = \tau_{\text{max}}$ . Together with equation (6.9) this yields the model

$$\begin{aligned} \dot{x}_{\text{tp}} &= \begin{pmatrix} 0 & 1 \\ 0 & -\frac{d}{J} \end{pmatrix} x_{\text{tp}} + \begin{pmatrix} 0 \\ \frac{1}{J} \end{pmatrix} (\tau + \bar{\theta}_{\text{tp}}^T f_{\text{tp}}(\varphi)) \\ \left( D^2 + \frac{d}{J} D \right) \varphi &= \frac{1}{J} (\tau + \bar{\theta}_{\text{tp}}^T f_{\text{tp}}(\varphi)), \end{aligned} \quad (6.10)$$

where

$$\begin{aligned} x_{\text{tp}} &= [\varphi \quad \dot{\varphi}]^T, \\ \bar{\theta}_{\text{tp}} &= [T_{01} \quad T_{02} \quad k_{t1} \quad k_{t2}]^T \frac{R}{K_M n_g U}, \\ f_{\text{tp}} &= \begin{bmatrix} H(\varphi_{\text{lh}} - \varphi) & -H(\varphi - \varphi_{\text{lh}}) & \cdots \\ -(\varphi - \varphi_{\text{lh}}) H(\varphi_{\text{lh}} - \varphi) & -(\varphi - \varphi_{\text{lh}}) H(\varphi - \varphi_{\text{lh}}) \end{bmatrix}^T, \\ J &= J_{\text{mech}} \frac{R}{K_M n_g U}, \quad d = \left( d_{\text{mech}} + \frac{K_M^2 n_g}{R} \right) \frac{R}{K_M n_g U}. \end{aligned}$$

In order to apply indirect AMRAW to the throttle plate, a linear parametric model as given in (4.61) needs to be defined. In the following the linear parametric model

$$\tau_f = \theta_{\text{tp}}^T \phi_{\text{tp}} \quad (6.11)$$

with

$$\begin{aligned}\tau_f &= \frac{1}{\Lambda(D)} \tau, \\ \theta_{\text{tp}} &= \begin{bmatrix} J & d & \bar{\theta}_{\text{tp}}^T \end{bmatrix}^T, \\ \phi_{\text{tp}} &= \frac{1}{\Lambda(D)} \begin{bmatrix} D^2 \varphi & D \varphi & -f_{\text{tp},1}(y) & \cdots & -f_{\text{tp},4}(y) \end{bmatrix}^T,\end{aligned}\tag{6.12}$$

of the throttle plate is considered. Note that in difference to (4.61), the filtered saturated input have been defined as the output of (6.11). That allows an independent identification of the physical motivated parameters  $J$ ,  $d$  and  $\bar{\theta}_{\text{tp}}$ . The filter polynomial  $\Lambda(D)$  in (6.11) will be defined in the next section.

### 6.2.2 Application and Results

The method of indirect AMRAW from Table 4.3 has been applied to different throttle plates in order to show the capability of the indirect adaptive control method to quickly adapt the parameters and to achieve a prescribed performance. In order to make the plant parameter estimation scheme robust against modeling errors, it has been extended by projection as presented in Section 2.2.5. Hence, the parameter estimation scheme becomes

$$\begin{aligned}\dot{\hat{\theta}}_{\text{tp}} &= \begin{cases} P_{\text{ls}} \epsilon_{\text{tp}} \phi_{\text{tp}}, & \hat{\theta}_{\text{tp}} \in \mathcal{S} \\ P_{\text{ls}} \epsilon_{\text{tp}} \phi_{\text{tp}} - P_{\text{ls}} \frac{\nabla g \nabla g^T}{\nabla g^T P_{\text{ls}} \nabla g} P_{\text{ls}} \epsilon_{\text{tp}} \phi_{\text{tp}}, & \text{or } \hat{\theta}_{\text{tp}} \in \delta \mathcal{S} \text{ and } (P \epsilon_{\text{tp}} \phi_{\text{tp}})^T \nabla g \leq 0, \\ P_{\text{ls}} \epsilon_{\text{tp}} \phi_{\text{tp}} - P_{\text{ls}} \frac{\nabla g \nabla g^T}{\nabla g^T P_{\text{ls}} \nabla g} P_{\text{ls}} \epsilon_{\text{tp}} \phi_{\text{tp}}, & \text{otherwise,} \end{cases} \\ \dot{P}_{\text{ls}} &= \begin{cases} -\frac{P_{\text{ls}} \phi_{\text{p}} \phi_{\text{p}}^T P_{\text{ls}}}{1 + \phi_{\text{tp}}^T \phi_{\text{tp}}}, & \hat{\theta}_{\text{tp}} \in \mathcal{S} \\ 0, & \text{or } \hat{\theta}_{\text{tp}} \in \delta \mathcal{S} \text{ and } (P \epsilon_{\text{tp}} \phi_{\text{tp}})^T \nabla g \leq 0, \\ 0, & \text{otherwise,} \end{cases} \\ P_{\text{ls}}(0) &= P_{\text{ls}0}, \quad P_{\text{ls}}(t_r) = \rho_r,\end{aligned}\tag{6.13}$$

with

$$\epsilon_{\text{tp}} = \frac{\tau_f - \hat{\theta}_{\text{tp}}^T \phi_{\text{tp}}}{1 + \phi_{\text{tp}}^T \phi_{\text{tp}}}$$

and  $\mathcal{S} = \{\hat{\theta}_{\text{tp}} \in \mathbb{R}^6 \mid (\theta_p - X)^T (\theta_p - X) - R_{\mathcal{S}}^2 \leq 0\}$ . This definition of the admissible set  $\mathcal{S}$  for the plant parameters corresponds to a ball with a midpoint

$$X^T = \begin{bmatrix} \bar{J} & \bar{d} & \bar{T}_{01} & \bar{T}_{02} & \bar{k}_1 & \bar{k}_2 \end{bmatrix}$$

and with a radius  $R_{\mathcal{S}}$ .

For the initialization of the indirect AMRAW control scheme, the initial estimation of the plant parameters have been set to

$$\hat{\theta}(t)^T = \begin{bmatrix} 3 \cdot 10^{-4} & 0.089 & 0.13 & 0.07 & 0.04 & 0.065 \end{bmatrix}$$

based on a rough initial parameter identification. The admissible set of the estimated parameters have been defined by

$$X^T = [5 \cdot 10^{-4} \quad 0.1 \quad 0.2 \quad 0.1 \quad 0.06 \quad 0.08]$$

$$R_S = 0.1.$$

In normal operation of the throttle plate, its position is desired to track changing constant set points. In order to achieve this requirement, the internal model has been set to  $Q(D) = D$  which implicitly introduces an integrator in the control law of the basic controller given in Table 4.3. Therefore, four desired closed-loop poles need to be specified for  $A_d$ , which have been chosen to lie at  $-100$ . Also, the desired poles for the anti-windup scheme has been chosen to lie at  $-100$ , which leads to a desired system matrix of

$$A_{awr} = \begin{pmatrix} 0 & 1 \\ -10000 & -200 \end{pmatrix}.$$

The remaining tuning parameters of indirect AMRAW has been set to  $P_{ls}(0) = 10^5 I_{6 \times 6}$ ,  $\rho_0 = 1$ ,  $5 \cdot 10^4$  and  $\Lambda_e(D) = D^2 + 200D + 10000$ .

From this starting point, an experiment has been done with the first throttle plate, which is called TP1 in the following. A repeated step sequence with different step heights has been specified as reference signal. Note that such a reference signal is not special at all and can occur during normal operation of a throttle plate. The system response with the initial parameters and deactivated adaptation can be seen in the first graph of Figure 6.10. Apparently, the closed-loop performance is not sufficient to meet the requirements. Some strong oscillations around the desired set points can be observed. This is critical since it can lead to a varying air flow through the throttle plate and can also cause damage to the throttle plate if such oscillations occur near to a mechanical stop. In addition, a strange behavior can be observed when passing the "limp home position"  $\varphi = 0$  at about  $t = 2.8$ s. The throttle plate seems to bounce off the "limp home position" so that it moves in the wrong direction for a short time. The applied force seems not to be sufficient to overcome the initial torque of the spring which is active on the other side of the "limp home position".

The second, third, and fourth graph of Figure 6.10 show the closed-loop signals directly after starting the parameter adaptation. It can be seen that the estimated parameters change very quickly and also the closed-loop performance becomes better very quickly. It can also be observed that during adaptation the input saturates for the high step command upwards and downwards, which does not lead to divergence of the parameters. After ten seconds of adaptation, the parameter estimation has been deactivated. The closed-loop response with the adapted parameters is depicted in the last graph of Figure 6.10 and shows a very good tracking performance.

The same experiment has been carried out with a second throttle plate, called TP2 in the following. All tuning parameters have been adopted from the foregoing experiment. The initial values for estimated plant parameters have been chosen to be the estimated parameters at the end of the experiment with throttle plate TP1. The results are shown

in Figure 6.11. It can be seen that the performance for TP2 before adaptation is better than the performance of TP1 before its adaptation. However, overshoots and undershoots can be observed, which are undesired and critical for operation near to the mechanical stops of the throttle plate. After the start of parameter adaptation, it can be seen again that the parameter estimations change quickly and that the undesired behavior of the system response vanishes. Finally, after adaptation of the parameters the closed-loop performance of TP2 is similar to the performance of TP1.

The results of the presented throttle plate experiments clearly show a lot of benefits of the indirect AMRAW algorithm. It has been presented that a very quick adaptation of the plant parameters and therefore of the controller parameters can be achieved. This is possible even without a special excitation of the system. Therefore, it is not necessary to design a reference signal that allows for a reliable parameter estimation. Furthermore, it is not necessary to avoid input saturation during parameter adaptation, due to the anti-windup scheme. It has also been shown that the resulting closed-loop performance after adaptation is very good in the sense that no oscillations occur and that the rise time of the system is quite short. These properties of the presented AMRAW algorithm make it suitable for different applications. Firstly it could be used for automatic tuning purposes of throttle plates directly after their production. This would lead to the same initial closed-loop performance for different instances of the throttle plate even in the presence of production tolerances. In addition, the algorithm could be used to re-tune the control algorithm during regular maintenance. Hence, performance degradation due to aging could be avoided. Such re-tuning could also be activated in a safe operating condition of the motor and the car if a bad closed-loop performance has been detected before. This could reduce the time between parameter adaptation of the algorithm in comparison to the maintenance intervals and therefore lead to longer periods of an optimal throttle plate behavior. A last suitable application is mainly based on the parameter adaptation. It has been shown that the estimation of the plant parameters is quite fast. In addition the parameters have been chosen to have a physical interpretation. This makes it suitable for purposes of diagnostics, which can be used to detect defects or undesired changes of certain parts of the throttle plate.

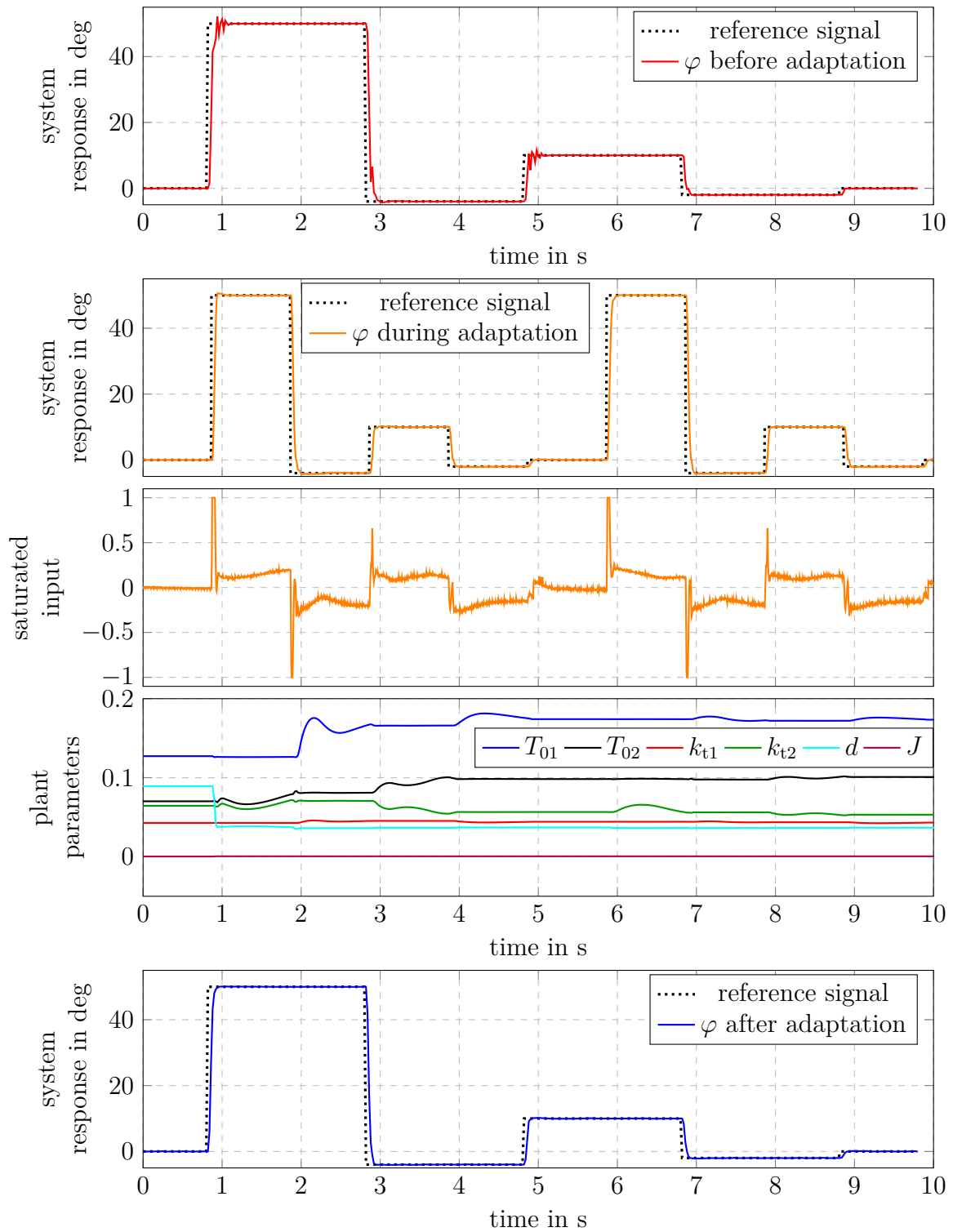


Figure 6.10: Closed-loop responses of throttle plate TP1 before, during, and after adaptation.

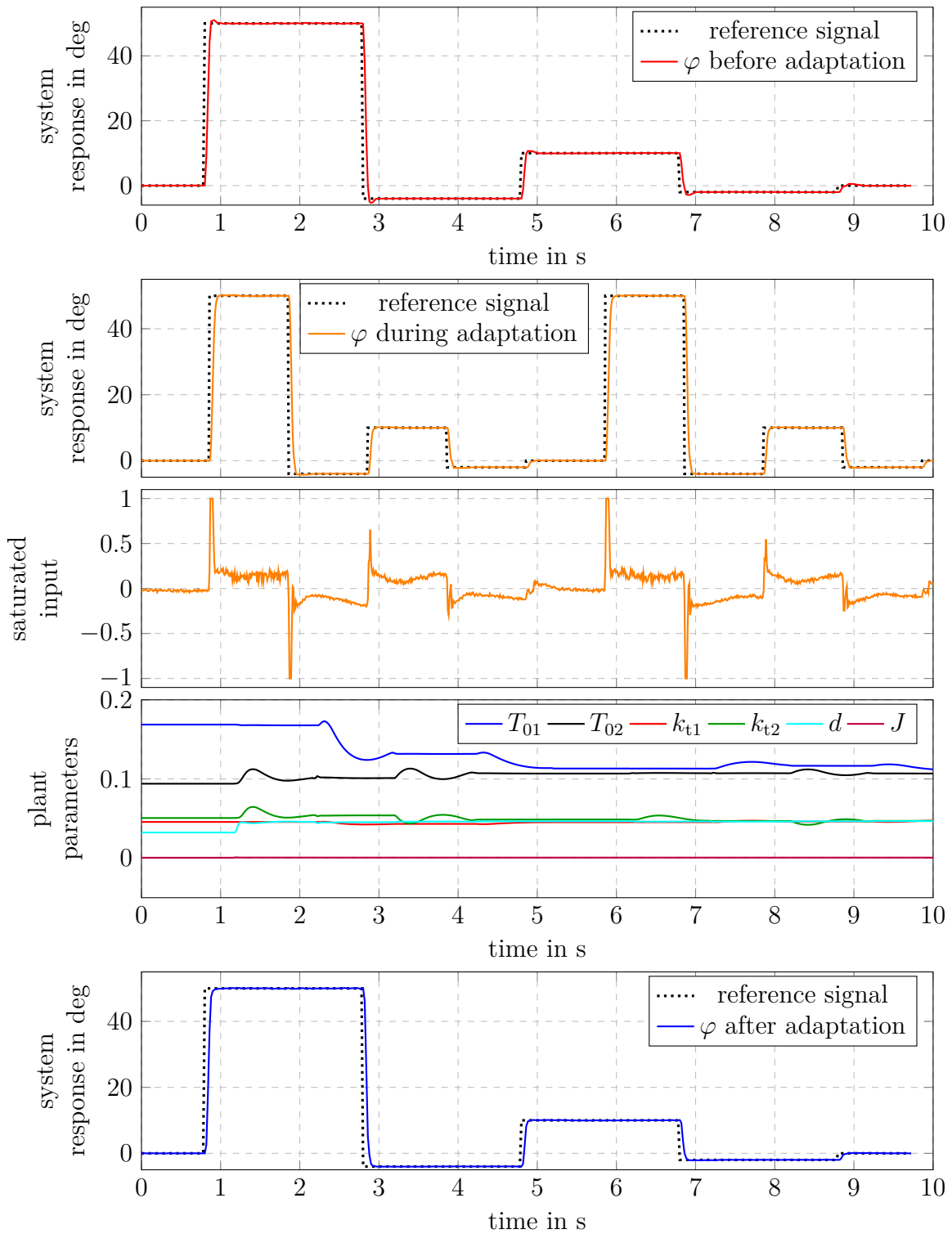


Figure 6.11: Closed-loop responses of throttle plate TP2 before, during, and after adaptation.

# Chapter 7

## Summary and Future Work

In this work, adaptive systems with input saturation have been examined. It has been shown that the application of basic adaptive control methods can lead to undesired effects on the closed-loop response if the input amplitude of the plant is limited. These effects involve slow closed-loop responses, oscillations of the plant output, and divergence of the estimated parameters. Additionally, for unstable open-loop plants global closed-loop stability can not be guaranteed any longer. Consequently, it has been concluded that a proper consideration of the input saturation for adaptive systems is absolutely necessary.

A review on existing anti-windup schemes for adaptive control in the literature revealed that multiple methods exist that address the issue of diverging parameters and that can guarantee bounded closed-loop trajectories under certain conditions on the plant and the closed-loop signals. Some of the reviewed methods additionally aim to avoid input saturation in order to reduce control deficiency. However, for none of the adaptive methods a performance analysis has been carried out analytically, experimentally or through simulations.

In order to address the issue of performance degradation in adaptive systems with input saturation, the new adaptive anti-windup method AMRAW has been introduced in this work. It extends basic adaptive control methods by a combination of two existing anti-windup concepts from the literature. Bounded closed-loop trajectories can be guaranteed if the new method based on MRAC is applied to open-loop stable plants. For unstable open-loop plants, certain conditions on the closed-loop states have been derived to guarantee boundedness of the closed-loop signals. Moreover, it has been shown for first order systems that the additional tuning parameter of AMRAW can be used to determine how fast the unwanted saturation effects will be regulated.

Several results of simulation examples have been presented in order to verify the stability of the resulting closed-loop system for the direct and indirect AMRAW schemes. In addition, the results show that the new adaptive anti-windup method can be used to improve the closed-loop performance and to avoid parameter divergence when the limits of the input amplitude are actually encountered. These properties of AMRAW have also been verified by applying the new method to real-world experiments. The results of the helicopter benchmark experiment further show the general benefits of adaptive control

algorithms for plants with parameter uncertainties and that the extensions of AMRAW makes adaptive control applicable to input saturated plants. Moreover, the results of the throttle plate experiments show how the application of indirect AMRAW results in an automatic tuning method that is straight forward to apply and leads to a very good closed-loop behavior. Based on the theoretical examination, the simulations, and the experiments, some interpretations and proposals have been stated in order to facilitate the understanding of the adaptive control schemes and to lower the hurdles for real world applications of the proposed schemes.

### **Future Work**

Many technical plants are controlled by digital controllers with low sampling rates, which makes the application of discrete-time control algorithms necessary. In such cases, the adaptive algorithms presented in this work are not applicable without further considerations. Hence, future work should involve these considerations and the derivation of discrete-time AMRAW methods, which allow for an improvement of performance for discrete-time input saturated adaptive closed-loop systems.

Not only a limited input amplitude can lead to a deterioration of the closed-loop performance in adaptive systems, but also a rate limitation of the controlled input. The method of MRAW can be used to address rate limitations for known plant parameters as shown e.g. in [15, 39, 40]. Therefore, an extension or modification of AMRAW which allows for a consideration of rate limitations would be beneficial for adaptive control of plants, which suffer from a limited input rate. Note that for indirect adaptive control with state-feedback an adaptive MRAW scheme for rate limitations has already been presented in [70].

In this work, the method of AMRAW has been derived for SISO systems. However, not all technical applications can be divided into multiple SISO systems, but have to be considered as a MIMO plant. For these applications, it is necessary to extend AMRAW to account for multiple inputs and outputs. Especially for plants with redundant actuators, this will include the allocation of the control signal inside the anti-windup scheme.

In Remark 5.2 possible ways of tuning the desired anti-windup dynamics in AMRAW have been proposed. These tuning procedures require either extensive simulations with different combinations of plant and controller parameters or a re-tuning after the closed-loop performance has become unacceptable. In order to find a more systematic tuning procedure a combination of the robust approach, as presented e.g. in [49, 155], with the adaptive approach, which has been presented in this work, should be considered.

The amplitude limits of technical systems are not always perfectly known or might even change during lifetime. A recommendation to implement AMRAW in order to avoid problems due to underestimation of the amplitude limits has been stated in Remark 5.5. In addition, the results of the helicopter experiment suggest that AMRAW is robust against overestimation of the input amplitude limits. However, future work should involve a rigorous examination of the robustness of AMRAW in the case of erroneous assumptions of the input amplitude limits. Results of such examinations will help to decide if AMRAW can be used for a plant with uncertain amplitude limits.



# Appendix A

## Definitions, Theorems and Lemma regarding Stability Analysis of Adaptive Systems

Some important definitions, theorems, and lemma are given in this appendix that are often utilized for stability analysis of adaptive dynamical systems. None of the lemma or theorems are proven here, but references are stated that present such proofs. The following definitions, theorems, and lemma are partially adopted from [94] and [60].

### A.1 Lyapunov Stability

A dynamical system of the form

$$\dot{x} = f(t, x) \tag{A.1}$$

is considered, with  $f : [0, \infty) \times \mathcal{B} \rightarrow \mathbb{R}^n$  and the domain  $\mathcal{B} \subset \mathbb{R}^n$ . It is assumed that  $f$  satisfies all necessary and sufficient conditions for the existence and uniqueness of the solution of (A.1) (see e.g. [78, 94]) for all initial conditions  $x(t_0) = x_0 \in \mathcal{B}$ . Stability analysis of the system (A.1) is done by inspecting the stability properties of its equilibrium points, which are defined in the following.

**Definition A.1.** *The state  $x_e$  is an equilibrium point of the system (A.1), if*

$$f(t, x_e) \equiv 0 \quad \forall t \geq t_0.$$

**Definition A.2.** *An equilibrium point  $x_e$  of (A.1) is stable in the sense of Lyapunov if for arbitrary  $t_0 \geq 0, \epsilon > 0$  there exists a  $\delta(\epsilon, t_0) > 0$ , such that  $\forall \|x_0 - x_e\| \leq \delta$  the system trajectories will satisfy  $\|x(t) - x_e\| < \epsilon \forall t \geq t_0$ . If  $\delta$  does not depend on  $t_0$ , the equilibrium point is said to be uniformly stable.*

**Definition A.3.** *An equilibrium point  $x_e$  of (A.1) is asymptotically stable in the sense of Lyapunov, if it is stable and there exists a  $\delta(t_0)$  such that the system trajectories will satisfy  $\lim_{t \rightarrow \infty} \|x(t) - x_e\| = 0$  if  $\|x_0 - x_e\| \leq \delta$ .*

**Definition A.4.** An equilibrium point  $x_e$  of (A.1) is uniformly asymptotically stable in the sense of Lyapunov, if it is uniformly stable and there exists a  $\delta$  for any  $t_0 \geq 0$  and  $\epsilon > 0$ , independent of  $(t_0, \epsilon)$ , and a  $T(\epsilon) > 0$ , independent of  $t_0$ , such that the system trajectories will satisfy  $\|x(t) - x_e\| < \epsilon \quad \forall t \geq t_0 + T(\epsilon)$  if  $\|x_0 - x_e\| \leq \delta$ .

**Definition A.5.** The stability definitions A.2-A.4 are said to be global, if  $\lim_{\epsilon \rightarrow \infty} \delta = \infty$  in the respective cases.

If an equilibrium point of the system (A.1) is stable in the sense of at least one of the definitions A.2-A.5, the solution  $x$  is said to be bounded. The concept of boundedness is defined in the following.

**Definition A.6.** A solution  $x$  of (A.1) is bounded, if  $\|x\| < \beta \quad \forall t \geq t_0$ , with a  $\beta > 0$ , which may depend on each solution.

**Definition A.7.** A solution  $x$  of (A.1) is uniformly bounded, if for any  $\alpha > 0$  there exists a  $\beta(\alpha)$ , independent of  $t_0$ , such that  $\|x\| < \beta(\alpha) \quad \forall t \geq t_0$  if  $\|x_0\| < \alpha$ .

The concept of Lyapunov stability has been defined above. The next definitions are useful to analyze the stability of a system with Lyapunov's direct method.

**Definition A.8.** A scalar function  $V(x) : \mathcal{B}_r \rightarrow \mathbb{R}$ , with the domain

$$\mathcal{B}_r = \{x \in \mathbb{R}^n : \|x\| \leq r\},$$

is called locally positive definite (semidefinite), if  $V(0) = 0$  and  $V(x) > 0$  ( $V(x) \geq 0$ ) for all nonzero  $x \in \mathcal{B}_r$  for some  $r > 0$ . The function is globally positive (semi)definite if  $\mathcal{B}_r = \mathbb{R}^n$ .

**Definition A.9.** A scalar function  $V(x) : \mathcal{B}_r \rightarrow \mathbb{R}$ , with the domain

$$\mathcal{B}_r = \{x \in \mathbb{R}^n : \|x\| \leq r\},$$

is called locally negative definite (semidefinite), if  $-V(x)$  is locally positive definite (semidefinite). The function is globally negative (semi)definite if  $\mathcal{B}_r = \mathbb{R}^n$ .

**Definition A.10.** A function  $V(x) : \mathbb{R}^n \rightarrow \mathbb{R}$  is called radially unbounded, if it is positive definite, strictly increasing on  $\mathbb{R}$ , and satisfies  $\lim_{\|x\| \rightarrow \infty} V(x) = \infty$ .

The definitions above allow the statement of the main theorem for stability analysis in the sense of Lyapunov.

**Theorem A.1** (Lyapunov's Direct Method). Let  $x_e = 0$  be an equilibrium point for (A.1). Suppose the initial conditions  $x(t_0 = 0) = x_0$  lie in the domain  $\mathcal{B}$  and there exists a continuously differentiable positive definite function on that domain:  $V(x) : \mathcal{B} \rightarrow \mathbb{R}$ . If the time derivative of this function is locally negative semi-definite,

$$\dot{V} = \frac{dV}{dx} f(t, x) \leq 0,$$

for all  $t \geq 0, x \in \mathcal{B}$ , then the equilibrium of the system is locally uniformly stable in the sense of Lyapunov. If  $\dot{V} < 0$  (locally negative definite), then the equilibrium point is uniformly asymptotically stable.

A proof of Theorem A.1 can be found in [78, 160]. The theorem above presents a method to verify stability as defined in A.2-A.4 by the properties of a function, defined in A.8-A.9. A positive definite function  $V(x)$  which is supposed to verify the stability of a system (A.1) is called a Lyapunov function candidate. If it satisfies the conditions in Theorem A.1,  $V(x)$  becomes a Lyapunov function. The concept of a Lyapunov function can be extended as follows.

**Theorem A.2.** *Let  $x_e = 0$  be an equilibrium point for (A.1). If  $V(x)$  is a radially unbounded Lyapunov function of the system, then the equilibrium is globally uniformly (asymptotically) stable.*

A proof of Theorem A.2 can also be found in [78, 160].

## A.2 Barbalat's Lemma

Barbalat's Lemma is especially useful to verify asymptotic convergence of states or signals of a system, even if Lyapunov's direct method (Theorem A.1) can just verify stability of the system ( $\dot{V}(x)$  semi negative definite). In order to state Barbalat's Lemma, the definition of uniformly continuous functions is necessary.

**Definition A.11.** *A function  $f(t) : \mathbb{R} \rightarrow \mathbb{R}$  is a uniformly continuous function, if for any  $\epsilon > 0$  there exists a  $\delta(\epsilon)$  such that  $\forall |t_2 - t_1| \leq \delta \Rightarrow |f(t_2) - f(t_1)| \leq \epsilon$ .*

**Lemma A.1** (Barbalat's Lemma). *If  $\lim_{t \rightarrow \infty} \int_0^t f(\tau) d\tau$  of the uniformly continuous function  $f(t) : \mathbb{R} \rightarrow \mathbb{R}$  exists and is finite, then  $\lim_{t \rightarrow \infty} f(t) = 0$ .*

The proof of Barbalat's Lemma can be found in [60, 78] The Lemma A.1 together with the two facts that a function is uniformly continuous if its derivative is bounded ([60, 94]), and that a nonincreasing function with lower bound has a limit for  $t \rightarrow \infty$  (Lemma 3.2.3 in [60]) lead to the following result which is adopted from [94].

**Corollary A.1.** *If a scalar function  $f : \mathbb{R} \rightarrow \mathbb{R}$  is twice continuously differentiable on  $[0, \infty)$ , has a finite limit, and has a bounded second derivative, then  $\lim_{t \rightarrow \infty} \dot{f}(t) = 0$ .*

## A.3 Meyer-Kalman-Yakubovich (MKY) Lemma

Before introducing the MKY Lemma, a definition for (strictly) positive real transfer functions is necessary. The following definitions and the MKY lemma are adopted from [60, 116, 147].

**Definition A.12.** *A function  $G(s)$  of the complex variable  $s = \sigma + j\omega$  is positive real (PR) if*

1.  $G(s)$  is real for real  $s$ , and

2. the real part of  $G(s)$ , i.e.  $\text{Re}(G(s))$ , for all  $s > 0$  satisfies  $\text{Re}(G(s)) \geq 0$ .

**Definition A.13.** A function  $G(s)$  of the complex variable  $s = \sigma + j\omega$  is strictly positive real (SPR) if  $G(s - \epsilon)$  is PR for some  $\epsilon > 0$ .

**Lemma A.2.** A rational function  $G(s)$  of the complex variable  $s = \sigma + j\omega$  is strictly positive real (SPR) if and only if

- $G(s)$  does not have any poles for  $\sigma \geq 0$ ,
- $\text{Re}(G(s)) > 0$  for all  $\omega \in (-\infty, \infty)$ , and
- $$\begin{cases} \lim_{\omega^2 \rightarrow \infty} \omega^2 \text{Re}(G(j\omega)) > 0 & \text{for } n^* = 1, \\ \lim_{\omega \rightarrow \infty} \text{Re}(G(j\omega)) > 0 & \text{for } n^* = 0, \text{ and} \\ \lim_{\omega \rightarrow \infty} \frac{G(j\omega)}{j\omega} > 0 & \text{for } n^* = -1. \end{cases}$$

A proof of Lemma A.2 can be found in [57]. Note that the second condition in Lemma A.2 is equivalent to a phase of  $G(s)$  in  $(-90^\circ, 90^\circ)$ .

**Lemma A.3** (Meyer-Kalman-Yakubovich (MKY) Lemma). A system with the Hurwitz matrix  $A$ , vectors  $B, C$  and a scalar  $d \geq 0$  is considered. If the transfer function

$$G(s) = C(sI - A)^{-1}B + d$$

of this system is SPR, then for any given  $L = L^T > 0$ , there exists a scalar  $v > 0$ , a vector  $q$  and a  $P = P^T > 0$  such that

$$\begin{aligned} A^T P + P A &= -q q^T - v L \\ P B - C^T &= \pm q \sqrt{2d} \end{aligned}$$

A proof of the MKY Lemma can be found in [101].

## A.4 Properties of Least-Squares Estimation with Covariance Resetting

The following theorem states the properties of the Least-Squares Algorithm presented in Section 2.2.3.

**Theorem A.3.** The Least-Squares Algorithm with Covariance resetting given in (2.52) has the following properties:

- i)  $\epsilon, \epsilon \sqrt{\phi_p^T \phi_p}, \hat{\theta}_p, \dot{\hat{\theta}}_p$  are bounded.
- ii)  $\epsilon, \epsilon \sqrt{\phi_p^T \phi_p}, \dot{\hat{\theta}}_p$  are square integrable.

A proof of Theorem A.3 can be found in [60].

# Appendix B

## Proofs

### B.1 Second Part of Proof of Theorem 4.1

In Section 4.1 the method of adaptive model recovery anti-windup for state-feedback has been introduced. Boundedness of the closed-loop signals in the case of a stable open-loop plant has already been established in the first part of the proof. The proof of the boundedness of the closed-loop signals for the case of an unstable open-loop plant is done in the following. The respective theorem is repeated here for clarity.

**Theorem 4.1.** *The control law (4.8) with a bounded reference signal  $|r(t)| \leq r_{\max}(t)$  together with the parameter update laws (4.13) and the reference model (4.10) applied to the plant  $G_{\text{nls}}$  in (3.2) results in bounded closed-loop signals if the plant is open-loop stable. Boundedness of the closed-loop signals for an unstable open-loop plant  $G_{\text{nls}}$  can be established under the following conditions:*

i) *The initial state of the closed-loop system satisfies*

$$x_{\text{ps}}(t_0)^{\text{T}} P_W x_{\text{ps}}(t_0) \leq \lambda_{\min}(P_W) \left( \frac{2 p_b \lambda (u_{\max} - \|\theta_{\text{nl}}\| o_{\text{nl}})}{|-q_0 + 2 p_b \lambda \|K_x^*\| + \|\theta_{\text{nl}}\| c_{\text{nl}}|} \right)^2. \quad (\text{B.1})$$

ii) *The reference signal does not exceed*

$$r_{\max} \leq \frac{q_0 (u_{\max} - \|\theta_{\text{nl}}\| o_{\text{nl}}) - \rho \eta D_{\text{aw}} \|x_{\text{aw}}\|}{\rho \eta |k_r^*|}. \quad (\text{B.2})$$

iii) *The initial value of (4.12) does not exceed*

$$V(t_0) \leq \frac{\lambda}{\lambda_{\max}(\Gamma_x)} \left( \frac{q_0 (2 p_b \lambda (u_{\max} - \|\theta_{\text{nl}}\| o_{\text{nl}})) - 2 p_b \lambda \rho \eta (|k_r^*| r_{\max} + D_{\text{aw}} \|x_{\text{aw}}(t_0)\|)}{N_{\max}} \right)^2 \quad (\text{B.3})$$

with

$$N_{\max} = 2 p_b \lambda \left[ \rho \eta \left( \|x_{\text{aw}}(t_0)\| \left[ 1 + \sqrt{\frac{\lambda_{\min}(\Gamma_{\text{aw}})}{\lambda_{\min}(\Gamma_x)}} \right] + r_{\max} \sqrt{\frac{\gamma_r}{\lambda_{\min}(\Gamma_x)}} + o_{\text{nl}} \sqrt{\frac{\lambda_{\min}(\Gamma_{\text{nl}})}{\lambda_{\min}(\Gamma_x)}} \right) + \left( 1 + c_{\text{nl}} \sqrt{\frac{\lambda_{\min}(\Gamma_{\text{nl}})}{\lambda_{\min}(\Gamma_x)}} \right) (2 p_b \lambda [u_{\max} - \|\theta_{\text{nl}}\| o_{\text{nl}}]) \right]$$

The matrix  $P_W = P_W^T > 0$  is the solution of the linear equation  $A_{\text{ref}}^T P_W + P_W A_{\text{ref}} = -Q_W$  with  $Q_W = Q_W^T > 0$  and  $q_0$  is the minimal eigenvalue of  $Q_W$ . In conditions (i) – (iii) the definitions of  $p_b \triangleq \|P_W B_p\|$ ,  $\eta \triangleq |-q_0 + 2 p_b \lambda \|K_x^*\| + \|\theta_{\text{nl}}\| c_{\text{nl}}]$ ,  $D_{\text{aw}} \geq \|K_x^* - K_{\text{aw}}^*\|$  and  $\rho \triangleq \sqrt{\frac{\lambda_{\max}(P_W)}{\lambda_{\min}(P_W)}}$  have been used, where  $\lambda_{\min}(\cdot)$  and  $\lambda_{\max}(\cdot)$  are the minimal and maximal eigenvalue, respectively.

*Proof.* In order to simplify notation in the proof, upper bounds for the estimation errors are defined as  $\tilde{K}_{x\max} > \|\tilde{K}_x\|$ ,  $\tilde{K}_{\text{awmax}} > \|\tilde{K}_{\text{aw}}\|$ ,  $\tilde{k}_{r\max} > |\tilde{k}_r|$ ,  $\tilde{\theta}_{\text{nlmax}} > \|\tilde{\theta}_{\text{nl}}\|$  and  $\tilde{k}_{\Delta\max} > |\tilde{k}_{\Delta}|$  such that an upper bound for the Lyapunov function (4.12) satisfies

$$V_{\max} = \lambda \frac{\tilde{K}_{x\max}^2}{\lambda_{\min}(\Gamma_x)} = \lambda \frac{\tilde{K}_{\text{awmax}}^2}{\lambda_{\min}(\Gamma_{\text{aw}})} = \lambda \frac{\tilde{k}_{r\max}^2}{\gamma_r} = \lambda \frac{\tilde{k}_{\Delta\max}^2}{\gamma_{\Delta}} = \lambda \frac{\tilde{\theta}_{\text{nlmax}}^2}{\lambda_{\min}(\Gamma_{\text{nl}})} > \|V\|. \quad (\text{B.4})$$

From this definition it can be deduced that

$$\begin{aligned} \tilde{K}_{\text{awmax}} &= \sqrt{\frac{\lambda_{\min}(\Gamma_{\text{aw}})}{\lambda_{\min}(\Gamma_x)}} \tilde{K}_{x\max}, & \tilde{k}_{r\max} &= \sqrt{\frac{\gamma_r}{\lambda_{\min}(\Gamma_x)}} \tilde{K}_{x\max}, \\ \tilde{\theta}_{\text{nlmax}} &= \sqrt{\frac{\lambda_{\min}(\Gamma_{\text{nl}})}{\lambda_{\min}(\Gamma_x)}} \tilde{K}_{x\max}, & \tilde{k}_{\Delta\max} &= \sqrt{\frac{\gamma_{\Delta}}{\lambda_{\min}(\Gamma_x)}} \tilde{K}_{x\max}. \end{aligned} \quad (\text{B.5})$$

The proof is divided into two parts in the following. In the first part the case of  $\Delta u = 0$  is examined, whereas in the second part the case  $\Delta u \neq 0$  is considered. In both cases the quadratic Lyapunov function candidate

$$W = x_{\text{ps}}^T P_W x_{\text{ps}} \quad (\text{B.6})$$

is chosen in order to establish boundedness of the closed-loop signals. At the end of the proof, the two separate parts are combined in order to derive conditions for stability.

Case  $\Delta u = 0$

The derivative with respect to time of (B.6) together with the closed-loop equation (4.11) results in

$$\begin{aligned} \dot{W} &= \dot{x}_{\text{ps}}^T P_W x_{\text{ps}} + x_{\text{ps}}^T P_W \dot{x}_{\text{ps}} = x_{\text{ps}}^T (A_{\text{ref}}^T P_W + P_W A_{\text{ref}}) x_{\text{ps}} \\ &+ 2 x_{\text{ps}}^T P_W \left[ B_p \lambda k_r^* r + B_p \lambda \left( \tilde{K}_x^T (x_{\text{ps}} + x_{\text{aw}}) + \tilde{k}_r r - \tilde{\theta}_{\text{nl}}^T f_{\text{nl}}(x_{\text{ps}}) - \tilde{K}_{\text{aw}}^T x_{\text{aw}} \right. \right. \\ &\left. \left. + K_x^{*\text{T}} x_{\text{aw}} - K_{\text{aw}}^{*\text{T}} x_{\text{aw}} \right) \right], \end{aligned} \quad (\text{B.7})$$

where matching conditions (2.6) and (4.7) have been used to substitute

$$B_p \lambda K_x^{*\top} x_{aw} - B_p \lambda K_{aw}^{*\top} x_{aw} = A_{\text{ref}} x_{aw} - A_{awr} x_{aw}.$$

Solving the Lyapunov equation  $A_{\text{ref}}^\top P_W + P_W A_{\text{ref}} = -Q_W$  for  $Q_W = Q_W^\top > 0$  and introduction of the definitions  $q_0 = \lambda_{\min}(Q_W)$ ,  $p_b = \|P_W B_p\|$  yields

$$\begin{aligned} \dot{W} &< -q_0 \|x_{ps}\|^2 + 2 \|x_{ps}\| p_b \lambda (|k_r^*| r_{\max} + \|K_x^* - K_{aw}^*\| \|x_{aw}\|) \\ &+ 2 \|x_{ps}\| p_b \lambda \left[ \tilde{K}_{x\max} \left( \|x_{ps}\| \left[ 1 + c_{\text{nl}} \sqrt{\frac{\lambda_{\min}(\Gamma_{\text{nl}})}{\lambda_{\min}(\Gamma_x)}} \right] + \|x_{aw}\| \left[ 1 + \sqrt{\frac{\lambda_{\min}(\Gamma_{aw})}{\lambda_{\min}(\Gamma_x)}} \right] \right. \right. \\ &\left. \left. + r_{\max} \sqrt{\frac{\gamma_r}{\lambda_{\min}(\Gamma_x)}} + o_{\text{nl}} \sqrt{\frac{\lambda_{\min}(\Gamma_{\text{nl}})}{\lambda_{\min}(\Gamma_x)}} \right) \right], \end{aligned} \quad (\text{B.8})$$

where the upper bound for the nonlinear function in (4.1) has been used. Since  $\dot{W} \leq 0$  is necessary for (B.6) to be a Lyapunov function, equation (B.8) can be rearranged to

$$\begin{aligned} \|x_{ps}\| &\left[ q_0 - 2 p_b \lambda \tilde{K}_{x\max} \left( 1 + c_{\text{nl}} \sqrt{\frac{\lambda_{\min}(\Gamma_{\text{nl}})}{\lambda_{\min}(\Gamma_x)}} \right) \right] \\ &\geq 2 p_b \lambda \left[ |k_r^*| r_{\max} + D_{aw} \|x_{aw}\| + \tilde{K}_{x\max} \left( \|x_{aw}\| \left[ 1 + \sqrt{\frac{\lambda_{\min}(\Gamma_{aw})}{\lambda_{\min}(\Gamma_x)}} \right] \right. \right. \\ &\left. \left. + r_{\max} \sqrt{\frac{\gamma_r}{\lambda_{\min}(\Gamma_x)}} + o_{\text{nl}} \sqrt{\frac{\lambda_{\min}(\Gamma_{\text{nl}})}{\lambda_{\min}(\Gamma_x)}} \right) \right], \end{aligned} \quad (\text{B.9})$$

where  $D_{aw} \triangleq \|K_x^* - K_{aw}^*\|$ . Hence it follows an upper bound for the plant state

$$\begin{aligned} \|x_{ps}\| &\geq \left( \frac{2 p_b \lambda \left[ |k_r^*| r_{\max} + D_{aw} \|x_{aw}\| + \tilde{K}_{x\max} \left( \|x_{aw}\| \left[ 1 + \sqrt{\frac{\lambda_{\min}(\Gamma_{aw})}{\lambda_{\min}(\Gamma_x)}} \right] \right) \right]}{q_0 - 2 p_b \lambda \tilde{K}_{x\max} \left( 1 + c_{\text{nl}} \sqrt{\frac{\lambda_{\min}(\Gamma_{\text{nl}})}{\lambda_{\min}(\Gamma_x)}} \right)} \right. \\ &\left. + \frac{2 p_b \lambda \tilde{K}_{x\max} \left( r_{\max} \sqrt{\frac{\gamma_r}{\lambda_{\min}(\Gamma_x)}} + o_{\text{nl}} \sqrt{\frac{\lambda_{\min}(\Gamma_{\text{nl}})}{\lambda_{\min}(\Gamma_x)}} \right)}{q_0 - 2 p_b \lambda \tilde{K}_{x\max} \left( 1 + c_{\text{nl}} \sqrt{\frac{\lambda_{\min}(\Gamma_{\text{nl}})}{\lambda_{\min}(\Gamma_x)}} \right)} \right). \end{aligned} \quad (\text{B.10})$$

The denominator of (B.10)  $q_0 - 2 p_b \lambda \tilde{K}_{x\max} \left( 1 + c_{\text{nl}} \sqrt{\frac{\lambda_{\min}(\Gamma_{\text{nl}})}{\lambda_{\min}(\Gamma_x)}} \right)$  is always positive as it is shown at the end of the proof.

Case  $\Delta u \neq 0$

For  $\Delta u \neq 0$ , the stability analysis has to be divided into another two sub-cases, namely  $\text{sign}(u) \neq \text{sign}(x_{ps}^\top P_W B_{ps})$  and  $\text{sign}(u) = \text{sign}(x_{ps}^\top P_W B_{ps})$ .

**(1):**  $\text{sign}(u) \neq \text{sign}(x_{ps}^\top P_W B_{ps})$

A representation of the closed-loop is derived by adding and subtracting the term  $B_p \lambda K_x^{*T} x_p$  to the plant model  $G_{nl,s}$ , which yields

$$\dot{x}_{ps} = A_{\text{ref}} x_{ps} + B_p \lambda u_{\text{max}} \text{sign}(u) - B_p \lambda K_x^{*T} x_p + B_p \lambda \theta_{nl}^T f_{nl}(x_{ps}). \quad (\text{B.11})$$

The derivative of the Lyapunov equation  $W$  with respect to time then becomes

$$\begin{aligned} \dot{W} &= -x_{ps}^T Q_W x_{ps} + 2 x_{ps}^T P_W B_p \lambda u_{\text{max}} \text{sign}(u) - 2 x_{ps}^T P_W B_p \lambda \left( K_x^{*T} x_{ps} - \theta_{nl}^T f_{nl}(x_{ps}) \right) \\ &\leq -q_0 \|x_{ps}\|^2 - 2 \|x_{ps}\| p_b \lambda u_{\text{max}} + 2 \|x_{ps}\| p_b \lambda (\|K_x^*\| \|x_{ps}\| + \|\theta_{nl}\| (o_{nl} + c_{nl} \|x_{ps}\|)) \\ &\leq \|x_{ps}\|^2 | -q_0 + 2 p_b \lambda \|K_x^*\| + \|\theta_{nl}\| c_{nl} | - 2 \|x_{ps}\| p_b \lambda (u_{\text{max}} - \|\theta_{nl}\| o_{nl}) . \end{aligned} \quad (\text{B.12})$$

This leads to an upper bound

$$\|x_{ps}\| \leq \frac{2 p_b \lambda (u_{\text{max}} - \|\theta_{nl}\| o_{nl})}{| -q_0 + 2 p_b \lambda \|K_x^*\| + \|\theta_{nl}\| c_{nl} |} \quad (\text{B.13})$$

for the plant state to establish  $\dot{W} \leq 0$ .

**(2):**  $\text{sign}(u) = \text{sign}(x_{ps}^T P_W B_p)$

In this case, the fact that  $\text{sign}(u) = \text{sign}(x_{ps}^T P_W B_p)$  leads to

$$\dot{W} = -x_{ps}^T Q_W x_{ps} + 2 |x_{ps}^T P_W B_p| \lambda u_{\text{max}} - 2 x_{ps}^T P_W B_p \lambda \left( K_x^{*T} x_{ps} - \theta_{nl}^T f_{nl}(x_{ps}) \right) \quad (\text{B.14})$$

Since the case  $\Delta u \neq 0$  is considered, which is equivalent to  $|u| > u_{\text{max}}$ , the inequality

$$\begin{aligned} |x_{ps}^T P_W B_p| \lambda u_{\text{max}} &= x_{ps}^T P_W B_p \text{sign}(x_{ps}^T P_W B_p) \lambda u_{\text{max}} \\ &< x_{ps}^T P_W B_p \text{sign}(x_{ps}^T P_W B_p) \lambda |u| \end{aligned}$$

is true and

$$x_{ps}^T P_W B_p \text{sign}(x_{ps}^T P_W B_p) \lambda |u| = x_{ps}^T P_W B_p \lambda u$$

leads to

$$\begin{aligned} \dot{W} &< -x_{ps}^T Q_W x_{ps} + 2 x_{ps}^T P_W B_p \lambda \left( K_x^T (x_{ps} + x_{aw}) + k_r r - K_{aw}^T x_{aw} - \hat{\theta}_{nl}^T f_{nl}(x_{ps}) \right) \\ &\quad - 2 x_{ps}^T P_W B_p \lambda \left( K_x^* x_{ps} - \theta_{nl}^T f_{nl}(x_{ps}) \right) \\ &= -x_{ps}^T Q_W x_{ps} + 2 x_{ps}^T P_W B_p \lambda \left( \tilde{K}_x^T x_{ps} + K_x x_{aw} + k_r r - K_{aw} x_{aw} - \hat{\theta}_{nl} f(x_{ps}) \right) \end{aligned} \quad (\text{B.15})$$

Adding and subtracting  $2 x_{ps}^T P_W B_p \lambda \left( K_x^{*T} x_{aw} - K_{aw}^{*T} x_{aw} + k_r^* r \right)$  results in

$$\begin{aligned} \dot{W} &< -x_{ps}^T Q_W x_{ps} + 2 x_{ps}^T P_W \left( B_p \lambda k_r^* r + B_p \lambda \left( \tilde{K}_x^T (x_{ps} + x_{aw}) + \tilde{k}_r r - \tilde{\theta}_{nl}^T f_{nl}(x_{ps}) \right) \right. \\ &\quad \left. - \tilde{K}_{aw}^T x_{aw} + K_x^{*T} x_{aw} - K_{aw}^{*T} x_{aw} \right), \end{aligned} \quad (\text{B.16})$$

which is the same relation as for the case  $\Delta u = 0$  and hence leads to the same lower bound for the plant state.



Combination of the Cases

For the system to be stable, conditions (B.10) and (B.13) have to be satisfied, which are equivalent to

$$\begin{aligned}
& x_{\text{ps}}^{\text{T}} P_W x_{\text{ps}} \geq \\
& \lambda_{\max}(P_W) \left( \frac{2 p_b \lambda \left( |k_r^*| r_{\max} + D_{\text{aw}} \|x_{\text{aw}}\| + \tilde{K}_{x\max} \left( \|x_{\text{aw}}\| \left( 1 + \sqrt{\frac{\lambda_{\min}(\Gamma_{\text{aw}})}{\lambda_{\min}(\Gamma_x)}} \right) \right) \right)}{q_0 - 2 p_b \lambda \tilde{K}_{x\max} \left( 1 + c_{\text{nl}} \sqrt{\frac{\lambda_{\min}(\Gamma_{\text{nl}})}{\lambda_{\min}(\Gamma_x)}} \right)} \right. \\
& \left. + \frac{2 p_b \lambda \tilde{K}_{x\max} \left( r_{\max} \sqrt{\frac{\gamma_r}{\lambda_{\min}(\Gamma_x)}} + o_{\text{nl}} \sqrt{\frac{\lambda_{\min}(\Gamma_{\text{nl}})}{\lambda_{\min}(\Gamma_x)}} \right)^2}{q_0 - 2 p_b \lambda \tilde{K}_{x\max} \left( 1 + c_{\text{nl}} \sqrt{\frac{\lambda_{\min}(\Gamma_{\text{nl}})}{\lambda_{\min}(\Gamma_x)}} \right)} \right)
\end{aligned} \tag{B.17}$$

and

$$x_{\text{ps}}^{\text{T}} P_W x_{\text{ps}} \leq \lambda_{\min}(P_W) \left( \frac{2 p_b \lambda (u_{\max} - \|\theta_{\text{nl}}\| o_{\text{nl}})}{|-q_0 + 2 p_b \lambda \|K_x^*\| + \|\theta_{\text{nl}}\| c_{\text{nl}}|} \right)^2, \tag{B.18}$$

respectively.

With the definitions of  $\eta \triangleq |-q_0 + 2 p_b \lambda \|K_x^*\| + \|\theta_{\text{nl}}\| c_{\text{nl}}|$  and  $\rho \triangleq \sqrt{\frac{\lambda_{\max}(P_W)}{\lambda_{\min}(P_W)}}$  it follows

$$\begin{aligned}
& \rho \eta \left[ 2 p_b \lambda \left( |k_r^*| r_{\max} + D_{\text{aw}} \|x_{\text{aw}}\| + \tilde{K}_{x\max} \left( \|x_{\text{aw}}\| \left[ 1 + \sqrt{\frac{\lambda_{\min}(\Gamma_{\text{aw}})}{\lambda_{\min}(\Gamma_x)}} \right] \right. \right. \right. \\
& \left. \left. + r_{\max} \sqrt{\frac{\gamma_r}{\lambda_{\min}(\Gamma_x)}} + o_{\text{nl}} \sqrt{\frac{\lambda_{\min}(\Gamma_{\text{nl}})}{\lambda_{\min}(\Gamma_x)}} \right) \right] \\
& \leq q_0 [2 p_b \lambda (u_{\max} - \|\theta_{\text{nl}}\| o_{\text{nl}})] \\
& \quad - 2 p_b \lambda \tilde{K}_{x\max} \left( 1 + c_{\text{nl}} \sqrt{\frac{\lambda_{\min}(\Gamma_{\text{nl}})}{\lambda_{\min}(\Gamma_x)}} \right) [2 p_b \lambda (u_{\max} - \|\theta_{\text{nl}}\| o_{\text{nl}})]
\end{aligned} \tag{B.19}$$

Rearranging leads to

$$\begin{aligned}
& \tilde{K}_{x\max} \left[ 2 p_b \lambda \left( \rho \eta \left[ \|x_{\text{aw}}\| \left( 1 + \sqrt{\frac{\lambda_{\min}(\Gamma_{\text{aw}})}{\lambda_{\min}(\Gamma_x)}} \right) + r_{\max} \sqrt{\frac{\gamma_r}{\lambda_{\min}(\Gamma_x)}} + o_{\text{nl}} \sqrt{\frac{\lambda_{\min}(\Gamma_{\text{nl}})}{\lambda_{\min}(\Gamma_x)}} \right] \right. \right. \\
& \left. \left. + \left( 1 + c_{\text{nl}} \sqrt{\frac{\lambda_{\min}(\Gamma_{\text{nl}})}{\lambda_{\min}(\Gamma_x)}} \right) (2 p_b \lambda (u_{\max} - \|\theta_{\text{nl}}\| o_{\text{nl}})) \right) \right] \\
& \leq q_0 [2 p_b \lambda (u_{\max} - \|\theta_{\text{nl}}\| o_{\text{nl}})] - 2 p_b \lambda \rho \eta (|k_r^*| r_{\max} + D_{\text{aw}} \|x_{\text{aw}}\|),
\end{aligned}$$

and hence an upper bound

$$\tilde{K}_{x\max} \leq \frac{q_0 [2 p_b \lambda (u_{\max} - \|\theta_{\text{nl}}\| o_{\text{nl}})] - 2 p_b \lambda \rho \eta (|k_r^*| r_{\max} + D_{\text{aw}} \|x_{\text{aw}}\|)}{N_{\max}} \tag{B.20}$$

for the estimation error results, where the denominator is given by

$$N_{\max} = 2p_b \lambda \left[ \rho \eta \left( \|x_{\text{aw}}\| \left[ 1 + \sqrt{\frac{\lambda_{\min}(\Gamma_{\text{aw}})}{\lambda_{\min}(\Gamma_x)}} \right] + r_{\max} \sqrt{\frac{\gamma_r}{\lambda_{\min}(\Gamma_x)}} + o_{\text{nl}} \sqrt{\frac{\lambda_{\min}(\Gamma_{\text{nl}})}{\lambda_{\min}(\Gamma_x)}} \right) \right. \\ \left. + \left( 1 + c_{\text{nl}} \sqrt{\frac{\lambda_{\min}(\Gamma_{\text{nl}})}{\lambda_{\min}(\Gamma_x)}} \right) (2p_b \lambda [u_{\max} - \|\theta_{\text{nl}}\| o_{\text{nl}}]) \right].$$

From this maximal estimation error it directly follows that

$$2p_b \lambda \left( 1 + c_{\text{nl}} \sqrt{\frac{\lambda_{\min}(\Gamma_{\text{nl}})}{\lambda_{\min}(\Gamma_x)}} \right) \tilde{K}_{x_{\max}} (2p_b \lambda (u_{\max} - \|\theta_{\text{nl}}\| o_{\text{nl}})) \\ \leq q_0 (2p_b \lambda (u_{\max} - \|\theta_{\text{nl}}\| o_{\text{nl}})) - PT,$$

where

$$PT = \tilde{K}_{x_{\max}} 2p_b \lambda \rho \eta \left( \|x_{\text{aw}}\| \left[ 1 + \sqrt{\frac{\lambda_{\min}(\Gamma_{\text{aw}})}{\lambda_{\min}(\Gamma_x)}} \right] + r_{\max} \sqrt{\frac{\gamma_r}{\lambda_{\min}(\Gamma_x)}} + o_{\text{nl}} \sqrt{\frac{\lambda_{\min}(\Gamma_{\text{nl}})}{\lambda_{\min}(\Gamma_x)}} \right)$$

is a positive term, and hence

$$q_0 \geq 2p_b \lambda \tilde{K}_{x_{\max}} \left( 1 + c_{\text{nl}} \sqrt{\frac{\lambda_{\min}(\Gamma_{\text{nl}})}{\lambda_{\min}(\Gamma_x)}} \right),$$

which already has been presumed for (B.10).

In addition, from the definition of  $\tilde{K}_{x_{\max}}$  in (B.4) an upper bound for  $V$  can be deduced as

$$V(t_0) \leq \frac{\lambda}{\lambda_{\max}(\Gamma_x)} \tilde{K}_{x_{\max}}^2.$$

Since  $\dot{V} \leq 0$ , this is equivalent to the upper bound given in condition iii) of Theorem 4.1. In order to satisfy  $\tilde{K}_{x_{\max}} > 0$  the condition ii) in Theorem 4.1 on the reference signal  $r$  is also necessary. Based on the boundedness of  $x_{\text{ps}}$  and  $e_{\text{sat}}$ , it directly follows that  $x_{\text{refs}}$  is bounded. Summation of the dynamical system of the reference model (4.10) and the anti-windup scheme (4.9) yields

$$\dot{x}_{\text{aw}} + \dot{x}_{\text{refs}} = A_{\text{ref}} (x_{\text{aw}} + x_{\text{ref}}) + B_{\text{ref}} r,$$

which is a stable system with bounded input  $r$ . Hence,  $x_{\text{aw}} + x_{\text{refs}}$  is bounded and therefore  $x_{\text{aw}}$  is bounded. From the control law (4.8) it then follows that  $u$  is bounded.  $\square$

## B.2 Proof of Theorem 4.2

**Theorem 4.2.** *For the first order plant (4.17) with limited input amplitude, the choice of two different AMRAW parameters  $k_{\text{aw}1}^* \in \mathbb{R}$  and  $k_{\text{aw}2}^* \in \mathbb{R}$  such that*

$$a_p + b_p k_{\text{aw}1}^* = a_{\text{aw}r1} < a_p + b_p k_{\text{aw}2}^* = a_{\text{aw}r2} < a_p$$

with  $a_{awri} < 0$  for  $i = 1, 2$ , will lead to  $|x_{aw1}| \leq |x_{aw2}| \quad \forall t > t_0$  for the corresponding unwanted behaviors  $x_{awi}$ ,  $i = 1, 2$ , if

- i) the input  $u_c$  is the same for both systems,
- ii) the initial conditions fulfill  $|x_{aw1}(t_0)| \leq |x_{aw2}(t_0)|$ ,  
where  $\text{sign}(x_{aw1}(t_0)) = \text{sign}(x_{aw2}(t_0))$ ,
- iii) the unwanted behaviors  $x_{aw1}$  and  $x_{aw2}$  do not change sign.

*Proof.* In the following, the results for the dynamic of the unwanted behavior  $x_{aw}$  will be derived for

$$\dot{x}_{aw} = a_p x_{aw} + b_p \lambda \Delta u_{caw}, \quad (\text{B.21})$$

which results from equation (4.18) with

$$\Delta u_{caw} = u_c - \text{sat}(u_c - k_{aw}^* x_{aw}) \quad (\text{B.22})$$

Five different cases will be considered to proof Theorem 4.2. A graphical interpretation of these cases is shown in Figure B.1, where the possible combinations of  $u_c$  and  $u_{awp} = -k_{aw}^* x_{aw}$  are shown for a fixed sign of  $u_c$ , respectively. In the following the different cases are shortly defined and described. Furthermore, for all cases it is concluded how the unwanted behavior  $|x_{aw}|$  grows or decays.

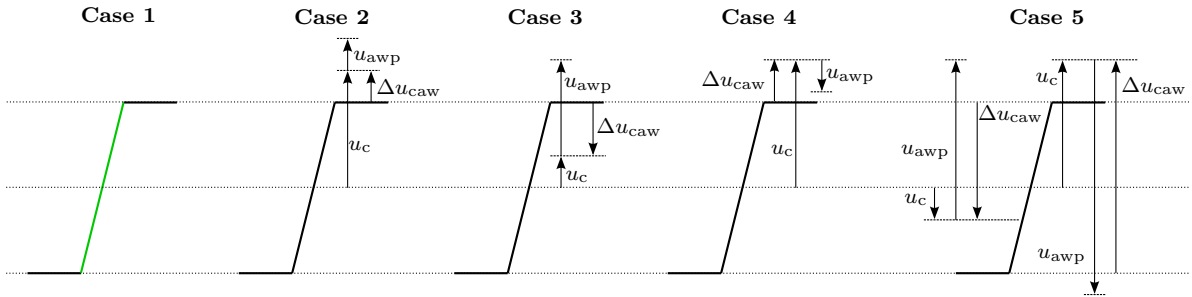


Figure B.1: Graphical interpretation of all cases that can occur for  $u_c - \text{sat}(u_c + u_{awp})$ .

### Description of the Cases:

**Case 1**  $|u_c + u_{awp}| \leq u_{\max}$ . This case includes all possible combinations of  $u_{awp}$  and  $u_c$  that does not lead to saturation.

In this case, it follows from equation (B.22) that  $\Delta u_{caw} = k_{aw}^* x_{aw}$  and therefore  $|x_{aw}|$  will decay with the desired dynamic  $a_{awr}$ .

**Case 2**  $|u_c| > u_{\max}$  and  $|u_c + u_{awp}| > u_{\max}$  where  $\text{sign}(u_c) = \text{sign}(u_{awp})$ . The sign of  $u_{awp}$  and  $u_c$  is the same in this case and the amplitude of  $u_c$  is greater than  $u_{\max}$ . Hence, the combination  $u_c + u_{awp}$  will always have the same sign as  $u_c$ , independently of the amplitude of  $u_{awp}$ .

In this case it follows that  $\text{sign}(\Delta u_{\text{caw}}) = \text{sign}(u_{\text{awp}})$  and therefore  $\text{sign}(\Delta u_{\text{caw}}) \neq \text{sign}(k_{\text{aw}}^* x_{\text{aw}})$ . Let the system stay in Case 2 throughout the time  $t_{c2}$ . Then a time-dependent fictitious gain  $k_{\text{awf}}(t_{c2})$  can be defined such that  $k_{\text{awf}}(t_{c2}) x_{\text{aw}} = \Delta u_{\text{caw}}(t_{c2})$  with  $\text{sign}(k_{\text{awf}}) \neq \text{sign}(k_{\text{aw}}^*)$ . From equation (B.21) it can be seen that

$$\dot{x}_{\text{aw}} = a_{\text{p}} x_{\text{aw}} + b_{\text{p}} \lambda k_{\text{awf}}(t_{c2}) x_{\text{aw}}$$

with

$$a_{\text{p}} + b_{\text{p}} \lambda k_{\text{awf}}(t_{c2}) > a_{\text{p}}$$

For a stable system, this can lead to a slower decay than in Case 1 or even a growth of the unwanted behavior. For an unstable system  $|x_{\text{aw}}|$  will grow.

**Case 3**  $|u_{\text{c}}| < u_{\text{max}}$  and  $|u_{\text{c}} + u_{\text{awp}}| > u_{\text{max}}$  where  $\text{sign}(u_{\text{c}}) = \text{sign}(u_{\text{awp}})$ . That means, the amplitude of  $u_{\text{c}}$  is smaller than  $u_{\text{max}}$  and the combination  $u_{\text{c}} + u_{\text{awp}}$  will always have the same sign as  $u_{\text{c}}$ , independently of the amplitude of  $u_{\text{awp}}$ . In contrast to Case 2, the amplitude of  $u_{\text{awp}}$  is not arbitrary but has to be greater than  $u_{\text{max}} - |u_{\text{c}}|$ .

In this case it follows that  $\text{sign}(u_{\text{awp}}) \neq \text{sign}(\Delta u_{\text{caw}})$  and hence

$$\text{sign}(\Delta u_{\text{caw}}) = \text{sign}(k_{\text{aw}}^* x_{\text{aw}}).$$

It can also be deduced, that  $|u_{\text{c}}| + |\Delta u_{\text{caw}}| < |u_{\text{c}}| + |u_{\text{awp}}|$  and therefore  $|\Delta u_{\text{caw}}| < |u_{\text{awp}}|$ . It follows that a time-dependent fictitious gain  $k_{\text{awf}}(t_{c3})$  can be found for the time  $t_{c3}$  the system stays in Case 3, such that  $k_{\text{awf}}(t_{c3}) x_{\text{aw}} = \Delta u_{\text{caw}}(t_{c3})$  with  $\text{sign}(k_{\text{awf}}(t_{c3})) = \text{sign}(k_{\text{aw}}^*)$  and  $|k_{\text{awf}}(t_{c3})| < |k_{\text{aw}}^*|$ . That means that  $a_{\text{p}} + b_{\text{p}} k_{\text{awf}}(t_{c3}) > a_{\text{awr}}$  but  $a_{\text{p}} + b_{\text{p}} k_{\text{awf}}(t_{c3}) < a_{\text{p}}$ . For a stable system, this will lead to a slower decay of the unwanted behavior than in Case 1. For an unstable system, it can lead to a slower decay than in Case 1 or even a growth of the unwanted behavior.

**Case 4**  $|u_{\text{c}}| > u_{\text{max}}$  and  $|u_{\text{c}} + u_{\text{awp}}| > u_{\text{max}}$  where  $\text{sign}(u_{\text{c}}) \neq \text{sign}(u_{\text{awp}})$  and  $|u_{\text{c}}| > |k_{\text{awi}}^* x_{\text{aw}}|$ . The first possibility of different signs of  $u_{\text{c}}$  and  $u_{\text{awp}}$  is described in this case. The amplitude of  $u_{\text{c}}$  is greater than  $u_{\text{max}}$  and the amplitude of  $u_{\text{awp}}$  is not high enough for the system to be in Case 1 or Case 5.

In this case it can be derived that  $|\Delta u_{\text{caw}}| > |u_{\text{awp}}|$  and  $\text{sign}(u_{\text{awp}}) \neq \text{sign}(\Delta u_{\text{caw}})$ . Let the system stay in Case 4 throughout the time  $t_{c4}$ . Then a time-dependent fictitious gain  $k_{\text{awf}}(t_{c4})$  can be found such that  $k_{\text{awf}}(t_{c4}) x_{\text{aw}} = \Delta u_{\text{caw}}(t_{c4})$  with  $|k_{\text{awf}}(t_{c4})| > |k_{\text{aw}}^*|$  and  $\text{sign}(k_{\text{awf}}) = \text{sign}(k_{\text{aw}}^*)$ . Therefore it can be derived that  $a_{\text{p}} + b_{\text{p}} k_{\text{awf}}(t_{c4}) < a_{\text{awr}}$  and the decay of  $|x_{\text{aw}}|$  is faster than in Case 1.

**Case 5**  $|u_{\text{c}} + u_{\text{awp}}| > u_{\text{max}}$  where  $\text{sign}(u_{\text{c}}) \neq \text{sign}(u_{\text{awp}})$  and  $|u_{\text{c}}| < |u_{\text{awp}}|$ . There are no restrictions for the amplitude of  $u_{\text{c}}$  in this case. In contrast to Case 4, the amplitude of  $u_{\text{awp}}$  is high enough to bring the input  $u_{\text{c}} + u_{\text{awp}}$  in the saturation with the opposite sign of  $u_{\text{c}}$ .

It directly follows from the definition of this case, that

$$|\Delta u_{\text{caw}}| < |u_{\text{awp}}| \quad \text{and} \quad \text{sign}(u_{\text{awp}}) \neq \text{sign}(\Delta u_{\text{caw}}).$$

Hence a time-dependent fictitious gain  $k_{\text{awf}}(t_{\text{c5}})$  with  $|k_{\text{awf}}(t_{\text{c5}})| < |k_{\text{aw}}^*|$  can be found, such that  $k_{\text{awf}}(t_{\text{c5}}) x_{\text{aw}} = \Delta u_{\text{caw}}(t_{\text{c5}})$  and  $a_{\text{p}} + b_{\text{p}} k_{\text{awf}}(t_{\text{c5}}) > a_{\text{awr}}$  and  $a_{\text{p}} + b_{\text{p}} k_{\text{awf}}^*(t_{\text{c5}}) < a_{\text{p}}$ . For a stable system, this will lead to a slower decay of the unwanted behavior than in Case 1. For an unstable system, the unwanted behavior can even grow.

The five cases above describe all possible combinations of  $u_{\text{c}} + u_{\text{awp}}$ . The different cases differentiate between  $|u_{\text{c}} + u_{\text{awp}}| < u_{\text{max}}$  and  $|u_{\text{c}} + u_{\text{awp}}| > u_{\text{max}}$  with the same and different signs of  $u_{\text{c}}$  and  $u_{\text{awp}}$ . This is summarized in the following:

$$|u_{\text{awp}} + u_{\text{c}}| \leq u_{\text{max}}$$

All possible combination of  $u_{\text{c}}$  and  $u_{\text{awp}}$  that lead to a smaller amplitude than  $u_{\text{max}}$  are described by Case 1.

$$|u_{\text{c}} + u_{\text{awp}}| > u_{\text{max}} \quad \text{and} \quad \text{sign}(u_{\text{awp}}) = \text{sign}(u_{\text{c}})$$

All possible combinations of  $u_{\text{c}}$  and  $u_{\text{awp}}$  with the same sign that lead to a higher amplitude than  $u_{\text{max}}$  are described by Case 2 for  $|u_{\text{c}}| > u_{\text{max}}$  and Case 3 for  $|u_{\text{c}}| \leq u_{\text{max}}$ .

$$|u_{\text{c}} + u_{\text{awp}}| > u_{\text{max}} \quad \text{and} \quad \text{sign}(u_{\text{awp}}) \neq \text{sign}(u_{\text{c}})$$

All possible combinations of  $u_{\text{c}}$  and  $u_{\text{awp}}$  with different sign that lead to a higher amplitude than  $u_{\text{max}}$  are described by Case 4 for  $|u_{\text{c}}| > |u_{\text{awp}}|$  and Case 5 for  $|u_{\text{c}}| \leq |u_{\text{awp}}|$ .

### Comparison of two systems:

In the next step of the proof, it is assumed that the system with  $k_{\text{aw}}^* = k_{\text{aw2}}^*$ , called  $G_{\text{aw2}}$  in the following, is in one of the five possible cases. For  $x_{\text{aw1}} = x_{\text{aw2}} = x_{\text{aw}}$  it is examined, which cases are possible for the system  $G_{\text{aw1}}$  with  $k_{\text{aw}}^* = k_{\text{aw1}}^*$ . In addition, the signals  $u_{\text{awp1}} = -k_{\text{aw1}}^* x_{\text{aw1}}$  and  $u_{\text{awp2}} = -k_{\text{aw2}}^* x_{\text{aw,2}}$  as well as  $\Delta u_{\text{caw1}}$  and  $\Delta u_{\text{caw2}}$  are used for the respective systems.

#### **$G_{\text{aw2}}$ in Case 1:**

System  $G_{\text{aw1}}$  can not be in Case 2 or Case 4:

Assume  $G_{\text{aw1}}$  to be in Case 2. Then  $|u_{\text{c}}| > u_{\text{max}}$  has to be true. Hence, for  $G_{\text{aw2}}$  to be in Case 1, an opposite sign of  $u_{\text{c}}$  and  $u_{\text{awp2}}$  is necessary. Since  $\text{sign}(k_{\text{aw1}}^*) = \text{sign}(k_{\text{aw2}}^*)$  this contradicts the assumption of  $G_{\text{aw1}}$  to be in Case 2. Hence,  $G_{\text{aw1}}$  can not be in Case 2.

Assume  $G_{aw1}$  to be in Case 4. For  $G_{aw1}$  it is then necessary that  $|u_c + u_{awp}| = |u_c| - |k_{aw1}^* x_{aw}| > u_{max}$  and  $|u_c| > u_{max}$ . Since  $\text{sign}(k_{aw1}^*) = \text{sign}(k_{aw2}^*)$  and  $|k_{aw2}^*| < |k_{aw1}^*|$  it follows that  $|u_c + u_{awp2}| = |u_c| - |k_{aw2}^* x_{aw}| > u_{max}$ . Therefore  $|u_c| - |k_{aw2}^* x_{aw}| \leq u_{max}$  for system  $G_{aw2}$  is not possible, which means that  $G_{aw1}$  can not be in Case 4.

Conclusion for  $G_{aw1}$  in Case 1, Case 3 or Case 5:

If  $G_{aw1}$  is in Case 1, it directly follows that  $|x_{aw1}|$  will decay faster than  $|x_{aw2}|$ .

If  $G_{aw1}$  is in Case 3, then a gain  $k_{awf1}(t_{c3})$  can be found such that  $k_{awf1}(t_{c3}) x_{aw} = \Delta u_{caw1}$ . It follows that  $|u_c| + |\Delta u_{caw1}| = u_{max}$  and therefore by definition of Case 1 and the fact that  $\text{sign}(k_{awf1}(t_{c3})) = \text{sign}(k_{aw2}^*)$  it results  $|k_{awf1}(t_{c3})| \geq |k_{aw2}^*|$ . Since  $k_{aw2}^*$  is chosen such that  $G_{aw2}$  is stable, the unwanted behavior of both systems will decay, but  $|x_{aw1}|$  will decay at least at the same rate as  $|x_{aw2}|$ .

If  $G_{aw1}$  is in Case 5, the same arguments as for Case 3 can be used.

### $G_{aw2}$ in Case 2:

The signal  $|u_c| > u_{max}$  is the same for both examined systems. It is known that  $\text{sign}(k_{aw1}^* x_{aw}) = \text{sign}(k_{aw2}^* x_{aw})$  and  $|k_{aw1}^*| > |k_{aw2}^*|$ . Therefore it can be seen that  $|u_c + u_{awp1}| > |u_c + u_{awp2}| > u_{max}$ , which shows that it is only possible for  $G_{aw1}$  to also be in Case 2. That means that the unwanted behavior of both systems will decay or grow at the same rate.

### $G_{aw2}$ in Case 3:

The signal  $|u_c| < u_{max}$  is the same for both examined systems, and from Theorem 4.2 it is known that  $\text{sign}(k_{aw1}^* x_{aw}) = \text{sign}(k_{aw2}^* x_{aw})$  and  $|k_{aw1}^*| > |k_{aw2}^*|$ . Therefore it can be seen that  $|u_c + u_{awp1}| > |u_c + u_{awp2}| > u_{max}$  and it is only possible for  $G_{aw1}$  to also be in Case 3. Since  $|\Delta u_{caw}|$  is the same for both systems, the same fictitious gain  $k_{awf}(t_{c3})$  can be found for them. Therefore both systems will decay or grow at the same rate.

### $G_{aw2}$ in Case 4:

For system  $G_{aw1}$  it is only possible to be in Case 1, Case 4, or in Case 5. These are the only cases where  $\text{sign}(u_c) \neq \text{sign}(u_{awpi})$  for  $i = 1, 2$  is possible.

If both systems are in Case 4, the unwanted behavior will decay for both systems at the same rate, since an identical fictitious gain for both systems can be found.

If system  $G_{aw1}$  is in Case 1, it follows that  $|u_{awp1}| \geq |\Delta u_{caw2}|$ . Hence, it results  $|k_{awf2}| \leq |k_{aw1}^*|$ , while both gains have the same sign. Therefore the unwanted behavior of system  $G_{aw1}$  will decay at least at the same rate as  $|x_{aw2}|$ .

If system  $G_{aw1}$  is in Case 5 the fact that  $u_c > u_{max}$  allows the conclusion that  $|\Delta u_{caw1}| > |\Delta u_{caw2}|$  with  $\text{sign}(\Delta u_{caw1}) = \text{sign}(\Delta u_{caw2})$ . This results in  $|k_{awf1}| > |k_{awf2}|$  for the fictitious gains of the systems. Therefore the decay of  $|x_{aw1}|$  is faster than that of  $|x_{aw2}|$ .

**$G_{aw2}$  in Case 5:**

If system  $G_{aw2}$  is in Case 5, it is known that  $\text{sign}(u_c) \neq \text{sign}(u_{awp2})$ . Hence, system  $G_{aw1}$  can not be in Cases 1-3, because  $\text{sign}(k_{aw1}^*) = \text{sign}(k_{aw2}^*)$ . Assuming  $G_{aw1}$  to be in Case 4 leads to the requirement  $|u_c| > |u_{\max}|$ . For this case it follows that  $|k_{aw2} x_{aw}| > |u_c|$ , which indicates  $|k_{aw2} x_{aw}| > |u_c|$ , since  $|k_{aw1}| > |k_{aw2}|$ . However, this contradicts the assumption of  $G_{aw1}$  being in Case 4. Hence, system  $G_{aw1}$  can only be in Case 5. In that case for both systems the same fictitious gain  $k_{awf1} = k_{awf2}$  can be found. Therefore the unwanted behavior for both systems will decay or grow at the same rate.

It has been shown that  $|x_{aw1}|$  will at most grow and at least decay at the same rate as  $|x_{aw2}|$  for all possible cases of  $G_{aw2}$ . Since the cases describe all possible dynamics of the system and it is guaranteed that  $x_{aw}$  does not change sign, it can be established that  $|x_{aw1}| \leq |x_{aw2}| \forall t > t_0$ .  $\square$

**B.3 Second Part of Proof of Theorem 4.3**

In Section 4.2 the method of adaptive model recovery anti-windup for output-feedback has been introduced. Boundedness of the plant state for the case of an open-loop stable plant has already been established in the first part of the proof. The proof of the boundedness in case of an unstable open-loop plant is done in the following. The respective theorem is repeated here for clarity.

**Theorem 4.3.** *The control law (4.27) with a bounded reference signal  $|r(t)| \leq r_{\max}(t)$  together with the parameter update laws (4.35)-(4.37) for  $n^* = 1$  or (4.40)-(4.42) for  $n^* \geq 2$  and the reference model (4.31) applied to the plant  $G_{\text{lims}}$  in (4.19) results in a bounded state of (4.21), if the plant is open-loop stable. Boundedness of the state for an unstable open-loop plant  $G_{\text{lims}}$  can be established under the following conditions:*

i) *The initial condition of the closed-loop state fulfills*

$$x_{cs}(0)^T P_W x_{cs}(0) \leq \lambda_{\min}(P_W) \left( \frac{2 p_b u_{\max}}{|-q_0 + 2 p_b \|\bar{\theta}^*\| \|C_t\|} \right)^2. \quad (\text{B.23})$$

ii) *The reference signal does not exceed*

$$r_{\max}(t) \leq \frac{u_{\max} q_0 - \rho \eta D_{aw} \|C_t\| \|x_{awc}\|}{\rho \eta |c^*|}. \quad (\text{B.24})$$

iii) *The initial values of the Lyapunov functions  $V$  in (4.38) and (4.43) fulfill*

$$\sqrt{V(t_0)} \leq \sqrt{\frac{1}{|c^*| \lambda_{\max}(\Gamma)} \left( \frac{2 p_b u_{\max} q_0 - 2 \rho \eta p_b \|c^*\| r_{\max} - 2 \rho \eta p_b D_{aw} \|C_t\| \|x_{awc}(t_0)\|}{N_{\max}} \right)} \quad (\text{B.25})$$

with

$$N_{\max} = 2 \rho \eta p_b \|C_t\| \|x_{\text{awc}}(t_0)\| \left( 1 + \frac{\lambda_{\min}(\Gamma_{\text{aw}})}{\lambda_{\min}(\Gamma)} \right) + 2 \rho \eta p_b r_{\max} + 4 p_b^2 u_{\max} \|C_t\|.$$

The matrix  $P_W = P_W^T > 0$  is the solution of the linear equation  $A_{\text{ref}}^T P_W + P_W A_{\text{ref}} = -Q_W$  with  $Q_W = Q_W^T > 0$  and  $q_0$  is the minimal eigenvalue of  $Q_W$ . In conditions (i) – (iii) the definitions of  $\bar{\theta} = [\theta_1^T \ \theta_2^T \ \theta_3^T]^T$ ,  $p_b \triangleq \|P_W B_c\|$ ,  $\eta \triangleq |2 p_b \|\bar{\theta}^*\| \|C_t\| - q_0|$ ,  $D_{\text{aw}} \geq \|(\bar{\theta}^{*\text{T}} - \theta_{\text{aw}}^{*\text{T}})\|$  and  $\rho \triangleq \sqrt{\frac{\lambda_{\max}(P_W)}{\lambda_{\min}(P_W)}}$  have been used, where  $\lambda_{\min}(\cdot)$  and  $\lambda_{\max}(\cdot)$  are the minimal and maximal eigenvalue, respectively. The matrix

$$C_t \triangleq \begin{pmatrix} 0 & I_{n-1 \times n-1} & 0 \\ 0 & 0 & I_{n-1 \times n-1} \\ C_p & 0 & 0 \end{pmatrix}$$

defines the mappings  $\bar{w} = C_t x_{\text{cs}}$  and  $w_{\text{aw}} = C_t x_{\text{awc}}$ .

*Proof.* The finite upper bounds  $\tilde{\theta}_{\max} > \|\tilde{\theta}\|$  and a bounded  $\tilde{\theta}_{\text{awmax}} > \|\tilde{\theta}_{\text{aw}}\|$  are defined such that

$$V_{\max} = \frac{1}{|c^*|} \frac{\tilde{\theta}_{\max}^2}{\lambda_{\min}(\Gamma)} = \frac{1}{|c^*|} \frac{\tilde{\theta}_{\text{awmax}}^2}{\lambda_{\min}(\Gamma_{\text{aw}})} > \|V\|, \quad (\text{B.26})$$

where  $V_{\max}$  is an upper bound for the Lyapunov equation  $\|V_1\|$  in (4.38) or  $\|V_2\|$  in (4.43). Consequently

$$\tilde{\theta}_{\text{awmax}} = \sqrt{\frac{\lambda_{\min}(\Gamma_{\text{aw}})}{\lambda_{\min}(\Gamma)}} \tilde{\theta}_{\max}. \quad (\text{B.27})$$

Since  $\tilde{c}$  is part of  $\tilde{\theta}$ , the relations

$$c = c^* + c - c^* = c^* + \tilde{c} \leq c^* + \tilde{\theta}_{\max} \leq \|c^*\| + \tilde{\theta}_{\max} \quad (\text{B.28})$$

result in an upper bound for  $c$ .

In the following, the Lyapunov function candidate  $W = x_{\text{cs}}^T P_W x_{\text{cs}}$  with positive definite  $P_W$  as the solution for Lyapunov equation  $A_{\text{refc}}^T P_W + P_W A_{\text{refc}} = -Q_W$  for a positive definite  $Q_W$  is utilized to show boundedness for all closed-loop signals. The stability analysis is divided into two parts, namely the cases  $\Delta u = 0$  and  $\Delta u \neq 0$ .

Case  $\Delta u = 0$ :

Starting with the combined open-loop system

$$\dot{x}_{\text{cs}} = A_c x_{\text{cs}} + B_c (u + \Delta u). \quad (\text{B.29})$$

from equation (4.21), adding and subtracting  $B_c (\bar{\theta}^{*\text{T}} (\bar{w}_s + w_{\text{aw}}))$ , where

$$\bar{w}_s = [w_{1s}^T \ w_{2s}^T \ y_{ps}]^T$$

yields

$$\dot{x}_{\text{cs}} = A_{\text{refc}} x_{\text{cs}} + B_c \left( u + \Delta u - \bar{\theta}^{*\text{T}} \bar{w}_{\text{us}} + \bar{\theta}^{*\text{T}} w_{\text{aw}} \right), \quad (\text{B.30})$$



with  $\bar{w}_{\text{us}} = \bar{w}_{\text{s}} + w_{\text{aw}}$ . Adding and subtracting  $B_{\text{c}} \theta_{\text{aw}}^{*\text{T}} w_{\text{aw}}$  and substitution of  $u = u_{\text{c}} - u_{\text{aw}} = \bar{\theta}^{\text{T}} \bar{w}_{\text{us}} + cr - \theta_{\text{aw}}^{\text{T}} w_{\text{aw}}$  results in

$$\begin{aligned} \dot{x}_{\text{cs}} &= A_{\text{refc}} x_{\text{cs}} + B_{\text{c}} \left( \Delta u + \tilde{\theta}^{\text{T}} \bar{w}_{\text{us}} - \tilde{\theta}_{\text{aw}}^{\text{T}} w_{\text{aw}} + \bar{\theta}^{*\text{T}} w_{\text{aw}} - \theta_{\text{aw}}^{*\text{T}} w_{\text{aw}} + cr \right) \\ &= A_{\text{refc}} x_{\text{cs}} + B_{\text{c}} \left( \Delta u + \tilde{\theta}^{\text{T}} (\bar{w} + w_{\text{aw}}) - \tilde{\theta}_{\text{aw}}^{\text{T}} w_{\text{aw}} + \bar{\theta}^{*\text{T}} w_{\text{aw}} - \theta_{\text{aw}}^{*\text{T}} w_{\text{aw}} + cr \right). \end{aligned} \quad (\text{B.31})$$

With

$$C_{\text{t}} = \begin{pmatrix} 0 & I_{n-1 \times n-1} & 0 \\ 0 & 0 & I_{n-1 \times n-1} \\ C_{\text{p}} & 0 & 0 \end{pmatrix} \quad (\text{B.32})$$

and

$$\bar{w}_{\text{s}} = \begin{pmatrix} w_{1\text{s}} \\ w_{2\text{s}} \\ y_{\text{ps}} \end{pmatrix} = C_{\text{t}} x_{\text{cs}}, \quad w_{\text{aw}} = \begin{pmatrix} w_{1\text{aw}} \\ w_{2\text{aw}} \\ y_{\text{aw}} \end{pmatrix} = C_{\text{t}} x_{\text{awc}}. \quad (\text{B.33})$$

equation (B.30) can be written as

$$\dot{x}_{\text{cs}} = A_{\text{refc}} x_{\text{cs}} + B_{\text{c}} \left( \Delta u + \tilde{\theta}^{\text{T}} C_{\text{t}} (x_{\text{cs}} + x_{\text{awc}}) - \tilde{\theta}_{\text{aw}}^{\text{T}} C_{\text{t}} x_{\text{awc}} + (\bar{\theta}^{*\text{T}} - \theta_{\text{aw}}^{*\text{T}}) C_{\text{t}} x_{\text{awc}} + cr \right). \quad (\text{B.34})$$

Therefore, the derivative of  $W$  with respect to time becomes

$$\begin{aligned} \dot{W} &= \\ &\left( A_{\text{refc}} x_{\text{cs}} + B_{\text{c}} \left( \Delta u + \tilde{\theta}^{\text{T}} C_{\text{t}} (x_{\text{cs}} + x_{\text{awc}}) - \tilde{\theta}_{\text{aw}}^{\text{T}} C_{\text{t}} x_{\text{awc}} + (\bar{\theta}^{*\text{T}} - \theta_{\text{aw}}^{*\text{T}}) C_{\text{t}} x_{\text{awc}} + cr \right) \right)^{\text{T}} P_{\text{W}} x_{\text{cs}} \\ &+ x_{\text{cs}}^{\text{T}} P_{\text{W}} \left( A_{\text{refc}} x_{\text{cs}} + B_{\text{c}} \left( \Delta u + \tilde{\theta}^{\text{T}} C_{\text{t}} (x_{\text{c}} + x_{\text{awc}}) - \tilde{\theta}_{\text{aw}}^{\text{T}} C_{\text{t}} x_{\text{awc}} + (\bar{\theta}^{*\text{T}} - \theta_{\text{aw}}^{*\text{T}}) C_{\text{t}} x_{\text{awc}} + cr \right) \right) \\ &= x_{\text{cs}}^{\text{T}} \left( A_{\text{refc}}^{\text{T}} P_{\text{W}} + P_{\text{W}} A_{\text{refc}} \right) x_{\text{cs}} \\ &+ 2 x_{\text{cs}}^{\text{T}} P_{\text{W}} B_{\text{c}} \left( \tilde{\theta}^{\text{T}} C_{\text{t}} (x_{\text{cs}} + x_{\text{awc}}) - \tilde{\theta}_{\text{aw}}^{\text{T}} C_{\text{t}} x_{\text{awc}} + (\bar{\theta}^{*\text{T}} - \theta_{\text{aw}}^{*\text{T}}) C_{\text{t}} x_{\text{awc}} + cr \right). \end{aligned} \quad (\text{B.35})$$

With the definitions  $q_0 \triangleq \lambda_{\min}(Q_{\text{W}})$ ,  $p_{\text{b}} \triangleq \|P_{\text{W}} B_{\text{c}}\|$ , and  $D_{\text{aw}} \triangleq \|\bar{\theta}^* - \theta_{\text{aw}}^*\|$ , it can be established that

$$\begin{aligned} \dot{W} &\leq -q_0 \|x_{\text{cs}}\|^2 + 2 \|x_{\text{cs}}\|^2 p_{\text{b}} \tilde{\theta}_{\text{max}} \|C_{\text{t}}\| + 2 \|x_{\text{cs}}\| p_{\text{b}} \tilde{\theta}_{\text{max}} \|C_{\text{t}}\| \|x_{\text{awc}}\| \left( 1 + \sqrt{\frac{\lambda_{\min}(\Gamma_{\text{aw}})}{\lambda_{\min}(\Gamma)}} \right) \\ &+ 2 \|x_{\text{cs}}\| p_{\text{b}} \left( \|c^*\| + \tilde{\theta}_{\text{max}} \right) r_{\text{max}} + 2 \|x_{\text{cs}}\| p_{\text{b}} D_{\text{aw}} \|C_{\text{t}}\| \|x_{\text{awc}}\|. \end{aligned} \quad (\text{B.36})$$

The state  $x_{\text{cs}}$  can be shown to be bounded if  $\dot{W} \leq 0$ . From (B.36) it follows Lyapunov stability of  $x_{\text{cs}}$  for

$$\begin{aligned} \|x_{\text{cs}}\| &\geq \frac{2 p_{\text{b}} \tilde{\theta}_{\text{max}} \|C_{\text{t}}\| \|x_{\text{awc}}\| \left( 1 + \sqrt{\frac{\lambda_{\min}(\Gamma_{\text{aw}})}{\lambda_{\min}(\Gamma)}} \right) + 2 p_{\text{b}} \left( \|c^*\| + \tilde{\theta}_{\text{max}} \right) r_{\text{max}}}{q_0 - 2 p_{\text{b}} \tilde{\theta}_{\text{max}} \|C_{\text{t}}\|} \\ &+ \frac{2 p_{\text{b}} D_{\text{aw}} \|C_{\text{t}}\| \|x_{\text{awc}}\|}{q_0 - 2 p_{\text{b}} \tilde{\theta}_{\text{max}} \|C_{\text{t}}\|} \end{aligned} \quad (\text{B.37})$$

At the end of this proof, it is shown that  $q_0 - 2p_b \tilde{\theta}_{\max} \|C_t\| > 0$  in the denominator of (B.37) is always true.

Case  $\Delta u \neq 0$ :

In this case, the system input is  $u_{\text{lim}} = u_{\max} \text{sign}(u)$  and the closed-loop system can be written as

$$\dot{x}_{\text{cs}} = A_c x_{\text{cs}} + B_c u_{\max} \text{sign}(u) + B_c \bar{\theta}^{*\text{T}} \bar{w} - B_c \bar{\theta}^{*\text{T}} \bar{w} = A_{\text{refc}} x_{\text{cs}} + B_c u_{\max} \text{sign}(u) - B_c \bar{\theta}^{*\text{T}} \bar{w}. \quad (\text{B.38})$$

For the time derivative of the Lyapunov function candidate it follows

$$\begin{aligned} \dot{W} &= x_{\text{cs}}^{\text{T}} \left( A_{\text{refc}}^{\text{T}} P_W + P_W A_{\text{refc}} \right) x_{\text{cs}} + 2 x_{\text{cs}}^{\text{T}} P_W B_c \left( u_{\max} \text{sign}(u) - \bar{\theta}^{*\text{T}} \bar{w} \right) \\ &= -x_{\text{cs}}^{\text{T}} Q_W x_{\text{cs}} - 2 x_{\text{cs}}^{\text{T}} P_W B_c \bar{\theta}^{*\text{T}} C_t x_{\text{cs}} + 2 |x_{\text{cs}}^{\text{T}} P_W B_c| u_{\max} \text{sign}(u) \text{sign}(x_{\text{cs}}^{\text{T}} P_W B_c). \end{aligned} \quad (\text{B.39})$$

Two different subcases, namely  $\text{sign}(u) = \text{sign}(x_{\text{cs}}^{\text{T}} P_W B_c)$  and  $\text{sign}(u) \neq \text{sign}(x_{\text{cs}}^{\text{T}} P_W B_c)$ , are distinguished in the following in order to establish boundedness of the closed-loop signals for the case  $\Delta u \neq 0$ .

**(1):**  $\text{sign}(u) = \text{sign}(x_{\text{cs}}^{\text{T}} P_W B_c)$ :

It follows from (B.39) that

$$\dot{W} = -x_{\text{cs}}^{\text{T}} Q_W x_{\text{cs}} - 2 x_{\text{cs}}^{\text{T}} P_W B_c \bar{\theta}^{*\text{T}} C_t x_{\text{cs}} + 2 |x_{\text{cs}}^{\text{T}} P_W B_c| u_{\max}. \quad (\text{B.40})$$

Since  $\Delta u \neq 0$  it follows that  $u_{\max} < |u|$  and hence  $|x_{\text{cs}}^{\text{T}} P_W B_c| u_{\max} \leq x_{\text{cs}}^{\text{T}} P_W B_c u$ , which leads to

$$\dot{W} \leq -x_{\text{cs}}^{\text{T}} Q_W x_{\text{cs}} - 2 x_{\text{cs}}^{\text{T}} P_W B_c \bar{\theta}^{*\text{T}} C_t x_{\text{cs}} + 2 x_{\text{cs}}^{\text{T}} P_W B_c u. \quad (\text{B.41})$$

Substitution of the control law

$$\begin{aligned} u &= u_c - u_{\text{aw}} = \bar{\theta}^{\text{T}} C_t (x_{\text{cs}} + x_{\text{awc}}) + c r - \theta_{\text{aw}}^{\text{T}} C_t x_{\text{awc}} \\ &= \bar{\theta}^{*\text{T}} C_t x_{\text{cs}} + \tilde{\theta}^{\text{T}} C_t x_{\text{cs}} + \bar{\theta}^{*\text{T}} C_t x_{\text{awc}} + \tilde{\theta}^{\text{T}} C_t x_{\text{awc}} + c r - \theta_{\text{aw}}^{*\text{T}} C_t x_{\text{awc}} - \tilde{\theta}_{\text{aw}}^{\text{T}} C_t x_{\text{awc}} \end{aligned}$$

in (B.41) yields

$$\begin{aligned} \dot{W} &\leq -x_{\text{cs}}^{\text{T}} Q_W x_{\text{cs}} - 2 x_{\text{cs}}^{\text{T}} P_W B_c \bar{\theta}^{*\text{T}} C_t x_{\text{cs}} \\ &\quad + 2 x_{\text{cs}}^{\text{T}} P_W B_c \left( \bar{\theta}^{*\text{T}} C_t x_{\text{cs}} + \tilde{\theta}^{\text{T}} C_t x_{\text{cs}} + \bar{\theta}^{*\text{T}} C_t x_{\text{awc}} \right. \\ &\quad \left. + \tilde{\theta}^{\text{T}} C_t x_{\text{awc}} + c r - \theta_{\text{aw}}^{*\text{T}} C_t x_{\text{awc}} - \tilde{\theta}_{\text{aw}}^{\text{T}} C_t x_{\text{awc}} \right) \\ &= -x_{\text{cs}}^{\text{T}} Q_W x_{\text{cs}} \\ &\quad + 2 x_{\text{cs}}^{\text{T}} P_W B_c \left( \tilde{\theta}^{\text{T}} C_t (x_{\text{cs}} + x_{\text{awc}}) - \tilde{\theta}_{\text{aw}}^{\text{T}} C_t x_{\text{awc}} + \left( \bar{\theta}^{*\text{T}} - \theta_{\text{aw}}^{*\text{T}} \right) C_t x_{\text{awc}} + c r \right), \end{aligned} \quad (\text{B.42})$$

which is the same as for  $\Delta u = 0$ . Hence  $\dot{W} \leq 0$  if (B.37) is true.

**(2):**  $\text{sign}(u) \neq \text{sign}(x_{\text{cs}}^{\text{T}} P_W B_c)$ :

In this case, the time derivative of  $W$  becomes

$$\begin{aligned} \dot{W} &\leq -x_{\text{cs}}^{\text{T}} Q x_{\text{cs}} - 2 x_{\text{cs}}^{\text{T}} P_W B_c \bar{\theta}^{*\text{T}} C_t x_{\text{cs}} - 2 |x_{\text{cs}}^{\text{T}} P_W B_c| u_{\max} \\ &\leq -x_{\text{cs}}^{\text{T}} Q x_{\text{cs}} + 2 |x_{\text{cs}}^{\text{T}} P_W B_c| \|\bar{\theta}^{*\text{T}} C_t x_{\text{cs}}\| - 2 |x_{\text{cs}}^{\text{T}} P_W B_c| u_{\max}. \end{aligned} \quad (\text{B.43})$$

If  $\|\bar{\theta}^{*\text{T}} C_t x_{\text{cs}}\| \leq u_{\text{max}}$  then  $\dot{W} \leq 0$ , which proves boundedness of  $x_{\text{cs}}$ .  
For  $\|\bar{\theta}^{*\text{T}} C_t x_{\text{cs}}\| > u_{\text{max}}$  the equation (B.43) is rewritten as

$$\dot{W} \leq -x_{\text{cs}}^{\text{T}} Q x_{\text{cs}} + 2 \|x_{\text{cs}}\| p_b \left( \|x_{\text{cs}}\| \|\bar{\theta}^*\| \|C_t\| - u_{\text{max}} \right). \quad (\text{B.44})$$

A negative definite  $\dot{W}$  can, therefore, be achieved for

$$\begin{aligned} & | -q_0 + 2 p_b \|\bar{\theta}^*\| \|C_t\| \|x_{\text{cs}}\|^2 - 2 \|x_{\text{cs}}\| p_b u_{\text{max}} \leq 0 \\ \iff & \|x_{\text{cs}}\| \leq \frac{2 p_b u_{\text{max}}}{| -q_0 + 2 p_b \|\bar{\theta}^*\| \|C_t\| |}. \end{aligned} \quad (\text{B.45})$$

### Combination of the Cases

It remains to combine the above cases in order to establish stability. From equation (B.45) and (B.37) it follows

$$x_{\text{cs}}^{\text{T}} P_W x_{\text{cs}} \leq \lambda_{\min}(P_W) \left( \frac{2 p_b u_{\text{max}}}{| -q_0 + 2 p_b \|\bar{\theta}^*\| \|C_t\| |} \right)^2, \quad (\text{B.46})$$

which is condition i) in the Theorem, and

$$\begin{aligned} & x_{\text{cs}}^{\text{T}} P_W x_{\text{cs}} \geq \\ & \lambda_{\max}(P_W) \left( \frac{2 p_b \tilde{\theta}_{\max} \|C_t\| \|x_{\text{awc}}\| \left( 1 + \sqrt{\frac{\lambda_{\min}(\Gamma_{\text{aw}})}{\lambda_{\min}(\Gamma)}} \right) + 2 p_b (\|c^*\| + \tilde{\theta}_{\max}) r_{\max}}{q_0 - 2 p_b \tilde{\theta}_{\max} \|C_t\|} \right. \\ & \left. + \frac{2 p_b D_{\text{aw}} \|C_t\| \|x_{\text{awc}}\|}{q_0 - 2 p_b \tilde{\theta}_{\max} \|C_t\|} \right)^2, \end{aligned} \quad (\text{B.47})$$

respectively, which together leads to the relation

$$\begin{aligned} & \lambda_{\max}(P_W) \left( \frac{2 p_b \tilde{\theta}_{\max} \|C_t\| \|x_{\text{awc}}\| \left( 1 + \sqrt{\frac{\lambda_{\min}(\Gamma_{\text{aw}})}{\lambda_{\min}(\Gamma)}} \right) + 2 p_b (\|c^*\| + \tilde{\theta}_{\max}) r_{\max}}{q_0 - 2 p_b \tilde{\theta}_{\max} \|C_t\|} \right. \\ & \left. + \frac{2 p_b D_{\text{aw}} \|C_t\| \|x_{\text{awc}}\|}{q_0 - 2 p_b \tilde{\theta}_{\max} \|C_t\|} \right)^2 \\ & \leq \lambda_{\min}(P_W) \left( \frac{2 p_b u_{\text{max}}}{| -q + 2 p_b \|\bar{\theta}^*\| \|C_t\| |} \right)^2. \end{aligned} \quad (\text{B.48})$$

Rewriting the above inequality as

$$\begin{aligned} & 2 p_b u_{\text{max}} q_0 - 4 p_b^2 u_{\text{max}} \tilde{\theta}_{\max} \|C_t\| \\ & \geq \sqrt{\frac{\lambda_{\max}(P_W)}{\lambda_{\min}(P_W)}} \left( 2 \eta p_b \tilde{\theta}_{\max} \|C_t\| \|x_{\text{awc}}\| \left( 1 + \frac{\lambda_{\min}(\Gamma_{\text{aw}})}{\lambda_{\min}(\Gamma)} \right) + 2 \eta p_b (\|c^*\| + \tilde{\theta}_{\max}) r_{\max} \right. \\ & \left. + 2 p_b \eta D_{\text{aw}} \|C_t\| \|x_{\text{awc}}\| \right) \end{aligned} \quad (\text{B.49})$$

where  $\eta \triangleq | -q + 2p_b \|\bar{\theta}^*\| \|C_t\|$ , leads to

$$2p_b u_{\max} q_0 - 2\rho\eta p_b \|c^*\| r_{\max} - 2\rho\eta p_b D_{\text{aw}} \|C_t\| \|x_{\text{awc}}\| \geq \tilde{\theta}_{\max} \left( 2\rho\eta p_b \|C_t\| \|x_{\text{awc}}\| \left( 1 + \frac{\lambda_{\min}(\Gamma_{\text{aw}})}{\lambda_{\min}(\Gamma)} \right) + 2\rho\eta p_b r_{\max} + 4p_b^2 u_{\max} \|C_t\| \right) \quad (\text{B.50})$$

with  $\rho = \sqrt{\frac{\lambda_{\max}(P_W)}{\lambda_{\min}(P_W)}}$ . This results in an upper bound for the parameter errors

$$\tilde{\theta}_{\max} \leq \frac{2p_b u_{\max} q_0 - 2\rho\eta p_b \|c^*\| r_{\max} - 2\rho\eta p_b D_{\text{aw}} \|C_t\| \|x_{\text{awc}}\|}{2\rho\eta p_b \|C_t\| \|x_{\text{awc}}\| \left( 1 + \frac{\lambda_{\min}(\Gamma_{\text{aw}})}{\lambda_{\min}(\Gamma)} \right) + 2\rho\eta p_b r_{\max} + 4p_b^2 u_{\max} \|C_t\|}. \quad (\text{B.51})$$

and hence in a bound for the initial value of the Lyapunov function

$$\sqrt{V(t_0)} \leq \sqrt{\frac{1}{|c^*| \lambda_{\min}(\Gamma)}} \left( \frac{2p_b u_{\max} q_0 - 2\rho\eta p_b \|c^*\| r_{\max} - 2\rho\eta p_b D_{\text{aw}} \|C_t\| \|x_{\text{awc}}\|}{2\rho\eta p_b \|C_t\| \|x_{\text{awc}}\| \left( 1 + \frac{\lambda_{\min}(\Gamma_{\text{aw}})}{\lambda_{\min}(\Gamma)} \right) + 2\rho\eta p_b r_{\max} + 4p_b^2 u_{\max} \|C_t\|} \right). \quad (\text{B.52})$$

The explicit term for  $\tilde{\theta}_{\max}$  in (B.51) leads to the relation

$$2p_b u_{\max} q_0 - 2\rho\eta p_b \|c^*\| r_{\max} - 2\rho\eta p_b D_{\text{aw}} \|C_t\| \|x_{\text{aw}}\| - \tilde{\theta}_{\max} \left( 2\rho\eta p_b \|C_t\| \|x_{\text{aw}}\| \left( 1 + \frac{\lambda_{\min}(\Gamma_{\text{aw}})}{\lambda_{\min}(\Gamma)} \right) + 2\rho\eta p_b r_{\max} \right) \geq \tilde{\theta}_{\max} 4p_b^2 u_{\max} \|C_t\|$$

which is equivalent to

$$2p_b u_{\max} q_0 \geq \tilde{\theta}_{\max} 4p_b^2 u_{\max} \|C_t\|,$$

which has already been presumed for the derivation for the case  $\Delta u = 0$ .

From equation (B.51) it can be deduced that

$$2p_b u_{\max} q_0 - 2\rho\eta p_b \|c^*\| r_{\max} - 2\rho\eta p_b D_{\text{aw}} \|C_t\| \|x_{\text{awc}}\| \geq 0, \quad (\text{B.53})$$

$$r_{\max} \leq \frac{u_{\max} q_0 - \rho\eta D_{\text{aw}} \|C_t\| \|x_{\text{awc}}\|}{\rho\eta |c^*|},$$

which is condition ii) in the Theorem.

With  $x_{\text{cs}}$  bounded, it follows that  $x_{\text{ps}}$  is bounded and hence  $y_{\text{ps}}$  is bounded. For a plant with relative degree  $n^* = 1$  it follows from the Lyapunov function  $V_1$  that the state  $e_{\text{sat}}$  is bounded. Together with the bounded plant state, this leads to a bounded state  $x_{\text{refs}}$  of the reference model. Summation of the anti-windup scheme (4.29) and the reference model (4.31) leads to the stable system

$$\dot{x}_{\text{aw}} + \dot{x}_{\text{refs}} = A_{\text{ref}} (x_{\text{aw}} + x_{\text{refs}}) + B_{\text{ref}} r,$$

with the bounded input  $r$ . Hence,  $x_{\text{aw}} + x_{\text{refs}}$  is bounded and therefore  $x_{\text{aw}}$  is bounded.  $\square$

# Appendix C

## Examples: Additional Results

### Example 2.1

An additional simulation has been carried out for Example 2.1, where all the tunable MRAC parameters have been the same as for the first part of the example. In order to achieve faster adaptation of the parameters, a different reference signal has been provided. It is a combination of the repeated sequence  $r_1 = (20, 0, 10, 0)$ , where each value is hold for 2 seconds, and  $r_2 = 9 \sin(5t) + 6 \sin(8t)$ . The system response and the estimated parameters are shown in Figure C.1. The adaptation of the controller parameters is faster than in Figure 2.4 for the repeated step change of the reference signal, which is due to the stronger excitation of closed-loop system by the reference signal  $r = r_1 + r_2$  (see Remark 2.3). However, such excitation is usually not desired during normal operation of a technical system.

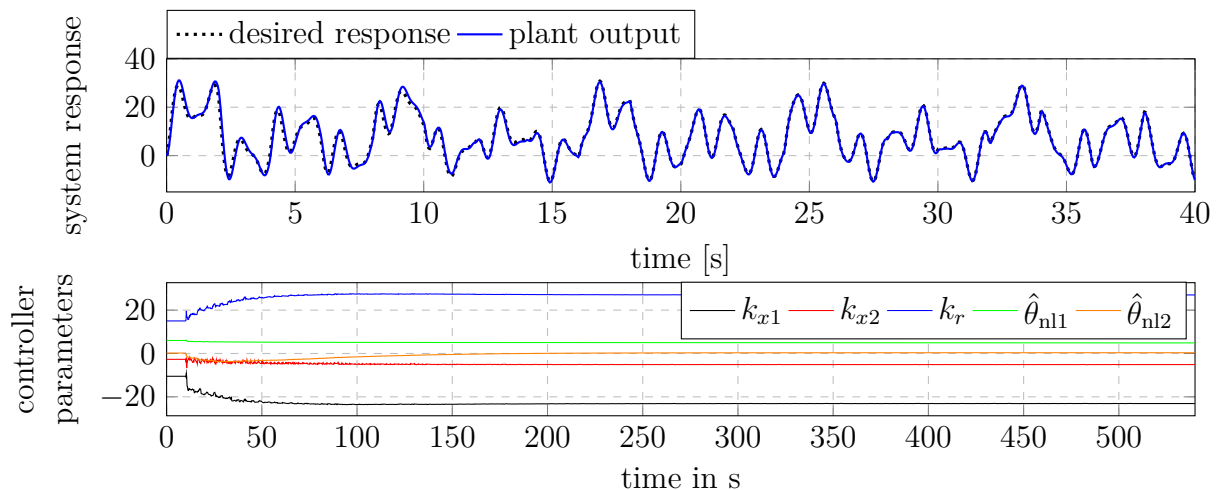


Figure C.1: Additional result of Simulation Example 2.1 for MRAC with state-feedback. First graph: System response at beginning of adaptation. Second graph: Estimations of controller parameters.

## Example 2.2

For output-feedback MRAC the same starting point as given in the introduction of Example 2.2 has been used for an additional simulation with the same reference signal as given in Appendix C. The results in Figure C.2 show that also for output-feedback MRAC adaptation of the parameters can be made faster with a reference signal that is more appropriate for parameter estimation.

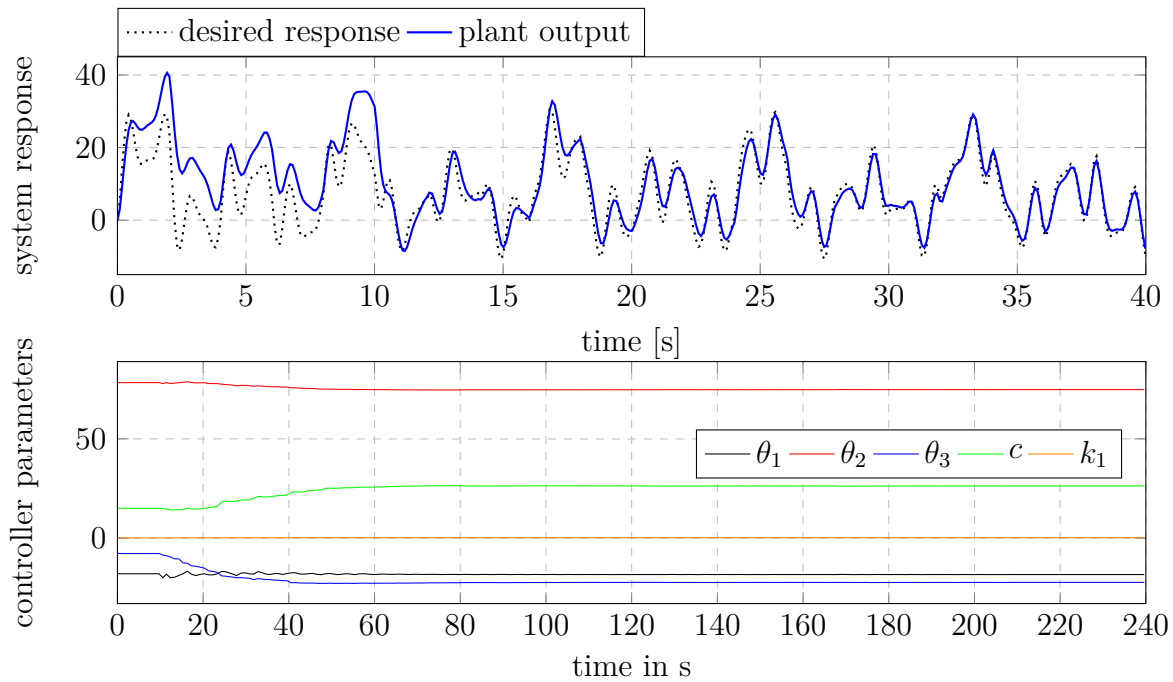


Figure C.2: Additional results of Simulation Examples 2.2 for MRAC with output-feedback. First graph: System response at beginning of adaptation. Second graph: Estimations of controller parameters.

## Example 2.3

For APPC the same starting point as given in the introduction of Example 2.3 has been used for an additional simulation with the same reference signal as given in Appendix C. The results in Figure C.3 show that for APPC, similar to the MRAC schemes before, adaptation of the parameters can be made faster with a reference signal that is more appropriate for parameter estimation.

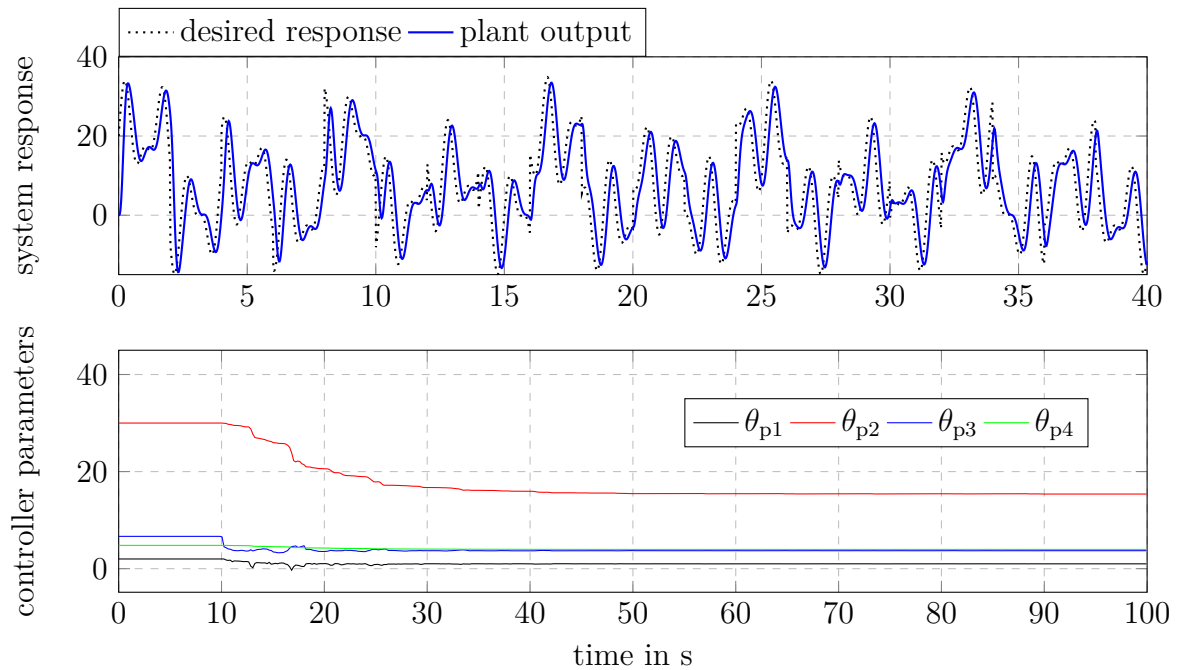


Figure C.3: Additional results of Simulation Example 2.3 for APPC. First graph: System response and controlled input at beginning of adaptation. Second graph: Estimations of controller parameters.

## Example 5.1

An additional simulation has been carried out for Example 5.1, where all the tunable AMRAW parameters have been the same as for the first part of the example. In order to achieve faster adaptation of the parameters the reference signal given in Appendix C have been used. The system response and the estimated parameters are shown in Figure C.4. It can be seen that similar to standard MRAC the stronger excitation of the closed-loop leads to faster parameter adaptation. However, the parameters do not reach their ideal values until the end of the simulation. For this example the excitation of the closed-loop is not sufficient to adapt the parameters to their ideal values in the given simulation time.

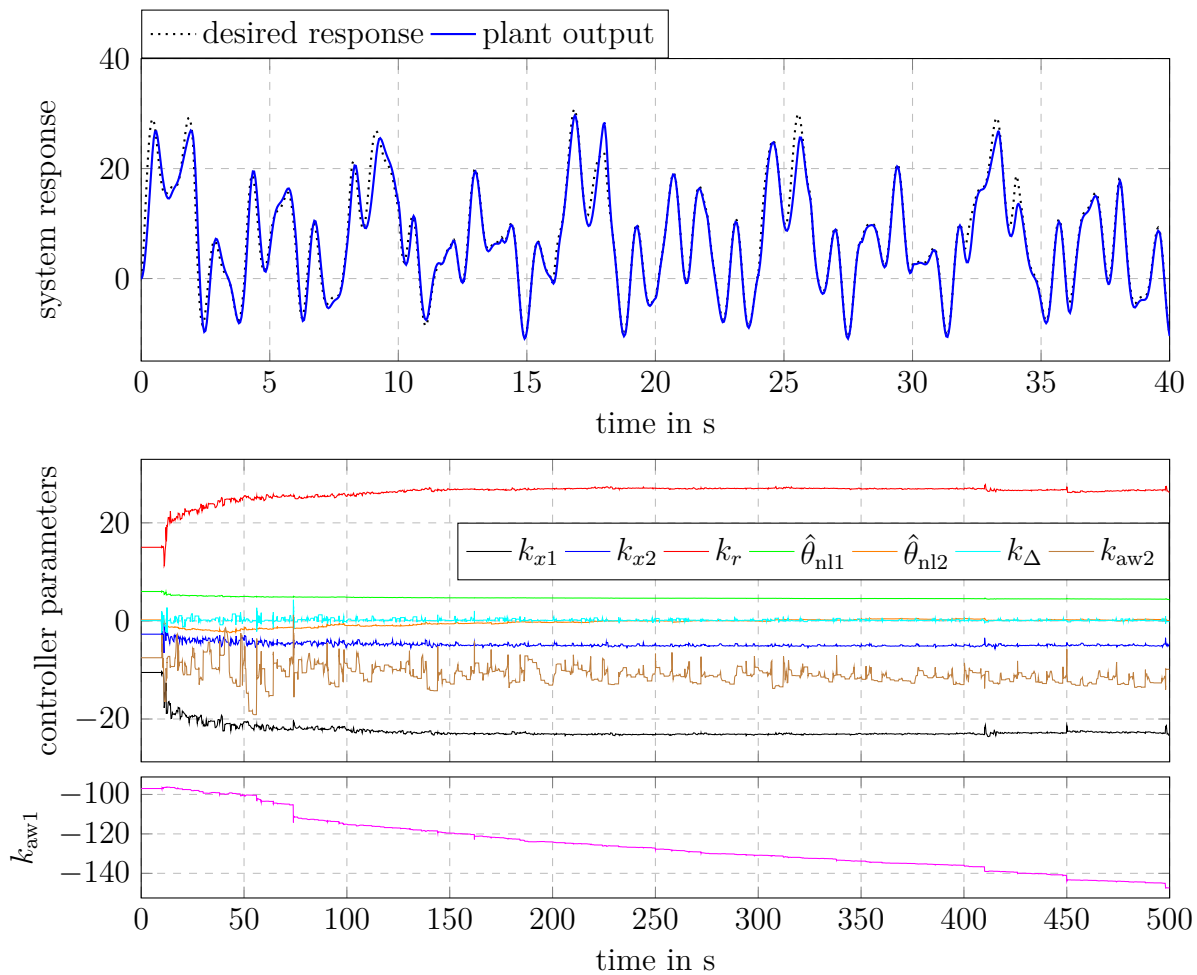


Figure C.4: Additional results of Simulation Example 5.1 for AMRAW with state-feedback. First graph: System response at beginning of adaptation. Second and third graph: Estimations of controller parameters.



## Example 5.2

An additional simulation has been carried out for Example 5.2, where all the tunable AMRAW parameters have been the same as for the first part of the example. In order to achieve faster adaptation of the parameters, the reference signal  $r = r_1 + r_2$  has been used, where the values of the repeating sequence  $r_1 = (10, 0, 5, 0)$  have been changed every two seconds and  $r_2 = 5 \sin(5t) + 3 \sin(8t)$ . The amplitudes of the reference signals have been reduced for this example in comparison to the preceding examples in order to avoid plant states where stabilization is not possible with the limited input amplitude. The results are shown in Figure C.5. It can be observed that the parameter estimation is a bit faster than for the step sequence in Figure 5.4. However, similar to the results in Appendix C, the excitation of the closed-loop is not sufficient for estimation of the ideal parameters in the given simulation time.

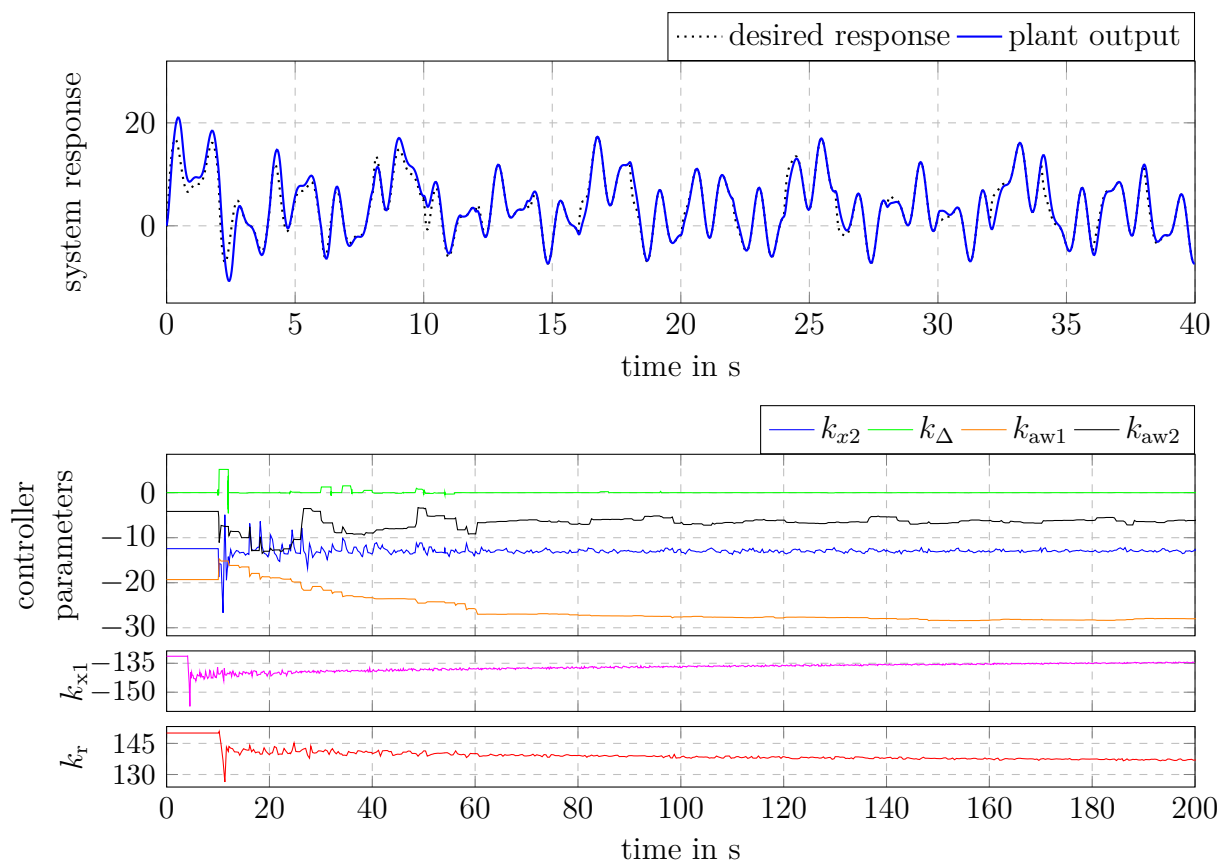


Figure C.5: Additional results of Simulation Example 5.2 for AMRAW with state-feedback for an unstable open-loop plant. First graph: System response at beginning of adaptation. Second, third and fourth graph: Estimations of controller parameters.



# List of Figures

|     |  |    |
|-----|--|----|
| 2.1 | Indirect adaptive control scheme. . . . .  | 8  |
| 2.2 | Direct adaptive control scheme: MRAC. . . . .  | 9  |
| 2.3 | Schematic representation of $G_{\text{ex1}}$ . . . . .   | 15 |
| 2.4 | Results of Simulation Example 2.1 for MRAC with state-feedback. . . . .  | 17 |
| 2.5 | Results of Simulation Example 2.2 for MRAC with output-feedback. . . . .   | 26 |
| 2.6 | Results of Simulation Example 2.3 for APPC. . . . .  | 33 |
| 2.7 | Comparison of MRAC with and without CRM. . . . .   | 36 |
| 3.1 | MRAC with ideal and constant controller parameters applied to the unstable input saturated plant $G_{\text{ex4}}$ . . . . .  | 43 |
| 3.2 | MRAC with ideal and constant controller parameters applied to the unstable input saturated plant $G_{\text{ex4}}$ , with inappropriate initial conditions for the plant state. . . . . | 44 |
| 3.3 | Comparison of simulation results for MRAC without anti-windup and with different initial conditions for the controller parameters. . . . .   | 44 |
| 3.4 | Simulation results of the parameter estimations for MRAC without anti-windup applied to $G_{\text{ex4}}$ . . . . .   | 45 |
| 3.5 | Basic structure of model recovery anti-windup. . . . .   | 47 |
| 3.6 | Simulation results for MRAC with and without KAAW applied to $G_{\text{ex4}}$ . . . . .  | 53 |
| 4.1 | Schematic illustration of the derivation of the adaptive anti-windup scheme. Note that the ideal anti-windup controller denotes the controller with ideal parameters. . . . .          | 58 |
| 4.2 | Schematic illustration of AMRAW for output-feedback plants. . . . .  | 70 |
| 5.1 | Results of Simulation Example 5.1 for KAAW and AMRAW with state-feedback before ( $t < 10\text{s}$ ) and after adaptation. . . . .   | 84 |
| 5.2 | Results of Simulation Example 5.1 for AMRAW with state-feedback, ideal controller parameters and different choices of the desired anti-windup poles. . . . .                           | 85 |

|      |   |     |
|------|---|-----|
| 5.3  | Results of the third part of Simulation Example 5.1 for KAAW and AMRAW with state-feedback before ( $t < 10$ s) and after adaptation. . . . .                 | 86  |
| 5.4  | Results of Simulation Example 5.2 for AMRAW with state-feedback before ( $t < 10$ s) and after adaptation. . . . .  | 89  |
| 5.5  | Result of Simulation Example 5.3 for KAAW and AMRAW for a first order system before ( $t < 3$ s) and after adaptation. . . . .                                | 90  |
| 5.6  | Simulation results for AMRAW for a first order system with ideal controller parameters and different choices of the desired anti-windup poles. . . . .        | 91  |
| 5.7  | Results of Simulation Example 5.4 for AMRAW with output feedback. . . . .   | 93  |
| 5.8  | Results of Simulation Example 5.4 for AMRAW with output-feedback, ideal controller parameters and different choices of the desired anti-windup poles. . . . . | 94  |
| 5.9  | Results of Simulation Example 5.5 for AMRAW with output-feedback applied to the unstable open-loop plant $G_{\text{ex4}}$ . . . . .                           | 95  |
| 5.10 | Results of Simulation Example 5.6 for indirect AMRAW with output-feedback. . . . .  | 98  |
| 5.11 | Simulation results for indirect AMRAW with output-feedback, ideal controller parameters, and different choices of the desired anti-windup poles. . . . .      | 99  |
| 5.12 | Simulation results for indirect AMRAW with output-feedback, where the input amplitude limit has been overestimated. . . . .                                   | 99  |
| 5.13 | Results of Simulation Example 5.7 for indirect AMRAW applied to the unstable open-loop plant $G_{\text{ex4}}$ . . . . .                                       | 101 |
| 6.1  | Experimental setup of the 3-DOF helicopter. . . . .   | 104 |
| 6.2  | MRAC with CRM applied to helicopter experiment. . . . .   | 107 |
| 6.3  | AMRAW with CRM applied to helicopter experiment. . . . .  | 107 |
| 6.4  | AMRAW applied to the helicopter experiment with different choices of the anti-windup poles. . . . .   | 108 |
| 6.5  | AMRAW applied to helicopter experiment with wrong initial parameters. . . . .   | 110 |
| 6.6  | AMRAW applied to helicopter experiment with changing position of mass $m_v$ . . . . .   | 111 |
| 6.7  | AMRAW applied to helicopter experiment with changing $\lambda$ and a reduction of the maximal force amplitude during operation. . . . .                       | 112 |
| 6.8  | Experimental setup of the throttle plate position control. . . . .  | 114 |
| 6.9  | Schematic structure of the throttle plate. . . . .  | 114 |
| 6.10 | Closed-loop responses of throttle plate TP1 before, during, and after adaptation. . . . .   | 119 |
| 6.11 | Closed-loop responses of throttle plate TP2 before, during, and after adaptation. . . . .   | 120 |

---

|     |   |     |
|-----|---|-----|
| B.1 | Graphical interpretation of all cases that can occur for $u_c - \text{sat}(u_c + u_{\text{awp}})$ .                 | 133 |
| C.1 | Additional result of Simulation Example 2.1 for MRAC with state-feedback.   | 143 |
| C.2 | Additional results of Simulation Example 2.2 for MRAC with output-feedback. . . . .                                 | 144 |
| C.3 | Additional results of Simulation Example 2.3 for APPC. . . . .  | 145 |
| C.4 | Additional results of Simulation Example 5.1 for AMRAW with state-feedback. . . . .                                 | 146 |
| C.5 | Additional results of Simulation Example 5.2 for AMRAW with state-feedback for an unstable open-loop plant. . . . . | 147 |

# List of Tables

- 2.1 Summary of state-feedback MRAC. . . . . 14
- 2.2 Summary of output-feedback MRAC. . . . . 23
- 2.3 Summary of the polynomial approach of output-feedback APPC with compensation of matched uncertainty. . . . . 31
  
- 4.1 Summary of AMRAW with state-feedback. . . . . 63
- 4.2 Summary of AMRAW for output-feedback. . . . . 71
- 4.3 Summary of indirect AMRAW based on the polynomial approach of APPC. 75
  
- 6.1 Plant parameters and force characteristic for helicopter benchmark experiment. . . . . 105

# Bibliography

- [1] Daniel Y. Abramovitch and Gene F. Franklin. On the stability of adaptive pole-placement controllers with a saturating actuator. *IEEE Transactions on Automatic Control*, 35(3):303–306, 1990.
- [2] Daniel Y. Abramovitch, Robert L. Kosut, and Gene F. Franklin. Adaptive control with saturating inputs. In *25th IEEE Conference on Decision and Control*, pages 848–852, 1986.
- [3] Maruthi R. Akella, John L. Junkins, and Rush D. Robinett. Structured model reference adaptive control with actuator saturation limits. In *AIAA/AAS Astrodynamics Specialist Conference and Exhibit, Boston, MA*, pages 308–315, 1998.
- [4] Liron I. Allerhand, Dieter Schwarzmann, and Jonas Missler. Performance guarantees and performance optimization of mrac for non-minimum phase systems. In *54th IEEE Annual Conference on Decision and Control*, pages 5642–5647, 2015.
- [5] Benedikt Alt, Jan P. Blath, Ferdinand Svaricek, and Matthias Schultalbers. Self-tuning control design strategy for an electronic throttle with experimental robustness analysis. In *IEEE American Control Conference*, pages 6127–6132, 2010.
- [6] Boris Andrievsky, Dimitri Peaucelle, and Alexander L. Fradkov. Adaptive control of 3DOF motion for LAAS helicopter benchmark: design and experiments. In *IEEE American Control Conference*, pages 3312–3317, 2007.
- [7] A. M. Annaswamy, E. Lavretsky, Z. T. Dydek, T. E. Gibson, and M. Matsutani. Recent results in robust adaptive flight control systems. *International Journal of Adaptive Control and Signal Processing*, 27(1-2):4–21, 2013.
- [8] A.M. Annaswamy and Jo-Ey Wong. Adaptive control in the presence of saturation non-linearity. *International Journal of Adaptive Control and Signal Processing*, 11(1):3–19, 1997.
- [9] Anuradha M. Annaswamy and S.P. Karason. Discrete-time adaptive control in the presence of input constraints. *Automatica*, 31(10):1421–1431, 1995.
- [10] S. Arimoto, S. Kawamura, and F. Miyazaki. Bettering operation of dynamic systems by learning: a new control theory for servomechanism or mechatronic system. In *Proceedings of 23rd Conference on Decision and Control*, pages 1064–1069, 1984.

- [11] Karl J. Åström and Björn Wittenmark. *Adaptive Control - Second Edition*. Prentice Hall, 1994.
- [12] K. J. Åström and B. Wittenmark. On self-tuning regulators. *Automatica*, 9:185–199, 1973.
- [13] Karl J. Åström. Theory and applications of adaptive control - a survey. *Automatica*, 19(5):471–486, 1983.
- [14] Karl J. Åström, Tore Hägglund, Chang C. Hang, and Weng K. Ho. Automatic tuning and adaptation for PID controllers-a survey. *Control Engineering Practice*, 1(4):699–714, 1993.
- [15] Corneliu Barbu, Sergio Galeani, Andrew R. Teel, and Luca Zaccarian. Non-linear anti-windup for manual flight control. *International Journal of Control*, 78(14):1111–1129, 2005.
- [16] Miroslav Barić, Ivan Petrović, and Nedjeljko Perić. Neural network-based sliding mode control of electronic throttle. *Engineering Applications of Artificial Intelligence*, 18(8):951–961, 2005.
- [17] Itzhak Barkana. Simple adaptive control—a stable direct model reference adaptive control methodology—brief survey. *International Journal of Adaptive Control and Signal Processing*, 28(7-8):567–603, 2014.
- [18] Dennis S. Bernstein and Anthony N. Michel. A chronological bibliography on saturating actuators. *International Journal of robust and nonlinear control*, 5(5):375–380, 1995.
- [19] Thomas Bierling. *Comparative Analysis of Adaptive Control Techniques for Improved Robust Performance*. PhD thesis, TU München, 2013.
- [20] Marc Bodson and William A. Pohlchuck. Command limiting in reconfigurable flight control. *Journal of Guidance, Control, and Dynamics*, 21(4):639–646, 1998.
- [21] C. Bohn and D.P. Atherton. An analysis package comparing pid anti-windup strategies. *IEEE Control Systems*, 15(2):34–40, 1995.
- [22] Mou Chen, Peng Shi, and Cheng-Chew Lim. Adaptive neural fault-tolerant control of a 3-DOF model helicopter system. *IEEE Transactions on Systems, Man, and Cybernetics: Systems*, 46(2):260–270, 2016.
- [23] Ming-Chih Chien and An-Chyau Huang. Adaptive control for flexible-joint electrically driven robot with time-varying uncertainties. *IEEE Transactions on Industrial Electronics*, 54(2):1032–1038, 2007.
- [24] Aniruddha Datta and James Ochoa. Adaptive internal model control: design and stability analysis. *Automatica*, 32(2):261–266, 1996.



- [25] J. Benton Derrick and David M. Bevly. Adaptive control of a farm tractor with varying yaw dynamics accounting for actuator dynamics and saturations. In *IEEE International Conference on Control Applications*, pages 547–552, 2008.
- [26] J. Benton Derrick, David M. Bevly, and Andrew K. Rekow. Model-reference adaptive steering control of a farm tractor with varying hitch forces. In *IEEE American Control Conference*, pages 3677–3682, 2008.
- [27] Josko Deur, Danijel Pavković, and Nedjeljko Perić. An adaptive nonlinear strategy of electronic throttle control. In *Electronic engine controls*. SAE, 2004.
- [28] Josko Deur, Danijel Pavkovic, Nedjeljko Peric, Martin Jansz, and Davor Hrovat. An electronic throttle control strategy including compensation of friction and limp-home effects. *IEEE Transactions on Industry Applications*, 40(3):821–834, 2004.
- [29] Mario Di Bernardo, Alessandro Di Gaeta, Umberto Montanaro, and Stefania Santini. Synthesis and experimental validation of the novel lq-nemcsi adaptive strategy on an electronic throttle valve. *IEEE Transactions on Control Systems Technology*, 18(6):1325–1337, 2010.
- [30] Manuel A. Duarte and Kumpati S. Narendra. Combined direct and indirect approach to adaptive control. *IEEE Transactions on Automatic Control*, 34(10):1071–1075, 1989.
- [31] Guy A. Dumont and Mihai Huzmezan. Concepts, methods and techniques in adaptive control. In *Proceedings of the 2002 American Control Conference*, pages 1137–1150, 2002.
- [32] H. Durrant-Whyte. Practical adaptive control of actuated spatial mechanisms. In *IEEE International Conference on Robotics and Automation. Proceedings*, volume 2, pages 650–655, 1985.
- [33] Zachary T. Dydek, Anuradha M. Annaswamy, and Eugene Lavretsky. Adaptive control and the nasa x-15-3 flight revisited. *IEEE Control Systems*, 30(3):32–48, 2010.
- [34] Howard Elliott, Roberto Cristi, and Manohar Das. Global stability of adaptive pole placement algorithms. *IEEE transactions on automatic control*, 30(4):348–356, 1985.
- [35] Lars Eriksson and Lars Nielsen. Non-linear model-based throttle control. Technical report, SAE Technical Paper, 2000.
- [36] Zheng Fang, Weinan Gao, and Lei Zhang. Robust adaptive integral backstepping control of a 3-DOF helicopter. *International Journal of Advanced Robotic Systems*, 9, 2012.
- [37] G. Feng, C. Zhang, and M. Palaniswami. Adaptive pole placement control subject to input amplitude constraints. In *Proceedings of the 30th IEEE Conference on Decision and Control*, pages 2493–2498, 1991.

- [38] G. Feng, C. Zhang, and M. Palaniswami. Stability analysis of input constrained continuous time indirect adaptive control. *Systems & control letters*, 17(3):209–215, 1991.
- [39] Fulvio Forni, Sergio Galeani, and Luca Zaccarian. Model recovery anti-windup for plants with rate and magnitude saturation. In *European Control Conference (2009)*, pages 324–329, 2009.
- [40] Fulvio Forni, Sergio Galeani, and Luca Zaccarian. Model recovery anti-windup for continuous-time rate and magnitude saturated linear plants. *Automatica*, 48(8):1502–1513, 2012.
- [41] A.L. Fradkov, B. Andrievsky, and D. Peaucelle. Adaptive control design and experiments for laas "helicopter" benchmark. *European Journal of Control*, 14:329–339, 2008.
- [42] Sergio Galeani, Sophie Tarbouriech, Matthew Turner, and Luca Zaccarian. A tutorial on modern anti-windup design. In *IEEE European Control Conference*, pages 306–323, 2009.
- [43] Travis E Gibson, Anuradha M Annaswamy, and Eugene Lavretsky. Closed-loop reference models for output-feedback adaptive systems. *arXiv preprint arXiv:1210.8220*, 2012.
- [44] Travis E. Gibson, Anuradha M. Annaswamy, and Eugene Lavretsky. On adaptive control with closed-loop reference models: transients, oscillations, and peaking. *IEEE Access*, 1:703–717, 2013.
- [45] Adolf Hermann Glattfelder and Walter Schaufelberger. *Control systems with input and output constraints*. Springer Science & Business Media, 2012.
- [46] Graham C. Goodwin and Kwai Sang Sin. *Adaptive filtering prediction and control*. Courier Corporation, 2014.
- [47] Goodwin, Graham C. and Ramadge, Peter J. and Caines, Peter E. Discrete-time multivariable adaptive control. *IEEE Transactions on Automatic Control*, 25, 1980.
- [48] R Grepl. *Modelling and Control of Electromechanical Servo System with High Nonlinearity*. INTECH Open Access Publisher, 2010.
- [49] Gene Grimm, Andrew R Teel, and Luca Zaccarian. Robust lmi-based linear anti-windup design: Optimizing the unconstrained response recovery. In *Decision and Control, 2002, Proceedings of the 41st IEEE Conference on*, volume 1, pages 293–298. IEEE, 2002.
- [50] Zhou Han and Kumpati S. Narendra. New concepts in adaptive control using multiple models. *IEEE Transactions on Automatic Control*, 57:78–89, 2012.

- [51] John B Heywood. *Internal combustion engine fundamentals*, volume 930. Mcgraw-hill New York, 1988.
- [52] Peter Hippe. *Windup in control: its effects and their prevention*. Springer Science & Business Media, 2006.
- [53] Heather S. Hussain, Megumi Matsutani, Anuradha M. Annaswamy, and Eugene Lavretsky. Robust adaptive control in the presence of unmodeled dynamics: A counter to rohrs counterexample. In *AIAA Guidance Navigation and Control Conference*, 2013.
- [54] Hussain, Heather S. and Annaswamy, Anuradha M. and Lavretsky, Eugene. A new approach to robust adaptive control. In *American Control Conference (ACC), 2016*, pages 3856–3861, 2016.
- [55] P. Ioannou and Konstantinos Tsakalis. A robust direct adaptive controller. *IEEE Transactions on Automatic Control*, 31(11):1033–1043, 1986.
- [56] Petros Ioannou and Baris Fidan. *Adaptive Control Tutorial*. siam, 2006.
- [57] Petros Ioannou and Gang Tao. Frequency domain conditions for strictly positive real functions. *IEEE Transactions on Automatic Control*, 32(1):53–54, 1987.
- [58] Petros A. Ioannou and Aniruddha Datta. Robust adaptive control: a unified approach. *Proceedings of the IEEE*, 79(12):1736–1768, 1991.
- [59] Petros A. Ioannou and Petar V. Kokotovic. Instability analysis and improvement of robustness of adaptive control. *Automatica*, 20(5):583–594, 1984.
- [60] Petros A. Ioannou and Jing Sun. *Robust Adaptive Control*. tapir akademisk forlag, 2003.
- [61] Rolf Isermann and Marco Münchhof. *Identification of dynamic systems: An introduction with applications*. Springer, Heidelberg and New York, 2011.
- [62] Mitsuaki Ishitobi, Masatoshi Nishi, and Kazuhide Nakasaki. Nonlinear adaptive model following control for a 3-DOF tandem-rotor model helicopter. *Control Engineering Practice*, 18(8):936–943, 2010.
- [63] Mitsuaki Ishitobi, Masatoshi Nishi, and Kazuhide Nakasaki. Nonlinear adaptive model following control for a 3-dof tandem-rotor model helicopter. *Control Engineering Practice*, 18:936–943, 2010.
- [64] S. Jagannathan and Mohammed Hameed. Adaptive force-balancing control of mems gyroscope with actuator limits. In *Proceedings of the American Control Conference*, volume 2, pages 1862–1867, 2004.
- [65] Yonghwan Jeong, Seonwook Kim, Kyongsu Yi, Sangyong Lee, and ByeongRim Jo. Design and Implementation of Parking Control Algorithm for Autonomous Valet Parking. Technical report, SAE Technical Paper, 2016.

- [66] Xiaohong Jiao, Jiangyan Zhang, and Tielong Shen. An adaptive servo control strategy for automotive electronic throttle and experimental validation. *IEEE Transactions on Industrial Electronics*, 61(11):6275–6284, 2014.
- [67] Eric N. Johnson and Anthony J. Calise. Pseudo-control hedging: a new method for adaptive control. In *Advances in navigation guidance and control technology workshop*, pages 1–23, 2000.
- [68] Eric N. Johnson and Anthony J. Calise. Neural network adaptive control of systems with input saturation. In *Proceedings of the IEEE American Control Conference*, volume 5, pages 3527–3532, 2001.
- [69] Nazli E. Kahveci, Petros Ioannou, et al. An indirect adaptive control design with anti-windup compensation: stability analysis. In *46th IEEE Conference on Decision and Control*, pages 1294–1299, 2007.
- [70] Nazli E. Kahveci and Petros A. Ioannou. Indirect adaptive control for systems with input rate saturation. In *IEEE American Control Conference*, pages 3396–3401, 2008.
- [71] Nazli E. Kahveci, Petros A. Ioannou, and Maj D. Mirmirani. A robust adaptive control design for gliders subject to actuator saturation nonlinearities. In *IEEE American Control Conference*, pages 492–497, 2007.
- [72] Nazli E. Kahveci, Petros A. Ioannou, and Maj D. Mirmirani. Adaptive lq control with anti-windup augmentation to optimize uav performance in autonomous soaring applications. *IEEE Transactions on Control Systems Technology*, 16(4):691–707, 2008.
- [73] Mitsuru Kanamori and Masayoshi Tomizuka. Model reference adaptive control of linear systems with input saturation. In *Proceedings of the 2004 IEEE International Conference on Control Applications*, volume 2, pages 1318–1323, 2004.
- [74] I.P. Kanellakopoulos, P.V. Kokotovic, and A.S. Morse. Adaptive output-feedback control of systems with output nonlinearities. *IEEE Transactions on Automatic Control*, 37(11):1666–1682, 1992.
- [75] S.P. Kárason and A.M. Annaswamy. Adaptive control in the presence of input constraints. *IEEE Transactions on Automatic Control*, 39:2325–2330, 1994.
- [76] Howard Kaufman, Itzhak Barkana, and Kenneth Sobel. *Direct Adaptive Control Algorithms*. Springer, 1998.
- [77] Hassan K Khalil. Adaptive output feedback control of nonlinear systems represented by input-output models. *IEEE Transactions on Automatic Control*, 41(2):177–188, 1996.
- [78] Hassan K. Khalil. *Nonlinear systems*. Pearson, Harlow, 3. ed., new internat. ed edition, 2014.

- [79] Ata M. Khan, Ataur Bacchus, and Stephen Erwin. Policy challenges of increasing automation in driving. *IATSS research*, 35(2):79–89, 2012.
- [80] Khedekar, Darshan C. and Truco, Amelia C. and Oteyza, Diego A. and Huer-tas, Guillermo F. Home Automation—A Fast-Expanding Market. *Thunderbird International Business Review*, 2016.
- [81] Myke King. *Process Control: A Practical Approach*. John Wiley & Sons, 2016.
- [82] P.V. Kokotovic, M. Krstic, and I. Kanellakopoulos. Backstepping to passivity: recursive design of adaptive systems. In *Proceedings of the 31st IEEE Conference on Decision and Control*, pages 3276–3280, 1992.
- [83] Gerhard Kreisselmeier. An approach to stable indirect adaptive control. *Automatica*, 21(4):425–431, 1985.
- [84] Gerhard Kreisselmeier and Brian Anderson. Robust model reference adaptive control. *IEEE Transactions on Automatic Control*, 31(2):127–133, 1986.
- [85] Miroslav Krstic, Ioannis Kanellakopoulos, and Peter V. Kokotovic. *Nonlinear and adaptive control design*. Wiley, 1995.
- [86] Matthew Kuipers and Petros A. Ioannou. Multiple model adaptive control with mixing. *IEEE Transactions on Automatic Control*, 55:1822–1836, 2010.
- [87] I.D. Landau, Reglia Lozano, M’Saad Mohammed, and Karimi Alireza. *Adaptive Control - Algorithm, Analysis and Applications*. Springer, 2011.
- [88] Yoan D. Landau. Adaptive control: The model reference approach. *IEEE Transactions on Systems, Man, and Cybernetics*, pages 169–170, 1984.
- [89] E. Lavretsky and N. Hovakimyan. Stable adaptation in the presence of input constraints. *System & Control Letters*, 55:722–729, 2007.
- [90] Eugene Lavretsky. Transients in output feedback adaptive systems with observer-like reference models. *International Journal of Adaptive Control and Signal Processing*, 29(12):1515–1525, 2015.
- [91] Eugene Lavretsky et al. Combined/composite model reference adaptive control. *IEEE Transactions on Automatic Control*, 54(11):2692, 2009.
- [92] Eugene Lavretsky and Naira Hovakimyan. Positive  $\mu$ -modification for stable adaptation in the presence of input constraints. In *Proceedings of the 2004 American Control Conference*, pages 2545–2550, 2004.
- [93] Eugene Lavretsky and Naira Hovakimyan. Positive  $\mu$ -modification for stable adaptation in dynamic inversion based adaptive control with input saturation. In *Proceedings of the 2005 American Control Conference*, pages 3373–3378, 2005.

- [94] Eugene Lavretsky and Kevin A. Wise. *Robust and Adaptive Control with Aerospace Applications*. Springer-Verlag London, 2013.
- [95] Alexander Leonessa, Wassim M. Haddad, and Tomohisa Hayakawa. Adaptive tracking for nonlinear systems with control constraints. In *Proceedings of the 2001 IEEE American Control Conference*, volume 2, pages 1292–1297, 2001.
- [96] Alexander Leonessa, Wassim M. Haddad, Tomohisa Hayakawa, and Yannick Morel. Adaptive control for nonlinear uncertain systems with actuator amplitude and rate saturation constraints. *International Journal of Adaptive Control and Signal Processing*, 23(1):73–96, 2009.
- [97] Jesse Levinson, Jake Askeland, Jan Becker, Jennifer Dolson, David Held, Soeren Kammel, J. Zico Kolter, Dirk Langer, Oliver Pink, Vaughan Pratt, et al. Towards fully autonomous driving: Systems and algorithms. In *IEEE Intelligent Vehicles Symposium (IV)*, 2011.
- [98] Lennart Ljung. *System identification: Theory for the user*. Prentice Hall PTR, 2nd ed edition, 1999.
- [99] Rogelio Lozano and Bernard Brogliato. Adaptive control of a simple nonlinear system without a priori information on the plant parameters. *IEEE Transactions on Automatic Control*, 37(1):30–37, 1992.
- [100] Jan Lunze. *Regelungstechnik*. Springer-Lehrbuch. Springer, Berlin [u.a.], 7., überarb. Aufl edition, 2013.
- [101] K.R. Meyer. On the existence of Lyapunov function for the problem of Lur’e. *Journal of the Society for Industrial and Applied Mathematics, Series A: Control*, 3(3):373–383, 1965.
- [102] Richard H. Middleton, Graham C. Goodwin, David J. Hill, and David Q. Mayne. Design issues in adaptive control. *IEEE Transactions on Automatic Control*, 33:50–58, 1988.
- [103] Middleton, R.H. and Goodwin, G.C. Adaptive computed torque control for rigid link manipulations. *Systems & Control Letters*, 10(1):9–16, 1988.
- [104] Jonas Missler, Dieter Schwarzmann, and Liron Allerhand. On the influence of filter choice in output-feedback mrac during adaptation transients. *IFAC-PapersOnLine*, 48(11):505–510, 2015.
- [105] R. Monopoli. Adaptive control for systems with hard saturation. In *Proceedings of 14th Conference on Decision and Control*, 1975.
- [106] R V. Monopoli. Model reference adaptive control with an augmented error signal. *IEEE Transactions on Automatic Control*, 19(5):474–484, 1974.

- [107] Umberto Montanaro, Alessandro di Gaeta, and Veniero Giglio. Robust discrete-time mrac with minimal controller synthesis of an electronic throttle body. *IEEE/ASME Transactions on Mechatronics*, 19(2):524–537, 2014.
- [108] A Morse. Global stability of parameter-adaptive control systems. In *18th IEEE Conference on Decision and Control including the Symposium on Adaptive Processes*, pages 1041–1045, 1979.
- [109] A. Stephen Morse. Supervisory control of families of linear set point controllers—part 1: Exact matching. *IEEE Transactions on Automatic Control*, 41:1413–1431, 1996.
- [110] A. Stephen Morse. Supervisory control of families of linear set-point controllers—part 2: Robustness. *IEEE Transactions on Automatic Control*, 42:1500–1515, 1997.
- [111] A. Stephen Morse, David Q. Mayne, and Graham C. Goodwin. Application of hysteresis switching in parameter adaptive control. *IEEE Transactions on Automatic Control*, 37:1343–1354, 1992.
- [112] K. Narendra and A. Annaswamy. Robust adaptive control in the presence of bounded disturbances. *IEEE Transactions on Automatic Control*, 31(4):306–315, 1986.
- [113] K. Narendra, Yuan-Hao Lin, and L. Valavani. Stable adaptive controller design, part ii: Proof of stability. *IEEE Transactions on Automatic Control*, 25(3):440–448, 1980.
- [114] KS Narendra and LS Valavani. Stable adaptive controller design—direct control. *IEEE Transactions on Automatic Control*, 23(4):570–583, 1978.
- [115] Kumpati S Narendra and Anuradha M. Annaswamy. Persistent excitation in adaptive systems. *International Journal of Control*, 45(1):127–160, 1987.
- [116] Kumpati S. Narendra and Anuradha M. Annaswamy. *Stable adaptive systems*. Dover Publications, Mineola, N.Y., 2005.
- [117] Kumpati S. Narendra and Zhou Han. A new approach to adaptive control using multiple models. *International Journal of Adaptive Control and Signal Processing*, 26:778–799, 2012.
- [118] Kumpati S. Narendra, Yu Wang, and Wei Chen. Extension of second level adaptation using multiple models to siso systems. In *2015 IEEE American Control Conference*, pages 171–176, 2015.
- [119] Maciej Niedźwiecki. *Identification of time-varying processes*. Wiley, Chichester and New York, 2000.
- [120] Roger D Nussbaum. Some remarks on a conjecture in parameter adaptive control. *Systems & Control Letters*, 3(5):243–246, 1983.

- [121] Marcin Odelga, Abdelhamid Chriette, and Franck Plestan. Control of 3 DOF helicopter: a novel autopilot scheme based on adaptive sliding mode control. In *2012 IEEE American Control Conference*, 2012.
- [122] Andreas Ortseifen. *Entwurf von modellbasierten Anti-Windup-Methoden für Systeme mit Stellbegrenzungen*. VDI Verlag GmbH, Düsseldorf, 2013.
- [123] Andreas Ortseifen and Jürgen Adamy. A new design method for mismatch-based anti-windup compensators: Achieving local performance and global stability in the siso case. In *IEEE American Control Conference*, 2011.
- [124] Andreas Ortseifen and Jürgen Adamy. A performance-oriented, non-iterative, local design method for mismatch-based anti-windup compensators. In *IEEE International Symposium on Computer-Aided Control System Design*, 2011.
- [125] G.A. Pajunen and Michael Steinmetz. Model reference adaptive control for exponentially convergent systems with input and output constraints. In *26th IEEE Conference on Decision and Control*, volume 26, pages 831–836, 1987.
- [126] Cesar C. Palerm and Wayne Bequette, B. Direct model reference adaptive control and saturation constraints. In *Proceedings of The 15th Triennial IFAC World Congress*, 2002.
- [127] T.J. Pallett. Electronic throttle control system including mechanism for determining desired throttle position, June 1996. US Patent 5,526,787.
- [128] Yaodong Pan, Umit Ozguner, and Oguz H. Dagci. Variable-structure control of electronic throttle valve. *IEEE Transactions on industrial electronics*, 55(11):3899–3907, 2008.
- [129] Konstantinos G Papadopoulos and Nikolaos I Margaritis. Optimal automatic tuning of active damping pid regulators. *Journal of Process Control*, 23(6):905–915, 2013.
- [130] Danijel Pavković, Joško Deur, Martin Jansz, and Nedjeljko Perić. Self-tuning control of an electronic throttle. In *Proceedings of 2003 IEEE Conference on Control Applications*, pages 149–154, 2003.
- [131] Danijel Pavković, Joško Deur, Martin Jansz, and Nedjeljko Perić. Adaptive control of automotive electronic throttle. *Control Engineering Practice*, 14(2):121–136, 2006.
- [132] Anthony N. Payne. Adaptive one-step-ahead control subject to an input-amplitude constraint. *International Journal of Control*, 43(4):1257–1269, 1986.
- [133] Dimitri Peaucelle, Boris Andrievsky, Vincent Mahout, and Alexander Fradkov. Robust simple adaptive control with relaxed passivity and PID control of a helicopter benchmark. *IFAC Proceedings Volumes*, 22(1):2315–2320, 2011.



- [134] Zheng Qu and Anuradha M. Annaswamy. Adaptive Output-Feedback Control with Closed-Loop Reference Models for Very Flexible Aircraft. *Journal of Guidance, Control, and Dynamics*, 39(4):873–888, 2015.
- [135] Zhen Ren and Guoming G. Zhu. Modeling and control of an electric variable valve timing system for SI and HCCI combustion mode transition. In *Proceedings of the 2011 American Control Conference*, pages 979–984, 2011.
- [136] Charles E. Rohrs, Lena Valavani, Athans Michael, and Stein Gunter. Robustness of continuous-time adaptive control algorithms in the presence of unmodeled dynamics. *IEEE Transactions on Automatic Control*, 30:881–889, 1985.
- [137] Carlo Rossi, Andrea Tilli, and Alberto Tonielli. Robust control of a throttle body for drive by wire operation of automotive engines. *IEEE Transactions on control systems technology*, 8(6):993–1002, 2000.
- [138] Emanuel Sachs, R-S Guo, Sungdo Ha, and Albert Hu. Process control system for vlsi fabrication. *Semiconductor Manufacturing, IEEE Transactions on*, 4:134–144, 1991.
- [139] Shankar Sastry. *Nonlinear Systems: Analysis, Stability, and Control*, volume 10 of *Interdisciplinary Applied Mathematics*. Springer New York, New York, NY, 1999.
- [140] Shankar Sastry and Marc Bodson. *Adaptive control: Stability, convergence, and robustness*. Dover books on engineering. Dover Publications, Mineola, N.Y., 2011.
- [141] H. Sato, Japan Ibaraki, T. Sueno, T. Toyama, and M. Mikawa. High accuracy magnet power supply for proton synchrotron by repetitive control. In *22nd Annual IEEE Power Electronics Specialists Conference*, 1991.
- [142] Dieter Schwarzmann. *Nonlinear Internal Model Control with Automotive Applications*. PhD thesis, Ruhr-Universität Bochum, 2007.
- [143] J. Shan, H.-T. Liu, and S. Nowotny. Synchronised trajectory-tracking control of multiple 3-dof experimental helicopters. *IEE Proceedings-Control Theory and Applications*, 152(6):683–692, 2005.
- [144] Jean-Jacques E. Slotine and Weiping Li. Composite adaptive control of robot manipulators. *Automatica*, 25(4):509–519, 1989.
- [145] Jing Sun. A modified model reference adaptive control scheme for improved transient performance. *IEEE Transactions on Automatic Control*, 38(8):1255–1259, 1993.
- [146] Kok K Tan, Qing-Guo Wang, and Chang C. Hang. *Advances in PID control*. Springer Science & Business Media, 2012.
- [147] Gang Tao. *Adaptive control design and analysis*. Wiley-Interscience, Hoboken, N.J., 2003.

- [148] Gang Tao. Multivariable adaptive control: A survey. *Automatica*, 50(11):2737–2764, 2014.
- [149] S. Tarbouriech and M. Turner. Anti windup design: an overview of some recent advances and open problems. *IET Control Theory and Application*, 3:1–19, 2009.
- [150] Sophie Tarbouriech, Germain Garcia, João Manoel Gomes da Silva Jr., and Isabelle Queinnec. Linear systems subject to control saturation-problems and modeling. In *Stability and Stabilization of Linear Systems with Saturating Actuators*, pages 3–48. Springer, 2011.
- [151] Sophie Tarbouriech, Germain Garcia, João Manoel Gomes da Silva Jr., and Isabelle Queinnec. *Stability and stabilization of linear systems with saturating actuators*. Springer Science & Business Media, 2011.
- [152] M. Thiel, D. Schwarzmann, M. Schultalbers, and T. Jeinsch. Indirect adaptive pole placement control with performance orientated anti-windup for electronic throttle plates. In *24th Mediterranean Conference on Control and Automation*, pages 461–466, 2016.
- [153] Manus Thiel, Dieter Schwarzmann, Anuradha M Annaswamy, Matthias Schultalbers, and Torsten Jeinsch. Improved performance for adaptive control of systems with input saturation. In *American Control Conference*, 2016.
- [154] Manus Thiel, Dieter Schwarzmann, Matthias Schultalbers, and Torsten Jeinsch. Adaptive model recovery anti-windup for output-feedback plants. In *Proceedings of The 20th IFAC World Congress*, accepted for publishing 2017.
- [155] Matthew C. Turner and Ian Postlethwaite. A new perspective on static and low order anti-windup synthesis. *International Journal of Control*, 77:27–44, 2004.
- [156] Sandor M. Veres and Derek Wall. *Synergy and Duality of Identification and Control*. Taylor & Francis, 2000.
- [157] Antonio Visioli. Modified anti-windup scheme for pid controllers. In *IEE Proceedings-Control Theory and Applications*, volume 150, pages 49–54. IET, 2003.
- [158] Antonio Visioli. *Practical PID control*. Springer Science & Business Media, 2006.
- [159] Hui Wang and Jing Sun. Modified model reference adaptive control with saturated input. In *Proceedings of 31st Conference on Decision and Control*, 1992.
- [160] M.H. Wassim and V.S. Chellaboina. *Nonlinear dynamical systems and control*, 2008.
- [161] H. P. Whitaker, J. Yamron, and A. Kezer. Design of model reference adaptive control systems for aircraft. Technical report, Instrumentation Laboratory, MIT, Cambridge, 1958.

- [162] Kevin A. Wise, Eugene Lavretsky, and Naira Hovakimyan. Adaptive control of flight: theory, applications, and open problems. In *American Control Conference*, pages 6–pp, 2006.
- [163] Björn Wittenmark and Karl J. Åström. Practical issues in the implementation of self-tuning control. *Automatica*, 20(5):595–605, 1984.
- [164] Wittenmark, Björn. Adaptive dual control methods: An overview. In *IFAC Symposium on Adaptive Syst. in Control and Signal Proc*, pages 67–72, 1995.
- [165] Ye Xudong, Jiang Jingping, S.D. Brierley, J.N. Chiasson, E.B. Lee, S.H. Zak, Michael A. Demetriou, and Marios M. Polycarpou. Adaptive nonlinear design without a priori knowledge of control directions. *IEEE Transactions on Automatic Control*, 1998.
- [166] Bong-Jun Yang, Anthony J. Calise, and James I. Craig. Adaptive output feedback control with input saturation. Technical report, Georgia Institute of Technology, 2003.
- [167] Cishen Zhang. Discrete-time saturation constrained adaptive pole assignment control. *IEEE Transactions on Automatic Control*, 38(8):1250–1254, 1993.
- [168] Cishen Zhang and Robin J. Evans. Amplitude constrained adaptive control. *International Journal of Control*, 46(1):53–64, 1987.
- [169] S. Zhao, J.-X. Xu, et al. Online automatic tuning of a proportional integral derivative controller based on an iterative learning control approach. *IET Control Theory & Applications*, 1(1):90–96, 2007.
- [170] Bo Zheng and Yisheng Zhong. Robust attitude regulation of a 3-DOF helicopter benchmark: theory and experiments. *IEEE transactions on industrial electronics*, 58(2):660–670, 2011.
- [171] Jing Zhou and Changyun Wen. Adaptive control of systems with input saturation. In *Adaptive Backstepping Control of Uncertain Systems*, pages 189–197. Springer, 2008.

# Theses

- The input amplitude of technical plants is always limited. Hence, input saturation is highly relevant for industrial control applications.
- Especially in systems with high performance requirements saturation of the plant input is encountered frequently and therefore plays an important role for the closed-loop behavior.
- An input saturation of the plant can not only cause a reduction of the closed-loop performance but can also lead to an unstable closed-loop system if the input of an unstable open-loop system is saturated.
- Control algorithms for industrial applications need to work for plants that can change due to aging, environmental conditions or small defects. Moreover, the control algorithms has to work for several instances of the same system which potentially differ due to e.g. production tolerances.
- Adaptive control algorithms provide methods to adjust the controller parameters such that the closed-loop behavior gets as close as possible to a desired behavior even for uncertain or changing plant parameters.
- Indirect adaptive control approaches basically allow to combine arbitrary controller structures with arbitrary recursive parameter estimation schemes. However, closed-loop stability has so far only been guaranteed for certain combinations of controller structures and estimation schemes.
- Modern direct model reference adaptive control algorithms are based on a rigorous stability analysis that yields stable parameter estimation laws and bounded closed-loop signals as well as an asymptotically stable tracking error.
- Model reference adaptive control aims to force the closed-loop system to follow a given reference model, where the stable system matrix and the input matrix are design parameters and can be chosen by the designer.
- The extension of model reference adaptive control (MRAC) by a closed-loop reference model leads to an improvement of the closed-loop performance during the parameter estimation transients and is therefore highly relevant for practical applications of MRAC.
- If adaptive control methods are applied to real technical processes it is absolutely necessary to consider extensions regarding robustness, e.g. a dead zone modification and parameter projection. Otherwise unmodeled dynamics or disturbances can lead to an unstable closed-loop system.
- If an input saturation of the plant is not considered correctly for the controller design, an undesired closed-loop behavior is likely to occur. Such an undesired behavior can often be connected to the integral part of the controller or slow controller

dynamics. However, also the characteristics of the controlled plant can give rise to undesired windup effects.

- Multiple extensions for adaptive control methods exist that allow to take input saturation into account and result in stable closed-loop systems. However, none of these methods provide degrees of freedom to explicitly address the closed-loop performance.
- In adaptive systems the parameter estimations introduce additional states in the closed-loop system. Therefore, these states and their initial values are important for the closed-loop stability, for windup-phenomena, and for undesired closed-loop effects in the presence of input saturation.
- The method of model recovery anti-windup (MRAW) allows for a separate treatment of the saturation effects by introducing a dynamical system as an extension of the closed-loop system. Since the additional dynamical system can be interpreted in terms of the plant model, MRAW is well suited for the framework of adaptive control.
- In order to guarantee stability of the estimated parameters in model reference adaptive control (MRAC) the desired dynamic has to be achievable for the closed-loop system. If the input of the controlled plant is limited, the reference model has to be extended in order to take the input saturation into account in the desired dynamic.
- The additional dynamical system introduced by the method of MRAW can be split up in a desired anti-windup dynamic and in an adaptive controller. The controller parameters needs to be adjusted by a suitable update law in order achieve the desired anti-windup dynamic. This structure is similar to the model reference adaptive control structure and hence can be treated in a similar way.
- The newly introduced method of adaptive model recovery anti-windup (AMRAW) based on model reference adaptive control (MRAC) results in a stable closed-loop system under certain conditions on the plant and on the initial closed-loop states.
- Adaptive model recovery anti-windup (AMRAW) introduces an additional degree of freedom in the closed-loop, that allows to influence the closed-loop performance if the input saturation is encountered without changing it when the input stays unsaturated.